INFRARED ACTIVITY IN INTERACTING GALAXIES

by

Gillian Susan Wright

Astrophysics Group
Blackett Laboratory
Imperial College of Science and Technology
LONDON SW7 2BZ

A thesis submitted for the degree of
Doctor of Philosophy of the University of London

November 1985

ABSTRACT

INFRARED ACTIVITY IN INTERACTING GALAXIES

Recent bursts of star-formation are thought to be responsible for most of the IR excesses exhibited by many types of galaxy. A IR study of interacting and merging galaxies is especially important because they form a class of objects in which a readily understood mechanism for triggering a starburst may be effective.

For the first stage of this study JHKL photometry of about 50 morphologically representative interacting galaxies was obtained. The most striking result is that for about 80% of the systems observed, one member showed a K-L colour index significantly redder than normal. Several mechanisms for this excess are considered and it is concluded that the galaxy colours are best understood as thermal radiation from warm dust heated by hot young stars.

Confirmation of the interpretation of the near-infrared colours is obtained from 10 and 20μm photometry of several of the interacting galaxies. These data are used to derive some of the parameters of the starbursts, such as starformation and supernova rates. The starbursts in interacting galaxies are shown to be about an order of magnitude more luminous than those previously known. For the morphologically defined subset of interactions in which two disc galaxies have merged to form a single disturbed object, the IR luminousities are about an order of magnitude more luminous still.

For the ultra-luminous merging galaxy NGC6240, near infrared spectroscopy of the 1.22μm rotation-vibration line of H_2, and the Paα hydrogen recombination line is used to examine in more detail the characteristics of this super starburst. A simple physical picture of a mechanism by which an interaction may trigger a starburst, based on the molecular hydrogen observations, is developed.

In summary the work presented in this thesis suggests strongly that interactions between galaxies, and especially ongoing mergers, frequently induce unusually intense nuclear IR activity. The source of this activity is most likely to be a recent burst of star-formation.

ACKNOWLEDGEMENTS

Firstly, I should like to thank my supervisor, Bob Joseph, for his enthusiasm and encouragement and for giving me the benefit of his broad understanding of physics and astronomy. By recognising the seminal importance of studying IR activity in interacting galaxies before its current popularity and initiating this project, he provided me with the opportunity to participate in a developing field of research. Special thanks are also due to Norna Robertson for her moral support and many useful and illuminating discussions.

Many friends and collegues have provided helpful advice, assitance and encouragement. Peter Meikle was a collaborator whose advice was much appreciated. The UKIRT staff provided practical assistance and useful discussions. Ian Gatley deserves special mention for his interest and for teaching, by example, the efficient use of UKIRT time. Richard Wade also provided much useful advice, particularily on the techniques of IR spectroscopy. This thesis could not have been printed without the BBC microcomputer software written by Steve Hart. Tom Hicks produced the pictures of "the Antennae" for chapter 1. I would also like to thank Pam Harvey for typing the original draft of chapter 1 into the word processor. Finally, but by no means least, I thank Jack Abolins, Simon Chase, Chris Collins and especially James Graham, for many stimulating discussions concerning interacting galaxies, supernovae and the rest of the universe, and for generally being cheerful observing companions.

I acknowledge the financial support of an SERC studentship for two and a half years.

CONTENTS

LIST OF TABLES

LIST OF FIGURES

CHAPTER 1

WHY STUDY INTERACTING GALAXIES ?

1.1 Introduction

Active galactic nuclei have been recognised for little more than two decades, and in this period we have progressed from discovery to formulating theories of how the various types of activity may be causally or evolutionarily related. Many fundamental astrophysical problems have been raised along the way, and the answers to a great number of these have yet to be found.

The need for energy generation by processes other than thermonuclear burning in stars first became obvious with the discovery of the variability of the highly luminous quasars, and the small ($\lesssim$ 1pc) sizes this variability implied. Indeed the first measures of the variability of a quasar, 3C48, were made before its redshift was known (Matthews and Sandage 1963). The controversy over the energy generation mechanism and whether the redshifts of quasars are cosmological is still continuing. The currently favoured source of the high luminosity, implied by a cosmological redshift, and rapid variability is gravitational energy released by accretion onto a collapsed object in the core.

Seyfert galaxies had been known as very luminous galaxies with compact stellar like nuclei showing conspicuous emission lines since about 1943 (Seyfert 1943). However it was not until 1968 that the optical variability of the classic Seyfert galaxy NGC4151 was measured (Pacholczyk et al. 1968). High luminosity in a compact volume, and variabilty on a short timescale, are the fundamental similarities between Seyfert nuclei and quasars which have led to the proposals of a common energy generation mechanism for both. The link between Seyferts and quasars has become more established with the recent observations showing that quasars are often embedded in galaxy-like haloes of luminous material (cf. Balick and Heckman 1982)

It was in this atmosphere of recent discovery of active nuclei that the pioneering infrared measurements of galaxies were made. Not surprisingly, the first 10μm detection of an extra-galactic source was 3C273 (Low and Johnson 1965). However, one of the most unexpected results of the initial far-infrared observations of galaxies were the large IR excesses of many galactic nuclei, not just the previously known Seyferts (e.g. Kleinman and Low 1970, Rieke and Low 1972). Despite attempts to relate this IR activity to the activity seen in the optical, comparison of the spectra with those of galactic sources, showed the energy source to be best explained as thermal emission from dust (e.g. Kleinman and Low 1969). By the early 1970's a number of investigators had suggested that many aspects of this powerful IR activity could arise from episodes of extremely intense formation of massive stars (e.g. Harwit and Paccini 1975, Reike and Low 1975). The identification of the luminosity source as hot young stars rests largely on indirect evidence, e.g. the spectra are typical of galactic HII regions, and the IR radiation is extended on a scale that is difficult to reconcile with the hypothesis of a single compact nuclear source. This starburst interpretation for the IR activity in most galaxies came of age with the demonstration by Rieke et al. (1980) that a recent burst of star formation could account, in detail, for all of the observed properties of the canonical IR galaxies M82 and NGC253. Rieke (1980) pointed out that these galaxies, if placed at a slightly greater distance would have many of the characteristics of type 2 Seyfert galaxies, and suggested starbursts as the energy source for these as well.

The existence of starburst nuclei raises a number of important astrophysical questions. How is the process of star formation affected by the nuclear environment, and what mechanism initiates and sustains the star formation activity? (e.g. Rieke 1981). Furthermore it has become apparent that nuclear non-thermal activity, as evidenced by variability for example, and intense star-formation activity in a ~ 1 kpc^3 nuclear volume are frequently coincident (cf. Smith 1984). This has led to suggestions that the coincidence is not merely fortuitous, but that a starburst may evolve into a compact nucleus or that non-thermal activity can trigger nuclear star formation.

The work presented in this thesis has been concerned with the first of these questions, i.e. elucidating the triggering mechanism and characteristics of nuclear bursts of star formation, as evidenced by IR activity. In this chapter the rationale for an infrared survey of nuclear star-formation rates in interacting galaxies is developed. The early phases of stellar evolution and the conditions necessary for star formation to occur are briefly described and related to the observed location and characteristics of star formation in galaxies. This provides a context in which to discuss the properties of starburst nuclei, and the relevance of interacting galaxies to this phenomenon is explained. The nature of galaxy-galaxy interactions, as deduced from numerical models is described and the existing evidence for a connection between interactions and activity (especially starbursts) is reviewed. Finally the advantages of using IR observations to study this problem are emphasised.

1.2 Star formation in galaxies

1.2.1 Physics of star formation

In this section simple physical arguments are used to discuss the basic conditions in the interstellar medium which must be met, if stars are to form by the collapse of interstellar material. This leadsrnaturally to an appreciation of why star formation is observed to occur in certain regions of the galaxy.

If the internal pressure (due to thermal velocities, rotation, magnetic fields, etc.) in a cloud of interstellar gas becomes small compared to its self-gravity, the cloud becomes unstable and begins to collapse. The thermal energy of a spherical gas cloud is

$$W_T = \frac{A\rho T}{\mu} \frac{4}{3} \pi R^3$$

and its gravitational energy is

$$W_G = -\frac{GM^2}{R} \sim -G\rho^2 R^5$$

where $A = 3/2\ k/m_p$,
G = gravitational constant,
and, μ = mean atomic or molecular weight.

Thus, for a given density, ρ, and temperature, T, the potential energy of a gas cloud increases as a higher power of the radius (R^5) than the thermal energy (R^3). So there is a limiting mass, the Jeans mass, which a cloud of given ρ and T must have if it is to satisfy this most basic condition for collapse. Quantitatively, for collapse of a homogenous spherical cloud to occur the cloud mass must therefore be greater than the Jeans mass

$$M_J = (AT/_{\mu G})^{3/2} \ (4/_3 \ \pi)^{3/2} \ \rho^{-1/2} \qquad 1.1$$

Clouds smaller than the Jeans mass are stable while larger ones can spontaneously collapse. Refinements to this equation which are made to allow for inhomogeneity etc. have only a small effect (Gunn 1980). Equation 1.1 shows that an ordinary interstellar gas cloud will not contract under its own gravitation. For example in the solar neighbourhood $\rho < 1$ atoms cm^{-3}, $T \sim 150$ K and $M_J \geq 10^5 \ M_\odot$. Only very large, massive clouds or very cool dense clouds are unstable enough for spontaneous collapse. If, for example $\rho \sim 30 \ cm^{-3}$, and $T \sim 40K$ then $M_J \sim 10^3 \ M_\odot$, which is more typical of the sizes observed for cold molecular clouds. In general, for collapse on the mass scales of stars ($\sim M_\odot$), some mechanism for generating a higher density or lowering the temperature is required. Equation 1.1 can be used to derive the densities needed if a cloud of about stellar mass is to collapse to form a single star, for stars of different masses. Assuming a favourably cold temperature, $T \sim 10$ K, gives a lower limit of $\rho \sim 6 \times 10^2 \ cm^{-3}$ for an O5 star but $\rho \sim 8 \times 10^4 \ cm^{-3}$ for an A0 star. Densities as high as $10^2 - 10^3 \ cm^{-3}$, are observed in some localised regions in the interstellar medium (cf. Spitzer 1964). So although an O star may form in some favorably cold dense region it is very difficult for an isolated low mass star to form. The collapse of an interstellar cloud to form $\sim M_\odot$ stars is described in the following paragraph.

Under normal conditions, as the cloud contracts the temperature and hence the pressure rises and slows the contraction. However the cold dense clouds in which contraction can be initiated are optically thin to IR radiation. So the gravitational energy released by the contraction is not expended in heating up the gas but escapes as IR radiation and the cloud continues to collapse in free fall. From equation 1.1 $M_J \propto T^{3/2} \rho^{-1/2}$, so if a large optically thin cloud starts to collapse at constant temperature, the density increases and M_J decreases. After the original cloud has contracted, smaller masses within it become unstable and start to contract and the cloud breaks up into a number of smaller denser fragments. This process shows qualitatively why young stars tend to be found in clusters or associations. Detailed numerical simulations of the collapse of uniform rotating cloud show that the number of collapsing "cores" formed varies approximately inversely as the Jeans mass. For example two protostars are formed when the cloud mass is about twice the Jeans mass. In general a hierarchical structure of fragments develops, with the final mass of each protostar depending on how much mass it accretes after its formation. These models predict a power law mass spectrum for the stars formed (Larson 1978), as indeed is observed for stars in the Galaxy.

In order to collapse and fragment, the cloud must, however, overcome a number of other energy barriers. The first of these is that when a cloud fragments the energy in the magnetic fields becomes larger relative to the gravitational potential energy. Consider a cloud with initial energies of E_m and E_p which breaks up into n fragments. Each fragment has magnetic energy ~ $1/n\ E_m$, and potential energy ~ $n^{-5/3}\ E_p$, and so on fragmentation E_m / E_p increases as $n^{2/3}$. Collapse and fragmentation will stop when $E_m = E_p$, and unless the magnetic field is very small initially (~ 10^{-7} Gauss, von Hoerner 1975) this limits the collapse. Secondly, since molecular clouds rotate with the galaxy, they have angular momenta. If the angular momentum stays constant as the cloud contracts, the rotational velocity increases as $v_r \sim R^{-1}$. Three dimensional contraction stops when the Keplerian velocity, $(GM/R)^{1/2}$ is reached and the cloud then contracts to a thin disc. This is a serious problem. For example if a cloud of mass $1M_\odot$ and ρ ~ 30 cm^{-3} is to contract to a stellar density of ~ 1 g cm^{-3}, its radius must contract by about 10^7 times. But if the cloud keeps its angular momentum from the galactic rotation it can only contract by about a factor of 50. Thus considerable transport of angular momentum is needed and it is thought that this can occur via turbulent friction between a disk and a massive core, or the rotating field lines of the protostar, or via stellar winds after the density becomes high enough that the ionization of the cloud drops. The detailed mechanisms by which the above two problems are circumvented are not yet fully understood. The angular momentum problem may be one of the reasons why star formation generally is observed to be inefficient.

Assuming the obstacles are overcome, the sub-clouds formed by fragmentation of the initial gravitationally unstable cloud will continue to collapse in free fall until the radius is small enough and the density high enough that the cloud becomes opaque to IR radiation. The cloud then continues to contract, but more slowly, the temperature in the central regions grows rapidly and a large temperature differential develops between the inner and outer layers. The gravitational energy is transported from the dense collapsing interior by convection and a dense cocoon of dust and gas forms around the star-like nucleus. The collapse of the core halts when the temperature has risen sufficiently to trigger thermonuclear burning and a main sequence star is formed. While the stellar core is surrounded by its optically thick circumstellar shell, the luminosity of the core is absorbed by dust and re-radiated in the infrared. Very young stars are therefore detected by their infrared emission. The association between IR emission and star formation is one of the principal reasons why IR astronomy has had such a large impact on the study of HII regions and starburst nuclei.

1.2.2 Mechanisms for achieving the conditions for star formation

Since gravity alone will not cause a typical cloud to collapse it is not surprising that locations where star formation is observed in galaxies are generally those where some mechanism exists for compressing or cooling the interstellar medium and so reducing the Jeans mass. The principal mechanisms and the locations in a galaxy where they operate are briefly described below.

One possibility for producing external pressure on a molecular cloud is an ionization front driven by a previous generation of early type stars. This mechanism is observed as "contagious star formation" (e.g. Habing and Israel 1979) in OB associations. The stars are often distributed in subgroups, starting with the oldest stars at one end of an elongated association, with much younger stars at the other. Usually the oldest subgroup is relatively free of interstellar material, while the youngest is associated with a molecular cloud which often contains HII regions and IR sources that probably represent a new generation of star formation. The Orion complex is a well studied example. However, not all star formation can be contagious. Even if most massive stars are formed this way, it is unlikely that low mass stars can trigger the formation of other stars since their dynamical effect on the interstellar medium is small (Silk 1980). There is considerable observational evidence that compression of interstellar clouds by the shock wave from a supernova explosion triggers star formation (Madore 1980a). So this is another way of maintaining star formation, given a previous generation of stars.

In spiral galaxies, if the spiral structure is maintained by a Lin-Shu density wave, large scale spiral shock waves could cause sufficient compression for star formation to be triggered. Alternatively, enhanced coalescence of clouds due to the increase in density would form bigger clouds which will ultimately collapse when they reach the Jeans mass. The observations of narrow bands of blue stars and HII regions on the leading edge of spiral arms is generally consistent with this theory. Since a large amount of gas is also observed, in each cycle of a spiral density wave only a small fraction of the available gas is actually turned into stars and so the star formation is not very efficient (e.g. Woodward 1976).

Some star formation seems to be spontaneous since star formation is observed in regions other than OB associations and grand-design spiral arms. Coalescence of clouds to form a cloud of larger mass which would collapse when the Jeans mass is reached is a possibility. A more efficient mechanism is a collision between two clouds, which drives a shock front into the clouds, thus compressing the cloud gas. For example, if two gas clouds of density 1 cm^{-3} collide at 100 km s^{-1}, the shocked gas cools in less than 10^6 years and, with a finite heavy element content, it can reach temperatures as low as 10-100K and densities as high as 10^4-10^5 cm^{-3} (Larson and Tinsley 1978). From section 1.2.1 such conditions should be extremely favorable for triggering star formation. Some dusty molecular clouds may develop denser colder cores due to thermal instabilities. Dust in the outer regions of the cloud may shield the interior from heating by the interstellar radiation field. Molecular emission may then be efficient enough to cause the core to cool further, and so the internal pressure would drop and trigger gravitaitonal collapse.

In summary, the large scale processes which trigger star formation are not yet understood quantitatively, although several possible mechanisms have been suggested which qualitatively agree with observations.

Recent estimates suggest that in general the efficiency of star formation in molecular clouds in the Galaxy is ~ 5-10% (Cohen and Kuhi 1979)

1.2.3 Parameters describing starformation in galaxies.

Since at present there is so little understanding of the triggering mechanisms for star formation, empirical studies of star formation in galaxies are used to try to glean information about the relevant mechanisms for star formation. The basic quantities which can be derived from observations to give the general characteristics of star formation in a galaxy are the current rate of star formation, its initial mass function (IMF), the upper and lower mass cutoffs, and the location of the star formation. The latter was outlined above and the others are discussed below. The lifetime of a star and the amount of gas which it returns to the interstellar medium are strong functions of its mass, and so knowledge of the initial mass function is as fundamental to describing the characteristics of star formation as the rate of star formation. In this section the definitions of these fundamental parameters are given, and their observationally derived properties are discussed.

Salpeter (1955) originally defined the IMF $\Psi(M)$ as

$$r\Psi(M) = \frac{d\dot{N}(M)}{d\ \ln M} = M\,\frac{d\dot{N}(M)}{dM}$$

where r is the rate of starformation per unit time,
$\dot{N}(M)$ is the rate of star formation per unit mass,
and M is the stellar mass.

so that the total mass of stars formed per unit time up to a given mass limit is given directly by the integral of $\Psi(M)$ over mass

$$\frac{dM}{dt} = r \int_0^M \Psi(M)\ dM$$

He showed that the IMF can be fitted by a power law in a given range of masses $\Psi(M) \propto M^{-\alpha}$ where $\alpha \sim 1.35$ for high mass stars. More recent determinations of the IMF in the Galaxy are discussed below.

In many recent starburst models (e.g. Rieke et al. 1980, Telesco and Gatley 1984) an alternative definition of the IMF as the differential mass spectrum

$$\Psi(M) = \frac{d\dot{N}(M)}{dM}$$

is used, in which case the mass of stars formed per unit time is given by

$$\frac{dM}{dt} = r \int_0^M M \, \Psi(M) \, dM$$

With this definition of the IMF, the index of the power law fit is different by a factor of M^{-1}, so Salpeters result corresponds to $\alpha \sim 2.35$. To be consistent with the later work discussed in this thesis it is this latter definition of the IMF which is refered to when discussing recent determinations of the slope of the power law fit to the IMF in the following section.

The initial mass function (IMF) for the Galaxy has been derived from star counts in the solar neighbourhood for both clusters and field stars (cf. Lequeux 1980). Lequex finds that it is best fitted by a power law (the Salpeter Law) where $\alpha \sim 3$ for $M > 2.5\ M_\odot$. For low mass stars with masses in the range .1 to 1 $M_\odot$ the IMF appears to be much flatter with $\alpha \sim 1.3$. There is little observational evidence for how the two relatively well defined portions of the IMF fit together in the intermediate mass range. One of the most recent and accepted determinations of the IMF is that by Miller and Scalo (1979). They derive $\alpha = 1.4$ for stars with masses 0.1 - 1 $M_\odot$, $\alpha = 2.5$ in the mass range 1.6 - 10 $M_\odot$ and $\alpha = 3.3$ for 10 - 60 $M_\odot$ stars. These slopes, together with the "local" upper and lower mass cutoff's, 60 - 100 $M_\odot$ and ~ 0.1 $M_\odot$ respectively (Boisse et al. 1981, Miller and Scalo 1979), are taken to be generally applicable to global star formation in galaxies. The derivation all these results is uncertain because they depend on the assumption that the distribution of stars in space is uniform (Lequex 1980). Furthermore, there is strong evidence in favour of variations in the upper limit to the IMF, especially as a function of galacto-centric distance in our galaxy and M101 (cf. Lequex 1980). This may be due to a relation between the IMF and metallicity, in the sense that the smaller the heavy element fraction, the greater the fraction of high mass stars, as predicted by theories of star formation (e.g. Khan 1974).

Since stars form from interstellar gas, star formation rates are often estimated relative to the mass of gas or total mass of a galaxy. Comparing the number of stars in a given region of the H-R diagram for different galaxies provides the most direct measure of the relative rates of formation of stars on a global scale. Since this depends on observing newly-formed stars, and low mass stars are difficult to detect in their early phases, these star formation rates relate mainly to stars of mass > 1 $M_{\odot}$. Star counts exist for only a few galaxies and the main result of this work is that the present rate of star formation is approximately the same in the LMC and the solar neighbourhood, but is four times smaller in the SMC.

Less direct methods such as studies of HII regions at optical, infrared or radio wavelengths have shown that there are large variations in the rate of star formation within the galaxy. Radio and far-infrared maps indicate a concentration of gas and HII regions round the galactic centre in a ring of radius ~ 5 kpc. Serra et al. (1980) find that the far-IR luminosity per unit surface of the galactic disc is about 10 times higher at ~ 5 kpc than at ~ 10 kpc, and they argue that the excess arises from a significant population of young stars. An excess at 2.4 μm (Maihara et al. 1978), due to almost entirely to red giants, shows that this high star formation rate is not a recent phenomenon.

For more distant galaxies, infrared luminosities and optical spectra have been used to argue that many galaxies exhibit very copious star formation in their nuclear regions, as described in the following sections.

1.3 Starburst galaxies

Intense star formation might be expected to occur in the nuclei of galaxies because this is where the potential well is deepest so material may accummulate and be compressed more readily there. Nuclei in which this seems to occur have been termed "starbursts" because the available gas has to be processed into new stars at a rate which is too high to be sustained indefinitely, in order to account for the large numbers of new stars necessary to produce the luminosities. The optical, IR and radio evidence is briefly reviewed and then the characteristics of starbursts in the few galaxies that have been studied in detail are described.

1.3.1 Optical evidence for starbursts

The UBV photometric colours of galaxies are in general consistent with the idea that galaxies have the same age and IMF, with decreasing star formation rates, where the timescale for star formation to decline varies with morphological type. A very recent burst of star formation produces hot stars, which make a galaxy bluer in U-B than the normal U-B, B-V relation. Searle et al. (1973) first used the starburst hypothesis to explain the colours of a few blue dwarf galaxies. These unusually small, low luminosity galaxies have colours so extreme that they mimic those of HII regions. Similar evolutionary models of star formation rates have been used by Huchra (1977) and Biermann and Fricke (1977), to explain the blue colours of Markarian galaxies in terms of a composite galaxy, consisting of a galaxy with properties similar to an ordinary spiral with a burst of star formation of varying strength (20-50% of the light at V) superimposed.

HII regions produce strong optical emission lines, so bright starburst nuclei are expected to show optical emission lines and these have recently been used to derive more details about recent starbursts. In an extensive survey of galaxies with starburst nuclei, Balzano (1983) finds that the line ratios of [OIII]/Hβ and [NII]/Hα are similar to those found in galactic HII regions. This, together with the narrowness (FWHM < 250km s^{-1}) and Gaussian profiles of the lines, strongly suggests that the ionization mechanism is photoionization by UV radiation from hot stars. All the observed characteristics can be consistently explained by a large episode of star formation which is confined to the central nucleus and lasts from 10^7 to 10^8 years. Like Seyfert galaxies, starburst galaxies have strong nuclear emission lines but the characteristc line widths and ratios can be used to distinguish them from the Seyferts.

1.3.2 Radio emission from starbursts

The radio sources associated with nearly all bright spiral galaxies are generally very weak and diffuse. However there are a few cases where the radio power is ten or more times larger than normal. These stronger radio sources might be similar to those found in radio galaxies, being powered by accretion processes. Alternatively, the radio flux could be due to supernovae and HII regions produced in an enormous burst of star formation. Unresolved (< 1 pc) radio sources are not thought to be related to star formation or supernova remnants, but to be the result of the accretion onto a compact object which is thought to power the luminosity of some Seyfert galaxies and double lobed radio galaxies. Extended nuclear sources can on the other hand can be understood in terms of the starburst hypothesis (cf. Hummel et al. 1984).

Both thermal and non-thermal radio emission are expected from a recent burst of star formation. The thermal flux arises from free-free emission from HII regions ionized by young stars, while non-thermal synchrotron emission arises from supernova remnants and the particles supernovae inject into the galaxies' magnetic field. For a sample of 33 radio bright spirals, Condon et al. (1982) shows that there is no evidence for beaming in the central sources, while many of them are ~ 1 kpc in size and coextensive with optical emission line regions or IR sources, indicative of regions of intense star formation. The radio luminosities can be explained by synchrotron emission associated with supernova remnants if supernovae are produced at a rate of 1^{-10} yr.

Recently, Turner and Ho (1983) have conducted a much more detailed study of the radio emission from three starburst nuclei. By mapping the galaxies with very high angular resolution at both 2 cm and 6 cm wavelengths, they constructed "spectral index maps" of the nuclei. Regions of flat spectral index indicative of young stars are separated from negative spectral index areas of smooth synchrotron emission. The thermal fluxes, a direct measure of the number of ionizing photons, correspond to > 3 x 10^4 young stars, consistent with a massive burst of star formation as the source of the radio luminosities.

1.3.3 IR emission from starbursts

One of the most surprising results of early infrared astronomy was the large 10μm excesses of many galactic nuclei (e.g. Rieke and Lebofsky 1979). The infrared continuum spectra of these galaxies are very similar to those of HII regions in the galaxy and indicate that most of the IR emission from these galaxies is thermal reradiation by dust.

(For QSO's and some type 1 Seyferts the IR emission mechanism may be nonthermal.) Where observed, the spectra of these IR excess galaxies show a number of IR absorption and emission features also detected from galactic HII regions. The probable association of infrared emission with nuclei containing dense molecular clouds detected through CO emission (Rickard et al. 1977) confirms the similarity. The spectral similarity led Harwit and Pacini (1975) to suggest bursts of star formation as the origin of strong infrared radiation from galaxies.

Far-infrared observations (e.g. Telesco and Harper 1980) show that most of the galaxies bright at 10μm have even larger excesses at 100μm, corresponding to luminosities of ~ 10^9 to 5 x 10^{10} $L_\odot$. Complete thermonuclear burning of a primordial abundance of hydrogen and helium can release ~ 0.8% of the total mass as energy. So for a galaxy of mass M, the minimum mass luminosity ratio achieveable is

$$\frac{M}{L} \sim \frac{M}{0.008Mc^2/t}$$

where t is the time during which the energy is released. For the age of a galaxy ~ 10^{10} years, this corresponds to M/L ~ 0.1. Typical mass-luminosity ratios for galaxies with infrared excesses are very low, ~ 0.001 - 0.5 (Rieke 1978), implying that if the energy source heating the dust is thermonuclear it occurs over timescales < 10^{10} years. Recently produced luminous young stars can account for the observed luminosity and low M/L ratios, and so the star formation is thought to be occuring in a short lived burst.

A prominent IR characteristic of a burst of star formation is that the infrared luminosity dwarfs the luminosity at all other wavelengths. Where it has been resolved the emission is typically extended over an area ~ 100 - 600 pc in diameter, co-extensive with HII regions (Rieke 1976) and is consistent with emission by dust heated by sources spread throughout the emitting region.

Rieke and Lebofsky (1978) showed that > 40% of bright nearby spirals have strong nuclear emission at 10μm. A survey of galaxies in the Virgo cluster (Scoville et al. 1984) also suggests that many spiral nuclei are strong 10μm emitters. Although they detected (> 2σ) only 18 of the 53 galaxies they observed, Scoville et al. made a statistical argument to show that virtually all the galaxies showed a significant 10μm excess. One surprising result was that the IR excesses, which they interpreted in terms of recent star formation, were uncorrelated with Hubble type or other global galaxy properties. These two infrared surveys show clearly that IR activity which is easily understood as due to a starburst is a common feature of galactic nuclei.

1.3.4 Some examples of starbursts in galaxies

In the following paragraphs the properties of a few galaxies with well-studied starburst nuclei are described in order to illustrate the success of the starburst hypothesis and its general features.

Two of the most extensively observed and modelled star-burst galaxies are M82 and NGC253. In their model Rieke et al. (1980) showed that the nuclear emission from these galaxies could be accounted for by a starburst if the non-thermal radio emission arises from a mixture of supernovae and free-free emission, the IR excess from dust grains heated by hot stars, the near-infrared flux from red giants formed earlier, the UV from the young stars themselves and the X-ray from remnants of stars and supernovae. Best-fitting models have an IMF slope ~ 3 (i.e. similar to the local IMF) and a burst age ~ .5 x 10^7 years. One striking result is that the lower mass cut off must be ~ 3.5 $M_\odot$, as opposed to < 1 $M_\odot$ for the local IMF (cf. 1.2.3). If lower mass stars are formed the models cannot account for all of the 2μm flux within the mass limit of the nucleus or the excitation conditions for the ionized gas. The required mass of recently formed stars necessary to explain the UV and FIR fluxes is comparable to the total mass of gas available so the star formation must be very efficient (> 50%) in terms of conversion of the interstellar medium into stars. Rieke et al. (1980) are able to explain all the observed galaxy properties, including the non-circular motions of the interstellar material, by this starburst model.

In contrast to M82 and NGC253, Moorwood and Glass (1982) find that the a starburst in the nucleus of NGC5253 must be much younger, < 10^7 years, to explain the lack of a 2μm excess due to red giants/super giants and the lack of any significant contribution from supernova remnants to the X-ray emission or radio flux . Comparing this result with the model of Van den Bergh (1980), in which star formation began in the outer parts of this galaxy ~ 10^8 - 10^9 years ago, suggests that this starburst has only recently propagated into the nucleus.

The optical, infrared and radio luminosities of NGC3690/IC694 have recently been interpreted successfully as the result of a burst of star formation by Gerhz et al. (1983). There is a very strong emission line flux from these interacting galaxies. There appear to be three regions of intense IR activity in this system: two nuclear sources and one extranuclear. This starburst is particularly interesting because, although it is not located in the nucleus, it has a luminosity comparable to the brightest starbursts in galactic nuclei (~ 10^{10} $L_{\odot}$). Telesco et al (1985) suggest that this star formation region has been caused by the gravitational interaction between the two galaxies. They also show that the starburst in NGC3690 is significantly younger than that in IC694 and find, suggestively, that the difference in ages is about a galactic rotation time. Again the data is best fitted by an IMF biased towards high mass stars ($M > 6$ $M_{\odot}$), and a high supernova rate of ~ 2 yr^{-1} is predicted.

1.3.5 Starburst properties and puzzles

Based on the currently known examples, the global properties of a burst of recent star formation are: (1) most of the bolometric luminosity is emitted as (extended) infrared emission; (2) it has a very low mass/luminosity ratio; (3) narrow but bright optical emission lines which resemble those from HII regions are often observed (4) strong non-thermal radio emission is frequently coincident with the IR emission and (5) UV and X-ray excesses have sometimes been found. Models of starbursts in a few galaxies all suggest that the formation of low mass stars is suppressed and the conversion of gas into stars must be very efficient. The frequent occurrence of large infrared luminosities in many types of galaxy strongly suggests that bursts of star formation are a common feature of nuclei. Observations of starbursts are needed to quantify the characteristics found so far, and elucidate new ones.

The existence of starburst nuclei raises many interesting questions about star-formation processes. A crucial problem is what determines the IMF, which seems to biased towards high mass stars, compared to the more normal star formation described in 1.2.3. Larson (1977) has suggested that most massive stars may form only in regions of large scale dynamical disturbance or shock fronts. If this is so then a mechanism for creating the disturbance is needed. The efficiency of the star formation also suggests that some special mechanism is involved -- none of the proposed means of compressing the interstellar medium to trigger srar formation mentioned in section 1.2.2 seem to be suitable for generating the sudden formation of such large numbers of young stars. Nuclear starbursts certainly seem to have different characteristics than those more normally observed for star formation in the solar neighbourhood. Given the general problem of obtaining the right conditions for star formation to be initiated (cf. 1.2.1), the triggering mechanism for a starburst is far from obvious.

1.4 Interactions and starbursts

If disturbed gas motions and shock compression are of general importance for star formation (1.2.1) then star-formation rates might be very high in systems showing evidence of dynamical disturbances or shock fronts. Such galaxies should be a seminal class of galaxies in which to study the details of starbursts. In this section the dynamical disturbances in interacting galaxies and the evidence that bursts of star formation are occurring in these galaxies are reviewed.

1.4.1 Models of interacting galaxies

Interacting galaxies have one or more nearby companions and many of these appear to be joined by a luminous bridge of matter and/or to have long narrow tails and filaments or a peculiar disturbed morphology. A large variety of such galaxies has been catalogued by Arp (1966) and Vorontsov-Velyaminov (1959, 1977).

Toomre and Toomre (1972) and Wright (1972) showed that these features could be the result of purely tidal forces between the galaxies. This was important, because it had been thought that tides could produce only broad features, and exotic mechanisms involving the ejection of companions had frequently been proposed (cf. Vorontsov - Velyaminov 1969). A major result of this work was to show that the amount and form of tidal damage depends critically on the details of the passage of one galaxy past another. Retrograde interactions where the system angular momentum is in the opposite sense to the spin of the individual galaxies, tend not to produce tails or bridges. The amount of disruption is also critically-dependent on the inclination of the spin plane of the galaxy to the system orbital plane -- highly inclined passages cannot build bridges. Tail-building seems to be less affected by inclination, although if tails are to form on both galaxies they must have similar masses and interact very closely.

In order to illustrate the correctness of the tidal model, the Toomres modelled in detail the morphology of five well-known examples of interacting galaxies taken from the Arp Atlas (1966). The impressive success of their model for the long, thin crossed tails of the "Antennae" is illustrated in Figure 1.1. One criticism of this type of model is that it does not allow the test particles to have an initial dispersion in their velocities, as the gas and stars in real galaxies do. Including this effect would result in a much wider spread of the test particles in the model tails. A very deep photograph by Schweizer (1978) shows that the tails are in fact ~ 3 times wider than previously thought, consistent with the models. The limited amount of velocity information so far accummulated for members of interacting pairs suggests that models of tidal interactions account successfully for the dynamics as well as the morphologies of interacting galaxies (Toomre 1977).

The Toomres' models also showed that during an interaction material can be captured from one galaxy by the other. They noted that the orbits of the accreted material were very disturbed and often plunged deeply into the nucleus. This lead them to suggest that a tidal interaction could result in a sudden injection of fresh material being brought deep into the galaxy. This material, either from the disc of the galaxy itself or captured from its partner, could fuel prolific star formation in the nucleus. In the following section some of the dynamical evidence for disturbed gas motions in interacting galaxies is briefly summarised before the observations pertaining to the Toomres' hypothesis that interactions can trigger star formation in the nuclei of galaxies are reviewed.

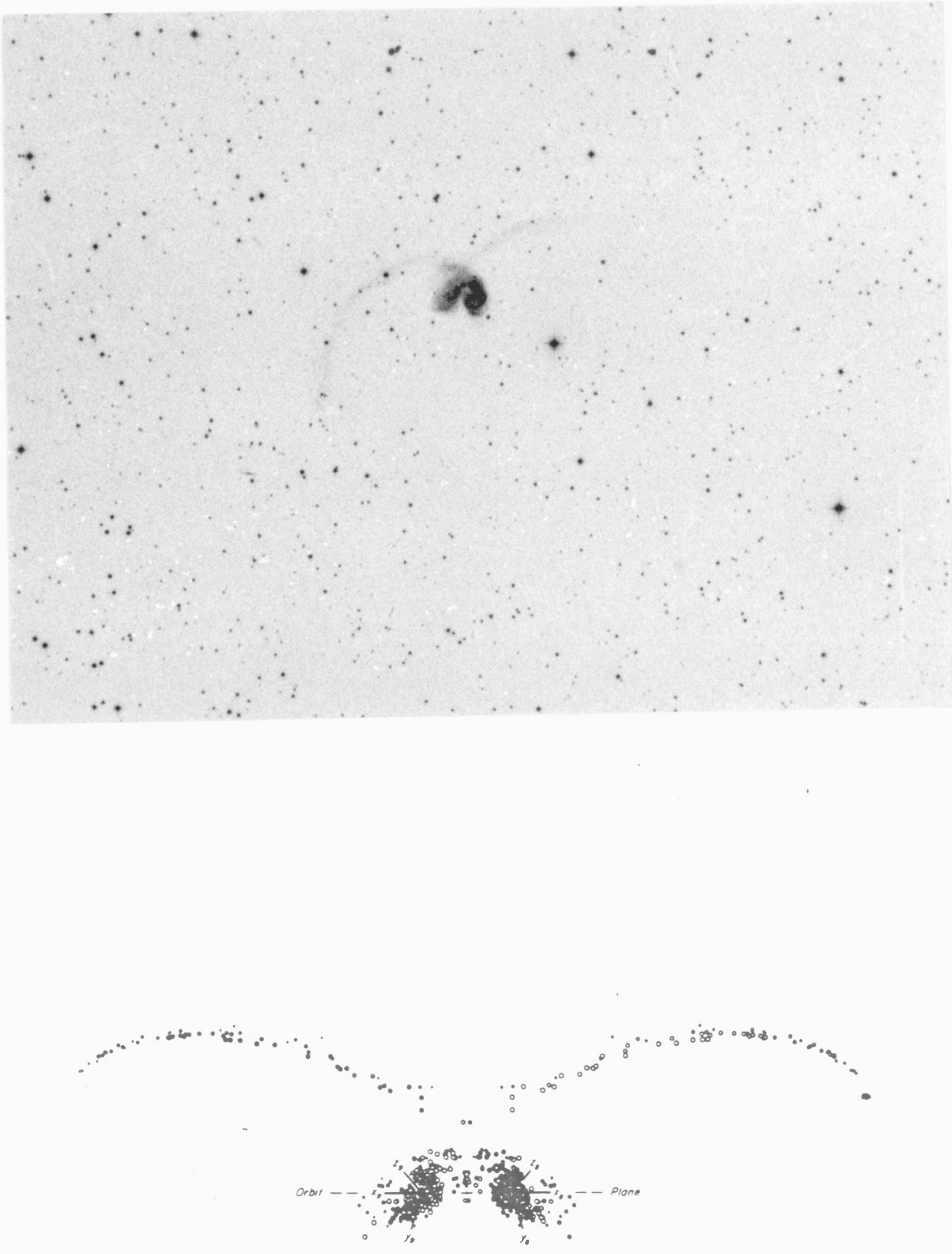

Figure 1.1 A comparison of the Toomre and Toomre (1972) simulation of NGC4038/39 with the appearance of the galaxies on the sky-survey plates.

1.4.2. HI studies of interacting galaxies

Radio studies of the HI gas dynamics and distribution in interacting galaxies are interesting for two reasons. Firstly, since HI discs around galaxies are often extended, the gas disc is sensitive to the tidal forces and a study of the HI velocity field may yield information about the detailed kinematics of the interaction. Secondly, if gas can be detected between interacting galaxies, especially in cases with no apparent optical bridge, this will provide direct observational evidence for the transfer of matter during the interaction, as well as confirming physical association.

Gallagher et al. (1981) and more recently Sulentic and Arp (1983) have shown that interacting galaxies often have strongly perturbed HI velocity fields. This result is interpreted as being caused by rapid changes in the gravitational potential due to the interaction. Heckman et al. (1983) have measured the sense of flow of material using HI absorption lines. They find evidence for both inflow and outflow. The most important result is that it is not only the disc gas which is disturbed, but also gas concentrated deep in the interior of the galaxy (ie. the inner ~ 2 kpc). So the interaction can indeed stimulate infall of gas which is close to the nucleus.

HI mapping of M81, M82 and NGC3077 by Van de Hulst (1978) and Davies (1978) have shown that an HI bridge connects M81 to NGC3077, M82 to M81 and both NGC3077 and M82 may have HI tails. Velocity gradients in these features suggest that they have a tidal origin. More than 50% of the total HI content of this system is involved in the tails and bridges, suggesting that large masses of gas are transported during a gravitational interaction.

1.4.3 Surveys of star formation in interacting galaxies

The quest for activity in interacting galaxies as a class has been persued in surveys ranging from radio to X-ray wavelengths with tantalizing, if somewhat ambiguous, results. The results of these surveys and their relevance to the suggestion that interacting galaxies may have starburst nuclei are summarised below and then, in the following section, evidence relating interactions between galaxies with more exotic activity is presented.

Larson and Tinsley (1978) have estimated star-formation rates in both normal and interacting galaxies from their UBV colours (cf. 1.3.3). For morphologically normal galaxies from the Hubble Atlas, they find that the colours form a narrow sequence in the UBV two colour diagram, as expected. In contrast, a sample of interacting galaxies taken from the Arp (1966) Atlas shows a much greater scatter in the diagram, both above and below the normal galaxy sequence and extending to much bluer and redder colours. These results cannot be explained by models with normal monotonically declining star formation rates, but can be explained by episodic star formation. A very recent burst produces hot stars which make a galaxy bluer in (U-B) than normal, but as the burst ages (U-B) becomes redder and after $\sim 5 \times 10^7$ yr it is redder than normal. Larson and Tinsley (1978) were able to show that the colour distribution for interacting galaxies could be explained if many of them experienced bursts of star formation involving a few percent of the total mass with durations $< 10^8$ years.

Smirnov and Komberg (1979) have studied star formation rates in interacting galaxies by comparing the UBV colours of 208 galaxies in pairs or groups with a sample of "isolated" galaxies. They interpret the result using a similar model to that of Larson and Tinsley, but find that some of the colours are best modelled with an "anti-burst" -- termination of star formation for some period. Durations of bursts and anti-bursts are $\sim 10^7$ yr. They find that 30-40% of the starburst galaxies have spiral companions, while galaxies with "anti-bursts" tend to have early type companions, and suggest that the rate of star formation is influenced by the gas in the companion. These are the not the only results which give an indication of a relation between the star formation and characteristics of the interaction, as discussed below.

White and Valdes (1980) show that close binary galaxies are systematically brighter than the equivalent field galaxies. Rough UBV colours for these galaxies show that they are also bluer (Sharp and Jones 1980). Thus an "obvious" explanation is that the interaction of the two galaxies induces star formation and this makes the galaxies brighter. There is also some weak evidence that bluer colours correspond to closer pairs (Sharp and Jones 1980). Furthermore, Madore (1980b) has shown in a study of companions to nearby spirals that spirals with many companions are systematically brighter than spirals with few companions, again suggesting that it is the interaction which causes the increased brightness.

As explained in 1.3.3, bright radio emission is now often thought to arise from a recent burst of star formation. However interest in the possibility of excess radio emission from multiple systems originally arose because of the clues this might give to the fuelling of other bright radio active galactic nuclei.

Wright (1974) and Sulentic and Kaftan-Kassim (1973) did not find any evidence for excess radio emission in the galaxies they studied. On the other hand, Sulentic (1976) carried out an extensive survey of the Arp Atlas at 6, 11 and 21 cm wavelengths and concluded that interacting galaxies were radio emitters approximately twice as often as more normal galaxies. In these radio surveys it is impossible to tell whether the emission is associated with one or both galaxies in the pair. Sulentic's results were confirmed by Stocke (1978), in a higher resolution survey, who also inferred that the interaction triggered the excess emission because closer physical pairs are more often detected than widely spaced ones. Both members of a small number of pairs were distinguished by Hummel (1981), who found them to have luminosities a factor of 2-3 higher than non-interacting galaxies. He suggests that the enhanced emission is triggered by the interaction, possibly as a result of infalling gas. Heckman (1983) confirms this result and additionally finds that merged pairs tend to be even brighter with ~ 5 times normal radio luminosities.

Since most interacting galaxies have non-thermal radio spectra and many have been shown to be extended radio sources, there is tantalizing evidence in the more frequent occurrence of stronger radio sources in interacting galaxies that the interaction is triggering star formation.

Fabbiano, Feigelson and Zamorani (1982) detected 40% of a sample of peculiar galaxies in the X-ray band using the Einstein Observatory. They concluded that the X-ray emission is most likely due to Population I X-ray binary systems, with young supernova remnants possibly adding a contribution.

In summary several types of evidence suggest that nuclear bursts of star formation occur in interacting galaxies. It is probable that the interaction causes disturbed gas to be dumped into the nucleus of one or both galaxies, where it becomes highly compressed in the deep potential well and generates a burst of star formation. However the evidence accumulated to date is essentially qualitative. For example the evidence from UBV colours depends on the interpretation of a scatter and so cannot provide quantitative information on the fraction of galaxies affected or the magnitude of the effect. For other studies such as radio and X-ray, there is still some debate about whether or not it is reasonable to interpret this emission in terms of a starburst, and the differences between starburst and non-starburst characteristics tend to be subtle (cf. Heckman et al. 1983b, Hummel et al. 1984)

1.5 Interactions and other activity

As described in the Introduction, other types of activity are also observed in galactic nuclei, which may or may not be associated star formation. There is in fact weak evidence that interacting galaxies are associated with Seyfert galaxies. Studies of the morphology of classical Seyferts have been carried out by Adams (1977) and Simkin et al. (1980). Adams finds an apparent excess of Seyferts in disturbed and interacting systems -- 10% compared to 6% for normal galaxies. Simkin et al. (1980) have suggested that some of the disturbed morphological appearance of Seyfert galaxies may be a result of the activity itself, if it is fed by gas from the disk. So the evidence is rather weak. If accretion processes are invoked to explain Seyfert activity there is the problem of supplying enough material to maintain the luminosity. This is where interactions may be involved. Just as the tidally induced flow of material deep into the nucleus of a galaxy can trigger a burst of star formation, so it can provide the necessary fuel to feed an accretion disc around a compact object. Since infrared excesses are a common feature of Seyfert galaxies, an IR survey of the nuclear star formation rates in interacting galaxies such as that proposed below may also provide information about the association between interactions and Seyfert galaxies, and perhaps between Seyfert type activity and starbursts.

1.6 Utility of infrared observations

The results described in this chapter which lead naturally to the desirability of a survey of the IR activity in interacting galaxies, to search for evidence of recent bursts of star formation in their nuclei, can be summarised as follows. Many galaxies appear to have massive nuclear bursts of star formation, and one of the main signatures of these starbursts is luminous IR emission. Unravelling the mechanisms by which these starbursts are initiated is a major astrophysical challenge. Interactions between galaxies have been suggested as a possible source of fresh gas to fuel the starburst, while tidal forces in the interaction may provide the necessary compression of the gas to trigger fragmentation and star formation. Observations of starbursts in interacting galaxies are not only important to elucidate the processes which may trigger a starburst, but also because investigations of the rate of star formation in different galaxies provide a wide range of environments in which to study the processes of star formation itself.

There is some evidence from optical and radio observations that interacting galaxies do have nuclear bursts of star formation. However these surveys have been inconclusive. In the optical, UBV photometry can be severely affected by extinction, and in any case does not uniquely determine the age of a starburst or its IMF (cf. Struck-Marcell and Tinsley 1978). Additionally, the number of young stars can only be determined via evolutionary models. Spectroscopic studies of line ratios yield these quantities more directly. However such studies are difficult to carry out for a large number of faint galaxies and are also subject to extinction problems. Young stars form in regions embedded in dust (cf. section 1.2) so dust is always associated with bursts of star formation. Radio observations can be difficult to interpret, because the angular resolution achieved is often not sufficient to distinguish which galaxy(ies) in a pair or group are associated with the emission. Also the spectra are generally dominated by synchrotron emission so that a direct measure of the number of Lyman continuum photons and hence the number of young stars is not possible. Additionally a wide range of source morphologies is observed (e.g. compact to extended over ~ 1 kpc) and there is still controversy over where the borderline between those associated and not associated with star formation lies (e.g. Balick and Heckmann 1982).

Infrared observations of starbursts do not seem to involve these complications. Most of the bolometric luminosity of the galaxies is emitted at IR wavelengths by the heated dust that is associated with young stars or protostars. Since it was the frequent occurrence of these large IR luminosities and low M/L ratios which suggested star bursts were a common phenomenon it is reasonable to suppose that intense bursts of star formation can occur in regions so deeply embedded in dust that they are not necessarily seen optically at all. M82 and NGC253 are examples of star-burst galaxies where UBV colours do not reveal anomalously high star formation rates (Larson 1978). A survey of the IR emission from interacting galaxies could provide strong evidence for (or against) an association between interactions and high rates of star formation. Mass-luminosity ratios will provide much more direct estimates of the star formation rate and efficiency than observations at other wavelengths. By resolving the IR sources it should be possible to separate the genuine starbursts from Seyfert-type activity. Rieke (1978) noted that his (unpublished) 10μm observations of a few interacting galaxies indicated higher luminosities than those of the spiral galaxies with IR excesses which he had been studying. Thus IR observations of interacting galaxies may show the degree to which their activity differs from that in "normal" spirals.

In this chapter the rationale for the IR observations of interacting galaxies discussed in the following chapters has been presented. The recent availability of reasonable mid-IR sensitivity has led to other investigators persuing observational programmes with similar aims to the work described herein, and their results are now briefly summarised. Lonsdale et al. (1984) have detected 11 out of 20 morphologically selected interacting galaxy systems at 10μm. They argue that these systems have on average a significantly higher infrared luminosity than non-interacting galaxies and interpret the enhanced infrared luminosities as due to bursts of star formation. Cutri et al. (1985) detected only 13 galaxies out of a complete sample of 39 pairs selected from the Karachentsev (1972) Catalogue of Isolated Pairs of Galaxies, of which they observed 30 pairs at 10μm. Cutri et al. argue that a statistical comparison of the nuclear properties of these galaxies with samples of non-interacting galaxies shows that a population of galaxies with extremely luminous 10μm emission is unique to the interacting sample.

Because the sensitivity limitation due to photon noise from warm telescopes is rather severe at 10μm, an alternative strategy to that used in the work described above was chosen for the first stage in the study of interacting galaxies presented in this thesis. This is to use near-infrared colours to infer the presence of a steeply rising mid-IR continuum. In the following chapter the details of the rationale for this approach are presented. The results from a near infrared survey of a wide range of interacting galaxies are then discussed.

CHAPTER 2

A NEAR INFRARED SURVEY OF INTERACTING GALAXIES

2.1 Introduction

In Chapter 1 the importance of a systematic study of star formation and other activity in interacting galaxies was outlined, and a survey of their IR emission was proposed. This chapter describes a near-infrared survey of a variety of morphological types of interacting systems to search for evidence of IR activity in their nuclei. As discussed in section 1.3.3 large infrared luminosities and correspondingly small mass/luminosity ratios are characteristic features of recent bursts of star formation in galactic nuclei. In a starburst galaxy most of the energy of the young star forming regions is absorbed by dust and reradiated in the infrared. Measurements of the infrared luminosities of interacting galaxies should therefore be decisive in determining if large scale bursts of star formation are triggered by interactions between galaxies, as suggested in section 1.4.

Regions where stars have recently formed have infrared energy distributions with maximum flux densities at ~ 50-100μm and so an accurate measure of the infrared and hence bolometric luminosity requires far-infrared(~100μm) photometry. However, since the radiation at ~ 5-30μm originates from dust that is closer to the heating sources and therefore hotter (≧100K) the continuum spectra have a characteristic quaisi-thermal shape and a good estimate of L_{bol} can generally be obtained by extrapolating from measurements made at 10 and 20μm to the FIR. (cf Scoville et al. 1983). Photometry at these wavelengths is difficult to achieve for most extragalactic sources because they are very faint compared to the high background emission from the telescope and atmosphere, so long integration times are necessary. Since the objective was to survey a wide variety of morphological types of interacting galaxy, 10μm photometry was not very practical. The usefulness of near infrared colours to infer luminous 10-100μm emission is outlined in the next paragraph.

If there is substantial far-infrared emission then its presence will also be observable as excess emission at L (3.4μm). A qualitative measure of this excess can be obtained from the K-L colour, which will be significantly redder than normal galaxy colours. This is illustrated in Figure 2.1 where a typical FIR spectrum is shown added to the near infrared spectrum of a normal galaxy. The near infrared (JHKL) colours of normal galaxies are dominated by late-type stars and hence correspond approximately to the colours of a 3500K blackbody; J-H ~ 0.7, H-K ~0.3, K-L ~ 0.3. For most galaxies for which a FIR spectrum has been measured the flux density increases approximately proportional to λ^2 to the mid-infrared. A good example of a normal galaxy is M31 which has a nuclear K-L colour of 0.34 (Sandage et al. 1969), a "flat" near to mid IR spectrum and a mass/luminosity ratio of 48 (Rieke and Lebofsky 1978). In contrast the archetypal starburst galaxies M82 and NGC253 have K-L' colours of 0.86 and 1.38 respectively (L'~3.6μm) with mass/luminosity ratios of 0.04 and 0.002 which, as described in section 1.2.3 cannot be maintained by a normal population of stars (Rieke et al. 1980, Rieke & Low 1975, Telesco & Harper 1980, Rieke & Lebofsky 1978). Since photometry at JHKL can be done much more quickly than longer wavelength photometry the infrared activity in interacting galaxies is best investigated initially at these wavelengths.

2.2 Observations

The galaxies chosen for study were selected from the Atlas of Arp(1966) to cover a wide range of morphological types. These included a) systems with both weak and well developed tidal tails, b) spiral galaxies with small compact companions (like M51), c) systems where one or both galaxies have a peculiar, disturbed appearance, d) pairs where both galaxies seemed almost identical, e) members of small groups, and f) a range of apparent closeness of interaction from systems which appear to be coalescing to widely separated pairs. Finally, the brighter examples of these types were chosen to try to ensure that they could be detected at L, in the absence of an excess, with reasonable integration times. Except for the few merging systems it is probable that the galaxies have at least one companion, even although this is not always shown in the photographs in the Arp Atlas. Physical association is indicated by the clear bridges of matter joining the galaxies, the lack of significant differences in their redshifts, and their apparent proximity. The maximum recessional velocity difference between a pair in the sample is ~ 600 kms^{-1} for Arp 120, which is of the order of the velocity dispersion observed in nearby clusters, and the mean is much

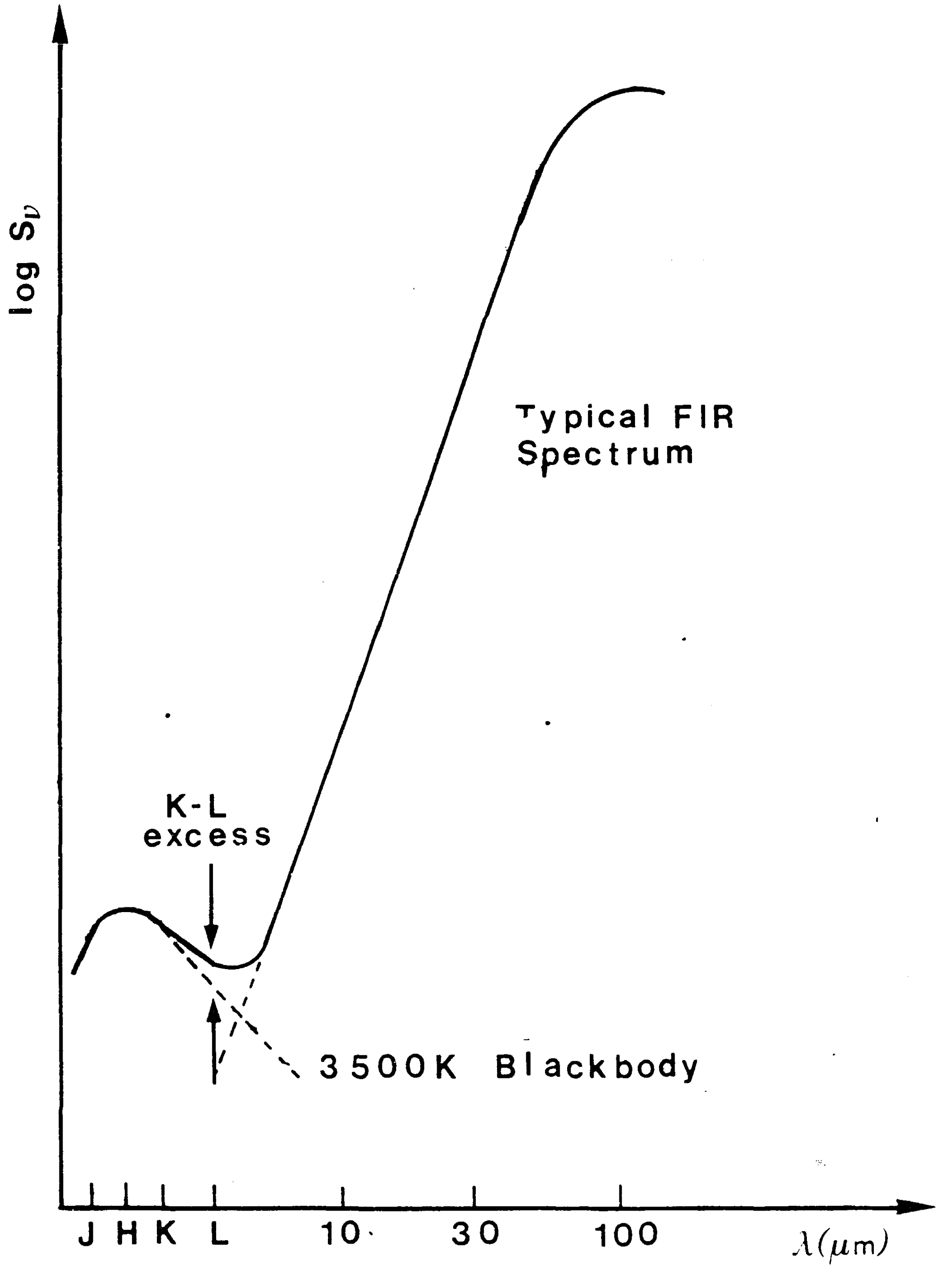

Figure 2.1 The relation between a red K-L colour index and a far-infrared excess.

smaller than this, ~ 150 kms^{-1}. The two galaxies for which companions are not secure because of the absence of velocity information are denoted by the comment "Probable pair with.." in Table 2.2.

The UK Infrared Telescope (UKIRT) was used during March and September 1982 to obtain JHKL (1.25, 1.65, 2.2, 3.45 μm) photometry for both members of 20 pairs of galaxies and for only one member of another 6 pairs. Since then a few more systems have been observed as "backup" or "filling in" objects on other observing runs. The galaxies were found using either the coordinates for optical nuclei published by Gallouet et al. (1971, 1973, 1975), or coordinates measured from the Palomar Sky Survey plates. The infrared signal was detected at K on the stripchart and the location where this signal peaked was found. Since the emission at K arises principally from old red stars, this position is most accurately the nucleus of the galaxy, ie. the centre of its potential well. In most cases this position coincided with the optically brightest spot to within the aperture used. Apertures of 12" were used in March 1982 while 8" apertures were used in September 1982 and for subsequent observations. Since the galaxies span a large range of angular sizes the use of different apertures does not affect comparisons between the data on different galaxies. Large chopper throws (60-100") were used to minimise contamination of the colours by disc material.

2.3 Data reduction

Several faint standard stars were observed frequently during each night to monitor changes in atmospheric extinction and/or instrumental sensitivity. These were selected from the lists of Elias & Frogel (1982) and the UKIRT calibration star sheets. From graphs of calibration magnitude as a function of airmass it was apparent that the stars BS4828 and BS6902 always gave inconsistent results, so these were not used to calibrate the data. Other scatter in the calibration data were due to variable weather and drifts in sensitivity. The galaxy photometry was therefore calibrated using a star which was observed close in time and airmass. In the few cases where this was not possible a star close in time was used together with the mean extinction law for the night. Photometry of the stars HD1160, GL105.5, BD+2.2957, BS9524, BS6353, BS1152 and BS4550 (with corrections for extinction where necessary) was used to calibrate the galaxy photometry.

The uncertainty in calibration was the main source of error in the JHK photometry, while the photometric precision at L was usually limited by the signal-to-noise ratio achieved. Generally the colours of the calibration stars remained consistent during a night even if their observed magnitudes varied, so the scatter around the mean airmass curves is an over estimate of the uncertainty in the colours. Depending on the quality of the night this scatter ranged from ~ 0.03 to ~ 0.2 magnitudes but was typically ~ 0.03-0.04 magnitudes. Errors in the J-H and H-K colours of the galaxies were also estimated by calibrating using the "next best" star, and by using the mean extinction curve for the night. Comparing these colours with those derived from the best estimate of the calibration gave a mean difference of ~ 0.025 magnitudes. The galaxy NGC 2798 was observed on two nights in 1982 March, thus giving another estimate of the reproducibility of the colours. The photometry for this galaxy is presented in Table 2.1, for both nights on which it was observed. The discrepencies in the J-H and H-K colours are ~ 0.09 and ~ 0.07 magnitudes respectively. Unfortunately the night of 16 March was not photometric and the calibration for this night is extremely poor, so this table should represent much larger uncertainties than normal. In fact no data taken on this night was used, and most of the discrepancy in the colours of NGC2798 is likely to be due to the poor photometry on the 16 March. Overall, the quality of the calibration suggests that the J-H and H-K colours of the galaxies are accurate to about 0.03 magnitudes. In April 1984 the galaxy NGC4438 was observed using UKIRT at JHKL' in an 8" aperture as part of another programme. The difference between these new measurements and the original photometry is ~ 0.05 magnitudes in J-H and ~ 0.01 magnitudes in H-K. A final estimate of the reproducibility of the photometry may be obtained by comparing the results of Lawrence et al. (1984) for NGC4438, NGC5929 & NGC5930 in a 6" aperture with our measurements for these galaxies. The mean colour differences are ~ 0.06 in J-H and ~ 0.03 in H-K, which are of the order of their quoted error estimates. Overall the estimate from the quality of the calibration curves that the J-H and H-K colours are typically known to ~ 0.03 magnitudes is consistent with these recent measurements. The error in K-L varies much more from galaxy to galaxy, depending on the signal to noise ratio achieved and is therefore quoted separately for each galaxy. Where high photometric precision was obtained the error in the colour due to systematic uncertaintities was estimated using the methods described above.

Table 2.1

Repeated Observations of NGC2798

Night(1982)	J	H	K	L	J-H	H-K	K-L
3 March	11.08	10.25	9.85	9.16	0.83	0.40	0.69
16 March	11.32	10.40	9.93	9.26	0.92	0.47	0.67

Galactic extinction corrections were applied using the cosecant law (Sandage 1973) and the van de Hulst reddening curve No.15 (Johnson 1968). Because of the small size of the extinction at infrared wavelengths uncertainties due to the choice of reddening law are much less than the photometric errors in the data. Corrections for flux in the reference beam and K-corrections have not been applied since these are both small compared to the photometric precision. The corrected photometric data is presented in Table 2.2, together with the recessional velocities of the galaxies and the error in the K-L colour.

2.4 Interpretation of the near-infrared colours

Near infrared colours can be usefully summarised in terms of JHK and HKL two-colour diagrams, and the distribution of the interacting galaxies in these diagrams is now discussed.

The data from Table 2.2 is plotted in a JHK colour-colour diagram in Figure 2.2 and in the HKL plane in Figure 2.3. Normal spiral nuclei are generally considered to have the colours

$$J-H = 0.7\pm0.1, \quad H-K = 0.3\pm0.1, \text{ and } K-L = 0.3\pm0.2$$

(cf. Johnson 1966, Sandage et al. 1969, Glass 1973, Allen 1976), and these regions of the two colour diagrams are outlined in Figures 2.2 and 2.3. Examination of these figures shows that the most striking feature of the data is that whereas nearly all the galaxies have approximately normal J-H, H-K colours, about half exhibit a distinct K-L excess, i.e. K-L $\geqq$ 0.5. This excess is unlikely to be a systematic effect due to the use of a fixed beam size, although this may play a small role in the

Table 2.2

JHKL observations of interacting galaxies

Arp Number	NGC/Other Identity	$V_o^{(1)}$	J	J-H	H-K	K-L	Aperture (arcsec)	Notes
318	0833		11.81	0.59	0.58	0.2 ± 0.2	8	
	0835		11.29	0.81	0.36	0.3 ± 0.1	8	
200	1134	3595	11.86	0.79	0.40	0.4 ± 0.1	8	Probable companion UGC 02362
186	1614	4643	11.80	0.75	0.60	1.1 ± 0.1	5	
243	2623	5355	13.30	0.76	0.83	0.8 ± 0.1	5	
143	2444	3994	11.86	0.79	0.22	0.3 ± 0.08	12	
	2445	4020	12.81	0.84	0.37	0.8 ± 0.2	12	IR source 3"E, 3"S of nucleus
82	2535	4016	12.84	0.71	0.25	0.3 ± 0.2	12	
	2536	4061	13.20	0.67	0.20	0.8 ± 0.2	12	
283	2798	1709	11.08	0.83	0.40	0.69 ± 0.04	12	(2)
	2799	1738	13.99	0.74	0.22	0.1 ± 0.4	12	
94	3226	1254	11.42	0.82	0.18	0.13 ± 0.06	12	
	3227	1050	10.74	0.86	0.43	0.81 ± 0.03	12	Seyfert Galaxy
270	3395	1595	12.57	0.59	0.43	0.4 ± 0.1	12	
	3396	1650	12.61	0.63	0.24	0.7 ± 0.1	12	
214	3718	1095	10.83	0.93	0.30	0.33 ± 0.03	12	Companion NGC 3729
294	3786	2745	11.88	0.79	0.39	0.63 ± 0.06	12	
	3788	2323	11.72	0.77	0.28	0.14 ± 0.06	12	
83	3799	3479	13.42	0.66	0.21	0.4 ± 0.2	8	
	3800	3462	12.53	0.75	0.37	0.6 ± 0.1	8	
244	4038	1447	11.86	0.79	0.34	0.3 ± 0.06	12	
	4039	1430	11.88	0.78	0.25	0.34 ± 0.06	12	
18	4088	822	11.67	0.83	0.35	0.62 ± 0.06	12	(2); Companion NGC 4085

Table 2.2 / contd.

Arp Number	NGC/Other Identity	V_o (1)	J	J-H	H-K	K-L	Aperture (arcsec)	Notes
120	4435	793	10.19	0.85	0.29	0.23 ± 0.03	12	
	4438	182	10.28	0.97	0.33	0.32 ± 0.02	12	
242	4676A	6631	12.58	0.77	0.67	0.6 ± 0.1	12	
	4676B	6590	12.48	0.80	0.27	0.1 ± 0.2	12	
193	I883	6942	13.20	0.99	0.60	1.7 ± 0.08	8	
240	5257	6791	12.59	0.82	0.35	0.4 ± 0.1	12	
	5258	6615	12.27	0.79	0.38	0.6 ± 0.1	12	(2)
239	5278	7710	12.84	0.72	0.33	0.15 ± 0.2	8	
	5279	7744	13.25	0.66	0.33	0.26 ± 0.15	8	
84	5394	3496	12.05	0.88	0.34	0.5 ± 0.1	12	
	5395	3505	12.21	0.84	0.25	0.1 ± 0.1	12	
271	5426	2296	11.97	0.73	0.28	0.3 ± 0.09	12	
	5427	2483	12.04	0.74	0.28	0.6 ± 0.1	12	
199	5544	3292	12.70	0.71	0.25	0.7 ± 0.2	12	
	5545	3302	12.98	0.74	0.33	0.3 ± 0.2	12	
297	5753		12.26	0.84	0.16	0.05 ± 0.1	12	(2); 2 galaxies in field of 4
	5755		13.17	0.96	0.33	0.69 ± 0.07	12	
90	5929	2696	11.97	0.83	0.27	0.4 ± 0.1	12	
	5930	2875	11.52	0.83	0.34	0.63 ± 0.06	12	
91	5954	2210			0.26	0.3 ± 0.2	8	K = 10.29; Companion 5953
220	I4553	5400	13.38	1.13	0.87	0.92 ± 0.05	5	
188	A1605+55		12.91	0.80	-0.39	0.1 ± 0.2	8	Probable companion MGC 09-26-54
209	6052	4821	13.40	0.61	0.32	0.58 ± 0.07	8	
	6240	7590	11.83	1.03	0.63	0.83 ± 0.03	8	
102	A1718+49B	7420	12.65	0.80	0.45	0.7 ± 0.2	8	Companion A1718+49A; Source 3"W of nuclei
93	7284		12.33	0.76	0.40	0.4 ± 0.3	8	
	7285		12.76	1.49	0.22	0.6 ± 0.2	8	

Table 2.2 / contd.

Arp Number	NGC/Other Identity	V_o (1)	J	J-H	H-K	K-L	Aperture (arcsec)	Notes
319	7318A	6976	12.16	0.73	0.31	0.2 ± 0.1	8	
	7318B	6011	12.64	0.65	0.35	0.1 ± 0.1	8	
	7319	6878	13.05	0.60	0.48	0.8 ± 0.1	8	
86	7752	5125	13.26	0.71	0.36	1.2 ± 0.4	8	
	7753	5328	12.64	0.85	0.38	0.4 ± 0.2	8	
112	7805	4948				0.3 ± 0.1	8	K = 10.8
	7806	4827			0.44	0.7 ± 0.1	8	K = 11.18

Notes

(1) Velocities from de Vaucouleurs et al. (1976) except for N2445 and N5395, from Botinelli et al (1982), N1134, N7805 and N7806 from Huchra et al, (1983) and I4553 from Soifer et al, (1984).

(2) Source was extended in North-South directions at K,

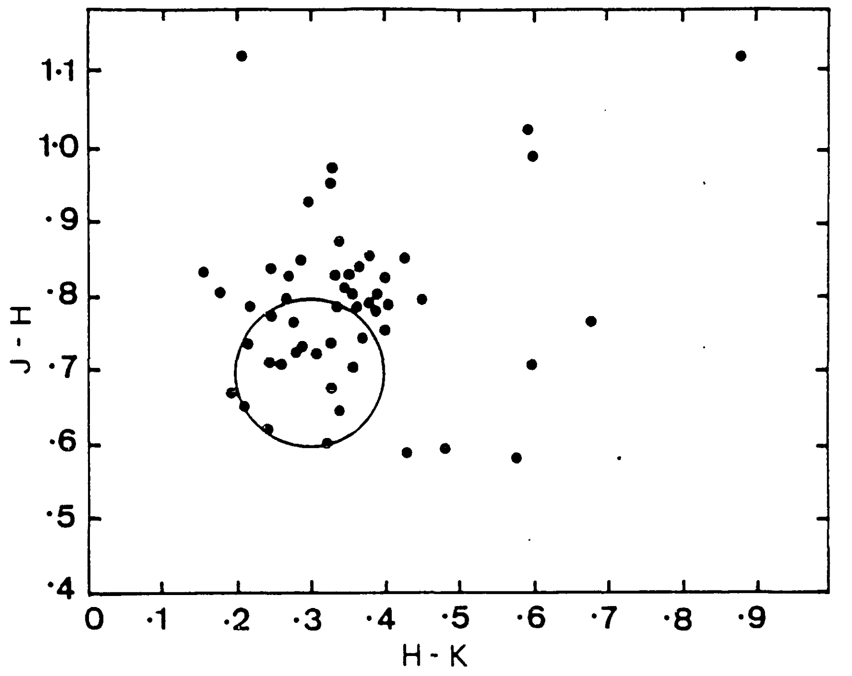

Figure 2.2 JHK two colour diagram for all the galaxies in Table 2.2. Normal galaxy colours lie within the circle.

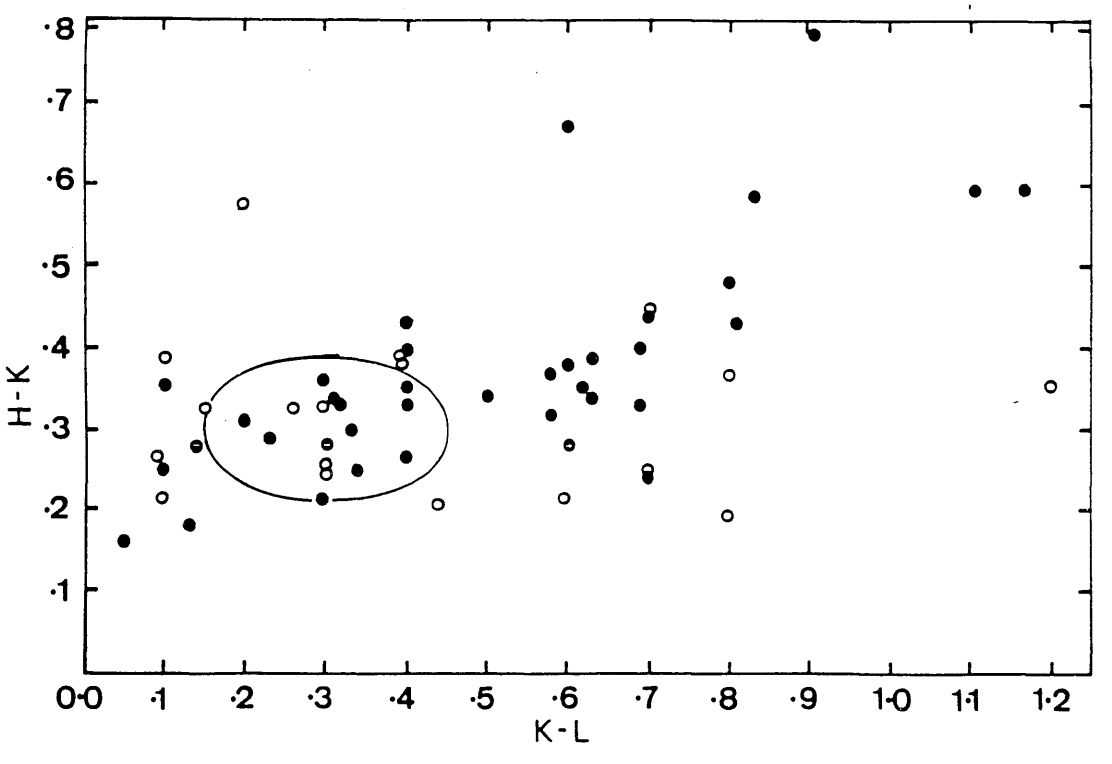

Figure 2.3 HKL colour-colour diagram for all the galaxies in Table 2.2. Normal galaxy colours lie within the ellipse. An open circle is used to indicate data with errors in K-L > 0.1.

figures. Typically the smaller the aperture relative to the galactic nucleus the redder the colour (e.g. Griersmith et al. 1982) but the red K-L colours are not limited to nearby or large galaxies. Thus the JHKL colours of the interacting galaxies show that in about half the sample there is excess emission over that of a normal stellar population. The astrophysical interpretation of this K-L excess is the subject of the rest of this section.

In the following paragraphs the constraints which can be placed on the astrophysical processes in these galaxies by their near infrared colours are discussed. The approach is to investigate the effect of important physical processes on the infrared colours of a normal galaxy and display the synthesised colours on JHK and HKL diagrams for comparison with the data. Model colours for internal reddening, power-law continua, free-free emission and thermal dust radiation added in varying proportions to the normal stellar emission of galaxies are described in turn below. These are then used in section 2.4.2, with additional data at radio wavelengths, to determine the most likely cause of the red K-L colours.

2.4.1 Model galaxy colours.

The effect of internal reddening on the galaxy colours was evaluated using the simple assumption that the standard Van de Hulst extinction curve was applicable. The effect on the colours of increasing extinction is shown as a line in Figures 2.4 and 2.5, where the tick marks represent increasing magnitudes of extinction at V.

Power law continua of the form $S_\nu \propto \nu^\alpha$ have been found in some Seyfert galaxies. Such emission might be expected if there were a collapsed object in the nucleus of a K-L excess galaxy, and the interaction were providing the fuel to "feed the monster" as suggested by Gunn (1979). When a power law of index α is added to the stellar emission from a galaxy, the A-L colour is given by

$$A-L = -2.5 \log_{10} \left\{ (1-x)\, 10^{-\frac{2}{5}(A-L)_s} + x \left({}^{\nu_A}\!/\!_{\nu_L} \right)^{\alpha} \, {}^{F_0(L)}\!/\!_{F_0(A)} \right\}$$

Where A is either J H or K, x is the fraction of the total flux at L arizing from the non-stellar component, α is the power law index, the subscript s denotes a normal population of stars, and $F_0(A)$ is the flux from a zero magnitude star at A. A power law of slope -1.5 was chosen to represent a putative non-thermal contribution to the IR emission from these galaxies because it typifies those Reike (1978) found for Seyfert 1 galaxies after subtracting the stellar continuum and also characterises the optical-infrared spectra of quasars.

Thermal bremsstrahlung emission from ionised gas may also contribute to the near-infrared colours of the galaxies. Since an optically thin free-free continuum can be aproximated by S_ν ~ constant, a mixture of normal stellar emission and free-free emission is a special case of the power-law mixture described above with $\alpha = 0$. The fraction of the total 3.5μm flux arizing from the free-free continuum, x, is indicated by the tick marks on the lines drawn in Figures 2.4 and 2.5.

Thermal emission from dust grains is one of the most common sources of infrared radiation in galactic nuclei (cf. Reike & Lebofsky 1979). Thermal spectra have the form

$$S_\nu \propto \alpha_\nu B_\nu(T) \; ,$$

where $B_\nu(T)$ is the Planck function, $\alpha_\nu \propto \nu^n$ and typically $0 \leqq n \leqq 2$. Broad band colours for dust emission added to a stellar continuum were calculated for black-body emissivity and several temperatures. The K-L colours for these mixtures are given by

$$K-L = -2.5 \log_{10} \left\{ (1-x)\, 10^{-2/5(K-L)_s} + x\, 10^{-2/5(K-L)_{BT}} \right\}$$

where the subcript s refers to the intrinsic colours of the stars, $(K-L)_{BT}$ is the K-L colour of a black-body of temperature T, and x is the fraction of the total 3.5μm light contributed by thermal emisson. H-L and J-L colours, and hence H-K and J-H, are computed similarly. The line drawn on Figure 2.5 corresponds to a temperature of ~ 300K. A steeper emissivity at a given temperature moves the peak of the spectrum to shorter wavelengths and would therefore tend to curve the line drawn on Figure 2.5 up and to the left, as would a higher temperature than ~ 450K. An equivalent line has not been drawn on Figure 2.4 because for these temperatures even if there is a large contribution to the L flux, the J-H and H-K colours are unaffected by the black-body emission. Much higher temperatures would be required. A temperature of ~ 300-400K should be representative of a typical contribution to the near-infrared colours from thermal dust emission, because it characterises the dust temperatures giving the observed continuum spectra of galaxies in the range 4-30μm.

2.4.2 The interpretation of the K-L excess

Distinguishing uniquely the nature of a near infrared excess from the JHK and HKL two colour diagrams alone is not possible. For example by adjusting the index of the power law contribution and/or the temperature of the thermal contribution lines drawn in Figure 2.5 these two lines can be made to coincide. However, given that representative parameters have been chosen, the diagrams can be used to establish the mechanism which is most likely to be the cause of the red K-L colours in the sample as a whole and then additional data may be used to substantiate this interpretation. In this section the capability of internal reddening, free-free emission, non-thermal emission, and thermal emission from dust, to explain the red K-L colours is evaluated by comparing the model galaxy colours drawn on Figures 2.4 and 2.5 with the distribution of the data points. Radio data for these galaxies is then used to further constrain the possible emission mechanisms.

Figures 2.4 and 2.5 show that although the J-H , H-K colours are scattered around the reddening line this is not the case for the H-K , K-L colours. It is clear from these figures that whereas most of the JHK colours are consistent with internal reddening alone, the HKL colours cannot be accounted for by this mechanism. Moreover Figure 2.6 shows that there is no correlation between galaxy inclination and K-L colour. This is in contrast to what might be expected if the K-L colour excess were due to internal reddening in the galaxies, since with increasing inclination a greater depth of obscuring material is in the line of sight to the nucleus. For Arp 242, the only galaxy whose HKL colours are close to the reddening line in Figure 2.5, the JHK colours indicate $A_V = 2$ at most, which is insufficient to account for the observed K-L colour. Since the red K-L colours cannot be accounted for by internal reddening alone they must be due to some non-stellar emisson process and the model lines for these are compared to the data in the following paragraph.

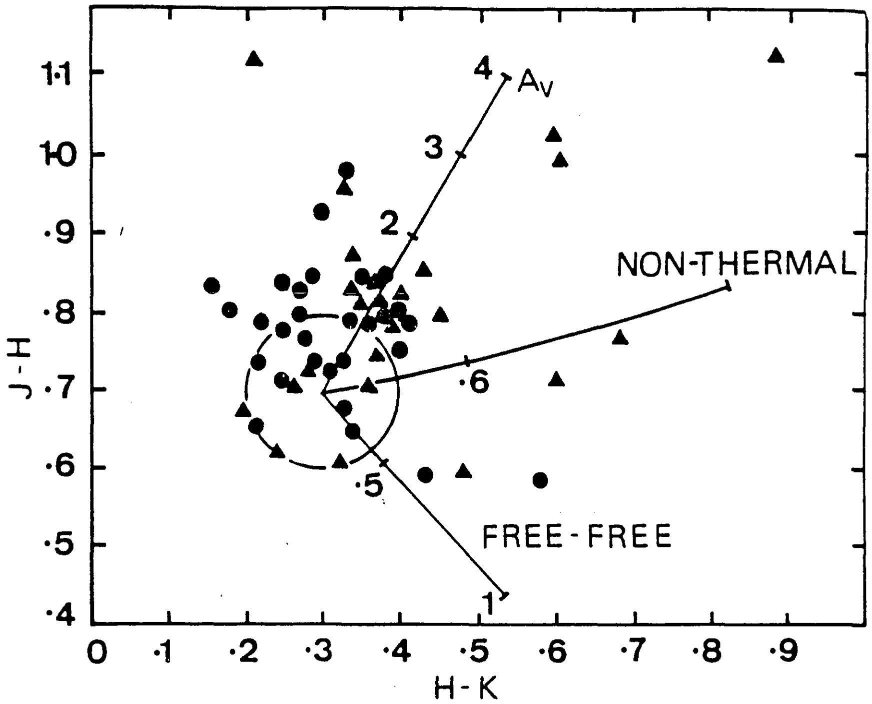

Figure 2.4 JHK colour-colour diagram comparing the colours of all the sample galaxies with the model galaxy colours of section 2.4.1. Tick marks on the reddening line indicate magnitudes of extinction at V. Tick marks on the free-free and non-thermal lines indicate the fraction of the total flux at **L** contributed by these components. A triangle is used to indicate galaxies for which the K-L colour is greater than 0.5.

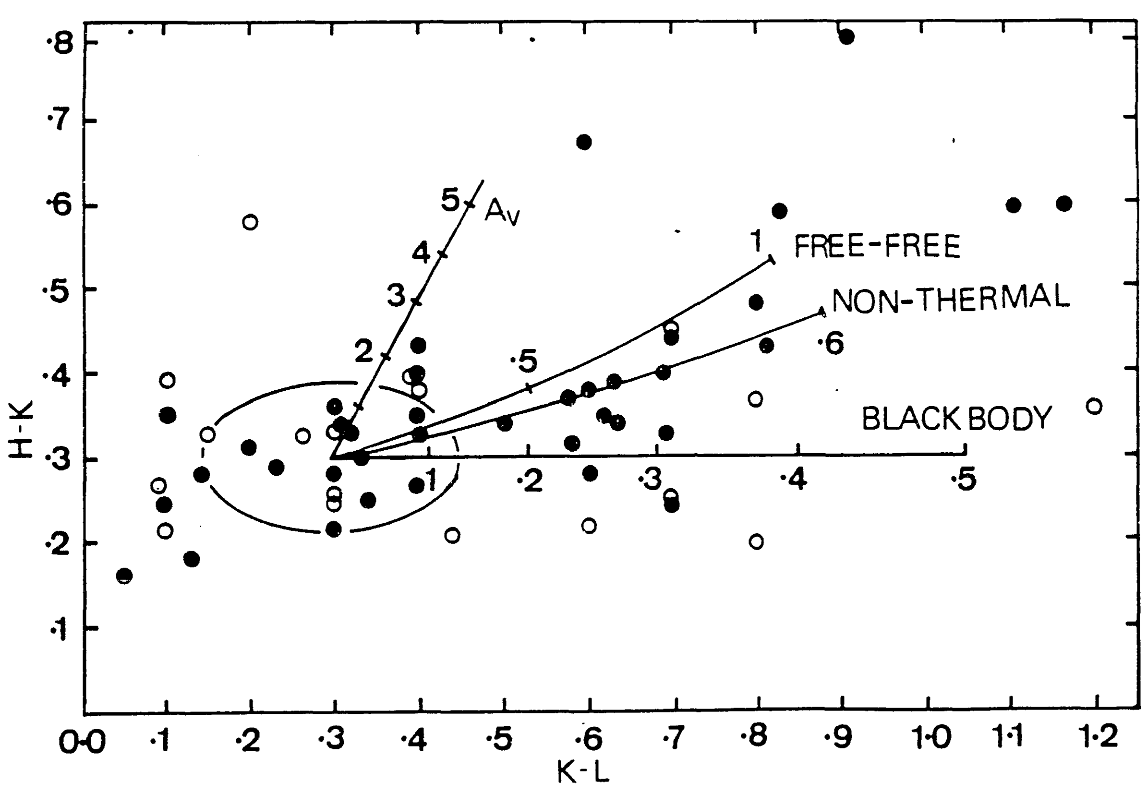

Figure 2.5 HKL two colour diagram comparing the colours of the galaxies in Table 2.2 with the model colours of section 2.4.1. Tick marks on the reddening line indicate magnitudes of extinction at V. Tick marks on the free-free, blackbody and non-thermal lines show the fraction of the total L flux contributed by these components. Data for which the error in K-L is > 0.1 is indicated by an open circle.

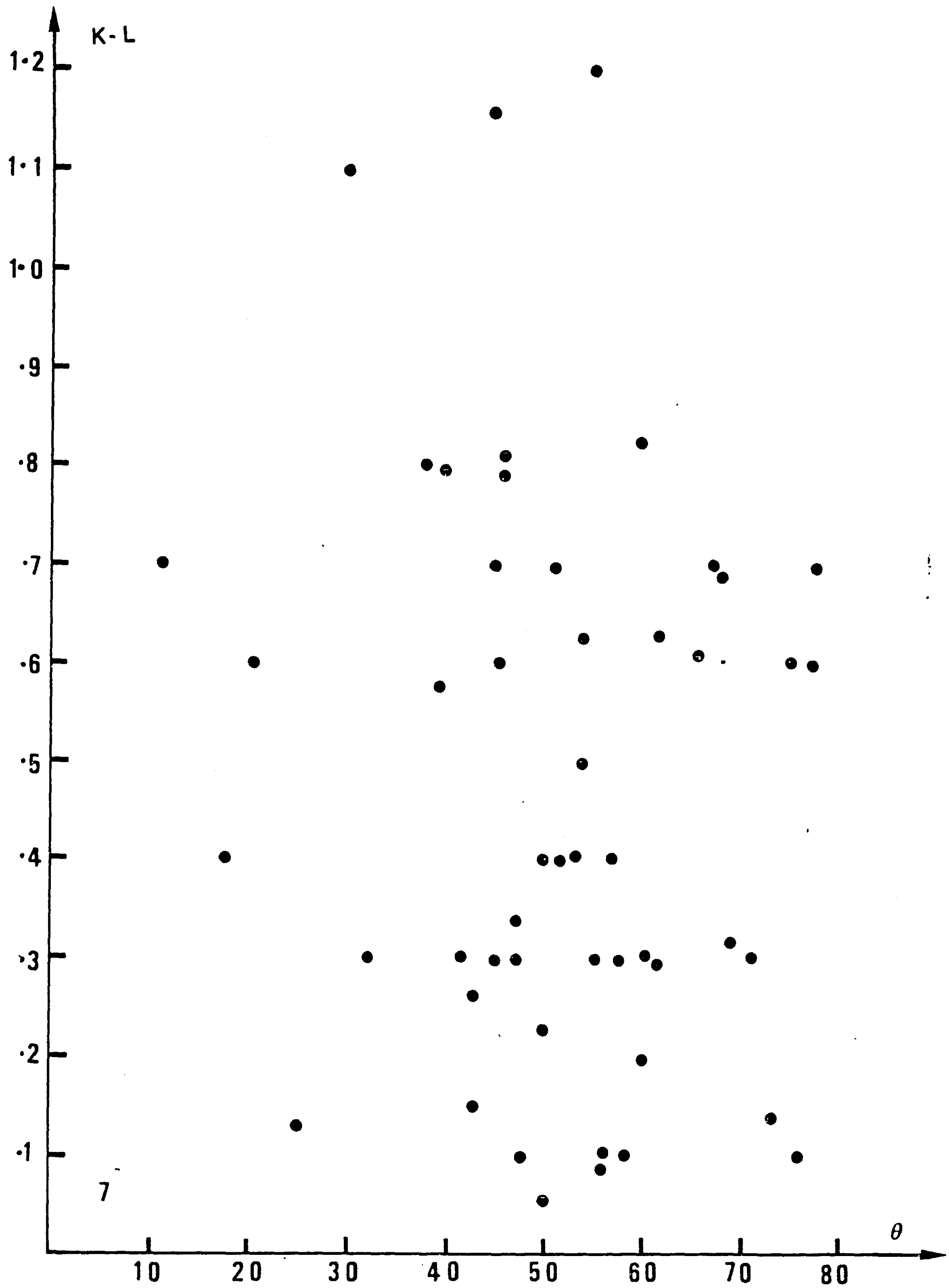

Figure 2.6 K-L colour as a function of galaxy inclination. The inclination angle, θ, was estimated from the axial ratios given in de Vaucoleurs, de Vaucoleurs and Corwin (1976).

Firstly the data in Figure 2.5 is scattered randomly around the "black-body" line and tends to lie below the non-thermal and free-free lines. Although a few galaxy colours lie close to the latter two lines, in general these mechanisms result in H-K colours significantly redder than normal, unlike the interacting galaxy sample for which the mean H-K colour is 0.35 ± 0.08. Secondly a sufficient contribution from free-free or non-thermal emission to give the observed K-L colours would result in a distribution of JHK colours significantly different from that in Figure 2.4. The few galaxies whose colours lie close to the free-free and non-thermal lines in the JHK plane do not have consistent K-L colours. Thirdly given that the JHK colours in general indicate the presence of 1-2 magnitudes of reddening, it is clear that the non-thermal and free-free lines do not fit the HKL colours of the interacting galaxies particularily well. Thus comparision of the data with simple models of possible emission mechanisms in these galaxies in Figures 2.4 and 2.5 suggests that the best interpretation of the K-L excesses is that they arise from the addition of warm thermal emission to the stellar spectrum exhibited by normal galaxies in the JHKL wavebands.

This qualitative conclusion can be greatly strengthened, both for individual galaxies whose colours lie close to the non-thermal or free-free lines on the HKL plane and for the whole sample, by the consideration of the radio emission from these galaxies. The constraints which are placed on the contributions from non-thermal and free-free emission in these galaxies by their observed radio flux densities and spectral indices are now discussed.

The radio data presented in Table 2.3 provide a further argument that non-thermal emission is unlikely to account for most of the K-L excesses observed. Limits to any contribution to the 3.5μm flux density from the same source responsible for the non-thermal radio emission can be obtained by extrapolating the radio measurements to the infrared. For six of the K-L excess galaxies radio measurements with angular resolution sufficient to distinguish between the pair of galaxies exist in the literature. This data is supplemented by radio flux densities, or upper limits, and spectral indices for 13 K-L excess galaxies which are unresolved from their companions. The spectral indices were used to extrapolate all of these radio flux densities to 3.5μm. An index of -0.7 was adopted where no spectral index has been measured. Also given in

Table 2.3

Estimated limits to a non-thermal L excess

Galaxy*	Frequency MHz	Flux mJy	Spectral* Index	Extrapolated L Flux (mJy)	Observed L Excess (mJy)
N2798	2695	66[1]	-0.6	0.13	32
N3227	2695	54[1]	-0.7	0.04	51
N5930	2695	40[1]	-1.0	0.001	19
N5394	2695	18[1]	-0.6	0.035	10.8
N2445	1415	20[2]	(-0.7)	0.009	5.5
N4676	1415	21[2]	(-0.7)	0.009	7.8
N6240	1413	230[8]	-0.85	0.02	22
Arp193	5000	34[5]	-0.7	0.04	11
Arp220	2380	312[9]	-0.6	0.5	9
Arp240	2695	40[1]	-0.78	0.012	6
Arp18	4800	84[3]	-0.77	0.044	11.2
Arp270	1400	123[4]	-0.93	0.004	2.9
Arp86	5000	32[5]	-0.76	0.02	4.4
Arp102	5000	96[6]	-0.82	0.03	5.5
Arp319	1400	100[5]	-1.38	2×10^{-4}	4.7
Arp271	1415	10[7]	(-0.7)	0.004	4.8
Arp294	5000	<0.05[5]	(-0.7)	<0.05	8.5
Arp83	2700	<0.06[5]	(-0.7)	<0.04	3.5
Arp112	2700	<0.05[5]	(-0.7)	<0.03	7

Notes

* For galaxies identified by an Arp number the radio flux is the total for the pair. Bracketts denote an assumed radio spectral index.

References

1) Stocke et al. (1978)
2) Burke and Miley (1973)
3) Gioia et al. (197?)
4) Klein et al. (1983)
5) Sulentic (1976)
6) Stocke (1978)
7) Hummel (1981)
8) Condon et al. (1982)
9) Condon (1980)

Table 2.3 is the excess flux at 3.5μm which is needed to account for the K-L colours, calculated by assuming that the stellar contribution at L corresponds to K-L = 0.3. It is evident from Table 2.3 that the 3.5μm flux densities derived from extrapolating the radio measurements are too small by factors of 200-10,000 to account for the excess over a ~ 3500K blackbody which is present in these galaxies. In fact this limit is even stronger because the continuum spectra of non-thermal extragalactic sources generally steepen between the radio and infrared. Table 2.3 includes radio measurements or upper limits for all of the galaxies which lie close to the non-thermal line in Figure 2.5. Thus if the K-L excesses are due to a non-thermal component in the near infrared it cannot be simply related to the non-thermal radio emission and the spectrum must have a rather contrived shape. Together with the fact that the "non-thermal" line in Figure 2.5 does not fit the data very well, this suggests most strongly that non-thermal emission cannot account for the majority of the K-L excesses.

Limits to the free-free flux density at 3.5μm can similarly be derived from the radio data e.g. for the six resolved pairs listed in Table 2.4. This data is listed in Table 2.4 with the angular size of the radio source and the observed flux density at L. As the table shows, the nuclear radio sources have angular sizes comparable to the apertures used for the infrared measurements. Since the radio spectra are generally non-thermal any free-free emission must be a small fraction of the radio flux densities listed in Table 2.4. For a plasma of temperature T the free-free absorption coefficient is

$$\alpha_\nu \propto \nu^{-2}\, g_\nu(T),$$

where $g_\nu(T)$ is the Gaunt factor. So, the infrared and radio free-free emission from an optically thin plasma are related by

$$S_\nu \propto \nu^{-2}\, g_\nu(T)\, B_\nu(T)$$

If $h\nu \ll kT$, $$S_\nu \propto g_\nu(T) = \ln\left[4.95\times10^{7}\,(T^{3/2}/\nu)\right]$$

Assuming a temperature T ~ 2 × 10^4K the free-free flux density at 2695MHz should be ~ 20 times the free-free flux at 3.5μm. Comparison of the radio and infrared flux densities in Table 2.4 shows that any infrared free-free emission must be ≦ $1/20$ of the total flux at L for these six K-L galaxies. Clearly this is neglible compared to the ~ 50% of the total L flux which from Figure 2.5 must be free-free emission if this mechanism is to account for the K-L colours. This result, which includes two of the four galaxies lying closest to the free-free line in figure 2.5, N2798 & N3227, is likely to typify the entire K-L excess group (cf. Table 2.3). In conclusion, these limits and the poor fit of the "free-free" line to the data in Figures 2.4 and 2.5 show that free-free emission does not make a significant contribution to the observed K-L excesses.

Table 2.4
Radio data for pairs with a K-L excess

Arp number	NGC	K-L	Radio flux density (mJy)	Radio spectral index	Radio size (arcsec)	3.5μm Flux density (mJy)
143	2445	0.8	20[1]		< 22	12
	2444	0.3	< 6			
283	2798	0.7	66[2]	-0.6	2.5x2.5	54
	2799	0.1	<20			
94	3227	0.8	54[2]	-0.7	3 x 3	87
	3226	0.3	20			
242	4676A	0.6	21[1]		< 22	15
	4676B	0.1	5			
84	5394	0.5	18[2]	-0.6	5 x 6	20
	5395	0.1	<20[3]			
90	5930	0.6	40[2]	-1.0	3 x 5	32
	5929	0.4	23			

Notes
1 Radio data at 1415MHz from Burke & Miley (1973)
2 Radio data at 2695MHz from Stocke et al. (1978)
3 Radio upper limit at 1415MHz from Hummel (1981)

Since the radio emission from these interacting galaxies has been used to confirm the earlier conclusion that neither free-free emission nor non-thermal radiation can explain the red K-L colours, the remaining possibility is that, as previously suggested, the K-L excesses are due to thermal emission from dust. This interpretation is now examined in more detail.

Thermal IR emission from galaxies is commonly interpreted as indicating recent star formation, since it is also observed from HII regions in our galaxy. If the K-L excess galaxies have experienced recent bursts of star formation and the stellar radiation from hot young stars is thermalised by dust and reradiated in the FIR, then their spectra should be similar to those of well known "infrared" galaxies. A K-L excess is then due to the addition of a warm, luminous quasi-thermal spectrum to the normal stellar spectrum, which, as found above, is the best explanation of the K-L excesses in these interacting galaxies. If this interpretation of the K-L excesses is correct, and a K-L excess indicates that recent bursts of star formation have occurred in the nuclei of these galaxies, then there should be evidence of this activity at other wavelengths. The radio data in Table 2.4 provides one example supporting this interpretation. For all six pairs of interacting galaxies it is the K-L excess galaxy which is the brighter radio source in the pair. The radio luminosities of the bright components are comparable to those of radio-bright spirals (Condon et al. 1982) and they also exhibit similar non-thermal spectra. These features have been interpreted by Condon et al. as resulting from the high rate of supernovae and consequent supernova remnants associated with bursts of star formation. Thus the correlation of K-L excesses with bright radio emission further confirms the interpretation of a K-L excess as evidence of a recent burst of star formation.

In conclusion, about half the interacting galaxy sample have a K-L colour significantly redder than normal. The most plausible interpretation of this K-L excess is that it is the result of thermal emission from dust heated by the early type stars produced in a recent burst of star formation.

2.5 Relations between morphology and recent star formation.

In section 2.4 the K-L excesses present in about half the programme galaxies are interpreted as evidence that they have experienced recent bursts of star formation. The occurence of K-L excesses in the various types of interacting systems is now examined, to explore possible relations between the morphology of the interaction and recent star formation. These features are then related to the physical picture of interactions that emerges from the dynamical studies of Toomre and Toomre (1972) and Wright (1972).

2.5.1 Star formation in all types of pairs of galaxies.

The data in Table 2.2 includes JHKL photometry for both members of 22 pairs of galaxies. The HKL colours of these galaxies are shown in Figure 2.7, where the members of each pair are identified by their number in the Arp Atlas. Examination of this figure shows that for 18 of the 22 pairs one galaxy has a K-L excess and the other member of the pair has a normal K-L colour. Most importantly, in no case have **both** galaxies in an interacting pair shown a K-L excess. This is very striking in several systems in which both galaxies are remarkably similar in morphology and size e.g. Arp271 and Arp240. The radio measurements presented in table 2.4, if interpreted as in section 2.4.2, also suggest that there is more star formation in one member of a pair than the other. In every case there is at least a factor of 2 difference in radio flux density between the two galaxies in a pair. There are in the literature two cases in which both galaxies in a pair show strong infrared excesses NGC3690/IC694 (Allen 1976) and NGC5253/5236 (Glass 1973), and there are two K-L excess galaxies in this survey for which the colour of the companion was not measured. Never-the-less, the HKL colours of this comprehensive sample show most clearly that a characteristic of interacting pairs is that there is usually much more star formation in the nucleus of one member of the pair than the other.

This feature of the results can be understood on the basis of the numerical studies of Toomre and Toomre (1972) and Wright (1972). As emphasised in section 1.3.1 these show that during a close encounter material is redisributed between and within the galaxies, often far enough into the nuclear region to fuel a burst of star formation. However, the amount of disruption is critically dependant on the spin of the protagonists relative to the system angular momentum and on the inclination of their spin planes to the system orbital plane. Maximum tidal disruption and transfer of material occurs when a galaxy orbits its companion in the same plane and sense of direction as the rotation of the companion. Since in any arbitrary interaction between two galaxies conditions close to these are more likely to be met for one galaxy than for the other, it is not surprising that a burst of star formation preferentially appears in one member of the pair.

If recent star formation is triggered by the interaction then the

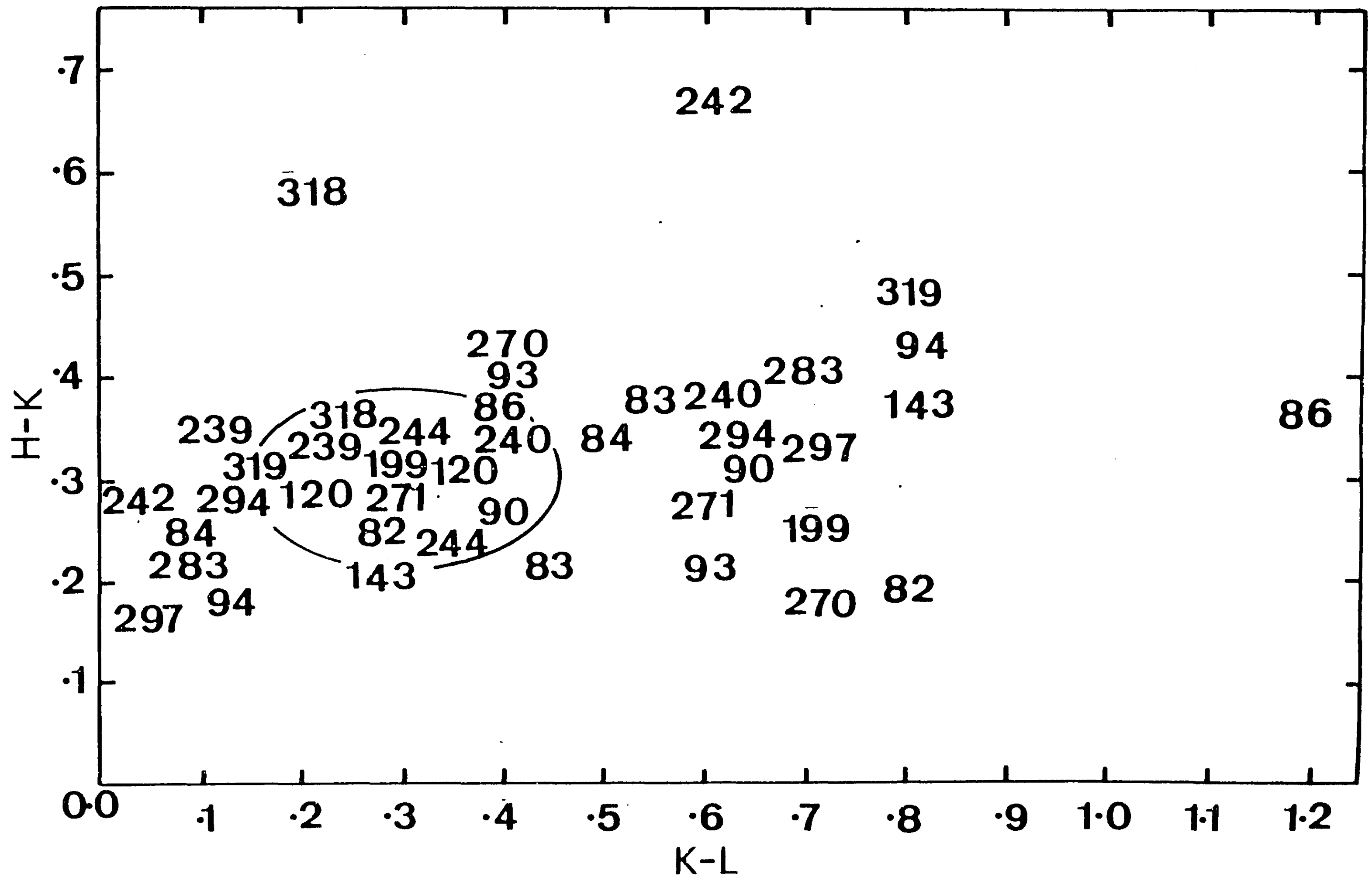

Figure 2.7 HKL colour-colour diagram for 22 pairs of galaxies. The members of each pair are identified by their number in the Arp (1966) Atlas.

amount of star formation may depend on how closely the galaxies interact. Some evidence for this is apparent in a study of ~ 600 pairs of galaxies selected from Karachentsev's (1972) Catalogue of isolated pairs of galaxies at 2695 and 5000MHz (Stocke 1978), where there is a correlation between the physical separation of the pair and radio detection percentage. The closer a pair the more likely it is to be a radio source. Stocke suggests that the effect can be understood if transfer of material between the galaxies fuels a starburst or accretion onto a collapsed object. In view of these results it is important to test whether the K-L colours of this sample of interacting galaxies show a similar effect. Figure 2.8 is a graph of separation (in Kpc) against K-L colour of the redder galaxy in each pair. It is obvious from this figure that despite a range of more than an order of magnitude in separation, there is no significant trend in the K-L colours. A K-L colour is a measure of the amount of excess emission, normalised to the brightness of the stellar component. It may be that the amount of excess, which must be some function of the number of young stars, rather than the relative excess depends on the separation of the galaxies and some systematic effect e.g. the brighter galaxies being the closest pairs, is masking the relationship for K-L colours. However, Figure 2.9 shows that there are no trends in L excess as a function of separation for these galaxies. A more physically meaningful parameter should be the separation of the pair relative to the size of the galaxies. L excess is plotted as a function of the separation of the pair in units of the major diameter of the larger galaxy as catalogued in de Vaucouleurs et al. (1976) in Figure 2.10. Again, no correlation is apparent. Some of the possible explanations of this apparent contradiction are discussed in the following paragraph.

One of the major differences between this IR survey and that described above is that nearly all of the galaxies show infrared excesses whereas only about half of the radio sample is "active". The latter sample includes more wide pairs of otherwise normal galaxies than the IR sample which is composed pairs with morphological features indicating interaction between the galaxies. The infrared sample therefore consists entirely of galaxies in which the conditions conducive to transfer of material to fuel star formation are likely to exist. Although the separation of a pair may be a crude measure of the strength of the tidal effect for widely spaced pairs, for pairs which

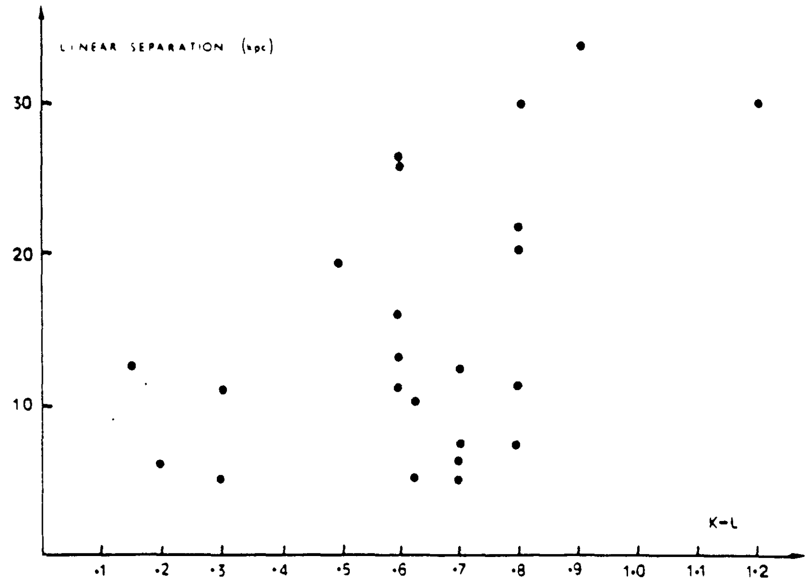

Figure 2.8 Linear separation of pairs of galaxies against the K-L colour of the reddest galaxy.

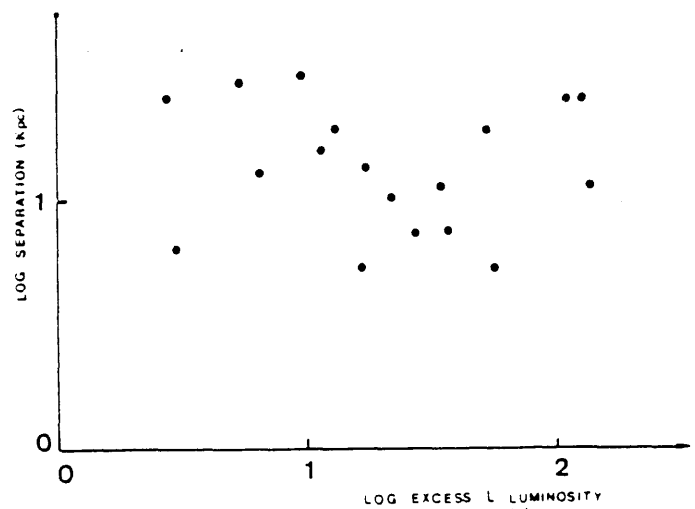

Figure 2.9 Linear separation of pairs of galaxies against excess luminosity at L.

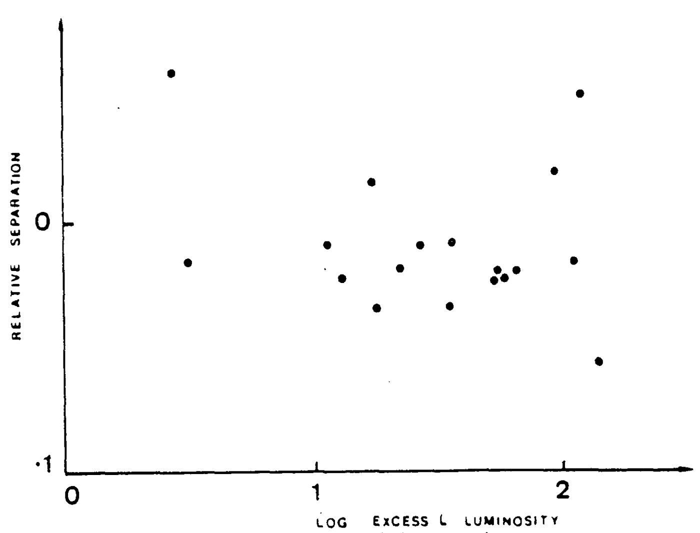

Figure 2.10 Graph showing the relative separation of pairs of galaxies against the excess luminosity at L.

are already interacting closely enough to cause tidal disturbances the amount of induced star formation is likely to depend more on the detailed parameters of the interaction, such as the relative inclinations of the galaxies. Finally, it may be that neither a K-L colour nor an L excess is a sufficiently sensitive measure of the intensity of a starburst to reflect subtle differences in the star formtion activity with the separation of the interaction.

2.5.2 Starbursts in pairs with well-developed "tails"

Another subset of the programme galaxies comprises those with long tidal tails. It is interesting to study the incidence of recent star formation in these pairs because, from the dynamical models, well-developed tidal tails indicate that the interaction must be at an advanced stage. The criterion for membership of this class is, however, somewhat subjective. Systems have been included if they have one or more "tails" whose length is at least twice the galaxy diameter and which seem to be unbound, in contrast to what appear to be loosely-wound spiral arms. The 7 systems (13 galaxies) fitting this criterion, including two marginal cases, are plotted in the HKL plane in Figure 2.11. Galaxies which do not have a tail themselves were included in the figure if they are paired with a companion which does have a well developed tail. This figure shows that for four of the seven pairs of galaxies with tails, one member of the pair has a K-L excess and evidently has a starburst nucleus.

The fact that a significant number of the galaxies in systems with well-developed tidal tails exhibit a K-L excess suggests immediatly that either a starburst can have a duration as long as the time required to develop a tail, or that starbursts may be delayed, or both. Toomre and Toomre (1972) and Wright (1972) find that tail-building requires a period ~ 10^8 years from the time when morphological disturbances first become apparent and that the tails can persist for ~ 10^9 years. Larson and Tinsley (1978) and Reike et al. (1980) found that the durations of model starbursts which best fit their data were generally < 10^8 years. This suggests that starburst activity has been delayed in some of the systems which we observed. These times also suggest that in the systems with tidal tails but without K-L excesses it is possible for any starburst activity to have died out.

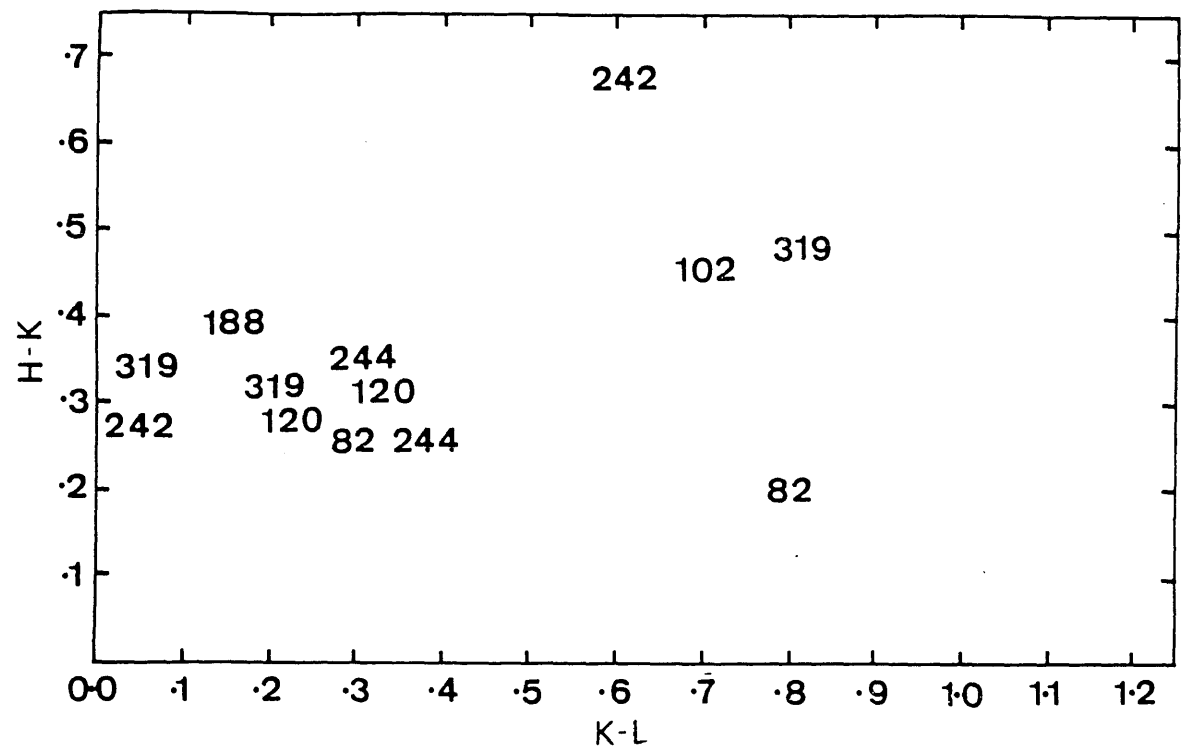

Figure 2.11 HKL colour-colour diagram for systems with well developed tidal tails. The galaxies are identified by their Arp numbers.

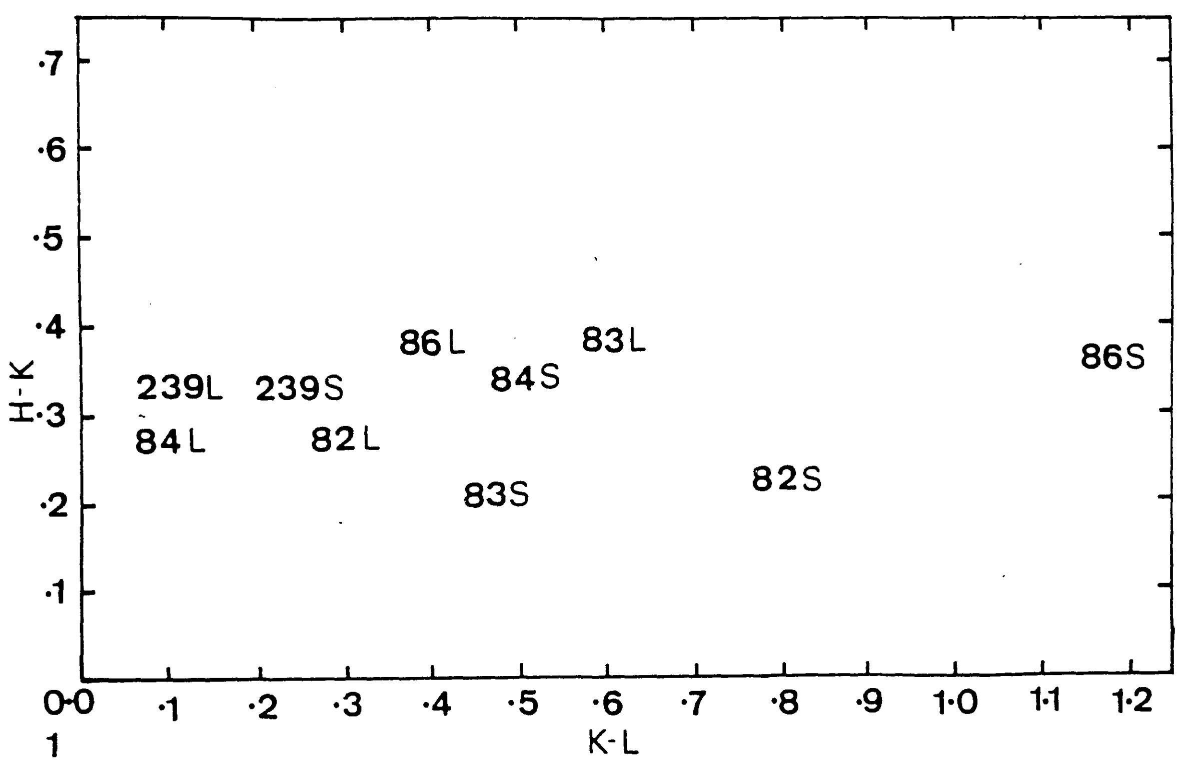

Figure 2.12 HKL two colour diagram for M51-like pairs. Arp numbers are followed by the letters L and S to denote the large and small member respectively.

2.5.3 Starbursts in "M51" types

The HKL colours for five "M51-like" pairs of galaxies in the sample, those with a compact companion at the end of one arm of a large spiral galaxy, are presented in Figure 2.12. The letters **L** and **S** denote the large and small members of each pair. In four of these systems one galaxy has a K-L excess and in three of these it is the compact companion which has the K-L excess. This is unlikely to be an aperture effect since one expects that the larger the aperture, relative to the galactic nucleus, the bluer the colour (e.g. Griersmith, Hyland and Jones 1982). Thus for this admittedly small statistical sample a burst of star formation seems to be preferentialy triggered in the small companion.

M51 itself may be showing similar behaviour. The smaller companion, NGC 5195, has a K-L colour of 0.5 (Penston 1973) whereas the colour of the nuclues of M51 itself is K-L = 0.3 (Ellis, Gondhalekar and Efstathiou 1982). The M/L ratio of the nucleus of M51 is 3 (Telesco and Harper 1980), which although it does not indicate an intense short lived starburst, it is not inconsistent with the presence of more young stars than normal. M51 is a strong infrared source and has been mapped at 2μm and 10μm by Telesco (1984) and in the far-infrared by Telesco and Harper (1980) and Smith (1982). The major result of these studies is that low surface brightness thermal emission from M51 extends over $\geqq$ 3kpc. Telesco (1984) shows that the 10μm luminosity is powered by large numbers of young stars and that it tends to coincide with the many bright HII regions and dust lanes seen in optical pictures of M51. Overall however, although M51 is very luminous ($\sim 10^{10}\ L_{\odot}$) these results do not show the centrally concentrated luminuos nuclear emission seen in starburst galaxies like NGC253. In NGC5195 there seems to be more evidence for a nuclear starburst. Firstly, taking the estimate of Smith (1982) for the total luminosity of NGC5195, $\sim 5 \times 10^{9}\ L_{\odot}$, and the rotation curve of Schweizer(1977) to give an estimate of the mass, $3 \times 10^{9}\ M_{\odot}$, its M/L ratio is ~ 0.4, which is likely to indicate a recent burst of star formation (c.f. section 1.2.3). Secondly, Smith (1982) derives a dust temperature of ~ 70K in NGC5195, similar to that found in other starburst galaxies and his map shows that the emission from NGC5195 is more centralised than that from M51. Taken together these points strongly suggest that a recent burst of star formation is occuring in the compact companion but not in the nucleus of the larger galaxy of the pair.

That the starburst occurs preferentially in the compact companion can be qualitatively understood in terms of how tightly material is bound in the two galaxies. Material in the outer regions of the larger galaxy will be relatively more loosely bound, and it is therefore more likely to be stripped and captured by the companion. This effect has appeared in the Toomre and Toomre (1972) simulation of an interaction between a disc of particles and a compact companion of smaller mass. Wright (1972) makes a related point when he notes that the disruption caused by the larger galaxy on the smaller is much less than vice-versa. In terms of its own radius the small galaxy is relatively further away from the large one and so is more likely to gain material than to lose it in the interaction. The extensive luminous material spread around the companion to M51 (van den Bergh 1969) has been interpreted as observational confirmation of these features of the dynamical models of M51-type systems.

2.5.4 Frequency of starbursts in interacting galaxies

As noted in section 2.5.1 for 18 out of 22 pairs one galaxy has a K-L excess and the other member has not. Of the remaining 11 systems observed, K-L excesses were found for 7 galaxies, although they either do not have a companion or it was unobserved. For the other 4 cases there was no K-L excess in the galaxy observed but since the companion was unobserved this does not imply that there is no K-L excess in these pairs. Overall therefore, a K-L excess was found for 25 out of 33 interacting systems studied. This suggests a frequency of starbursts in these interacting systems of ~ 80%. This sample is highly selective in the sense that spectacularly disturbed systems were chosen for the survey. However it was selected without prior knowledge of any previous records of activity in these systems and it should therefore be representative of the activity characteristics of strongly interacting galaxies. To the extent to which this is true, the JHKL survey shows that interactions may be very efficient triggers of IR activity in galaxies. The frequency with which starbursts are triggered by extreme interactions could even be higher than 80%. Three of the five systems in which no K-L excesses were found (Arps 244,120 and 188) have well-developed tidal tails. As discussed in section 2.5.2, this could indicate that the interaction is sufficiently old that any evidence of a starburst would have faded away. In conclusion, this survey of interacting galaxies suggests that interactions which cause strong morphological distortions are extremely efficient in triggering bursts of star formation in interacting galaxies.

2.6 Summary and conclusions

In a survey at JHKL of 55 interacting galaxies of various types about half the galaxies were found to have a K-L colour significantly redder than normal galaxy colours. From the distribution of the near infrared colours in the JHK and HKL planes, supplemented by constraints derived from radio measurements, the K-L excesses were found to be due to the addition of luminous thermal emission to the stellar spectrum exhibited by normal galaxies. The most plausible nature of this thermal component is that it arises from dust heated by young stars produced in a recent burst of star formation, since the emisson from the nuclei of similar infrared galaxies galaxies such as M82 are thought to be due to recent bursts of star formation. Additionally for at least six of the K-L excess galaxies bright non-thermal radio emission may be interpreted as due to a high rate of supernovae, thereby supporting the correlation between a K-L excess and a burst of star formation.

The major result of the survey is that starbursts could be triggered by interactions with an efficiency of almost 100%. A prominent feature of the data is that starbursts are only found in one member of each interacting pair in the sample. The occurence of recent star formation in different morphological types of interacting galaxy is physically consistent with the dynamical studies of interacting systems. The data also suggest that two other features which may characterise interaction induced starbursts are a delay of ~ 10^8 years in the starburst activity after the time of closest approach in some systems, and a tendency for the small companion in M51 like systems to be more likely to undergo a burst of star formation than vice-versa.

Clearly further infrared observations at longer wavelengths are required to confirm and quantify these strong indications of recent star formation in interacting galaxies. By observing the galaxies in the mid infrared more detailed parameters of the starbursts, such as star formation rates and mass-luminosity ratios may be derived. Starbursts driven by interactions between galaxies can then be directly compared to the starbursts seen in other galaxies. Follow up observations at 10 and 20μm of several of the interacting galaxies are discussed in Chapter 3.

CHAPTER 3

10 MICRON OBSERVATIONS OF INTERACTING GALAXIES

3.1 Rationale for longer wavelength observations

The major result of the survey described in Chapter 2 was that one member of nearly every pair of interacting galaxies observed showed a K-L colour significantly redder than normal galaxy colours, as would be expected if there were a large far-infrared excess due to a recent burst of star-formation. The advantage of carrying out a survey of IR activity by using near-infrared colours is that good signal-to-noise can be obtained in a relatively short observation time and so a large number of objects can be covered. However, the major disadvantage is that the near-infrared colours can provide only qualitative information about the luminosities and emission processes. Observations at longer wavelengths are needed to confirm and quantify the nuclear activity inferred from the JHKL survey, and to further constrain the interpretation of this activity as due to a massive burst of star-formation. The principal uses of 10 and 20μm photometry are briefly described below.

For star-forming regions in our galaxy, much (often all) of the luminosity of the young stars is reradiated at IR wavelengths by dust. Determination of the IR luminosity is therefore vital to establish the intensity of the star-formation activity. Although most of the IR luminosity is generally emitted at $\lambda \geqq 30\mu m$, reasonable estimates can be made by extrapolating from shorter (10-20μm) wavelength measurements (cf. Telesco 1984). Dust can also reradiate the energy from non-thermal activity in a nucleus, powered by accretion onto a compact object, in the IR. These two possible energy sources for the IR luminosity can be discriminated by measuring the spatial extent of the mid-IR emission. For a single compact object heating a dust cloud, the temperature will decrease rapidly with increasing distance from the source and the more distant dust therefore radiates at longer wavelengths. By comparison, star-forming regions are extended, with luminosity sources distributed over several hundred parsecs, and the dust will therefore radiate in the mid-IR over a larger region.

In this chapter the results of 10 and 20μm photometry of some of the galaxies in the K-L survey are presented. This data is supplemented by observations from the literature for galaxies in the K-L sample and similar interacting galaxies in order to provide as comprehensive an overview as possible of the mid-IR activity in interacting galaxies. The extent to which mid-IR nuclear photometry confirms the JHKL survey results is examined and then observations of the extent of the IR emission, as well as data at optical and radio wavelengths, are used to examine the emission mechanisms and energy sources in these galaxies. Interaction-induced activity is compared quantitatively with activity in other galaxies and the extent to which the strength of the interaction influences the magnitude of the activity is discussed. Finally, the data are used to develop a self-consistent picture of star-formation processes in this sample of interacting galaxies.

3.2 Observations and data reduction

The galaxies were chosen from the JHKL survey with priority being given to those galaxies which were brightest at L, because sensitivity at 10μm is sufficiently poor that the faint galaxies in the sample would be difficult to detect if their 10μm excesses were similar to those in other IR galaxies such as M82. Within the constraints imposed by sensitivity, observations were made of some of each of the types of interacting galaxy discussed in section 2.5. One galaxy which did not show a K-L excess was also observed. The observations were made at UKIRT during February 1983, February 1984 and January 1985. On all three occasions the weather conditions were extremely poor, with about half the available time being lost. In addition the performance of the UKIRT bolometer was always below standard and a great deal of time was also lost due instrumental problems. Thus far fewer follow-up observations of the JHKL survey galaxies were obtained than was intended, and the selection of objects presented here was largely influenced by their availability at a time when it was possible to observe them.

The 10 and 20μm measurements were made at the location of the peak of the emission at K. This had been determined in the course of the previous near-infrared observations, and for those cases in which an easily-seen nucleus was not apparent on the UKIRT TV the offset from the K-peak to a nearby guide star had been measured. Unfortunately, at the time these observations were made the dichroic used to deflect the IR beam into the dewar did not cover the entire focal plane which the TV crosshead was free to travel over. So large (≧ 70") offsets measured by moving the TV can differ from the true offset by the size of the refraction in the dichroic. Furthermore since the bolometer is generally mounted on a different port at the Cassegrain focus to the near-infrared photometer, a mis-centering by more than this amount can arise if the offsets measured on the cross-head for one system are then used with the other. As a result of these problems it is likely that the IR beam was not fully centred on the source when the 10μm measurements of NGC4088 and NGC2445 (which are large nearby galaxies with numerous bright HII regions) were made.

Different photometers were used for the observations in 1983, 84 and 85 and so slightly different apertures were used on each occasion. Also in order to keep the noise to a minimum ~ 5 arcsec apertures were sometimes used, in preference to the 8 arcsec apertures which would be more comparable to the JHKL observations. Of course the smaller aperture was also used in the cases where we attempted to resolve the nuclear source. The aperture used for each observation is given in the table of results. The largest chopper throws possible without increasing the noise to intolerable levels, typically 20 - 40 arcsec, were used to minimise the likelihood of chopping within the source.

Calibration stars were observed frequently to monitor changes in extinction and sensitivity during the night. Observations of the stars BS2990, BS4069, BS6406 and BS5340, whose magnitudes at 10 and 20μm are listed in Gehrz et al. (1974), were used to calibrate the data. The uncertainties due to the flux calibration and in the extinction curves are small compared to the statistical errors in the measurements. The galaxy data were generally calibrated using a star which was observed before or after the galaxy observation at a similar airmass to the galaxy, so corrections for atmospheric extinction were neglible compared to the statistical errors in the galaxy data. On the few occasions where this was not possible the mean extinction law for the night was used to correct for atmospheric extinction. Some of the galaxies were observed more than once through the same aperture, either on different nights in the same observing run or repeated, usually because of poor signal-to-noise, on a subsequent run. No differences larger than 1 sigma were found between the measurements and so for these galaxies the weighted mean of the individual observations was taken as the best measure of the flux. A galaxy was assumed to have been detected if the measurement was ≧ 3 σ. The reduced data for the detected galaxies is presented in Table 3.1(a), while 3 σ upper limits for those galaxies observed but not detected are listed in Table 3.1(b).

Given the observational problems in obtaining 10μm photometry and the low signal-to-noise ratios achieved for some of the galaxies it is important to compare the results with previous and subsequent observations of these galaxies by other observers. For those galaxies for which 10μm observations are now available in the literature the independant measurements are compared in Table 3.2. With the exception of NGC1614, all of the results agree within the errors quoted, and no systematic differences ,except, perhaps, some aperture effects, are apparent. For NGC1614 the 10μm photometry was obtained at the postion of the K-peak measured from a guide star and further observations at different postions suggest that the emission is extended and probably not coincident with the peak of the emission at K. The total flux evident from this map is consistent with there being a centering difference between the measurements in this work and the others in Table 3.2.

Altogether 16 of the K-L excess galaxies were observed at 10μm and of these 11 were detected. The upper limits for the non-detected galaxies are not strong enough to be inconsistent with the infrared excess inferred from the JHKL photometry. Before considering the extent to which 10μm photometry confirms the JHKL observations in more detail, the sample is extended with observations of interacting galaxies from the literature.

3.2.1 Data from the literature for JHKL sample galaxies

Subsequent to the completion of the JHKL survey described in Chapter 2 there have been two major attempts to survey the 10μm emission from interacting galaxies by other groups (Lonsdale et. al. 1984, Cutri and McAlary 1985). Several of the galaxies in these samples were also in the JHKL study and so data is now available for a larger fraction of the sample. All new data for galaxies in the JHKL study, including upper limits (3σ), is presented in Table 3.3. Observations of the

Table 3.1(a)

Detections of interacting galaxies in the JHKL sample

Galaxy NGC	Arp	Aperture	10µm Flux mJy	20µm flux mJy
1614	186	5	480 ± 35	
2623	243	4	80 ± 12	460 ± 70
2798	283	8	520 ± 104	1911 ± 260
		5	190 ± 18	
3227	94	8	313 ± 63	726 ± 123
		5	330 ± 14	
3627	317	4	71 ± 12	
3786	294	8	47 ± 18	
4038	244[1]	5	45 ± 12	341 ± 103
4088	18	8	60 ± 22	
5394	84	4	114 ± 20	
5930	90	8	147 ± 35	774 ± 154
		5	112 ± 25	
6240		4	124 ± 15	1100 ± 120

1) Observations were made at "Knot B" in Rubin et al. (1970)

Table 3.1(b)

Upper limits for galaxies in the JHKL sample

Galaxy NGC	Arp	Aperture (arcsec)	3σ 10µm limit (mJy)
2445	143	8	90
3396	270	8	96
5258	240	8	96
5929	90	8	99
6052	209	5	180
A1718 +49B	102	5	60

Table 3.2

Comparison of UKIRT photometry with other observations

Galaxy NGC	Galaxy Arp	Aperture (arcsec)	10µm Flux (mJy)	References
1614	186	5	480 ± 35	This work
		8	630 ± 20	Lebofsky & Rieke (1979)
		4.5	840 ± 50	Lonsdale et al. (1984)
2445	143	8	<90	This work
		4.5	68 ± 13	Lonsdale et al. (1984)
2623	243	4	80 ± 12	This work
		4.5	93 ± 12	Lonsdale et al. (1984)
		5.5	105 ± 9	" " " "
3396	270	8	<96	This work
		6	55 ± 7	Cutri & McAlary (1985)
3627	317	4	71 ± 12	This work
		5.7	110 ± 22	Rieke & Lebofsky (1978)
3786	294	8	47 ± 18	This work
			52 ± 6	Cutri & McAlary (1985)
5258	240	8	<96	This work
		6	<22	Cutri & McAlary (1985)
5394	84	4	114 ± 20	This work
		6	187 ± 62	Cutri & McAlary (1985)
5929	90	8	<99	This work
		6	43 ± 14	Cutri & McAlary (1985)
5930	90	8	147 ± 35	This work
		6	155 ± 23	Cutri & McAlary (1985)

Table 3.3

10μm Observations of JHKL sample galaxies in the literature

Galaxy NGC	Arp	Aperture (arcsec)	10μm Flux mJy	Reference
3395	270	6	26 ± 9	Cutri & McAlary (1985)
3718	214	5.5	<45	Lonsdale et al. (1984)
3788	294	6	<17	Cutri & McAlary (1985)
3799	83	6	<10	" " " "
3800	83	6	28 ± 7	" " " "
4438	120	4.5	33 ± 8	Lonsdale et al. (1984)
4676B	242	4.5	<60	" " " "
IC883	193	5.5	154 ± 9	" " " "
5257	240	6	<18	Cutri & McAlary (1985)
5395	84	6	<18	" " " "
IC4553	220	total	480	Soifer et al. (1984)
7752	86	12	116 ± 82	Cutri & McAlary (1985)
7753	86	12	<188	" " " "
7805	112	12	<210	" " " "

galaxies for which photometry was presented above are not included in this table since they are listed in Table 3.2. All of the observations of the JHKL sample galaxies are used in the following discussion.

3.3 Comparison of 10μm and K-L results

In section 2.1 it was argued that if there is a substantial IR excess at 10-100μm then its presence will also contribute to the flux at L and will be reflected in a K-L colour which is significantly redder than normal. If this is so, a correlation between K-L colour and 10μm luminosity would be expected because a larger 10μm excess would result in a redder K-L colour (i.e. a larger L excess) and 10μm luminosity and K-L colour are both distance independant. The 10μm luminosity was calculated using equation 3.3. Figure 3.1 is a plot of 10μm luminosity against K-L colour for all the galaxies in the JHKL sample for which 10μm photometry is available. There is a good correlation over more than two orders of magnitude in 10μm luminosity. A linear regression of 10μm luminosity against K-L colour gives a slope of 0.23 with a significance of 4.6 σ. This suggests strongly that the source of the 10μm emission is also responsible for the red K-L colours. Another way of examining this question is to test whether the L excess is directly related to the 10μm excess, i.e. the 10μm flux. For galaxies with a K-L colour greater than 0.3, the L excess was determined by assuming that the colour index of the stellar continuum is K-L = 0.3, as in 2.4.2. The galaxies NGC3718, 3799 were not included because their L excess, calculated in this way, is less than the accuracy with which the L flux is known. Figure 3.2 is a plot of 10μm flux as a function of the excess flux at L for these galaxies. Despite the uncertainty, due to the scatter in the K-L colours of normal galaxies, in determining the L excess, there is clearly a correlation between the two. For this correlation a linear regression gives a slope of 0.02 with a 5 σ significance. Thus the L excesses are the continuation into the near-infrared of the excesses seen at 10μm.

One of the major results of the JHKL survey was that the induced activity was only found in one member of each pair in the sample. As expected from the above, this result is also confirmed for those pairs in which 10μm observations of both members of a pair have been obtained, as shown in Table 3.4. The 10μm luminosity of one member of the pair is always significantly greater than that of the other. Thus

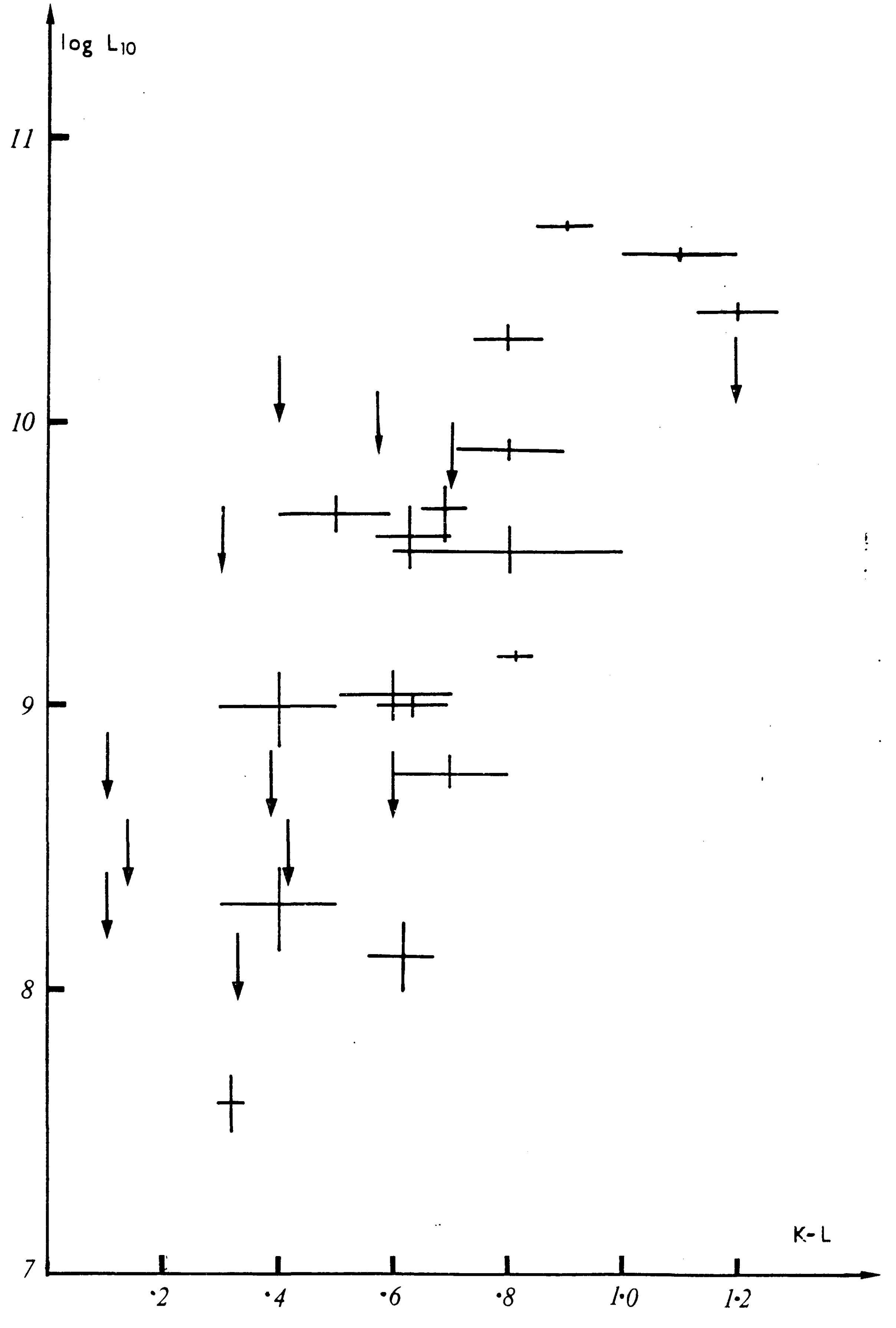

Figure 3.1 The correlation between 10μm luminosity (L_{10}) and K-L colour.

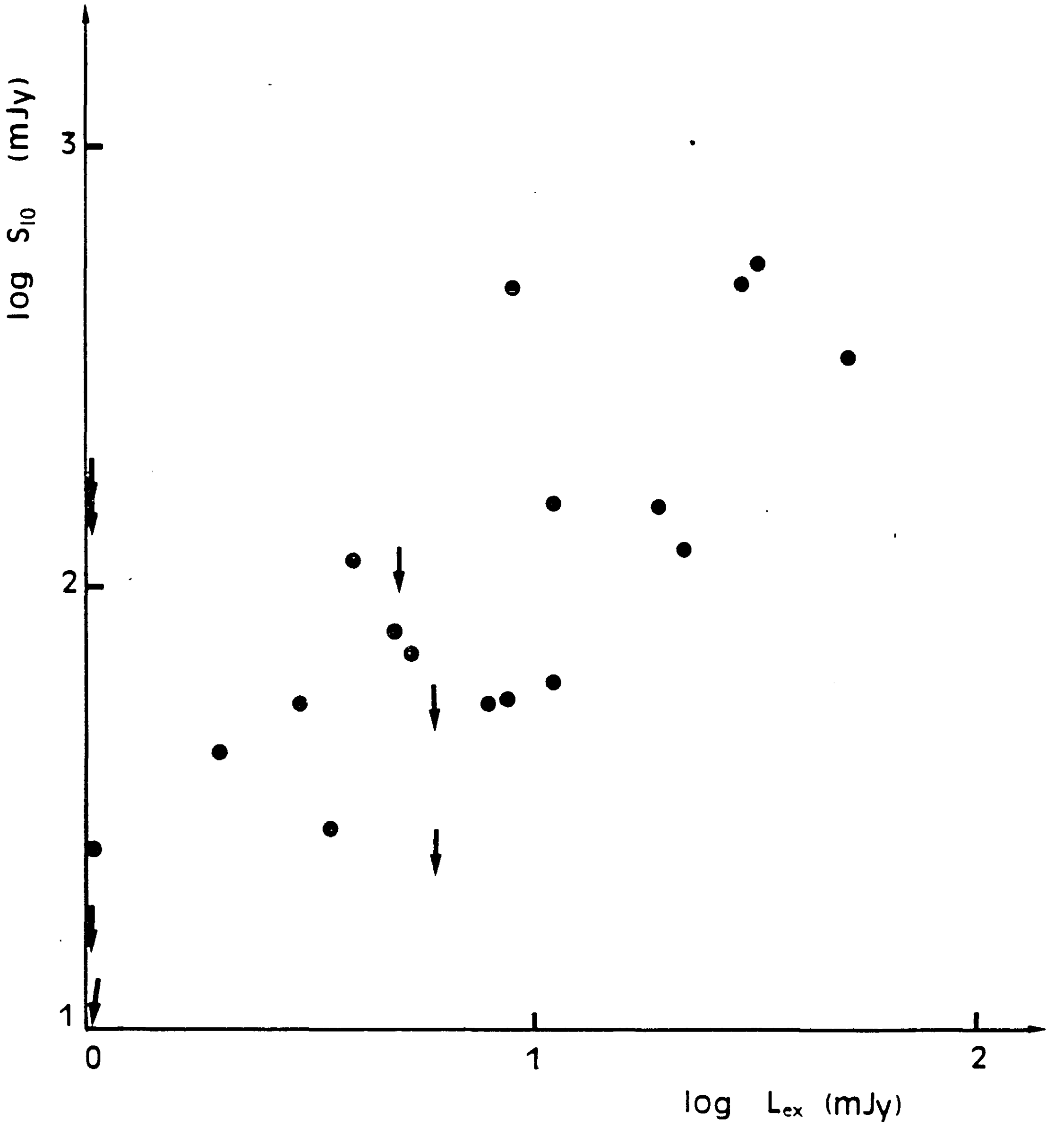

Figure 3.2 10μm flux (S_{10}) as a function of <u>excess</u> flux at L (L_{ex}).

there is more activity induced in one member of these pairs than in the other. As explained in section 2.5, this is qualitatively consistent with dynamical studies of galaxy interactions.

Table 3.4

10μm observations of both members of pairs

Galaxy Pair[1]	NGC	10μm Flux mJy	K-L
A270	3396	55 ± 7	0.70
	3395	26 ± 9	0.40
A294	3786	52 ± 6	0.63
	3788	<17	0.14
A83	3800	28 ± 7	0.60
	3799	<10	0.40
A84	5394	114 ± 20	0.50
	5395	<6	0.10
A90	5930	155 ± 23	0.63
	5929	43 ± 14	0.40

1) In this column A denotes the Arp number for the pair, while K is the number of the pair in the Karachentsev catalogue.

In summary the 10μm results show that JHKL photometry is a powerful and efficient tool to investigate IR activity in the nuclei of galaxies. The correlations found between 10μm luminosity and K-L colour and between 10μm and L excesses confirm the inferences of activity from the near infrared colours. So the conclusions based on JHKL photometry in Chapter 2, for example, that interactions are effficient in inducing IR activity and the appearance of this activity in systems of different morphological types is consistent with the results of numerical simulations of interactions, are borne out by the 10μm follow-up observations. In the following section the sample of interacting galaxies with 10μm photometry is extended by including observations in the literature for other interacting galaxies not in the original JHKL sample. Using this larger sample the degree to which 10μm observations confirm the interpretation of the K-L survey as showing that the IR activity in interacting galaxies is most likely due to a recent burst of star-formation is examined.

3.4 10μm photometry of other interacting galaxies

There are now observations in the literature for several interacting galaxies not included in the original JHKL survey, which have similar morphological features to the survey galaxies. Lonsdale et. al. (1984) present results for a sample selected from the Arp Atlas on the basis of morphological characteristics similar to the selection of objects for Chapter 2. Indeed, some of these galaxies were on the observing lists for the JHKL survey but were not observed due to lack of telescope time. Cutri and McAlary (1985), on the other hand have constructed a complete, magnitude limited sample of disturbed pairs of galaxies in the Karachentsev (1972) catalogue with the aim of achieving a statistical comparison of the detection rates and luminosity function of interacting compared to normal galaxies. (Unfortunately their conclusions are weakened by the large number of upper limits and the absence of an equally well defined comparison sample.) Their selection criteria from the Karachentsev catalogue are approximately equivalent in morphological terms to the selection of objects for Chapter 2 - they are all pairs with either obvious bridges and tails or extremely disrupted structure. Finally, a number of interacting galaxies have been observed as part of other observational programmes e.g. 10 of the 39 galaxies in the Rieke and Lebofsky (1979) survey of bright spirals are in the Arp Atlas. There have also been a few detailed studies of interacting systems which have included 10μm measurements (e.g. Gehrz et al. 1983, Telesco and Gatley 1984).

By combining all other 10μm measurements of interacting galaxies with the observations of the JHKL survey galaxies, the most comprehensive overview of the mid-IR characteristics of interacting galaxies will be obtained. Table 3.5 therefore summarises the 10μm photometry of other interacting galaxies which will be used in the following discussion to supplement the results for the JHKL survey galaxies. Galaxies are only included in this sample if they obviously fall into the types of interaction selected for the JHKL survey. So for example, those galaxies in the Arp Atlas which resemble dusty spirals with no obvious companions are not included even if 10μm observations are available. The sample is not complete, and because it is based on observations by different authors it is also not a survey to a uniform sensitivity level. Thus a statistical analysis of detection rates or luminosity

Table 3.5

Other interacting galaxy detections in the literature

Galaxy NGC	Pair[1]	Aperture (arcsec)	10μm Flux mJy	Reference
520	A157	5	460	Condon et al. (1982)
2341	K125	6	65 ± 8	Cutri & McAlary (1985)
2342	K125	6	·65 ± 8	" " " "
U3395	K140	6	97 ± 9	" " " "
2964	K210	6	110 ± 11	" " " "
2992	A245	4.5	255 ± 12	Lonsdale et al. (1984)
3256	VV65	15	1700 ±150	Graham et al. (1984)
3310	A217	map	1000	Telesco & Gatley (1984)
3656	A155	5.5	37 ± 6	Lonsdale et al. (1984)
3808A	A87	4.5	50 ± 11	" " " "
4038	A244[2]	4.5		Lonsdale et al. (1984)
4194	A160	6	320 ± 45	Rieke & Low (1972)
4568	K347	8	62 ± 19	Cutri & McAlary (1985)
5953	A91	6	64 ± 10	Cutri & McAlary (1985)
7469	A298	5.9	600 ± 40	Lebofsky & Reike (1979)
7714	A284	6	250 ± 40	Rieke & Low (1972)
7761	K592	8	119 ± 20	Cutri & McAlary (1985)

notes: 1) A is the number of the Arp pair and K denotes number in the Karachentsev catalogue

2) Position M in the figure of Rubin et al. (1970)

functions for these galaxies, which would place the upper limits in context, is not justified. An appreciation of how typical upper limits compare to detected galaxies can be obtained from Cutri and McAlary (1985). Although the sample is not complete, because all the galaxies were selected for inclusion (and in all but a few cases for observation) on the basis of morphological features and without regard to evidence for star-formation or an active nucleus the properties of the sample galaxies should be representative of the characteristics of similar interacting galaxies. A study of the mid-IR luminsities and other features of these galaxies cannot be extrapolated to generalised conclusions for interacting galaxies of all types. However the results should represent the properties of galaxies which have undergone sufficiently strong interactions to cause significant tidal effects such as bridges and tails. For the rest of this chapter the combined sample consisting of the galaxies in Tables 3.1, 3.3 and 3.4 is considered as a whole.

3.5 Emission mechanisms and energy sources

Examples of the continuum spectra of the interacting galaxies for which more than one point is available are plotted in Figure 3.3. Despite the varying degrees of completeness of the spectra it is clear that they are all very alike, with a steep mid-IR rise similar to that of NGC253, which is also plotted in the figure. These spectra, which peak near 100μm and decrease with decreasing wavelength less rapidly than a simple black-body function, are characteristic of the thermal radiation from a population of dust grains which are at a range of temperatures. Such spectra are also commonly observed from galactic regions of star-formation. Continuum spectra with these features for galactic nuclei are therefore generally assumed to be indicative of a recent burst of star-formation, with the ultra-violet radiation from massive early-type stars thermalised by dust and reradiated in the IR. There are several more detailed observational tests of this interpretation which can be applied to many of the galaxies in this sample and these are discussed in the following sections.

3.5.1. The extent of the IR emission

Thermal IR emission is observed from the nuclei of Seyfert galaxies where it is thought that the dust is heated by the compact central

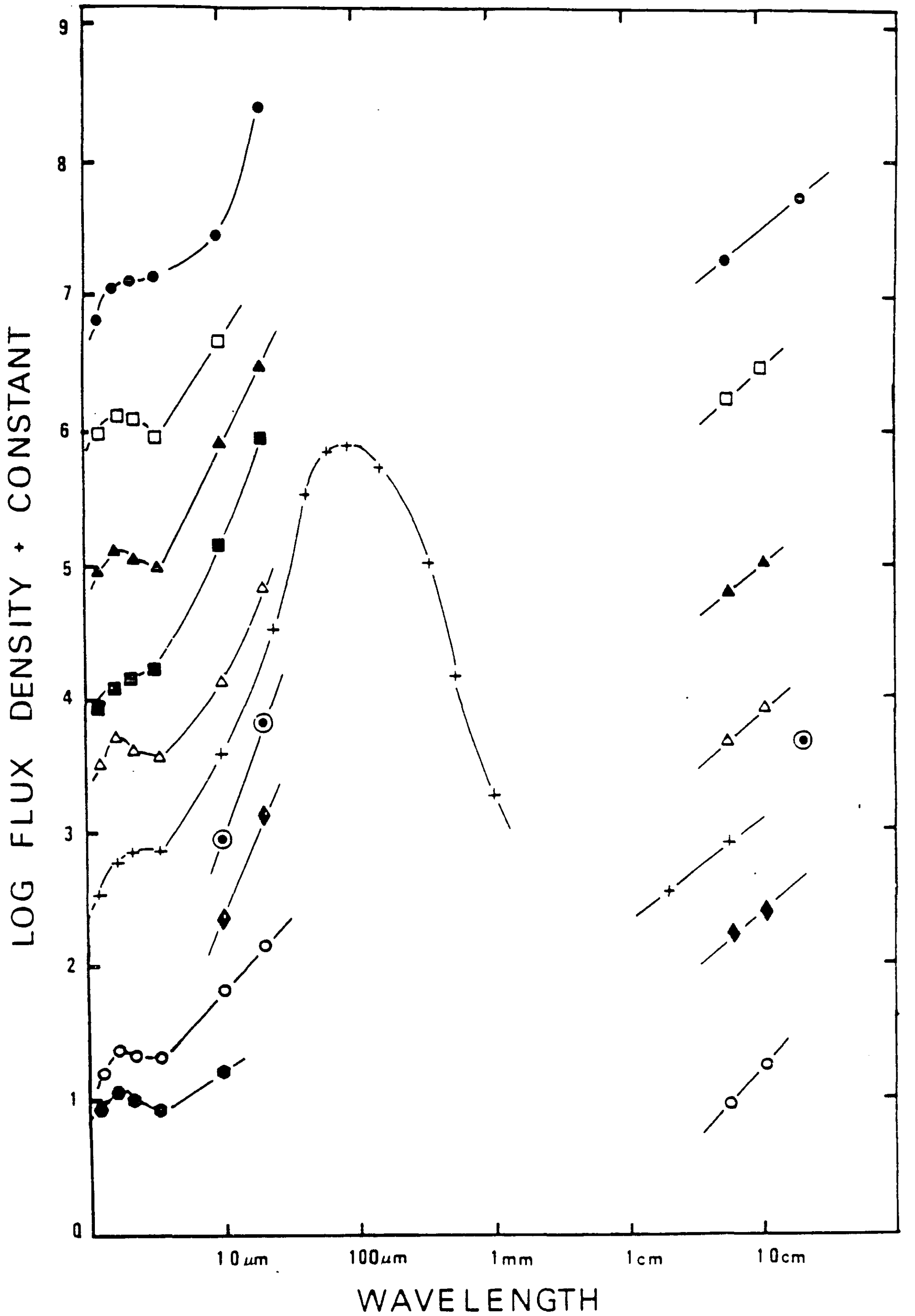

Figure 3.3 Continuum spectra of interacting galaxies. Near infrared data is given in Table 2.1. The mid IR photometry is from Table 3.1, except for NGC1614 (■) at 20μm which is from Lebofsky and Reike (1979) and NGC3786 (⬣) from Table 3.3. The radio data is taken from: NGC6240 (●), Condon et al. (1982); NGC2798 (▲), NGC5930 (△), NGC3227 (○), NGC5394 (□), Stocke et al. (1978); NGC2623 (◆), Condon (1980); NGC4038/39 (◉), Burke and Miley (1973). Data for NGC253, (+), are from Glass (1973), Rieke et al. (1973), Rieke & Low (1975), Hildebrand et al. (1977), Elias et al. (1978), Rieke & Lebofsky (1978), Telesco & Harper (1980) and Turner & Ho (1983).

source. The starburst hypothesis proposed above can be distinguished from this by measuring the extent of the IR emission. For a single source of luminosity L heating a dust cloud, the temperature of dust a distance R from the source is determined by the radiation balance of the grains,

$$e^{-\tau} \frac{L}{4\pi R^2} \bar{Q}_{uv} \pi a^2 \sim \sigma T_d^4 \bar{Q}_{IR} 4\pi a^2 \qquad 3.1$$

where,

Q_{uv} and Q_{IR} are the Planck mean emission and absorption coefficients,
a is the grain radius ,
T_d is the dust temperature, and
σ is the Stefan-Boltzmann constant

Since the dust is radiating at 10μm, $T_d \sim 300K$. Using typical values for interstellar dust, assuming $Q_{IR} \propto a\ T_d$, (e.g. Draine 1981) equation 3.1 gives

$$R \sim 50 T_d^{-5/2} (L/L_\odot)^{1/2} \quad pc \qquad 3.2$$

For a $10^{10}\ L_\odot$ source, $R \sim 3$ pc, so spatial extent at 10μm in galaxies on scales greater than ~ 3pc cannot be produced by a single compact source heating the dust, as would be required if the underlying nuclear energy source were accretion onto a compact object. Sellgren (1984) has argued that the near-IR emission from gaseous nebulae is the thermal emisison from very small (< 10 Å) dust grains heated by the arrival of a single high energy photons. Because such grains are not in thermal equilibrium, a compact nuclear source could power extended IR emission if a large proportion of the dust were these small "Sellgren grains". However there is currently little evidence for substantial amounts of this dust in the nuclei of galaxies, e.g. it has not been observed in known Seyfert nuclei. The IR emission from starburst galaxies is characterised by spatial extent on scales of 100's of parsec (e.g. Rieke 1976), and distributed sources such as hot young stars seem to be the best explanation of the extended warm dust emission. To investigate whether the IR emission from interacting galaxies is extended on scales similar to that observed for other starburst galaxies, we looked for spatial extent at 10μm for some of the interacting galaxies.

Table 3.6 summarises the results of mapping the galaxies NGC1614, 2798 and 3227 at UKIRT using a 5 arcsec beam. The data have been reduced as described in section 3.2. NGC1614 is clearly extended to the south and east. Figures 3.4 (a) and (b) show the S, E, W and SE measurements compared to the profiles of an unresolved source, determined by scanning across a star in the N-S and E-W directions. For the pixel to the SE the results have been compared to both beam profiles as if the offset was ~ 4" in one direction only, so that the overlap of beam area is the same as for the SE offset. Both to the S and to the SE the measured flux is significantly greater than that expected from a point source, and is strong evidence that the 10μm emission from NGC1614 is extended. This is consistent with the differences in flux between the measurements presented here and those of Lonsdale (1984) and Lebofsky and Rieke (1979) (cf. 3.2). Because the UKIRT photometry was taken at the position of the K peak (measured relative to a nearby guide star), these results suggest that the peak of the 10μm emission in NGC1614 is not coincident with the peak at K. For NGC2798 substantially less flux was detected with a 5 arcsec beam, 190±18 mJy, than with an 8 arcsec beam, 520±104 mJy. Both beams were centred on the optically brightest spot. In Figures 3.4(c) and (d) the off-centre measurements of NGC2798 are compared to the beam profiles determined by scanning across a star. The pixels in the 10μm map are consistent with the profile of an unresolved source. Because no 20μm beam profiles were measured it is difficult to quantitatively interpret the results of mapping NGC2798 at 20μm. However, assuming that a profile at 20μm would be broader than a 10μm profile (because the aperture size is close to the diffraction limit of UKIRT at 20μm), suggests that, within the photometric and pointing errors, these results also do not distinguish NGC2798 from a point source. The difference between the large and small aperture measurements remains an indication of extent, although the sensitivity and positional accuracy to measure the extent directly were not achieved. For NGC3227 the off-nuclear detections are compared to the beam profiles in Figures 3.4 (e) and (f). Despite having a signal-to-noise of only 3.4, the point in the south suggests extent of the source with a 1σ significance, as shown in Figure 3.4(f). In order to investigate further the extent of the IR emission in N3227, measurements of the K-L colour in non-nuclear positions were made using an 8 arcsec beam. A K-L colour of 0.85±0.23 was measured at a postion 8 arcsec west of the nucleus. Since K-L colour correlates well with 10μm excess (Figure 3.1) these results confirm that the IR emission is extended in

Table 3.6

5 arcsec aperture maps of galaxies

Galaxy	Chopper throw (arcsec)	Offset from nucleus (arcsec)	10μm Flux mJy	20μm Flux mJy
1614	30 E-W	0 , 0	480 ± 35	
		3E , 0	174 ± 24	
		3W , 0	64 ± 20	
		0 , 3S	530 ± 24	
		3E , 3S	260 ± 60	
2798	30 E-W	0 , 0	190 ± 18	700 ± 60
		2.5E , 0	99 ± 21	680 ± 100
		2.5W , 0	18 ± 14	160 ± 80
		0 , 2.5N	100 ± 18	560 ± 90
		0 , 2.5S		346 ± 100
		5E , 0		145 ± 97
3227	30 N-S	0 , 0	330 ± 14	
		3E , 0	23 ± 15	
		3W , 0	82 ± 17	
		0 , 3N	68 ± 19	
		0 , 3S	71 ± 21	

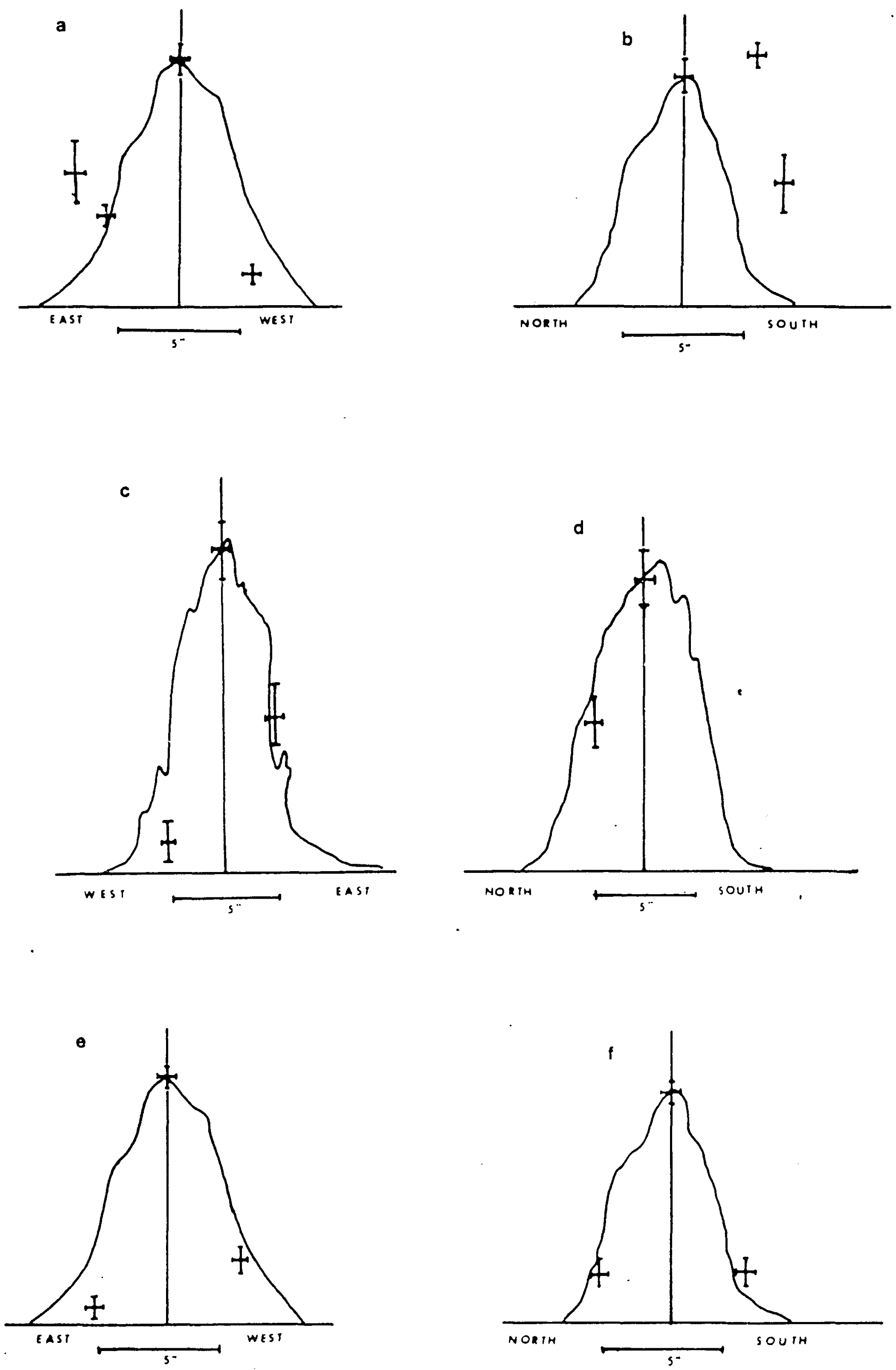

Figure 3.4 10μm photometry of pixels in NGC1614, NGC2798 and NGC3227 compared to the profiles of an unresolved source. The galaxy fluxes were scaled so that the peak flux corresponds to the height of the profile at beam centre. **a)** E-W and **b)** N-S scans of a star compared to the pixels measured in NGC1614, **c)** E-W and **d)** N-S beam profiles compared to photometry of NGC2798, **e)** E-W and **f)** N-S profiles compared to pixels measured for NGC3227.

NGC3227. The UKIRT measurements discussed here indicate that the IR sources in these galaxies are probably extended on scales ~ 5 arcsec or greater, which corresponds to 2, 0.8, and 0.6 kpc in NGC1614, 2798 and 3227 respectively.

For some of the other galaxies in the sample measurements of spatial extent at 10μm have been presented in the literature and these results are now summarised. Lonsdale et al. (1984) have mapped IC883 and find the emission to be extended to the North-West. From the difference between their large and small aperture measurements the source must be greater than 4.5 arcsec or 3 kpc in extent. As discussed in detail in section 4.3 the IR emission from NGC6240 must be extended on scales > 3kpc. For NGC3310 the maps of Telesco and Gatley (1984) show that the intense 10μm emission in this galaxy extends for more than 5kpc. Maps at 10μm and multi-aperture photometry at L' are used by Graham et al. (1984) to infer that the emission from NGC3256 is extended over at least 4kpc. Rieke et al. (1985) have mapped IC4553 at 10μm and conclude that the source is larger than 2kpc, although there is some debate about this result (Joseph 1985). Finally, some of the galaxies in Table 3.3 in which independent observations of the nuclei were compared, show evidence at the 1σ level for increased flux in the larger apertures. On the basis of this comparison it is likely that the IR emission from NGC2623 and NGC3627 is extended on a scale ~ 4 arcsec which corresponds to ~ 2kpc and 230pc respectively.

For the galaxies discussed in the above two paragraphs, if the dust is in thermal equilibrium, there must sources distributed throughout the emitting region, by comparison with equation 3.2. There is no case in which one of the sample galaxies been mapped at 10μm and shown to be compact. In contrast, for 7 of the 35 interacting galaxies detected at 10μm, there is a good indication of spatial extent at 10μm on scales > 1kpc. In addition there is data which suggests that the 10μm emission from a further 3 galaxies (NGC2623, 3627, IC4553) is also likely to be extended. For all these galaxies the observed spatial extent of the IR radiation indicates that the dust is unlikely to be heated by a single central source. A starburst interpretation fits much more naturally with the data.

3.5.2 Optical emission lines

Optical emission lines are a powerful probe of the physical conditions under which they arise and by providing information about the ionised gas in the nucleus enable the ultraviolet continuum which ionises it to be studied. Line intensity ratios may be used to distinguish between photo-ionisation by hot stars, by a strong power-law continuum (Seyferts) and low-ionisation nuclei (Liners) which could be ionised either by a weak power-law continuum or arise in the cooling regions behind shock fronts (e.g. Baldwin et al. 1981). If the starburst interpretation of the IR fluxes from interacting galaxies is correct then these galaxies should have optical spectra suggestive of recent star formation. There are optical spectra in the literature for 31 of the 35 interacting galaxies detected at 10μm (Keel et al. 1985, Heckman et al. 1983, Dahari 1985, Bushouse and Gallagher 1984, Balzano 1983). Figure 3.5 shows a diagnostic diagram, using the reddening insensitive ratios [OIII]/Hβ and [NII]/Hα, which differentiate between the excitation mechanisms (cf. Baldwin et al. 1981, Balzano 1983), with many of the interacting galaxy sample plotted. It is obvious that most of these fall in or near the "HII region" section of the diagram. Some authors have used other, similar, diagrams to classify galaxies for which these particular line ratios have not been measured, so not all of the classified galaxies are on this figure. Altogether, of the 31 galaxies for which optical spectra exist, 21 have been classified as having relative line intensities similar to those found in HII regions, 4 are classified as Liners and 6 as Seyfert galaxies. I have included NGC3256 in the HII region-like sample. Only a qualitative description of this spectrum has been given (Feast and Robertson 1978), but the spectrum is characterised by narrow linewidths, < 30 kms^{-1}, indicative of a starburst (cf. Feldman et al. 1982). The 4 galaxies with Liner type spectra are NGC6240, NGC2623, NGC3627 and NGC4438, and of these Keel et al. (1985) have classified the stellar continuum of NGC4438 as having a significant component due to early type stars. Spectra of sufficient senstivity to classify the continua of the others are not available. However for all three there is evidence suggesting that the IR emission is extended and hence that these also contain young stars in their nuclear regions. Heckman et al. (1983) note that the presence of a Liner-type nuclear spectrum does not necessarily rule out a substantial number of early type stars as well.

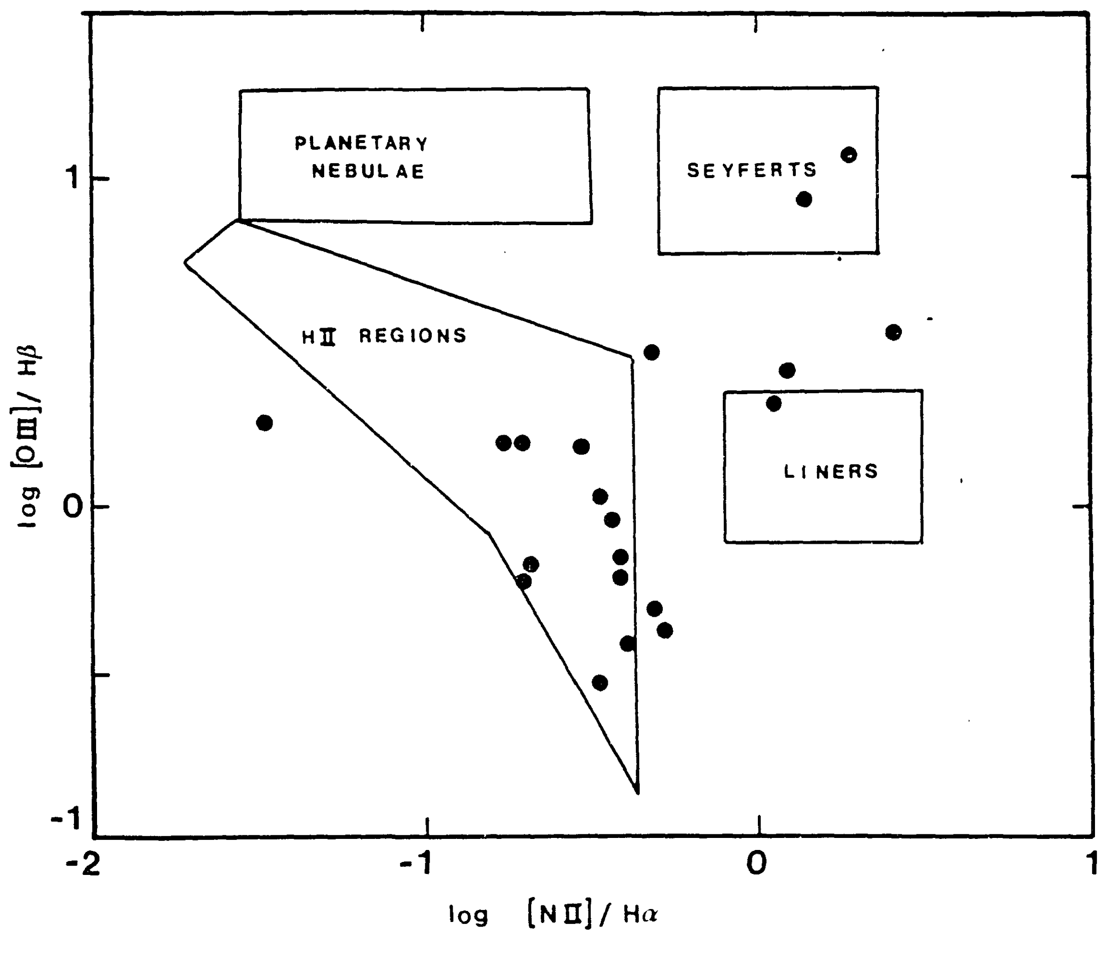

Figure 3.5 An [OIII] / Hβ , [NII] / Hα diagram for the interacting and merging galaxies.

The occurence of 6 Seyfert galaxies in the sample is probably not inconsistent with the number of Seyfert nuclei expected in a field sample of this magnitude range (see e.g. Keel et al. 1985). The Seyfert galaxies are NGC 3227, 3786, 5929, 7469, 2992, and 5953. It seems that in some Seyfert galaxies there is also intense star formation in the nuclear (i.e. the inner 1kpc) region (cf. Smith 1984). NGC1068 is a classic example of such a galaxy, and in this case about half of the IR lumimosity is provided by the Seyfert nucleus and about half by a surrounding extended disk of star formation (Telesco et al. 1984). There is evidence that three of the galaxies in this sample which are classified optically as Seyferts are composites with star formation as well as Seyfert activity in their nuclear regions. Jenkins (1984) has studied NGC5953 in detail and finds extremely luminous extended "nuclear" emission lines indicative of HII regions as well as the compact non-thermal core. The radio data for NGC2992 and NGC3227 all show a nuclear source extended on scales of 10-100 pc, consistent with a starburst (cf. 3.5.3). In addition the nuclear emission lines from NGC2992 are extended over ~ 7 arcsec (Heckman et al 1981), although they are unclassified. It was argued above that the IR emission from NGC3227 is sufficiently extended that distributed luminosity sources such as young stars are required to provide much of the luminosity. So, in these three Seyferts there is almost surely a starburst as well. Of the three Seyferts for which no further information is available NGC5929 is the companion to NGC5930, which has a starburst spectral classification and whose IR emission is 4 times stronger than that of NGC5929. Thus it is in the starburst member of this pair that the interaction has had the greatest effect, and it is NGC5930 which is included in the discussion of the properties of interaction induced activity in sections 3.5 and 3.6. To be conservative, the remaining two Seyferts are excluded from the discussion in these sections although it is quite likely that if observed in more detail they too would show indications of a recent burst of star formation.

3.5.3 Radio Observations

Condon et al. (1982), Hummel et al. (1984) and others have argued that steep spectrum, extended nuclear radio sources in spiral galaxies can be explained in terms of young supernovae and supernova remnants associated with recent bursts of star formation. In this section the characteristics of the radio emission from interacting galaxies detected at 10μm are examined to see if they fit this scenario. Radio data taken from the literature are summarised in Table 3.7. For 27 of the 35 interacting galaxies detected at 10μm, the radio source has been resolved and has a non-thermal spectrum, typically of index ~ -0.7. The two most compact sources are in NGC2623 and IC4553, with sizes ~ 0.5 arcsec (Condon 1980) which still corresponds to ~ 270pc in these galaxies. In contrast with the galaxies in Table 3.7, Kellerman et al. (1976) find that the Seyfert galaxy NGC3031 has a compact radio source of size ~ 10^{-3} arcsec (ie. < 1pc) with a spectral index of +0.1. The interacting galaxies do not seem to have the characteristic radio emission associated with Seyfert galaxies. Their radio properties are consistent with a starburst as the dominant luminosity source. The starburst model for the radio emission from these interacting galaxies is discussed in more detail in section 3.7.3.

3.5.4 Summary

Taken together the IR, optical and radio measurements on this group of interacting galaxies provides strong and consistent evidence that the IR emission from the majority of the galaxies is powered by recent bursts of star-formation. Only NGC3786, NGC5929, NGC7469, NGC3656 and UGC3395 were detected at 10μm and have no other evidence suggesting that star formation is occuring in their nuclei. For the latter two galaxies no optical or radio data was found in the literature. Thus it seems that starbursts are the dominant cause of the IR activity in interacting galaxies. In the following sections these starbursts are compared to the starbursts in other galaxies and the IR luminosities are used to derive typical physical parameters, such as star formation rates, of interaction induced starbursts. To be conservative the Seyfert galaxies NGC3786 and NGC7469 are excluded from this discussion because there is no other evidence for star formation in their nuclei. The inclusion in the sample of the other galaxies whose optical spectra are indicative of Seyfert or Liner-type activity will not affect the conclusions reached, since there is evidence that these galaxies have both a starburst and a Seyfert or Liner nucleus. In the Seyfert galaxy NGC1068 a burst of starformation accounts for half of the IR luminosity, and in a general overview of the properties of the star formation in interacting galaxies such factors of two have little significance.

Table 3.7

Radio data for interacting galaxies detected at 10μm

NGC	Pair[1]	Radio spectral index	Radio size[2] (arcsec)	References
520	A157	-0.68	~ 10	Condon et al. (1982)
1614	A186		≧ 3	Condon et al. (9182)
2341/2	K125	-1.0	E	Stocke et al (1978)
2445	A143		22	Burke and Miley (1973)
2623	A243	-0.8	0.5x0.4	Condon (1980)
2798	A283	-0.6	2.5x2.5	Stocke et al. (1978)
2964	K210	-0.9	E	Stocke et al. (1978)
2992	A245		~ 8	Condon et al. (1982)
3227	A94	-0.7	3x3	Stocke et al. (1978)
3256	VV65	-1.3		Wright (1974)
3310	A217	-0.7	~ 10	Hummel (1981)
3395	A270	-0.7	E	Stocke et al. (1978)
3627	A317	-0.73	E	Hummel (1980), Israel & Van de Hulst (1983)
4038	A244		E	Hummel (1980)
4088	A18	-0.77	E	Hummel (1980), Gioia et al (1982)
4194	A160	-0.7	~ 6	Hummel et al (1984)
4438	A120	-0.85	3-12	Hummel (1980)
4568	K347	-0.95	E	Stocke et al (1978)
I883	A193	-0.7	E	Sulentic (1976), Heckman (1983)
5394	A84	-0.6	5x6	Stocke et al. (1978)
5930	A90	-1.0	3x5	Stocke et al. (1978)
I4553	A220	-0.6	1.3x0.5	Condon (1980)
5953	A91	-1.0	E	Stocke et al. (1978)
6240		-0.85	~ 5	Condon et al. (1982)
7469	A298	-0.6	4x2	Stocke et al. (1978)
7714	A284	-0.93	3.5x2	Condon et al. (1982)
7761	K592	-1.0	4x8	Stocke et al (1978)

Notes

1) A and K are respectively number in the Arp and Karachentsev catalogues.
2) In this column E is used to denote galaxies whose radio emission has been clasified as extended although no size is given.

3.6 Infrared luminosities

As evidenced in Tables 3.1 3.3 and 3.4, the starbursts in interacting galaxies result in them being relatively bright 10μm sources. However it is the large infrared luminosities which these flux densities imply which are of physical interest. In Table 3.8 the 10μm luminosities of all the detected galaxies are presented. These have been computed using the formula

$$L_{10} = 4 \pi D^2 \nu S_\nu \qquad 3.3$$

where L_{10} is the luminosity at 10μm,
D is the distance in Mpc,
and S_ν is the 10μm flux density.

With the exception of IC4553 the distances for Table 3.8 were determined using the redshifts from de Vaucouleurs, de Vaucouleurs and Corwin (1976), assuming H_0 = 50 km s^{-1} Mpc^{-1}. The recessional velocity for IC4553 was taken from Soifer et. al. (1984). The galaxies in Table 3.7 have 10μm luminosities in the range $4 \times 10^7 - 5 \times 10^{10}\ L_\odot$. So some interacting galaxies have 10μm luminosities nearly two orders of magnitude larger than that of the canonical IR galaxy NGC253, for which $L_{10} \sim 6 \times 10^8\ L_\odot$.

One of the most luminous galaxies at 10μm, NGC3256, consists of a single body with long tidal tails. This is the primary morphological indication of that a merger of two disc galaxies has occurred (cf Toomre 1977). Mergers are the subset of interactions in which dynamical friction causes sufficient energy loss that the galaxies experience a severe orbital decay. Eventually the two galaxies lose their separate identities and appear as a single coalesced object. If grazing interactions can induce starbursts, (e.g. as evidenced by the JHKL survey), then galaxy-galaxy mergers might be expected to result in even more impressive starbursts since a merger should provide significantly more fuel for starformation than non-merging interactions. Heckman (1983) has found that his sample of merging galaxies are twice as likely to be radio loud than non-merging interacting galaxies.

In order to investigate this further, the subsample of merging galaxies

Table 3.8

10μm luminosities of interacting and merging galaxies

Galaxy NGC	Pair	L10 (LG)	Galaxy NGC	Pair	L10 (LG)
520	A157	8×10^{9}	3786*	A294	1×10^{9}
1614	A186	4×10^{10}	3800	A83	1×10^{9}
2341	K125	6×10^{9}	3808A	A87	6×10^{9}
2342	K125	6×10^{9}	4038	A244	6×10^{8}
2445	A143	4×10^{9}	4088	A18	1.3×10^{8}
2623	A243	8×10^{9}	4194	A160	7×10^{9}
2798	A283	5×10^{9}	4438	A120	4×10^{7}
U3395	K140	7×10^{9}	4568	K347	9×10^{8}
2964	K210	6×10^{8}	IC883	A193	2.5×10^{10}
2992	A245	2.5×10^{9}	5394	A84	5×10^{9}
3227	A94	1.5×10^{9}	5929	A90	1×10^{9}
3256		4×10^{10}	5930	A90	4×10^{9}
3310	A217	4×10^{9}	IC4553	A220	5×10^{10}
3396	A270	5×10^{8}	5953	A91	8.5×10^{8}
3395	A270	2×10^{8}	6240		2×10^{10}
3627	A317	8×10^{7}	7469*	A298	5×10^{10}
3656	A155	9×10^{9}	7714	A284	7×10^{9}
			7761	K592	7×10^{9}

* These two Seyfert galaxies are excluded from the analysis of the starburst luminosities and characteristics, as discussed in section 3.5.

is now separated out from the rest of the interacting galaxy sample. These galaxies have been selected from the lists of merging galaxies in the literature (Toomre 1977, Schweizer 1983, Heckman 1983). They are limited to those highly disturbed systems in which two disc galaxies have already coalesced. Thus systems such as "The Antennae" (Arp 244) on Toomre's (1977) list have been excluded because two galaxies are still clearly visible. The merging galaxies are NGC520, 2623, 3256, 1614, 6240, 4194, 3310, IC4553, 883. These nine mergers are thus the only merging galaxies which satisfy the morphological selection criteria for which 10μm photometry is available. Evidence that these galaxies are indeed the products of a merger includes tidal tails (NGC520, 2623, 3256) or remnants thereof (NGC6240, 1614, 4194, IC4553, 883), double nuclei (NGC6240, 2623) or the prescence of two velocity systems (NGC520). The shells or ripples seen in NGC3310 are also thought to be the result of a collision between two galaxies, seen in the late stages (Schweizer 1983). These galaxies are all among the most luminous galaxies in the interacting sample and the luminosities of merging galaxies and non-merging interacting galaxies are discussed in more detail in the following sections.

The astrophysical significance of the IR luminosities of interacting and merging galaxies is best appreciated by comparing them in detail with the 10μm luminosities of other types of galaxies. Luminosities calculated using equation 3.3 and the same value for H_0, for several classes of galaxies are shown in Table 3.9. Known interacting galaxies have been removed from the comparison sample. (They are included in the interacting one.)

Table 3.9

Nuclear 10μm Luminosities

Class of galaxy	N	Range (L⊙)	Mean (L⊙)	References
Merging	9	$4\times10^{9}-5\times10^{10}$	2×10^{10}	This work
Interacting	24	$4\times10^{7}-7\times10^{9}$	2.5×10^{9}	This work
Seyferts	50	$4\times10^{8}-10^{11}$	4×10^{10}	Rieke (1978)
Starbursts: M82		10^{9}		Rieke and
NGC253		6×10^{8}		Lebofsky(1978)
NGC2903		1×10^{8}		
Bright spirals	17	$10^{5}-7\times10^{8}$	2×10^{8}	"

It is apparent that the 10μm luminosities of the nuclear starbursts in these interacting galaxies are about an order of magnitude larger than those of canonical starburst galaxies such as NGC2903, NGC253, and merging galaxies are more luminous by about another order of magnitude. Of perhaps greater interest is comparison with Seyfert galaxies. The starbursts in merging galaxies are seen to overlap with the more luminous Seyferts, and only a few of the most luminous Seyferts outshine the merging galaxies at 10μm.

In conclusion, not only do strongly interacting galaxies frequently show IR activity indicative of recent bursts of star-formation, but these starbursts are typically about 10 times more luminous than those in non-interacting galaxies. This comparison is even more striking for the merging galaxies, which are among the most luminous IR galaxies known. The star formation activity present in these systems must be at least an order of magnitude more vigorous than in other starburst galaxies. Moreover for six of the merging galaxies (NGC6240, NGC3310, NGC3256, NGC1614, IC883, IC4553) the starburst seems to be extended over scales of several kpc, again significantly larger than other known starburst galaxies. The starbursts in many interacting galaxies and especially in merging galaxies, are indeed "super starbursts".

3.7 Properties of the starbursts in interacting and merging galaxies

The large IR luminosities may be given astrophysical significance by considering the numbers of, and rates of formation of, massive stars required to power them. In order to establish these parameters an estimate of the total (bolometric) luminosities of the galaxies is required. Typical starburst nuclei and HII regions exhibit maximum flux densities between 80 and 150μm, with most of the energy emerging beyond 30μm (Telesco and Harper 1980). Since the IR emission dominates that at other wavelengths, a total IR luminosity is a good measure of the bolometric luminosity. It has been demonstrated that the energy distributions of such star forming regions are sufficiently similar that an extrapolation from 10μm flux to total IR luminosity is accurate to better than a factor of three (Scoville et al 1983). The total IR luminosity can be estimated from the 10μm luminosity using,

$$L_{IR} = 15\ L_{10} \qquad 3.4$$

Thus the merging galaxies have IR (bolometric) luminosities of ~ 6×10^{10} to 8×10^{11} $L_{\odot}$ and the IR luminosities of interacting galaxies range from 6×10^{8} to 1.5×10^{11} $L_{\odot}$. Since the luminosity of an O5 star is ~ 7×10^{5} $L_{\odot}$, the nuclei of the interacing /merging galaxies must contain ~ 10^{3} to 10^{6} such stars. O stars have short (~ 10^{6} years) main sequence lifetimes and large masses, so a high rate of conversion of gas into such stars must be required to maintain the luminosities, and this is estimated in the following section.

3.7.1 Star-formation rates

The total luminosity of a starburst at a given time is determined by the luminosities of the stars formed, the relative number of stars formed in each mass interval, the length of time the starburst has been proceeding, and the overall number of stars formed per unit time. For simplicity, consider the formation of OBA stars in a starburst with a constant star-formation rate that has proceeded for a sufficiently long time so that equilibrium has been established and the death and birth rates of massive stars are equal. The initial mass function, the number of stars formed in the mass range m to m + dm, $\Psi(m)dm$ is normally written as a power law $\Psi(m) = Cm^{\gamma}$, where the constants C and γ depend on the mass range considered (cf. section

1.2.3). In this chapter a Miller-Scalo IMF is used. The luminosity per star and the main sequence lifetime of the stars can also be approximated by power law function of the mass so $l(m) = Am^{\alpha}$ and $tms(m) = Bm^{\beta}$, where l(m) and tms(m) are respectively the luminosity and main sequence lifetime of a star of mass m. The values of A, α, B, β, C and c, given in Table 3.10, are all taken from Telesco and Gatley (1984), upon whose models this analysis is based. The values of C are chosen to make the IMF piecewise continuous between the different mass ranges.

Table 3.10

Power law parameters for starburst models

Parameter	0.1-1.6M⊙	1.6-10M⊙	10-20M⊙	20-60M⊙	References
A	1.3	1.3	8.1	8.1	Allen 1973
α	3.6	3.6	2.8	2.8	Allen 1973
B		4.2×10^{9}	5.9×10^{7}	5.9×10^{7}	Miller and
β		-2.6	-0.8	-0.8	Scalo 1979
C	1	1	5.7	5.7	Miller and
γ	-1.4	-2.5	-3.3	-3.3	Scalo 1979

The total luminosity of the starburst is related to the numbers of OBA stars (1.6-60M⊙) formed by

$$L = K \int_{1.6}^{60} \Psi(m)\ l(m)\ tms(m)\ dm ,$$

where K is the constant that sets the overall magnitude of the star-formation rate. Integrating and substituting A,B,C,α,β,γ for 1.6-10 $M_{\odot}$ stars and 10-60 $M_{\odot}$ stars from Table 3.10,

$$L_{bol} = 7 \times 10^{9}\ K \qquad 3.5$$

The rate dM/dt at which the interstellar medium is converted to early type stars is

$$\dot{M} = K \int_{1.6}^{60} m\ \Psi(m)\ dm$$

from which

$$\dot{M} \sim 2 \times 10^{-10}\ L_{IR} \quad M_{\odot}/yr \qquad 3.6$$

assuming $L_{IR} \approx L_{bol}$.

This star formation rate, which has been estimated using the simplest possible assumptions, would change by about a factor of 2 if a starburst age ~ 10^7 years had been assumed, instead of OBA star formation in equlibrium. For a Miller-Scalo IMF extended to 0.1 $M_\odot$ the total rate of coversion of gas into stars of all mass ranges is about a factor of 3 times higher still

For the values of L_{IR} typical of interacting and merging galaxies, equation 3.6 shows that the ISM is being converted into early type stars at a phenomenal rate of ~ 0.1 to 140 $M_\odot$ yr^{-1}. For comparison the star formation rate in the Galaxy, deduced from observations in the solar neighbourhood, corresponds to ~ 0.003 $M_\odot$ yr^{-1} in a ~ 1 kpc diameter region, similar to that observed for the interacting and merging galaxy nuclei (cf. Miller and Scalo 1979).

3.7.2 Mass-Luminosity Ratios

The masses of the galaxies provide a powerful constraint on the length of time during which the star formation rates derived above can be maintained. Eventually the starburst will consume all of the available mass of gas. The most useful way to parameterise the mass available for star formation is in terms of the mass-to-total-luminosity ratio, M/L. As derived in section 1.2.4, the minimum mass to light ratio which can be maintained by thermonuclear energy generation for about a Hubble time is M/L ~ 1. An unevolved population of stars formed according to a solar neighbourhood IMF and extending from 0.1 to 60 $M_\odot$ has a mass-luminosity ratio < 0.01, while an old stellar population has M/L > 3 (cf. Struck-Marcell and Tinsley 1978). Thus a low value for the mass-luminosity ratio is evidence for significant recent star formation and implies that the star formation must be occuring in a short-lived burst.

So, to investigate the timescales for maintaining the starbursts in interacting and merging galaxies, an estimate of the mass within the region for which an IR luminosity has been derived is needed. Unfortunately, rotation curves from which masses can be estimated are available for only 6 interacting galaxies and 3 merging galaxies. For all of these, our apertures correspond to the region of the rotation curve which can be approximated by a straight line with the velocity at radius r proportional to r. The mass within the volume covered by the 10μm photometry has therefore been estimated from the rotational velocities by assuming a spherical homogeneous mass distribution:

$$M(r) = r\, v^2(r) / G$$

where M(r) is the mass within radius r,
v(r) is the rotational velocity at radius r,
and G is the gravitational constant.

Additionally, a total mass has been estimated for NGC2798 from the HI data of Peterson and Shostak (1977), which gives a total mass for the pair, by assuming that NGC2798 and NGC2799 are of equal mass. Masses for NGC6240 and NGC520 were estimated by assuming their measured line widths are due to doppler broadening due to rotation. Mass-to-light ratios for all these galaxies and references to the data from which the mass was derived are given in Table 3.11 below.

Table 3.11

The ratio of mass to total IR luminosity for 12 interacting galaxies

Galaxy NGC	Arp	M/L (solar units)	Reference
520	157	<0.01[1]	Stockton & Bertola (1980)
1614	186	0.003	Ulrich (1972)
2798	283	<0.4[1]	Peterson & Shostak (1977)
2992	245	0.001	Heckman et al. (1981)
3227	94	0.02	Rubin & Ford (1968)
3256		0.01	Feast & Robertson (1978)
3396	270	0.002	D'Odorico (1970)
3395	270	0.007	"
4088	18	0.02	Carozzi-Meyssonnier (1978)
4194	160	0.03	Demoulin (1969)
6240		<0.08[1]	Fosbury and Wall (1979)
7714	284	0.01	Demoulin (1968)

1) See note in text for method of estimating the mass.

All of the M/L ratios are very small and imply short-lived starbursts. The net rate of consumption of interstellar material in the formation of OBA stars, $\dot{M}_c$, can be estimated by allowing that massive stars ultimately return ~ 75% of their mass to the ISM. So from equation 3.6 above,

$$\dot{M}_c \sim 5 \times 10^{-11} L_{IR} \quad M_\odot/yr.$$

If 10% of the galaxy mass is gas, then the maximum duration t of the starburst is given by $\dot{M}_c\ t = M/10$, where M is the galaxy's mass, and hence

$$t \approx 2 \times 10^9\ M/L_{IR}.$$

So, the mass luminosity ratios of the interacting and merging galaxies imply that their interstellar gas will be consumed in very short timescales, ~ $5 \times 10^6 - 10^8$ years. For most of the galaxies then, if the starburst is to be maintained for periods > 10^7 years, fresh material must be supplied to the nuclear region on this timescale. Silk and Norman (1981) have shown that a galaxy-galaxy interaction can lead to departures from axial symmetry in the gravitational potential of a nucleus, and stimulate mass inflow rates of ~ 1-10 $M_\odot$/yr. Thus an interaction could, in ~ 10^6 years, replenish effectively the gas consumed in the starburst and thereby prolong its life. The duration of a starburst nucleus would then depend on the balance between interaction driven infall of material and the outflow which will result from the large number of supernovae produced in the burst (cf. Loose et al. 1983)

Whether the starburst is consuming gas already in the nucleus or infalling gas, the total mass of stars in the burst must be less than the observed mass. Since most of the mass is in low mass stars, the total burst mass is a sensitive function of the lower mass cut-off to the IMF. Thus the M/L ratio can be used in a more sophisticated analysis, to constrain the lower mass cut-off to the IMF of the star formation if the age of the starburst is known (cf. Rieke et al. 1980). For these interacting and merging galaxies direct information to determine the starburst age is not available. However the following order of magnitude arguement sets a lower limit to the starburst age. All of these galaxies have non-thermal nuclear radio emission, which has been interpreted in section 3.4.3 as arising from young supernovae and supernova remnants associated with the starburst. So in all of these galaxies the starburst must be sufficiently aged for SN to have formed and hence the starburst ages are > 10^7 years (Kronberg et al 1985). This age is therefore used to estimate the mass of stars formed in the starbursts in the interacting and merging galaxies.

In order to limit the lower mass cut-off to the IMF, an estimate of the mass of stars formed during the lifetime of the starburst, for different lower mass cut-offs is needed. For a Miller-Scalo IMF extending from 0.1 to 60 $M_\odot$, 60% of the mass is in stars less massive than 1.6 $M_\odot$ and 93% in stars with masses below 10$M_\odot$ (Telesco 1985). Since these stars have lifetimes longer than or of the order of the starburst age of 10^7 years, a good estimate of the mass of stars formed in the burst can be obtained simply from the star formation rate in $M_\odot$ yr^{-1} and the duration of the burst in years. Telesco (1985) has calculated the ratio $\dot{M}/L$ as a function of the starburst age and lower-mass cut-off to the IMF for a starburst in which the star formation rate is not a function of time. His results for a 10^7 year old starburst are summarised in Table 3.12. From this ratio and the starburst luminosity and age (~ 10^7 years), the total mass of stars formed in the burst can be computed for the various lower mass cut-offs to the IMF. The results for lower mass cut-offs of 0.1, 0.8, 3.2 and 6.5 $M_\odot$ are compared to the masses of the galaxies in Table 3.13. For all except NGC2798 and NGC6240, for which only poor limits to the nuclear mass are available, the total burst masses are about the same as the total mass estimated for the starburst regions if the IMF extends to 0.1 $M_\odot$. However, the starburst mass cannot account for all of the observed mass in the nuclear regions since the galaxies must also have the normal evolved stellar population. Therefore the IMF must have relatively few low mass stars in order to reasonably limit the mass that has been processed by the starburst. For example, since 10% of a galaxy's mass is a generous estimate of the mass of gas which would be available for star formation, it is reasonable to assume that starburst mass must be limited to about 10% of the observed nuclear mass. The tabulated mass which is nearest to 10% of the observed mass is underlined for each galaxy in Table 3.13. It is evident that, for all except the two galaxies with poor mass estimates, the lower mass cutoff to the IMF must be ~ 3 - 6 $M_\odot$ if the starburst mass is ~ 10% of the total mass. So, like the canonical starbursts in NGC253 and M82 (Rieke et al. 1980), the extremely luminous starbursts found in these interacting and merging galaxies have the remarkable feature that the star formation seems to be restricted massive stars only. If the starburst IMF is not restricted in this manner then a starburst model appears not to be a very good fit to the IR luminosities and masses

Table 3.12

M/L for various lower mass cut-offs to the IMF (10^7 year old burst)

Lower mass Cut-off(M⊙)	$\dot{M}$/L x10^{10}(M⊙yr^{-1}L⊙$^{-1}$)
0.1	10
0.8	6
1.6	4
3.2	2.5
6.5	1.2

Data taken from Telesco 1985

Table 3.13

Starburst masses compared to nuclear masses

Galaxy NGC	Mass ($M_\odot$)	Accumulated Starburst Mass, Lower Mass Cutoff ($M_\odot$) 0.1	0.8	1.6	3.2	6.5
520	1×10^9	1×10^9	7×10^8	5×10^8	3×10^8	1×10^8
1614	2×10^9	6×10^9	4×10^9	2×10^9	1×10^9	7×10^8
2798	3×10^{10}	7×10^8	4×10^8	3×10^8	2×10^8	9×10^7
2992	5×10^7	4×10^8	2×10^8	2×10^8	1×10^8	4×10^7
3227	4×10^8	2×10^8	1×10^8	8×10^7	5×10^7	2×10^7
3256	6×10^9	6×10^9	4×10^9	2×10^9	1×10^9	7×10^8
3396	2×10^7	7×10^7	4×10^7	3×10^7	2×10^7	8×10^6
4088	3×10^7	2×10^7	1×10^7	8×10^6	5×10^6	2×10^6
4194	3×10^9	1×10^9	6×10^8	4×10^8	2×10^8	1×10^8
6240	5×10^{10}	3×10^9	2×10^9	1×10^9	7×10^8	4×10^8
7714	1×10^9	1×10^9	6×10^8	4×10^8	3×10^8	1×10^8

of these galaxies. Not only is the star-formation restricted to massive stars, but because the starburst masses are of the same order as the masses of gas available, the star-formation in starburst galaxies must be extremely efficient. This conclusion can also be drawn from the estimates of the gas depletion timescales in the preceeding paragraph.

In the following section the implications of these high rates of star formation for the radio emission from supernovae are discused. The final section of this chapter then examines some of the broader implications of the high star formation rates in these galaxies, with particular reference to merging galaxies.

3.7.3 Radio and infrared emission.

It was suggested in section 3.5.3 that for most of the interacting and merging galaxies detected at 10μm, the radio emission has the spatial extent and spectral index expected if it arises from the supernovae and supernova remnants associated with the starburst. Since the 10μm luminosity is a measure of the number of massive stars formed in a starburst and the radio flux is proportional to the supernova rate which is a function of the number of massive stars, the starburst interpretation of the radio emission implies that there should be a correlation between the 10μm and radio flux densities. Condon et al. (1982) have shown that there is indeed such a correlation for the galaxies in their sample of radio bright spirals. These galaxies have infrared (10μm) to radio (1413MHz) flux ratios of 4 to within a factor of 2. Figure 3.6 is a plot of 10μm flux against flux at 1413MHz for all the interacting and merging galaxies for which radio data is available. For those galaxies without a radio flux measurement at 1413 MHz the flux was estimated from the flux at other frequencies using the measured spectral index. Although there is quite a wide scatter a clear correlation is evident. From the graph it is apparent that for this sample, the galaxies have, on average, an IR to radio flux ratio of ~ 3. This is slightly smaller than the typical value for galaxies in the Condon et al. sample, but it is well within the scatter. Furthermore, for galaxies in the Condon et al. sample this ratio was determined using radio fluxes only for those portions of the sources which lay within the 10μm apertures, and, because the data used for the interacting and merging galaxies was taken from a variety of sources

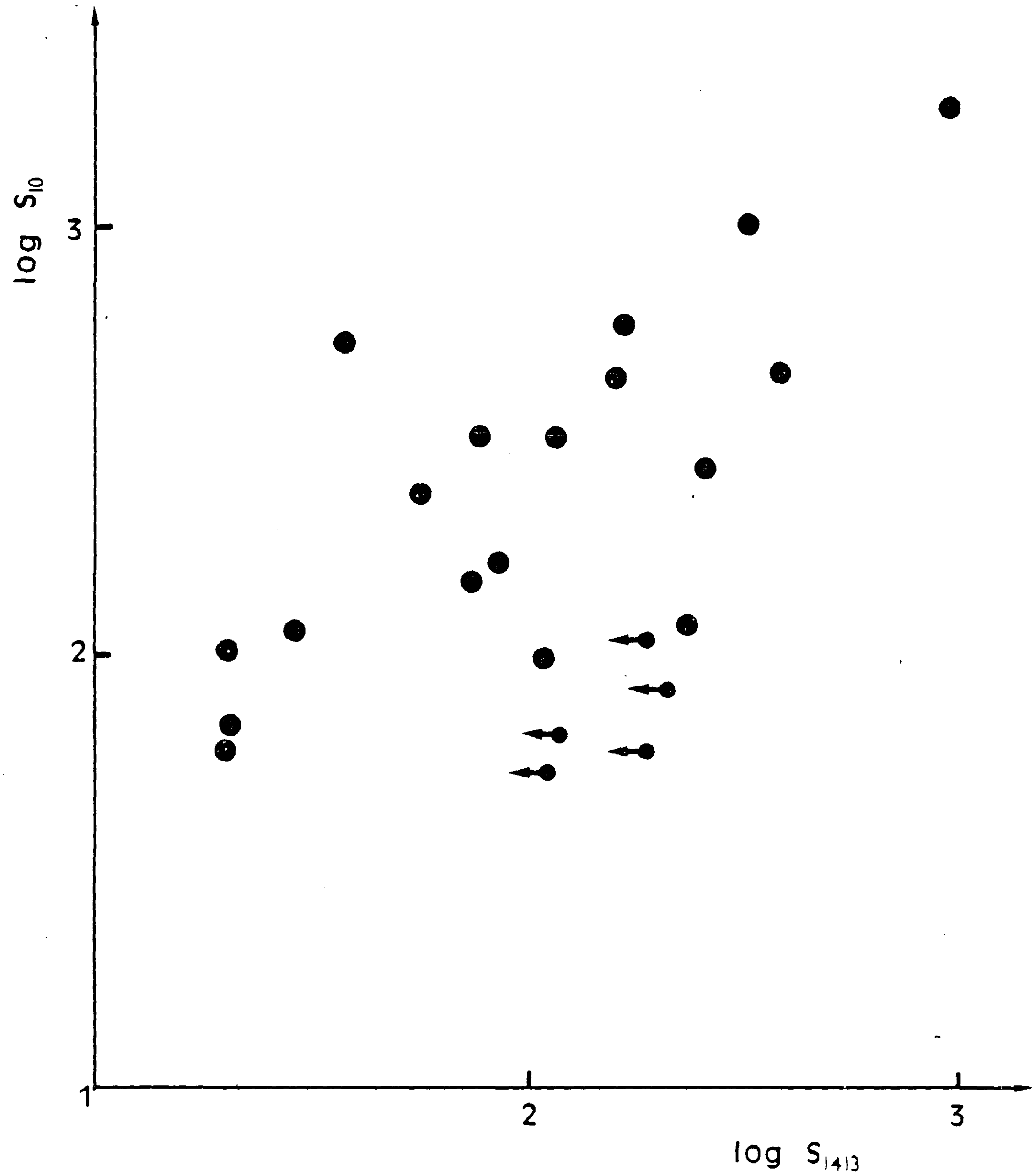

Figure 3.6 The correlation between IR (10μm) and radio (1413MHz) flux densities.

this was not always possible. In general the radio fluxes were tabulated in the literature for regions larger than the 10μm apertures and this may account for the slightly lower value for the IR to radio flux ratio as well as some of the scatter in Figure 3.6. The correlation in Figure 3.5 which spans more than two orders of magnitude in the radio and IR fluxes supports further the starburst interpretation of both the IR and radio data.

The simple starburst models discussed in sections 3.7.1 and 3.7.2 can be used to investigate whether the above relationship is of the right order to be consistent with a starburst model, because the luminosity of the starburst (derived from the 10μm flux) can be used to estimate the number of stars within a given mass range formed per year. Several authors have derived a relation between radio flux density and supernova rate based on the evolutionary models of galactic remnants (e.g. Kronberg and Biermann (1981), Condon et al.(1982), Ulvestad (1982)). For a starburst with a constant star formation rate, such as those discussed above, which is sufficiently evolved (~10^7 years) for supernovae to have occurred, the rates of formation and destruction of OB stars will be in equilibrium. So the supernova rate should be approximately equal to the star formation rate for these types of stars.

There are two types of supernova explosions which occur for different mass ranges of stars. Type 1 supernovae seem to arise from low mass stars with initial main sequence masses of ~ 5 $M_\odot$. However the favoured explosion mechanism involves evolution to a white dwarf, and the time taken to evolve to explosion is very long, ~ 5 x 10^8 to 10^{10} years. (Iben and Tutakov 1984). Such supernovae are therefore extremely unlikely to be associated with an on-going starburst and indeed are thought to be asociated with an old evolved population of stars. Type 2 supernovae evolve from stars more massive than ~ 10 $M_\odot$ and these supernovae are a direct consequence of a starburst.

Following 3.6.1, the number of stars more massive than 10 $M_\odot$ formed per unit time is simply

$$N = K \int_{10}^{60} \Psi(m)\ dm$$

where K is the constant which sets the overall star formation rate. For a 10^7 year old starburst with an IMF extending to 1.6 $M_\odot$, $L \approx 3 \times 10^9$ K (eqn. 3.5) and so substituting in the above with the values for C and γ from Telesco and Gatley (1984), as before,

$$N \sim 4 \times 10^{-12} L_{IR} \quad yr^{-1}$$

Using the relation between bolometric and 10μm luminosity (3.4) and the definition used to calculate the 10μm luminosities (3.3), the supernova rate R estimated from the rate of formation of massive stars derived from the 10μm flux, S_{10}, is

$$R \sim 5 \times 10^{-7} D^2 S_{10} \quad yr^{-1} \qquad 3.6$$

Because their calculation refers specifically to the radio flux at 1413 MHz the relation of Condon et al. (1982) is used to infer the supernova rate from the radio emission. They derive $R \sim L_{1413} / 10^{21}$ yr^{-1}. i.e.

$$R \sim 4 \times 10^{-6} D^2 S_{1413} \quad yr^{-1} \qquad 3.7$$

Equating 3.6 and 3.7 suggests that the IR to radio flux ratio for a starburst should be $\doteq$ 7. Given the large uncertainties in this estimate it is in surprisingly good agreement with the observed ratio of ~ 4. For example the uncertainty in the starburst age introduces an uncertainty of about a factor of 2 in the relation between 10μm flux and supernovae rate. This estimate is also extremely sensitive to the mass range of the IMF of the starburst which was assumed here to be limited to stars of mass greater than 1.6 $M_\odot$ because this seems to be a characteristic feature of starbursts. There are large uncertainties in the radio estimates because the supernovae in a starburst nucleus will occur under drastically different conditions to those for galactic supernovae. For example the supernova rate in M82 directly determined from observations of the variability of individual radio sources which are thought to be supernovae is 1 every 5 years i.e. R ~ 0.2 (Kronberg et al. 1985), whereas the supernova rate obtained by using the Condon et al. (1982) relation is R ~ 0.48. In summary, the proportionality of the radio and IR fluxes in interacting and merging galaxies is of the right order to support a starburst model for both the radio and the IR emission.

The starburst model for these interacting galaxies can be further investigated by calculating a supernova rate from the IR observations. Re-expressing eqn. 3.6 in terms of the 10μm lumimosity of the galaxies gives:

$$R \sim 6 \times 10^{-11} L_{10} \quad yr^{-1} \qquad 3.8$$

For the 10μm luminosities of interacting and merging galaxies in Table 3.8, which range from $4 \times 10^7 - 5 \times 10^{10}$ $L_\odot$, equation 3.8 shows that the corresponding supernova rates will be ~ 0.003 - 3 yr^{-1} . Such rates are not unreasonable compared to estimates of supernova rates derived from the observed number of supernovae, and are comparable to those derived for other starburst galaxies by e.g. Rieke et al. (1980) and Condon et al. (1982). The proportionality of radio and IR emission shows that the radio data is consistent with these supernova rates.

3.8 Discussion

As expected from the good correlation between 10μm luminosity and K-L colour and the results discussed in section 2.5 no correlation was found between 10μm luminosity and the strength of the interaction as measured by the relative separations of the galaxies. However at a very crude level there is evidence for this effect because the 10μm luminosities of merging galaxies are on average 10 times higher than those of interacting galaxies. Because the merging galaxies have a predicted dynamical evolution, and all 10μm data for galaxies which fit the morphological description has been presented, these data can be used to investigate some implications which are relevant to merging, but not to interacting, galaxies. In the following section some of the special consequences of super starbursts in mergers are discussed separately. More generally, the fact that galaxy-galaxy interactions have a drastic effect on nuclear star formation rates has implications for other types of activity and the evolution of galaxies, as described in section 3.8.2.

3.8.1 Consequences of super starbursts in merging galaxies

All of the merging galaxies in the sample are undergoing a super starburst phase, so does this mean that most merging galaxies should be found to be ultra-luminous IR galaxies? The dynamical simulations of Toomre & Toomre (1972) and Wright (1972) suggest that the morphological evidence for a merger in the form of tidal "tails" will persist for times of order 10^9 yr. Since merger candidates whose tidal tails have begun to disappear were selected, the remaining morphological distortions will probably disappear in about 5×10^8 yr (cf. Toomre 1977). Models of rapid star formation episodes result in starburst lifetimes of $\sim 10^8$ yr. Given the uncertainties in these numbers, it is likely that a significant fraction of the galaxies recognisable as mergers from the morphological criteria outlined in section 3.4 will be found in the super-starburst phase in their evolution, providing the super starburst is triggered at a late stage in the merger evolution.

Despite the relatively narrow age range of the merger sample, it seems to be possible to account for some of the spread in luminosities within the sample in terms of the age of the merger process. In Table 3.11 the luminosities of the galaxies are listed in a rough order of age. The faintness of the tidal "tails" and the degree of coalescence have been used as indicators of relative merger age, as was done by Toomre (1977). Although such an ordering is somewhat subjective, it is rather clear that NGC520 must be one of the youngest mergers in this group, since it is the only member of the sample in which two velocity systems are present in the spectra. NGC3310 must also be the oldest, since it has no tails remaining at all, and its "shells" or "ripples" indicate a very late stage in a merger (cf. Schweizer 1983). Comparing the IR luminosities in Table 3.11 it is apparent that the two youngest and the two oldest mergers are less luminous than the five "middle-aged" mergers.

Table 3.14

Luminosities of merging galaxies in order of increasing age

Galaxy	$L_{IR}(L_\odot)$
NGC520	1×10^{11}
NGC2623	1×10^{11}
NGC3256	6×10^{11}
NGC1614	6×10^{11}
IC883	4×10^{11}
NGC6240	5×10^{11}
IC4553	7×10^{11}
NGC4194	1×10^{11}
NGC3310	6×10^{10}

The appearance of an extremely luminous starburst as the natural consequence of a merger may also be significant for theories of the origin of (some) elliptical galaxies. Toomre (1977) and others have argued from the expected stellar velocity distributions and luminosity profiles of merger remnants that merging galaxies evolve into objects resembling elliptical galaxies. However, if this suggestion is correct, there must be some way for the embryonic elliptical galaxy to divest itself of the gas belonging to the galaxies before they merged. The super starburst phase of merger evolution can provide the mechanism for this. Massive, early-type stars produced in the starburst will end their lives as supernovae. Galactic winds driven by these supernovae may then sweep the galaxy free of gas (Matthews & Baker 1971). As Graham et al. (1984) have shown in the case of NGC3256, an exceptionally extended starburst with a bolometric mass-to-light ratio less than unity (solar units) can provide sufficient mechanical energy for ejection of all the gas in its vicinity. It is evident from Table 3.9 that the mass-to-light ratios of the merging galaxies NGC6240, 520, 1614 and 4194 are similar to NGC 3256, and substantially less than 1. If the M/L ratios and spatial extent are similar for the other merging galaxies in the sample, the remnant objects from all these mergers will be severely gas-depleted. Provided the other arguments relating mergers to ellipticals are valid, then it seems inevitable that these merging galaxies will indeed become indistinguishable from elliptical galaxies.

3.8.2 Wider implications of interaction induced starbursts

The fact that interacting galaxies have been shown to have IR active nuclei which are most likely to be due to a luminous burst of star formation, suggests that interactions may be important for other types of activity and galaxy evolution. These consequences are now briefly discussed.

Firstly, since interactions have been shown to trigger nuclear starbursts they can fuel other types of activity too. This is important, because, as described by Gunn (1979), the gas consumption rates necessary to provide the luminosities of nearby quasars by accretion onto a compact object are so high that there should be no low redshift quasars left. Such quasars are observed however, and this is where interactions may be involved. An interaction may trigger or re-trigger the activity in nearby quasars either by stripping gas from a companion or by perturbing existing gas into the nucleus i.e. by the same dynamical processes which are probably the explanation of the starbursts frequently found in interacting galaxies. Recently evidence has emerged that interactions are indeed associated with low redshift quasars. In a sample of 45 such quasars Hutchings and Campbell (1983) find 6 cases in which there is a bridge of material between a QSO and a neighbouring nucleus, a further nine with bridges that lack only redshift confirmation and in addition about 30% of the sample have nearby companions at the same redshift. The fact that interactions between galaxies are observed to trigger starburst activity greatly supports the suggestion that this interacting nature of nearby quasars is not a mere coincidence.

Secondly, interactions are likely to have played a major role in determining the evolution of most galaxies. About 2% of galaxies are observed to have morphological disturbances such as bridges and tails which indicate an ongoing interaction (Toomre & Toomre 1973). However such features are generally short lived with maximum lifetimes of $\sim 5 \times 10^8$ years. Thus if the current rate of interactions is representative, as many as 40% of all galaxies may have experienced a strong tidal interaction with a neighbour, for which the obvious results have died away. In fact the number of interactions in the past may have been much higher than the current rate suggests. The probabilty of a galaxy interacting is proportional to the number density of galaxies n, and,

$$n \propto (1 + Z)^3$$

So at higher redshifts a much larger fraction of all galaxies are interacting. The situation is slightly more complicated than this because at higher redshifts the peculiar velocities are also higher,

$$v_{pec} \propto 1 + Z$$

and there will be some time at which the increased probability of interaction due to the higher velocities will be negated by the fact that interactions are less effective at high velocities. However these simple order of magnitude arguments indicate that interactions must frequently occur in the evolution of galaxies at high redshifts. Thus it would not be surprizing if a greater proportion of high redshift galaxies show evidence of interaction induced activity. Furthermore, the frequecy of present day interactions, an extrapolation to higher redshift and the short timescales in which the morphologically obvious effects die away, all indicate that many apparently normal galaxies could have had a strong interaction in the past. The results presented in this chapter have shown that interactions between galaxies are associated with luminous IR emission arising from dust heated by young stars produced in a recent burst of star formation. So, since many "normal" galaxies are likely to have been interacting, an interaction induced starburst is probably common phase in the evolution of most galaxies. Star formation processes control the chemical evolution of galaxies, and since interaction induced starbursts are 1 - 2 orders of magnitude more luminous than starbursts triggered by other processes, with correspondingly higher star formation rates, interactions between galaxies must play a major role in determining metallicities and metallicity gradients. Previous starbursts, triggered by an interaction, might even be an explanation of the frequent occurence of Liner nuclei in apparently normal spirals (e.g. Keel 1983) because Terlevich and Melnick (1985) have argued that Liner type spectra are associated with old evolved starbursts. Finally, if galaxies have massive haloes then they are much more likely to interact, and star formation triggered by interactions may thus be even more frequent than the above discussion suggests. Understanding the processes of interaction induced star formation is fundamental to understanding the current properties of galaxies themselves.

3.9 Summary and Conclusions

Observations of interacting galaxies at 10μm confirm and quantify the results of the JHKL survey interacting galaxies. A good correlation was found between K-L colour, which was used as an index of IR activity in Chapter 2, and 10μm luminosity, thereby substantiating the major conclusions of this chapter. From the shape of the continuum spectra, the spatial extent of the IR and radio emission and the optical emission line intensities the energy source powering the IR luminosity is probably a massive burst of recent star formation. The IR luminosities of interacting galaxies are on average about an order of magnitude larger than those of typical starburst galaxies. This may be because the interaction can provide significantly more fuel to the nuclear region or because tidal compression may result in more efficient use of the fuel, or both. The subset of interactions which have resulted in the merger of two disc galaxies are the most luminous galaxies in the sample, by about an order of magnitude. i.e. they are about 100 times more luminous than "normal" starbursts. The IR luminosities of the merging galaxies exceed those of most classes of galaxies and rival those of the most luminous Seyfert galaxies.

Simple models of starbursts show that star formation rates in OBA stars of 1 - 140 $M_\odot$ yr^{-1} are required to maintain the high IR luminosities of these galaxies. For those galaxies for which mass estimates are available the starburst will consume the gas in ~ 10^7 years, unless there is significant refuelling of the nuclear region by gas from the disc. The star formation in these galaxies must be extremely efficient and the models suggest that the IMF of the starbursts in interacting and merging galaxies must be truncated at least to stars of mass > 1 $M_\odot$, a feature which Rieke et al (1982) also derive for the canonical starbursts in M82 and NGC253. Finally, the relative strengths of the radio and IR emission from these galaxies is consistent with the starburst models and supernova rates of ~ 1$M_\odot$ yr^{-1} are predicted on the basis of the IR luminosity.

Although no correlation between 10μm luminosity and separation of the pair of interacting galaxies was found, the fact that merging galaxies are found to be the most luminous galaxies is evidence that the amount of activity triggered does indeed depend on the strength of the interaction, as might be expected. For the merging galaxy sample there seems to be a suggestion of a rise and fall of star formation rate with merger evolution. One consequence of the super starbursts in merging galaxies is that the remnant of the merger may be swept free of gas by winds driven by supernovae resulting from the starburst, thus lending further support to suggestions that mergers will evolve into objects resembling elliptical galaxies. More generally, the frequent occurence of interaction induced star formation and the higher likelihood of interaction in the past suggests that interactions between galaxies have played an important part in the evolution of a significant fraction of all galaxies.

The observations presented in this chapter have been used to develop a general description of the properties of an interaction or merger driven starburst. It is qualitatively similar to, but quantitatively much more luminous than, other starbursts. In the following chapter more detailed observations of the ultraluminous merging galaxy NGC6240 are presented. These observations provide a clue to the processes by which an interaction may trigger such luminous starbursts.

CHAPTER 4

THE SUPER STARBURST IN NGC6240

In a study of a large number of interesting objects there is bound to be at least one which seems to merit special attention. As a result of the detailed investigation of Fosbury and Wall (1979) the merging galaxy NGC6240 was included on our observing lists early in 1983. In the course of checking preliminary lists of IRAS sources in Nature to see if any of the interacting galaxy sample were included, the IRAS source 1650+024P04 in Circular 4 was identified with NGC6240. The coordinates of the IRAS source agree with those of the galaxy to within 3" and examination of the Palomar sky survey plates showed that NGC6240 was the only visible non-stellar object in the 1 arcmin IRAS error box for the source. The IRAS measurements showed that this galaxy was one of the most luminous IR galaxies yet discovered, and a follow up programme of IR photometry and spectroscopy was immediately embarked upon.

In this chapter the details of the infrared emission from NGC6240 are described and used to develop a simple picture of the possible role of the merger in triggering a super starburst. Our IR photometry is analysed in section 4.2, the nature of the strong radio emission from NGC6240 is discussed in section 4.3, and in section 4.4 the results of IR spectroscopy and their implications are analysed. Finally, a simple model for the physical processes in NGC6240 is presented.

4.1 Description of NGC6240

The physical picture of NGC6240 which emerges from optical and radio studies is that of a merger between two gas rich galaxies. Photographs presented by Fosbury and Wall (1979) reveal that it is an extremely chaotic galaxy, with a prominent dust lane and three long plumes extending from the central region. CCD images obtained by Fried and Schulz (1983) show two distinct nuclei separated by ~ 2 arcsec. NGC6240 is a very strong radio source and the two nuclei are also clearly evident in the 4885MHz VLA maps of Condon et al. (1982). The optical spectra show intense emission lines arising from a region at least 10" in extent, and the optical emission line intensity ratios are thought to be indicative of shock excitation (Fosbury and Wall 1979, Fried and Schulz 1983). The two nuclei, the suggestion of shock excitation on large scales, and the morphological characteristics of this galaxy are all good evidence that this system is the result of a close interaction in which two colliding spiral galaxies have merged.

4.2 The infrared continuum spectrum

4.2.1 Results of IR photometry.

Photometry of NGC6240 was obtained using UKIRT in February 1984. As described in section 3.2, the peak of the emission at K was used as the position for longer wavelength photometry. This position was measured as accurately as possible (~ 2") relative to a nearby guide star and David King of RGO then measured the position of the guide star to a fraction of an arcsecond for us. Within the measurement errors the position of the IR source coincides with the nuclei described above. We are unable to distinguish between the two nuclei, since both fall within our ~ 4" aperture.

The results of 10 and 20μm photometry of NGC6240 at the position of the K peak are given in Table 4.1, along with the IRAS photometry published in Catalogued Galaxies and Quasars Observed with the IRAS Survey (1985). The UKIRT data was calibrated as described in section 3.2. The quoted photometric precision for this data is the signal-to-noise level achieved, the systematic errors being small compared to the statistical uncertainty. Calibration of the IRAS data is thought to be accurate to 4, 6, 6 and 10% at 12, 25, 60 and 100μm respectively. Much larger calibration errors ≥ 15% may arise at 60 and 100μm for very cold (T≤30K) sources due to uncertainties in the cut-off wavelengths of the filters and detectors. From the shape of its spectrum the fluxes for NGC6240 are unlikely to be affected by this. The errror on the mean flux from several scans of NGC6240 (the tabulated flux) was 4-8% at 12 and 25μm and 8-12% at 50 and 100μm. The catalogue source quality classification scheme showed no indication of confusion by other sources (none of the confusion flags were set) and the cirrus flags indicated that contamination of the fluxes by cirrus was very unlikely. Thus, aside from colour corrections, it is reasonable to assume that the IRAS fluxes for NGC6240 are accurate to ~ 8% at 12 and 25μm and ~ 12% at 60 and 100μm, and this is the precision quoted in Table 4.1.

Table 4.1

Photometry of NGC6240

Wavelength (μm)	Aperture	Flux (mJy)
10	4"	124 ± 15
20	4"	1100 ± 120
12	0.75'x4.5'	570 ± 46
25	0.75'x4.6'	3520 ± 280
60	1.50'x4.7'	23210 ± 2785
100	3.00'x5.0'	25880 ± 3106

4.2.2. Interpretation of the IR luminosity

The nuclear 10μm luminosity of NGC6240 inferred from the UKIRT photometry is 1.2×10^{10} $L_{\odot}$, assuming a Hubble constant of 50 km s^{-1} Mpc^{-1} and using the measured redshift of 7597 km s^{-1} (de Vaucouleurs, de Vaucouleurs & Corwin 1976). The continuum spectrum of NGC6240 showing the UKIRT photometry and the IRAS measurements together with published optical and radio data is drawn in Figure 4.1. Integrating this spectrum using the trapezoidal rule gives a bolometric luminosity of 1.9×10^{12} $L_{\odot}$. Almost all of this energy is emitted in the IR, with the optical and radio emission contributing ~ 10% of the total. This far-infrared data, in comparison with bolometric luminosities for canonical starburst and Seyfert galaxies, emphasises the results of section 3.5 for the 10μm luminosities of merging galaxies, i.e. the merging galaxy NGC6240 has a bolometric luminosity ~ 60 times larger than archetypal starburst galaxies such as M82 and NGC253 for which L_{bol} ~ 4×10^{10} $L_{\odot}$ (e.g. Rieke et al. 1980), and an oder of magnitude larger than the total luminosity of the Seyfert galaxy NGC1068 (cf. Telesco et al. 1984). The luminosity of NGC6240, ~ 2×10^{12} $L_{\odot}$, is comparable to that of Mkn231 and the ultra-high luminosity "IRAS" galaxies discussed by Houck et al. (1985), which have luminosities in the range 0.5 - 5×10^{12} $L_{\odot}$. Thus the IRAS results for NGC6240 show that its luminosity ranks it amongst the most luminous galaxies known.

Like all the galaxies discussed in section 3.5 the most basic question about NGC6240 is whether its luminosity is produced predominantly by an active nucleus or by an exceptionally strong burst of star formation. For NGC6240 in particular, both the shape of the infrared continuum emission and the inferred extent of the emission at 10μm provide an indication of the nature of the source powering the extreme luminosity, as discussed below.

The quasi-thermal IR continuum emission, evident in Figure 4.1, dominating the flux at shorter and longer wavelengths by 2 or 3 orders of magnitude and peaking near 100μm, is typical of that observed from known starburst galaxies. The recent work of Lawrence et al. (1985), in which the 1-20μm emission from samples of different classes of galaxy is contrasted, can be used to make the above comparison more quantitative. Empirically they find that type 1 Seyfert galaxies fit a power law ($S_\nu \propto \nu^n$) of index 1 to 1.5 from 1 to 10μm while Liners and Starburst galaxies have spectra dominated by the old stellar population in the near infrared and then fitted approximately by a power law from ~ 5 - 20μm. However, for the Liners the index of the power law fit ranges from 1 to 1.5 whereas for the starburst galaxies it lies in the range 2 to 4. For NGC6240 the rise from L through 20μm fits a power law of index 2.5, and on this basis the infrared continuum spectrum is most likely to have a starburst origin.

As described in section 3.5, the extent of the 10μm emission from the nucleus of a galaxy, in the absence of "Sellgren" grains, can also be used to infer whether a recent burst of star formation is likely to be powering the observed luminosity. Although there are no direct measures of the spatial extent of the IR emission in NGC6240, the extent at 10μm can be estimated as follows. Comparing the 10 and 20μm nuclear fluxes in a 4 arcsec aperture with the IRAS photometry at 12 and 25μm in a beam of approximately 1 arcmin diameter (Table 4.1), suggests that about half of the mid-IR emission comes from a region outside the central 4 arcsec. However because of the large apertures of the IRAS photometry this result does not distinguish between spatially extended nuclear emission (a starburst), a generally enhanced star-formation rate across the whole galaxy (with or without a compact nuclear source) or giant extra-nuclear HII region(s) such as that seen in NGC3690/IC694 (Gehrz et al. 1983). Rieke et al. (1985) have recently measured a 10μm flux of 250 ± 10 mJy in a 5.8 arcsec aperture

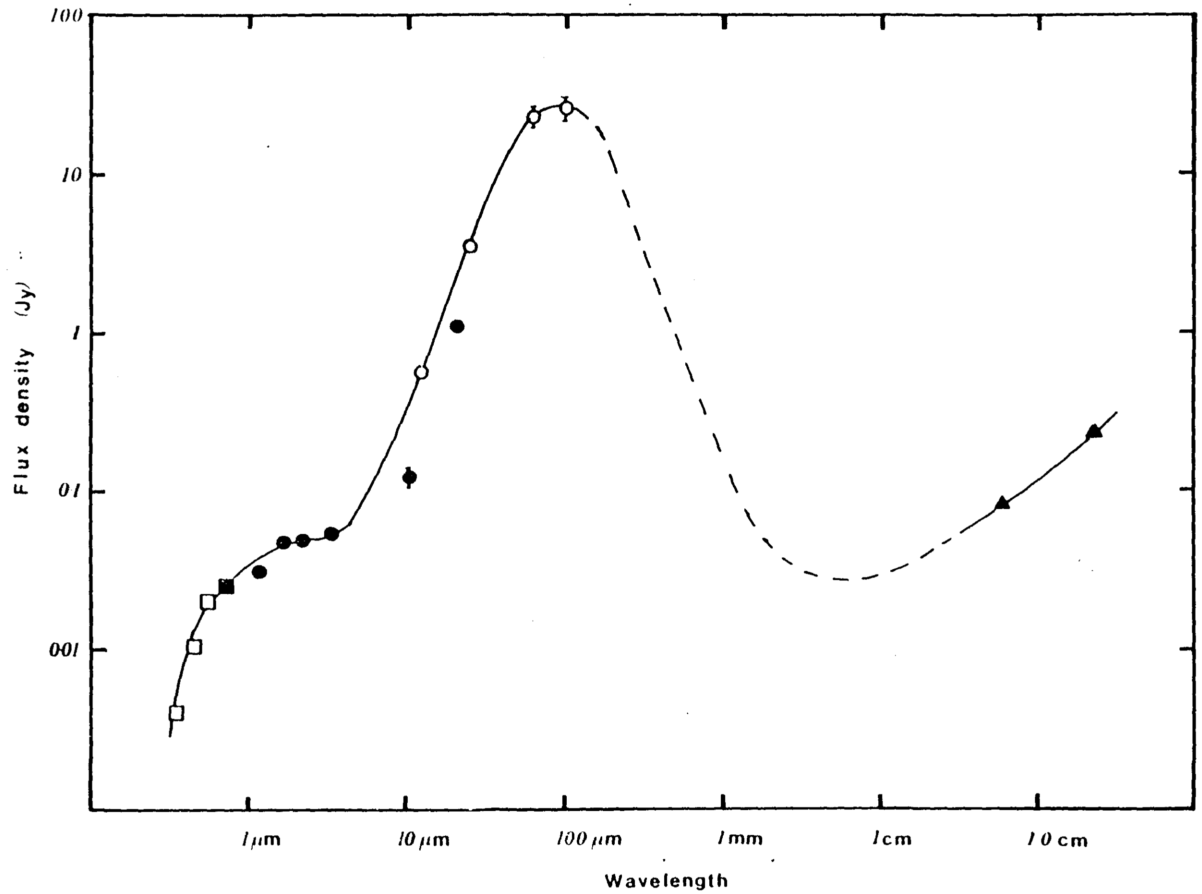

Figure 4.1 Continuum spectrum of NGC6240. Data are from: ● , Tables 2.1 and 4.1; ○ , Catalogued Galaxies and Quasars observed in the IRAS Survey, JPL, 1985; □ , Fosbury and Wall (1979); ■ , Fried and Schulz (1983); ▲ , Condon et al. (1982). The dashed interpolation is a Rayleigh-Jeans Spectrum with emissivity proportional to λ^{-1} joined smoothly to the data at longer and shorter wavelengths. For points plotted without error bars, the uncertainty in the flux is smaller than the size of the dots.

on the nucleus of NGC6240. Although this aperture may not be centred concentrically with the UKIRT measurements, comparing this result with those in Table 4.1 indicates that the nuclear 10μm source must be at least 6 arcsec in extent. Only about half of the IRAS lumimosity is associated with this region. At the distance of NGC6240, 6 arcsec corresponds to 4.5 kpc. Substituting the bolometric luminosity (2 x 10^{12} $L_{\odot}$) of NGC6240 in equation 3.2, a central compact luminosity source could heat dust in radiative equilibrium sufficiently for it to radiate at 10μm out to only ~ 10 pc. Thus the spatial extent of the 10μm emission from NGC6240 tends to rule out the possibility that the thermal IR emission arises from dust heated by a single compact object in the nucleus, as has been suggested for some Seyfert galaxies. As discussed in section 3.3, provided the dust in NGC6240 is not predominantly small grains, distributed luminosity sources are required to power the nuclear 10mm emission, and this fits naturally with a starburst origin for the luminous infrared continuum emission. Additionally, the IRAS results suggest that star formation is extended beyond the 4.5 kpc "nuclear" region observed by Rieke, although about half of the luminosity arises in this region.

In summary, the infrared luminosity is most easily understood as arising from a massive burst of star formation, in which the radiation from young, early-type stars is thermalised by dust and re-radiated in the IR. This starburst is about two orders magnitude more luminous than the most luminous non-interacting starburst galaxy NGC253 and is extended over an enormous region in excess of 4 kpc.

4.3 The radio emission from NGC6240

Non-thermal radio emission from interacting galaxies was used in section 2.4 to strengthen the interpretation of K-L excesses in terms of a recent burst of star formation, while in section 3.7.3, the relation between the 10μm and radio (1440 MHz) flux densities for a starburst was discussed. Since the extreme luminosity of NGC6240 has been interpreted above in terms of one of the most luminous and extended starbursts known, it is particularly interesting to examine the possibility that the radio emission from NGC6240 is also a consequence of this super starburst.

The radio luminosity of NGC6240, ~ 1 x 10^{23} W Hz^{-1} sr^{-1} at 1410 MHz, is exceptionally high for a "normal" galaxy and approaches that of the powerful radio galaxies (Fosbury & Wall 1979). It exceeds by about an order of magnitude the enhanced radio luminosities of interacting galaxies found by Sulentic (1976) and Hummel (1981). Condon et al. (1982) included NGC6240 in their VLA study of the radio emision from bright spiral galaxies and their maps show that the radio emission is co-extensive with the region of intense optical emission. As discussed in section 3.7.3 other bright radio galaxies in the Condon et al. sample have an IR (10μm)-to-radio (1445 MHz) flux density ratio of ~ 4, and most of the interacting galaxies are consistent with a ratio of ~ 3. This empirical relation can be understood in terms of a starburst model in which the radio emission arises from supernova remnants associated with the starburst. Comparing the 10μm flux density in Table 4.1 with the radio flux density for NGC6240 measured by Condon et al. for the central 5 arcsec gives a ratio of 0.5. Thus even relative to the high infrared luminosity of its starburst, NGC 6240 is over-luminous in the radio by almost an order of magnitude compared to the typical radio emission observed from other starburst galaxies. Evidently a simple starburst model is inadequate for NGC6240 and an additional energy source for the radio emission may be required.

Because they interpret the optical emission from NGC6240 in terms of shock excitation due to the merger (section 4.5), Fosbury and Wall (1979) suggest that the strong radio emission in NGC6240 is due to relativistic particles accelerated in the shock fronts. They argue that the unusually strong (> 6%) polarization of the radio emission from NGC6240 is evidence in favour of a mechanism such as this. Additionally it is physically reasonable that material will be shocked by the disruption that accompanies the merging of two galaxies. For pre-shock conditions with $B \sim 10^{-5}$ G, $N_e \sim 1$ cm^{-3} and a shock velocity of ~ 500 km s^{-1} Fosbury and Wall show that the radio emission from NGC6240 can indeed be provided by a collision-induced shock. This interpretation appears to be more consistent with the small IR-to-radio flux density ratio in this galaxy than a simple starburst model.

4.4 Near-infrared spectroscopy

The infrared photometry of NGC6240 and the radio and optical observations suggest that two processes are occurring with great vigour. There seems to be a starburst of extraordinary luminosity, coexisting with strong merger induced shocks. In order to find out more about the physical conditions in NGC6240, near infrared spectroscopy of the nucleus was obtained. The aims of this spectroscopy were two-fold. Firstly, observations of the near-infrared lines of molecular hydrogen might strengthen greatly the tentative evidence for large scale shocked regions in this galaxy, as outlined below. Secondly, observations of infrared hydrogen recombination lines would enable us to deduce more detailed properties of the starburst itself.

4.4.1 Molecular hydrogen emission

Infrared lines from hydrogen molecules arise from rotation-vibration transitions. The energy level diagram in Figure 4.2 summarises the notation used in describing the transitions from which individual lines arise. Observations of these lines in galaxies have only just become possible with the advent of sensitive spectrometers on large telescopes because, since they arise from electric quadrupole transitions, they are relatively faint ($A \sim 10^{-7}\ s^{-1}$). Atmospheric absorption limits the lines which can usefully be observed; Figure 4.3 shows the commonly observed molecular hydrogen lines which fall in the K-window.

Two important astrophysical mechanisms for producing vibrationally excited molecular hydrogen are: (a) inelastic collisions with atoms or molecules in a hot (T>1000K) gas (e.g. shocked gas) and (b) near-ultraviolet pumping in the electronically excited Lyman and Werner bands, followed by radiative cascade through the excited vibrational and rotational levels of the ground electronic state. For collisional excitation the population of the levels is thermal and determined by the temperature and density of the gas. A strong line, easy to observe in both cases, is the v=1-0 S(1) line at λ = 2.122μm. Table 4.2 shows the expected intensity ratios of other K-window lines to the v=1-0 S(1) line in the cases of UV and shock excitation for densities $\sim 10^3\ cm^{-3}$.

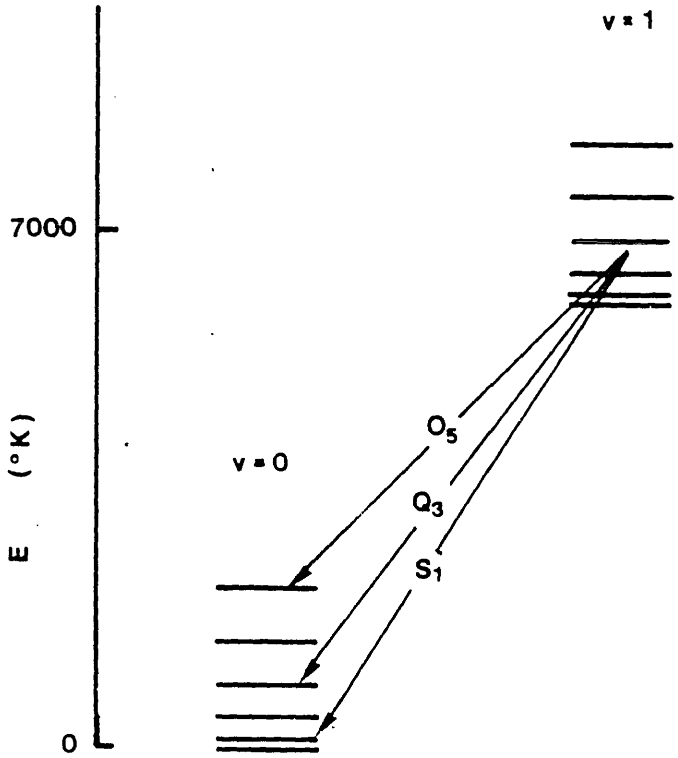

Figure 4.2 The three types of electric quadrupole rotation - vibration transitions of H_2. (Rotational levels are not to scale).

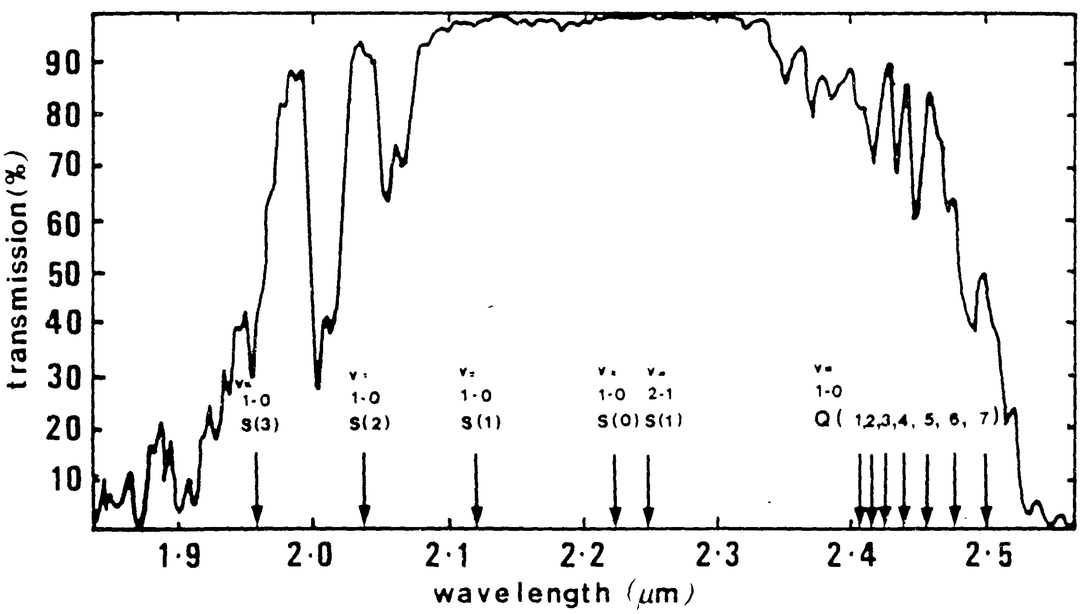

Figure 4.3 Commonly observed H_2 lines in the K window. The model atmospheric transmission spectrum is from Mountain (1983).

Table 4.2

Expected IR H_2 line ratios

Line	Shock(1) (10km/s)	UV pumping(2)
v=1-0S(0)	0.22	0.67
v=1-0S(1)	1.0	1.0
v=1-0S(2)	0.36	
v=1-0S(3)	0.95	
v=1-0Q(1-7)	2.4	2.7
v=2-1S(1)	0.10	0.55

(1) Hollenbach and Shull 1977

(2) Black and Dalgarno 1976

Infrared lines of H_2 have been detected from star formation regions in molecular clouds, planetary nebulae, a supernova remnant, the galactic centre and (as of June 1984) the galaxies NGC1068 and NGC3690. The Orion nebula is one of the most studied examples (Beckwith 1981). All of these are thought to be examples of collisionally excited H_2. In the case of star-forming regions the excitation is interpreted in terms of shocks due to the molecular outflows. For the two extragalactic detections, the H_2 emission is thought to originate in the large number of star-forming regions in these galaxies i.e. the integrated H2 emission from ~ 10^6 Orions is being observed.

Since we have inferred a very luminous starburst in NGC6240, it is reasonable to expect that there will be H_2 emission from the star-forming regions in the starburst, as is the case for NGC3690 and NGC1068. Additionally, since it is likely that material has been shocked during the merging process, it might be possible to detect H_2 emission due to more than just the starburst in NGC6240 and thereby strengthen the observational evidence for large scale shocks in this galaxy. So, the attempt to measure H_2 emission from NGC6240 was made with the aim of obtaining more detailed insight into physical processes in this galaxy.

4.4.2 Spectroscopy of NGC6240

Spectra centered on the v=1-0 S(1) and v=2-1 S(1) lines of H_2, redshifted to the recessional velocity of NGC6240, were measured at UKIRT in April 1984 using a 7 channel cooled grating spectrometer (CGSII) (Wade 1983) with a spectral coverage of ~ 0.023μm and a 5" aperture. Spectra centered on the redshifted Pa α hydrogen recombination line were also taken with this system at the same position. Paschen α was measured because Brackett α, at a rest wavelength of 4.051μm, is at the edge of the atmospheric transmission window at the redshift of NGC6240. Wavelength calibration and the instrumental resolution of 550 km s^{-1} were derived from observation of Brackett γ (λ = 2.166μm) in the planetary nebula NGC7027. This spectrum is shown in Figure 4.4. The spectra were ratioed with spectra of the star BS5447, which was observed at a similar airmass to NGC6240, to remove atmospheric extinction and absorption features. BS5447 is of type F2V and therefore did not show H recombination lines in absorption (which would create artificial emission features when the spectra were ratioed). This was especially important because Brackett γ is very close to the redshifted wavelength of the v=1-0 S(1) line in NGC6240. The H_2 results are discussed in the following section, while the recombination line results are presented in section 4.4.4.. A more detailed discussion of the implications of these results follows in section 4.5.

4.4.3 Molecular hydrogen in NGC6240

The full spectrum obtained for the v=1-0 S(1) line (the "S(1) line") measurement is shown in Figure 4.5. The S(1) line is clearly detected and, by comparison with Figure 4.4, also resolved. The width of the line ~ 800 km s^{-1} was estimated by assuming that both the instrumental profile and the line shape are Gaussian. The integrated line flux is (15 ± 1) x 10^{-17} W m^{-2} and for H_0 = 50 km s^{-1} Mpc^{-1} this corresponds to a luminosity of ~ 10^8 $L_\odot$. The luminosity in the S(1) line for NGC6240 of 10^8 $L_\odot$ may be compared with the luminosities of 3 x 10^6 and 3 x 10^7 $L_\odot$ in this line for NGC1068 and NGC3690 (Thompson et al. 1978, Fischer et al. 1983). Again, NGC6240 is extremely luminous compared to other galaxies. The data can be used to develop the following physical picture of the H_2 excitation in NGC6240.

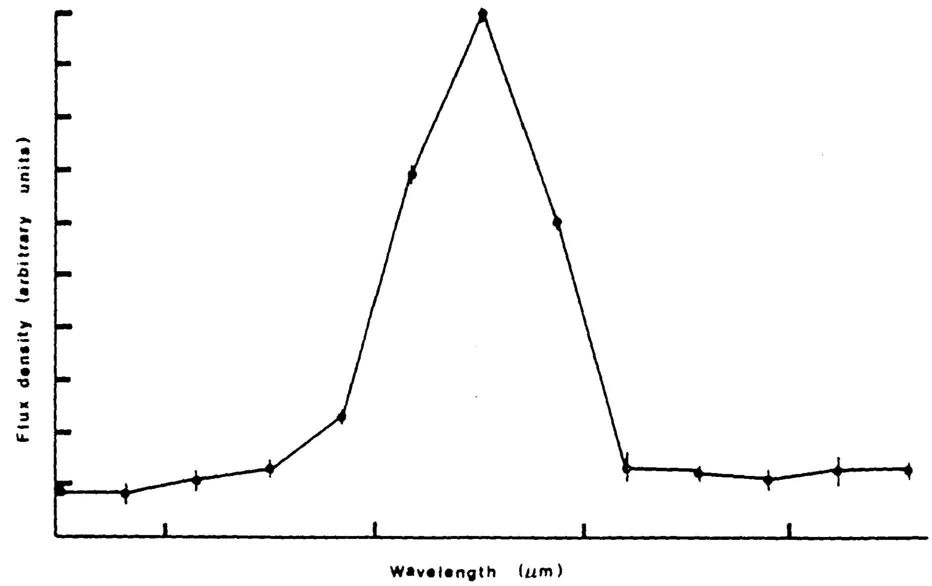

Figure 4.4 Brackett γ in NGC7027.

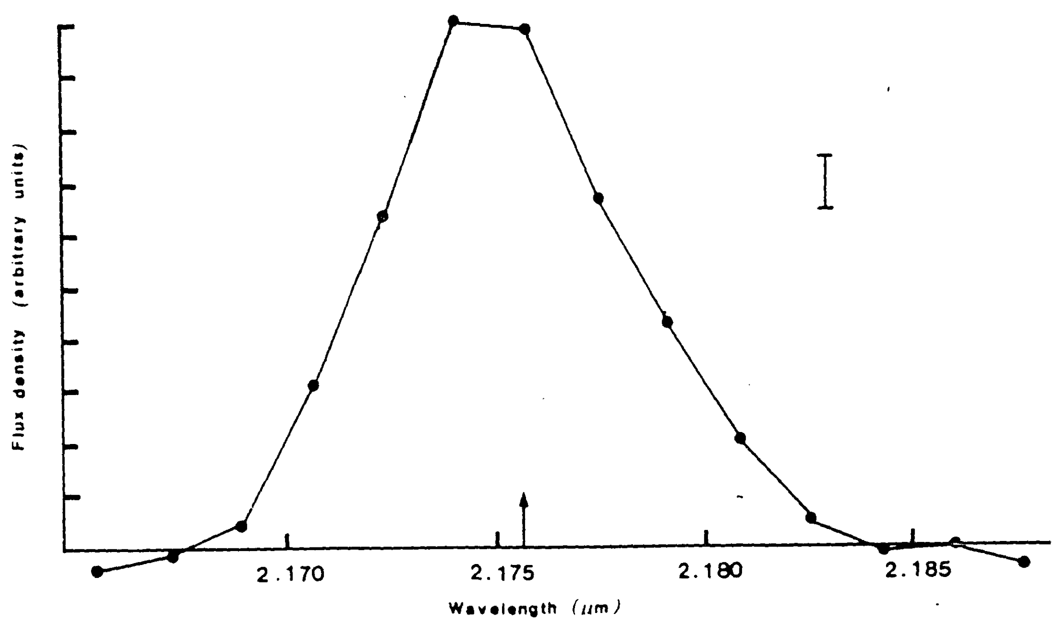

Figure 4.5 The v=1-0 S(1) line of H_2 in NGC6240. A typical 1σ error bar is indicated by the vertical bar. The arrow shows the wavelength of the 2.122μm v= 1-0 S(1) line of H_2 redshifted to the radial velocity of the galaxy. The spectrum has been ratioed with the standard, smoothed using a triangular function, and the continuum has beeen subtracted off.

Firstly, this gas is almost certainly excited by shock-heating as is the case for virtually all known examples of H_2 quadrupole emission. In NGC 6240, the width of the S(1) line (~ 800 km s^{-1}) is identical to the widths of optical emission lines seen in a similar aperture on the nucleus, and which are thought to be shock-excited (Fosbury and Wall 1979). Fluorescence following absorption of UV photons is considered to be the most plausible alternative mechanism for excitation of these rotation-vibration levels (section 4.4.1). In this case, the v=2-1 S(1) line should have about half the intensity of the v=1-0 S(1) line (Table 4.2). However, the v=2-1 S(1) line in NGC6240 was not detected at a sensitivity similar to that reached for the S(1) line detection, the 1σ upper limit being 4×10^{-17} Wm^{-2}. Although this limit is not strong it suggests that UV pumping is unlikely to contribute significantly to the excitation. It should be noted however that in the near-UV pumping models of Black & Dalgarno (1976) the line ratios were calculated assuming a local density n ~ 10^3 cm^{-3}. The line ratios become very sensitive to n if n ~ 10^5 - 10^6 cm^{-3}, when inelastic collision times become shorter than the radiative cascade lifetimes. In this situation the v=2 level population is suppressed by collisions: a v=0 molecule collides with a v=2 molecule and produces two v=1 molecules. For a T ~ 1000K gas these "resonant" vibrational transfers have rates many orders of magnitude larger than for transfer of vibrational to kinetic energy (Chu 1977). Thus for dense gas and near-UV pumping a v=2-1 S(1) line strength substantially less than that predicted by current models is possible. In view of this, the measured limit to the v=2-1 S(1)/v=1-0 S(1) line intensity ratio in NGC6240 cannot rule out the possibility that most of the H_2 is UV excited. In the following paragraph a simple analysis of the energetic requirements for near-UV pumping of the observed S(1) luminosity in NGC6240 is presented.

On absorption of a NUV (912-1100Å) photon an H_2 molecule either spontaneously decays to the vibrational continuum (~ 11% of the time) or to the bound vibrational states, where it cascades to v=0 (89%). For every cascading molecule there is a 1-3% chance that it will fall through a particular channel in the 1-0 band such as S(1). (Black and Dalgarno 1976). So if ~ 2% of the cascades result in a 1-0 S(1) photon, ~ 55 NUV photons must be supplied by the exciting source per S(1) photon. Moreover, for a typical cloud composition, H_2 molecules absorb at most 25% of the incident NUV flux; the rest is absorbed by dust

(Jura 1974, Hollenbach and Shull 1977). So the luminosity required to be emitted in the NUV in terms of L(S(1)), the observed luminosity in the 1-0 S(1) line, is

$$L \approx 55 \times 20 \; L(S(1)) \times 100/25 ,$$

since an 0.1μm photon has 20 times the energy of a 2μm photon. O-type stars emit about 25% of their total luminosity in the NUV (Hollenbach and Shull 1977) and so the total luminosity must be at least

$$L \approx 1.8 \times 10^{4} \; L(S(1))$$

For NGC6240, $L(S(1)) = 1 \times 10^{8} L_{\odot}$ and so the luminosity of NGC6240 in O stars must be $> 1.8 \times 10^{12} L_{\odot}$, if the H_2 is UV pumped. The ground-based 10 and 20μm photometry gives the appropriate luminosity for the nucleus of NGC6240 in an aperture similar to that used for the H_2 measurements. These data give an IR continuum shape similar to the large aperture IRAS data and extrapolating the spectrum implies a total luminosity of $\sim 0.5 - 1 \times 10^{12} L_{\odot}$. This is at best about half the above estimate of the luminosity in O stars needed to pump the H_2. Furthermore, this estimate is conservative and makes no allowance for filling factor; all of the NUV radiation from all of the stars is assumed to be incident on H_2 molecules. Thus even if all the luminosity of NGC6240 arises from O stars, there seems to be insufficient UV radiation to excite the H_2 by NUV pumping. Additionally, as discussed in section 4.4.4 the H recombination line measurements suggest that very little of the luminosity of NGC6240 may be provided by O stars. In conclusion, it is unlikely that NUV pumping contributes significantly to the excitation of the H_2 in NGC6240, and shocks remain as the most likely excitation mechanism.

Secondly, the mass of hot gas may be estimated by assuming local thermodynamic equilibrium at a temperature of ~ 2000K (Shull 1982). The V=1-0 S(1) line luminosity is related to the H_2 mass by

$$L(S(1)) = f \; A \; h\nu \; \frac{M(H_2)}{2 \; m_p}$$

where,

f is the fraction of hot molecules in the v=1, J=3 level

A is the Einstein spontaneous decay probability of the transition

$h\nu$ is the energy of the transition

m_p is the proton mass

and $M(H_2)$ is the mass of excited gas.

Substituting, $A = 3.5 \times 10^{-7}\ s^{-1}$ (Turner et al. 1977) and (for T~ 2000K) $f = 1.22 \times 10^{-2}$ (Scoville et al. 1982),

$$\frac{M(H_2)}{M_\odot} = 1.47 \times 10^{-3} \frac{L(S(1))}{L_\odot}$$

The luminosity of $10^8\ L_\odot$ then implies a mass of excited molecular gas of ~ $10^5\ M_\odot$ in NGC6240.

Thirdly, simple energetic arguments can be used to investigate the source driving the shocks. The gas cools to a temperature <1000K in about 3 years (Kwan 1977), so in NGC6240 the shock excites about $3 \times 10^4\ M_\odot$ of gas per year. The force $\dot{m}v$ required to drive such a shock at a speed of ~ 20 km s^{-1} is ~ 5×10^{36} dynes. By comparison, the radiation pressure, L/c, of this ultraluminous galaxy is ~ 10^{35} dynes. Despite the high luminosity, radiation pressure is clearly insufficient to drive the shocks which excite the H_2.

In section 4.2 the high IR luminosity of NGC6240 was interpreted in terms of a starburst of exceptional extent and intensity. An obvious mechanism for driving the shocks is mass outflow from the early type stars in the starburst. The ratio of the luminosity in the S(1) line to the total IR luminosity can be used to investigate the expected contribution of this process to the H_2 excitation in NGC6240. It should have a characteristic value if the H_2 is excited by mass outflow from young stars, and the IR luminosity is provided by the luminosity of the same stars thermalised by dust and reradiated in the IR. The ratio L(S(1))/ L(IR) is listed in Table 4.3 for Orion (Beckwith 1981), a "typical" star-forming region in the Galaxy, and NGC6240. As described above, an IR luminosity of $5 \times 10^{11}\ L_\odot$ is estimated to be the luminosity of the nucleus of NGC6240 in an aperture comparable to that used for the S(1) observations and this was therefore used in calculating the ratio for NGC6240. For comparison the table also includes the L(S(1))/L(IR) ratios for the other two galaxies for which H_2 has been detected (Thompson et al. 1978, Fischer et al. 1983) Table

4.3 shows that all the objects, with the exception of NGC6240 could be excited by mass outflow from star-forming regions similar to Orion. NGC6240 is clearly the exception by a factor of 10 or more, and this excess of shocked gas over that expected from star-forming regions alone is what might be expected when two gas rich galaxies merge.

Table 4.3

The ratio of luminosity in the S(1) line to total IR luminosity

Object	Ratio (L(S1)/LIR)
NGC6240	20×10^{5}
Orion	1.2×10^{5}
NGC3690	3×10^{5}
NGC1068	0.9×10^{5}

Since star-forming regions can account for only ~1/10 of the observed S(1) luminosity, it is likely that most of the H_2 excitation is due to cloud-cloud collisions during the merger. However, can the mechanical energy in a galaxy-galaxy colllision provide enough energy to heat the H_2 gas? Assuming a galaxy mass of ~ 10^{12} $M_{\odot}$, 10% of which is gas, and a relative velocity between the colliding galaxies of ~ 500 km s^{-1}, then this process supplies an energy of ~ 3 x 10^{59} ergs. For an efficiency of 0.002 in coupling shock energy into the S(1) line (Kwan and Scoville 1976), the mechanical energy in the collision can excite the gas at the observed rate for a time ~ 6 x 10^{7} years, which is a reasonable timescale compared to the lifetime of the merger process.

There are several important conclusions to be drawn from these H_2 measurements. Firstly, NGC6240 is an example of a merging galaxy and we have evidence for shocks driven by the tidal forces accompanying the violent dynamical relaxation. How common might such a phase of vigorous H_2 excitation be among merging galaxies generally? NGC6240 was chosen for observation because of its high IR luminosity and other peculiar features and so it is difficult to generalise on the basis of this galaxy. However, the dynamical simulations of Toomre and Toomre (1972) and Wright (1972) suggest that the tidal tails resulting from an interaction may persist for periods of the order of 10^{9} years. This is much longer than the 6 x 10^{7} years estimated above for the time that merger driven shocks can excite the H_2 gas and despite the uncertainties in this estimate the duration of H_2 excitation powered by the merger is unlikely to be much longer than 10^8 years. So if these timescales are even approximately correct, we would expect that only ~ 10% of the galaxies recognizable as mergers from their morphologies are currently under going a phase similar to that in NGC6240. Secondly, the existence of massive quantities of shocked molecular gas may have profound consequences for the efficiency and/or nature of star formation (cf. section 1.3) in these galaxies. In the following sections H recombination lines are used to derive more detailed parameters of the starburst itself and the optical data is re-examined in the light of the IR results. All of this information is then used in a discussion of the relation between the merger, H_2 emission and the starburst.

4.4.4 Recombination lines in NGC6240.

Perhaps one of the most intriguing results of the IR spectroscopy was the failure to detect the Paα hydrogen recombination line from NGC6240. The 1σ limit achieved for this line was 9×10^{-21} W cm^{-2}. Becklin et al. (1984) have independently achieved a similar result and they have a 1σ upper limit for Brγ of 0.2×10^{-20} W cm^{-2}. This is about 3 times brighter than the limit set by the above measurement of Paα, which corresponds to a Brγ flux of 7.5×10^{-22} W cm^{-2}, for case B recombination theory (Paα/Brγ = 12). In the following the 1σ upper limit to the Brγ flux from NGC6240 is therefore taken to be 7.5×10^{-22} W cm^{-2}.

Because it is difficult to avoid the conclusion that the IR luminosity of NGC6240 is due to a massive burst of star-formation this limit is surprisingly low. Table 4.4 shows the expected ratio of the luminosity in Brγ to the bolometric luminosity for HII regions excited by stars of different spectral types. This has been calculated using case B recombination theory (Osterbrock 1974, Giles 1977) and the data for early type stars in Panagia (1973).

Table 4.4

The ratio L(Brγ) to L_{tot} for ionisation by different stellar classes

Type	Ratio ($\times 10^{-5}$)
O5	22
O7	15
O9	9.4
B0	3.2
B0.5	0.56
B1	0.13

Using the luminosity of NGC6240 in a 5" aperture similar to the one used for the recombination line measurements, ~ 5×10^{11} $L_\odot$ (cf. 4.4.3), the upper limit derived above implies a limit to this ratio for the galaxy of

$$L(Br\gamma)/L_{bol} \leq 8 \times 10^{-6}.$$

This corresponds to the ratio expected from stars of type ~ B0, and thereby implies that there are very few of the hot O-stars normally associated with starbursts in NGC6240. There are several possible explanations of this result, which are difficult to distinguish between, given the current observations.

Firstly, it may simply be that the star-burst in NGC6240 is hidden behind a heavy degree of extinction. To acount for the observed limit to Brγ with obscuration would require about three magnitudes of extinction at K. If most of the luminosity arises from stars of type O5-O7, as might be expected for a starburst, A_V must be ~ 30 magnitudes, and this seems large compared to the reddening in other IR galaxies, e.g. NGC253 has A_V = 15 (Rieke et al. 1980). Secondly, the starburst may have had an IMF with fewer high mass stars. However this explanation would be contrary to the results found for all other starburst galaxies to date, in which it seems that the formation of low mass stars is suppressed (e.g. Rieke et al. 1980). Alternatively, a large population of B-stars could result if the starburst has aged sufficiently that all the O-stars formed initially have now ended their evolution, leaving the accumulated population of B-stars to power the luminosity. This would require $\geq 2 \times 10^8$ such stars to have formed in NGC6240. It is clear that more data is required to distinguish these possibilities and in particular a reliable measure of the extinction is of great importance. In the following section the nature of the excitation conditions in the optical spectrum are discussed and the implications for the starburst described.

4.5 Optical emission lines

There are two reasons why it is of interest to re-examine the optical data for NGC6240 in the light of the results from the infrared spectroscopy and photometry. Firstly, optical emission lines are a potentially powerful probe of the physical conditions under which they arise and therefore can be used to distinguish between various types of nuclear activity e.g. is Seyfert, starburst, Liner or shock emission dominating the optical spectrum? Secondly, the interpretation of the spectrum and the luminosity in the H recombination lines may illuminate the case presented above, which shows there is little evidence of early-type stars in NGC6240.

Several authors have obtained optical spectra of the nucleus of NGC6240 (Fosbury and Wall 1979, Fried and Schulz 1983, Heckman et al. 1983, Reike et al. 1985). However, only that of Fosbury and Wall (1979) has absolute flux calibration and lists a full table of the relative strengths of all the lines detected, and so this is the data used in the following discussion of line ratios. Fried and Schultz (1983) do have good spatial resolution and have resolved [NII] (λ 6548 & 6584 Å) from Hα over the entire region, and so their data is used where necessary to supplement the Fosbury and Wall (1979) data.

The forbidden-oxygen line ratios for NGC6240 resemble those of the Liners as defined by Heckman (1980). Using the reddening-insensitve line ratios in the classification scheme of Baldwin et al. (1981), NGC6240 is well within the region of "shock-excited" sources. Since this classification scheme was developed it has become very unclear whether galaxies with this type of spectrum are indeed collisionally excited or excited by a power-law non-thermal continuum with a low-ionisation parameter, similar to that which is generally believed to heat and ionise the emission line gas in both type 1 and 2 Seyfert galaxies (cf. Halpern and Steiner 1983). Currently, photoionisation by a non-thermal continuum is thought to be the more plausible because on many diagnostic diagrams (eg. [OIII]5007/Hβ vs. [OII]3727/[OIII]5007) the Liners are shown to form a natural sequence with Seyferts and Quasars with the ionisation parameter as the discriminating variable. However the possibility that both mechanisms are operating to different degrees in different objects cannot be ruled out (Aldrovandi & Contini 1983). NGC6240 is not included in any of the samples used in these analyses and on many of these diagrams would be at the extreme extent of the scatter. In other words it may not quite have a typical Liner spectrum. In Table 4.5 the measured line strengths relative to Hβ for NGC6240 from Fosbury and Wall (1979) are compared with the predictions of a) a model HII-region ionised by a O5 star (Stasinska 1982) b) the power-law photoionisation model of Ferland and Netzer (1983) which best fits the mean Liner spectrum, and c) shock models of Raymond (1979) for shocks of 120 km s^{-1} and 50 km s^{-1}. While it is obvious that the HII-region does not fit the data at all well, both the photo-ionisation and shock model (120 km s^{-1}) provide a reasonable fit. The shock model is perhaps a little better at fitting the spectrum if one recognises that a range of shock speeds would be physically more reasonable. While a clear distinction between the two models is dependent on observations of weak lines such as HeI (5876) or UV-lines (Ferland and Netzer 1983) for which there is no data for NGC6240, there are a number of other reasons why the shock model may be preferable for NGC6240.

Firstly, neither the emission line luminosities nor their spatial extent in NGC6240 are typical of Liners. From Heckman (1980), L(Hα) is typically $10^{39.5-41.5}$ erg s^{-1} whereas for NGC6240 L(Hα) is $10^{42.7}$, a factor of 10 higher. Ferland and Netzer (1983) derive the extent of the emission line zone from their model to have a radius ~ 130 pc, which is of the same order as the observed extent for those liners in which has been measured. Even if the increased luminosity of NGC6240 is attributed to an increase in the luminosity of the central source providing the ionising continuum, their model can only provide the ionisation over a region with ~ 1.3 kpc radius. In contrast both Fried and Schultz (1983) and Fosbury and Wall (1979) show that the emission lines in NGC6240 extend over a region of ~ 14 arcsec which corresponds to ~ 10 kpc, and Fried and Schultz (1983) demonstrate that the ionisation does not fall off in the extra-nuclear regions. Secondly, the emission lines are broad with widths ~ 700 km s^{-1} over regions much

Table 4.5

The optical lines from NGC6240 compared with models

Wavelength	Ion	Intensity (Hβ = 100) NGC6240	HII region	Liner Photoionisation	Shock v = 50kms^{-1}	Shock v = 120kms^{-1}
3727	[O II]	1230	191	640	1467	593
3869	[Ne II]	31	45		<1	42
4340	Hγ	34	47	47		
4363	[O III]	≤25	7.7	25	<1	26
4861	Hβ	100	100	100	100	100
4959, 5007	[O II]	180	670	290	5.4	570
5199	[N I]	43			7.6	26
5755	[N II]	<10			7.7	40
6300, 6363	[O I]	141	2.5	96	29.4	206
6563	Hα	300	280	310	320	299
6548, 6584	[N II]	525	16	160	311	240
6717, 6731	[S II]	262	25	250	156	170

larger than the relatively compact (~ 100 pc or so) broad line regions of Seyfert galaxies and again it is difficult to provide for this with the photo-ionisation models. Both of these features can be readily explained by a shock model in which clouds of shocked material are distributed and in bulk motion over the galaxy. Since there is also strong evidence for large quantities of shocked material in NGC6240 from the H_2 measurements, the optical spectrum is probably best understood in terms of shock excitation. The optical spectrum then indicates that much faster shocks than are necessary to excite the H2 are present. This point is discussed in more detail in the following section.

The optical emission lines can also be related to the IR recombination lines discussed in section 4.4.4. Fosbury and Wall derive Av = 4 from the ratio of Hα to Hβ and corrected for this extinction, their Hβ line flux is 6.5×10^{-20} W cm^{-2}. From case B recombination theory Brγ/Hβ = 0.028 so that the expected Brγ flux is ~ 1.8×10^{-21} W cm^{-2} which is comparable to the 2σ IR limit of 1.5×10^{-21} W cm^{-2}. However it should be noted that because essentially all of the optical emission could be accounted for in terms of shock excitation, any Brγ emission detected may also have a shock contribution. This makes the limit on the nature of the stars in the starburst even more stringent.

4.6 Discussion

NGC6240 is the result of a recent merger of two gas-rich spirals. Its infrared emission is best understood as arising from a starburst of exceptional extent and intensity, and implies a star-formation rate at least an order of magnitude higher than other starburst galaxies. Massive quantities of shocked molecular gas, in excess of that expected from star-foming regions alone, are observed and it is likely that the gas has been shocked directly as a result of the tidal disruption accompanying the merger of two galaxies. The optical spectrum also indicates shock excitation on large scales in this galaxy. All of these features are consistent with what might be expected when galaxies merge, and they provide a clue to the detailed mechanism by which the merging process may engender a massive burst of star-formation, as outlined below.

Firstly, the optical spectrum can only be understood in terms of shock excitation if the shock velocities are high (~ 100 km s^{-1}). If two gas-rich galaxies approach each other at a relative velocity of a few hundred km s^{-1}, as the galaxies begin to merge fast shocks of velocity ~ 100 km s^{-1} are induced in the gas due to cloud-cloud collisions. The merger of two galaxies is a violent event in which fast shocks, as evidenced by the optical spectrum of NGC6240 are to be expected. Further, since clouds will also be dragged through the diffuse gas in the galaxies almost all of the gas might reasonably be expected to be shocked. For shocks of ~ 100 km s^{-1}, the post shock gas is raised to a temperature of ~ 10^5 K. Since H_2 has a dissociation energy of only 4.48 eV (i.e. T ~ 7000K) any H_2 present before the interaction will be destroyed by such shocks. This is apparently in contradiction to the large quantities of molecular gas observed in NGC6240.

However, Draine and Salpeter (1979) have shown that a significant fraction of refractory dust grains survive shocks up to ~ 300 km/s. Hollenbach & McKee (1979) argue that this conclusion remains valid for densities up to ~ 10^7 cm^{-3}. These dust grains will provide sites for post-shock formation of H_2. Hollenbach & McKee go on to show that if the initial density is ≧ 10^3 cm^{-3} and the shock velocity is < 300 km/s, the post-shock gas can be fully molecular. Our detections of H_2 imply that 3 x 10^4 $M_\odot$ yr^{-1} are shocked in NGC6240. For any reasonable lifetime assumed for this process, it is evident that an efficient mechanism for H_2 formation, such as that discussed by Hollenbach and McKee, must be operating.

For a shock of 100 km s^{-1}, the post-shock gas can reach densities as high as 10^6 cm^{-3} and cool to temperatures as low as 100K, conditions which are highly conducive to star formation. The dense H_2 will rapidly cool, collapse, and fragment, producing a burst of star formation. Under such conditions gas could be converted into stars with exceptional efficiency, thus producing an episode of extremely luminous star formation. The dust required for the formation of the H_2 will thermalise the radiation from the newly formed stars and re-radiate it in the IR. Since the gas clouds experiencing these shocks will be distributed across the central regions of the two merging galaxies, the rapid star formation activity will have unusually large spatial extent. These are all characteristics of the super-starburst in NGC6240.

This picture of interaction-induced shocks which then trigger an unusually luminous starburst in a merging galaxy is physically coherent and plausible. However there remains at least one fundamental unanswered question concerning the details of this process. In NGC6240 we do not observe the H recombination radiation expected from the starburst. Some of the possible implications of this result for the starburst in NGC6240 are now described.

It is difficult to reconcile the suggestion made in section 4.4.4 that the starburst is evolved to such an extent that only B-stars remain, with the fact that we are still seeing evidence of the shocks which, as descibed above, are likely to be an efficient trigger for the starburst. However, it may be that a detailed model could account for these features in terms of a star formation rate which is now reduced (but still vigorous) compared to the rate at an earlier stage of the merger, with the B and A stars from this previous stage still producing a substantial luminosity.

To understand the low limit to the Brγ emission in terms of reddening involves a complex geometry for dust extinction in which $A_V \sim 30$ to the young stars, while the shocked regions only suffer an extinction $A_V \sim 4$, with which the (shock excited) optical line intensities are consistent. If the extinction to both the inferred starburst and the shocked gas is as high as $A_V \sim 30$, the mass of excited H_2 derived in section 4.4.3 is increased to 1.5×10^6 $M_\odot$ and the mechanical energy in a galaxy-galaxy collision can excite the gas at this rate for only $\sim 4 \times 10^6$ years. Compared to the lifetime of the merger process, this is much less reasonable than the earlier estimate of $\sim 6 \times 10^7$ years. The greater the extinction to the shocked H_2, the harder it becomes to explain its excitation. It is therefore unlikely that the shocked gas is seen through the same reddening necessary to account for the relatively low Brγ flux by extinction.

An "evolved" starburst model or a complex dust geometry could account for the observed properties of NGC6240 using a starburst involving star formation which has signatures not unlike those observed for Galactic HII regions or the spiral arms of other galaxies. Instead, it is possible that, because of the difference between conditions within the chaotic, shocked nuclear regions of NGC6240 and the ambient conditions surrounding Galactic star-forming regions, the hot young stars fail to produce their expected number of HII-regions. For example, repeated shocks and efficient post-shock cooling may have resulted in a density so high that there is self-shielding by the H_2 over a large region, and most of the gas remains in molecular form, despite the hot stars. If this is so then other nuclear starbursts, especially in merging or interacting galaxies might be expected to have similar features.

Alternatively, the IMF of the burst may have been determined by the extreme conditions in the nucleus, and the formation of high mass stars inhibited. In general, it seems that the conditions in the nuclei of other galaxies result in star-formation in which the production of high mass stars is enhanced relative to low mass stars (cf. sections 1.3.4 and 3.6.2). Shields and Tinsley (1976) have shown that a high metallicity inhibits the formation of high mass stars and the gas involved in the star-burst in NGC6240 may be enriched from star-formation in the disks of the two original galaxies. Such an IMF would be radically different from that observed in all other known starburst galaxies in which enriched material may equally well be involved. There is therefore no reason to prefer this scenario to the evolved starburst, extinction or self-shielding explanations of the low Brγ flux.

Finally, there is the possibility that the IR luminosity of NGC6240 is produced by a population of small dust grains, heated by a compact nuclear source. Small grains that suffer temporary heating to high temperatures by the absorption of a single photon have been proposed by Sellgren (1984) as an explanation of the 2 - 5μm emission from planetary nebulae. This type of grain heating differs from conventional heating in radiative equilibrium, in that the grain temperature less dependent on the distance to the source of radiation. So the extended 10μm emission discussed in section 4.2.2 might be produced by a compact source heating the dust. The low level of H recombination radiation could be explained if the nucleus was hidden behind a large amount of extinction. However, as for a reddened nuclear starburst, in this scenario the shocked H_2 gas must lie in a region outside of this extinction. Moreover, other properties of NGC6240 do not fit a model in which a compact active nucleus is the dominant source of luminosity. The optical line ratios, even if dereddened by tens of magnitudes, are not like those observed from

Seyfert galaxies and quasars (cf. section 4.5 and Figure 3.5). In addition the relationship of the extended steep spectrum radio source to the compact nucleus would have to be explained.

It is clear that determining in detail the physical conditions in the nucleus of NGC6240 will require a quantitative model linking all of the observed features. In general the observations are more consistent with a starburst coexisting with merger-driven shocks than with a compact nucleus, although this possibility cannot be entirely ruled out with the data presented in this chapter. Some observations which may illuminate further the nature of the inferred starburst in NGC6240 are suggested in the following chapter.

In conclusion, although some of the details of the starburst in NGC6240 are not understood, the molecular hydrogen observations have permitted a simple outline of how a merger may trigger a super-starburst to be presented. Since the conditions in merging galaxies are an extreme example of those in interacting galaxies in general, and the starbursts triggered in interacting galaxies appear also to be more vigorous than those in "normal" starburst galaxies (section 3.4) it is possible that similar processes operating at a lower level are also responsible for the frequent occurence of starbursts in interacting galaxies.

CHAPTER 5

SUMMARY, CONCLUSIONS AND SUGGESTIONS FOR FURTHER WORK

Interactions between galaxies lead to a redistribution of material and may thereby provide fresh fuel, either to feed a nuclear accretion disk or to maintain a starburst. Interacting galaxies should therefore be a seminal class of objects to study to further understanding of IR activity. The work presented in this thesis constitutes one of the first systematic studies of IR activity in interacting galaxies.

In order to elucidate the astrophysics of interaction triggered activity, near and mid-infrared photometry and near infrared spectroscopy were obtained and used to examine the frequency, luminosity and characteristics of IR activity in interacting galaxies. JHKL photometry is a rapid and efficient technique for identifying galaxies likely to exhibit IR excesses at longer wavelengths. In addition the near-infrared colours permit a preliminary assesment of the most likely underlying energy source for the IR luminosity. Longer wavelength photometry at 10 or 20μm provides a quantitative estimate of the total IR luminosity and hence the intensity of the activity. Near infrared spectroscopy allows a more detailed study of the physical conditions in the nucleus and can further illuminate the underlying mechanism for the IR luminosity. In the following section the astrophysical results, obtained by bringing the first two of these techniques to bear on representative samples of interacting galaxies and using the latter technique to study an extreme example, are summarised.

The major result of this survey is that interactions are extremely effective in triggering nuclear activity which seems most likely to be due to a recent burst of star formation. There is IR activity, evidenced by a red K-L colour or luminous 10μm emission, for one member of nearly every pair. Furthermore, the fact that the activity is seen in only one member of an interacting pair is physically consistent with what would be expected on the basis of the dynamical models of Toomre & Toomre (1972) and others, if the interaction is providing the fuel. From the JHKL colours and the shape of the mid-IR continuum spectra, the IR emission in these galaxies is the result of thermal emission by dust of an underlying continuum. The spatial extent of the IR emission, the extent and spectral index of the radio emission and the optical line ratios all consistent with a recent burst of star formation as the most plausible source of the infrared excesses. Thus it seems that galaxy-galaxy interactions are an efficient means of triggering starburst nuclei.

An equally important result is that the inferred starbursts in interacting galaxies are about an order of magnitude more lumnious than those of previously known starburst galaxies. Moreover, the morphologically defined subset of interactions in which a merger of two disk galaxies has occured are the most luminous galaxies in the sample i.e. they are 100 times more luminious than typical non-interacting starburst galaxies. Star formation rates of 1 - 140 $M_{\odot}$ yr^{-1} are required to power the high IR luminosities of the interacting and merging galaxies, and supernova rates of ~ 1 yr^{-1} are predicted. The radio data is consistent with this supernova rate, providing further support for the starburst interpretation. For a few of the interacting galaxies there is sufficient data to derive the model dependant result that, like the canonical starbursts in M82 and NGC253, the IMF of the star formation must be restricted to stars more massive than about 1MG.

NGC6240 is an example of one of the merging galaxies in the survey, and IRAS observations show that it is one of the most luminous galaxies known. A non-detection of IR hydrogen recombination radiation at the expected level in this galaxy shows that a simplistic starburst interpretation of the properties of interacting galaxies may not always be applicable when more refined observations are obtained. However this non-detection does not rule out a starburst as the major source of IR luminosity, for NGC6240 or other galaxies in the sample (if they have H recombination lines like NGC6240), although it does complicate this interpretation. The detection of 10^8 $L_{\odot}$ in the v=1-0 S(1) line of H_2, corresponding to a mass of ~ 10^5 $M_{\odot}$ of excited molecular gas in NGC6240, provides the first clue to the mechanism by which interactions between, and mergers of, disk galaxies may cause such luminous starbursts. Shocks generated in the interaction result in rapid and efficient formation of H_2 on the surfaces of dust grains and this dense gas very quickly engenders a burst of star formation. The dust grains on which the H_2 formed thermalise the radiation of the hot young stars and reradiate it in the IR, providing the luminous IR emission which is a characteristic feature of interacting and merging galaxies.

As well as showing that interactions are efficient triggers of unusually luminous IR activity, suggesting a mechanism by which the interaction triggers a starburst, and showing that mergers are extreme examples of this process and ultraluminous IR galaxies, there are a number of other characteristics of interaction induced starburst activity which are apparent as a result of this work. Firstly, in "M51-like" systems the compact companion seems to be more likely to aquire material from the larger galaxy and undergo a burst of starformation than vice-versa. Secondly, there is evidence of a delay of ~ 10^8 years after the time closest approach for the starburst activity in some systems. In the case of merging galaxies there is some suggestion of a rise and fall of star formation rate with merger evolution. One interesting consequence of the super starbursts found in merging galaxies is that the remnant of the merger is likely to be swept free of gas by the winds driven by the resulting supernovae, and this lends furhter support to suggestions that mergers will evolve into objects greatly resembling elliptical galaxies.

The above precis presents a physically consistent and plausible interpretation of the data in this thesis. However, this interpretation is not always generally accepted because the interaction could be providing the material to feed an accretion disk around a collapsed object in the nucleus. Although the observations are consistent with a starburst interpretation they cannot rule out this possibility. The "starbursts or monsters" debate (cf. Heckman et al. 1983) has become one of the central debates in interpreting nuclear activity in galaxies. It is an especially controversial topic for the merging galaxies because they are so extremely luminous, rivalling the most powerful Seyferts (thought to be "monster nuclei") in their IR luminosities. General arguements have been presented in favour of "starbursts" for most of the galaxies, but some also have optical line ratios or, in the case of NGC6240, IR recombination lines, which are more difficult to explain in the starburst scenario. Observations which will enable more persuasive arguements in favour, or otherwise, of star formaton as the dominant source of luminosity in interacting and merging galaxies are suggested in the following section. That interactions trigger extremely luminous starbursts, raises a number of other outstanding astrophysical questions, for example: What is the detailed mechanism by which the starburst is triggered?, Are the starbursts always more luminous? and is it because they are spatially more extended or are they more intense?, what other properties characterise the starbursts? and can they be related to the properties of the interaction?. Observations to explore several of the most important questions for which only tentative answers have been indicated in the previous chapters are now briefly discussed.

5.1 "Starbursts and monsters"

As mentioned above, the most important question concerning the IR activity in interacting galaxies which is still open to debate is whether or not the IR luminosity is provided by a burst of recent star formation or whether some more exotic luminosity source is required. Potentially one of the strongest arguements in favour of a starburst interpretaion was that discussed in section 3.5.1 viz. measuring the extent of the IR emission. Dust heated by a point source of 10^{10} $L_{\odot}$ cannot be hot enough to radiate at 10 μm over a distance of more than a few parsecs i.e. less than 1 arcsec. So, by mapping the extent of the nuclear IR emission it is possible to dicriminate between a single central source heating a dust cloud (a "monster") and luminosity sources which must be distributed over several hundreds of parsecs (a "starburst"). The observations of off-nuclear pixels in section 3.5.1 are weak, partly because of poor observational techniques. The analysis in that section shows clearly the importance of having better defined beam profiles, which could be obtained by integrating and offsetting on a star exactly as is done for the galaxies. In addition good signal to noise detections in the non-nuclear pixels are essential and it is not sufficient merely to detect a signal at a position where the beam is offset by half a beam-width. Finally taking care to minimise the pointing and offsetting errors is important. The observations of NGC1614 show clearly that the technique of comparing galaxy observations with those of a star will provide a strong arguement for extended IR emisson. There is one further difficulty with this approach which has recently arisen and which was briefly mentioned in the discussion at the end of chapter 4. The discovery of small dust grains, not in thermal equilibrium with the underlying energy source, in the Galaxy by Sellgren (1984) means that a compact nuclear source could concievably produce extended 10μm emission. Indeed this may be the explanation of the uncertainty about the spatial extent of the emission in IC4553 (section 3.5.1). Because of their small size these "Sellgren grains" will be unable to radiate effectively at longer wavelengths such as 20μm. Mapping the nuclear regions at 20μm, rather than at 10μm or in K-L as in chapter 3, therefore seems to be one of the clearest means of distinguishing between starbursts or monsters in the nuclei of interacting galaxies. A programme of mapping interacting galaxies at 20μm will be a key step towards solving what is currently one of the most important questions in extragalactic astronomy.

Another important step forward in understanding nuclear activity depends on elucidating the relationship beteen starburst and monster type activity. For example the optical spectra discussed in section 3.4.2, suggested that several of the galaxies had composite nuclei, with a starburst evident at some wavelengths and non-thermal activity dominating at others. The starburst may have been triggered as a by-product of the interaction feeding an accretion disk, or alternatively a starburst may have caused an accumulation of compact objects in the nucleus thereby triggering more exotic activity (cf. Weedman 1983). One way of testing whether interacting galaxies generally have both starburst and monster type activity, is to obtain data at wavelengths other than the IR or radio and compare them quantitatively with starburst models, to test whether a starburst alone can account for all of the observed activity. For example, X-ray observations can be compared with the expected X-ray luminosity from population I binaries and young supernova remnants associated with the starburst. Strong high excitation UV emission lines are difficult to produce with stars and would be evidence for a "monster", while absorption lines seen in the atmospheres of hot stars can provide direct evidence of a young stellar population and thereby support a starburst interpretation.

Galaxies with Liner type spectra may hold a clue to the relation between starburst and monster activity, because the excitation may be related to both Seyfert and starburst type activity. Such spectra may be provided by a weak active nucleus, a low ionisation version of the power law continuum observed from Seyfert galaxies. In this case it may be that all galaxies harbour a "monster" in their nuclei which is active in varying degrees depending on as yet unspecified conditions (cf. Keel 1983). Thus in the interacting galaxies the interaction may trigger a sufficiently strong starburst to hide this low level activity and sometimes (why ?) it may also trigger stronger "monster" activity. Terlevich and Melnick (1985) on the other hand, have argued that Liner type spectra are associated with old evolved starbursts and arise from the late stages of evolution of extremely massive stars formed in the burst. Alternatively, the spectrum may arise from shock excited gas associated with the shocks driving a young burst of starformation. It is clear that observational and theoretical work to distinguish all of these possibilities is important. The interacting galaxies with Liner type spectra, as well as evidence for a starburst may be very young starbursts, an older more evolved starburst, or it may be that this particular interaction has triggered some other form of activity as well. One possibility for distinguishing these scenarios would be measuring the depth of the CO features of Liner type galaxies. If the Terlevich and Melnick (1985) hypothesis is correct then these galaxies should have a greater proportion of super-giant stars and hence deeper CO features.

5.2 Luminosities

Whether or not the nuclear activity in interacting galaxies is due to "starbursts or monsters" it is important to follow up and confirm the indications that the activity in interacting and merging galaxies is significantly more luminous than that observed in other galaxies. This result is an indication that either the interaction provides more fuel to the nuclear region, and/or it causes the activity to use gas more efficiently. The evidence presented in chapter 3 is open to question because both the interacting galaxy sample and the comparison sample have not been defined in the best way for this type of study. The major fault is that the difference between interacting and non-interacting galaxies is likely to be exaggerated by Malmquist bias. On average the interacting galaxies are more distant than the comparison sample and so the luminous end of the distribution of luminosities in interacting galaxies is preferentially selected.

Ideally luminosity functions for samples of galaxies which are statistically complete should be compared. Becuase the selection criteria for the Arp Atlas are eclectic it cannot be used to define a statistically unbiassed sample. There are two catalogues which, because they contain all pairs of galaxies down to some magnitude limit selected using well defined criteria for interaction in terms of separation of the pair relative galaxy diameter, can be used to define such a sample. These are the Catalogue of Isolated Pairs of Galaxies in the Northern Hemisphere (Karachentsev 1972) and that of Bergvall (1981) which gives southern hemisphere galaxies. Both these catalogues also attempt to define the degree of morphological distortion in a systematic way, so it should be possible to select samples such as all pairs with bridges in a consistent manner. The Karachentseva (1972) catalogue of isolated galaxies, which contains all Zwicky galaxies whose nearest neighbours on the palomar plates, within a factor of four of the same diameter, lie further than 20 diameters away, would be a good source for a comparison sample in this type of study.

Cutri and McAlary have recently begun a statistical study of interacting galaxies, by selecting for observation at 10μm those galaxies in the Karachentseva list which have been classified "LIN" or "DIS" i.e. those pairs which show bridges or tails or distortion of the spiral structure in one or both of the galaxies. However their conclusions are weakened by the absence of a well defined comparision sample and the poor level of 10μm detections. To overcome this, there is a strong case for using JHKL photometry to look for excess radiation at L in this type of study, rather than 10μm photometry, as in the survey described in chapter 2. Well defined samples such as those described above will also be valuable for using the IRAS data, which will provide information about the global star formation rates, to study interacting galaxies. By providing a uniform survey of galaxies of all types over the whole sky, the IRAS results offer unique oppurtunities for comparing the luminosity and frequency of activity in different galaxy types.

The fact that interactions and mergers apparently induce bursts of star formation one to two orders of magnitude more luminous than starbursts in other galaxies suggests a further possibility which ought to be explored. There is some evidence that the largest luminosities in starbursts are not due to higher surface brightness, but to larger volumes of recent star formation activity (cf. Telesco 1984). Mapping the extent of the IR emission in the nuclear regions at 10 or 20μm will permit investigation of this question for the inferred star formation in interacting and merging galaxies. Such studies may also reveal interesting features in the star formation triggered in the inner few kpc. For example it is possible that the star formation is initiated along a shock front caused by the tidal disruption, and the morphology of the extended emission may therefore be related to the geometry of the interaction.

5.3 Triggering of the activity

The work presented in this thesis suggests strongly that interactions between galaxies are very efficient at causing unusually luminous bursts of star formation. However an understanding of the detailed mechanism by which the starburst is triggered remains elusive. The near infrared spectroscopic observations of NGC6240 presented in chapter 4 indicate the promise that future spectroscopic observations hold for investigating this problem. The idea that interaction driven shocks cause efficient molecule formation with the resueting dense molecular gas rapidly cooling, collapsing and fragmenting to trigger a massive burst of star formation, needs to be placed on a firmer footing both observationally and theoretically. Near-infrared spectroscopy holds the potential to provide a better understanding of the physics of the interaction between two galaxies, and further observations of other interacting and merging galaxies to search for H_2 excited by the shocks produced in the interaction are of paramount importance.

H_2 emission is also observed from star forming regions in molecular clouds. The evidence presented in chapter 4 that the H_2 in NGC6240 is excited directly by the merger rests largely on the comparison of the ratio L(S(1))/L(IR) for this galaxy with that for star forming regions. NGC6240 is a merging galaxy and is therefore likely to be disrupted by more and/or stronger shocks than would a non-merging interacting galaxy, so this comparison may not be sufficient to discriminate a contribution to the H_2 excitation from interaction induced shocks for other galaxies. A better way of looking for H_2 excited by interactions is to map the galaxies in one of the H_2 lines and compare this with the distribution of the star forming regions deduced either from mid-IR continuum maps or a map of the H recombination radiation. Shock excited H_2 should be extended over a large fraction of the galaxy if the shocks are indeed driven by the interaction or merger, as suggested for NGC6240. Duley and Williams (1985) have recently predicted the H_2 excitation immediately after reformation on dust grains, so observations of other H_2 lines and comparison with this model should enable further more detailed investigation of post-shock molecule formation in interacting and merging galaxies. Furthermore there should be varying amounts of excited H_2 in interactions of different ages e.g. there should be less in old mergers like NGC3310, which are expected to be more dynamically relaxed.

5.4 Characteristics of the star formation

Since star formation seems to be the dominant energy source in interacting galaxies, more refined observations to define with greater precision the characteristics of the starbursts will be critical in elucidating the effects of interactions. The IR H recombination lines Br α or γ can be used to obtain an indication of the underlying Lyman continuum ionising flux. Such observations are therefore vitally important for a quantitative interpretation of the IR luminosities in terms of star formation activity. For example, in the simple starburst models discussed in section 3.7, an estimate of the Lyman cotinuum flux could have been used together with the IR luminosity to provide an estimate of both the star formation rate and the starburst age (cf. Telesco 1985). Moreover, the IR H recombination line observations of NGC6240 are important because they illuminate some fundamental unanswered questions about the details of the inferred starburst in NGC6240. How many other interacting, merging or ordinary starburst galaxies appear to have a deficiency of ionising photons ? Answering this question should result in a significant step towards understanding the starburst in NGC6240. Another useful spectroscopic observation would be measuring the depth of the CO feature, which is an indicator of the dwarf-to-giant ratio in the stellar population. It too can therefore be used as an age constraining parameter in starburst models (cf. Rieke et al. 1980).

Refined starburst models, providing an estimate of the starburst age and star formation rate will permit a more detailed investigation of the timescales during which the nucleus can fuel the starburst, provided a good estimate of the mass is available. It may be possible to show that in some of the galaxies the starburst is sufficiently long lived that it must be fuelled directly by interaction driven infall, and to compare the necessary rate with dynamical models interactions. Good mass estimates can also be used with models to explore further the suggestions that the lower mass cut-off to the IMF of the star formation must be rather high if starbursts are to account for the luminosites within the age and mass limits. Most importantly, low mass-lumniosity ratios are one of the clearest indicators that a nucleus is active, in the sense defined by Balick and Heckman (1982), by showing the emission to be "qualitatively unusual and quantitatively energetic compared to the evolution of normal stars". Since rotation curves are available for very few interacting galaxies, observations to obtain this information, initially for the most intersting examples, should be undertaken.

5.5 What about the disk?

At present very little is known about environmental effects on galaxy disks or the role of the galaxy's disk in fueling the nucleus. The studies presented in this thesis have been concerned solely with the effects of interactions on nuclear activity. Interactions must, however, act via the disk on the nucleus. It is clear that the nuclei of interacting galaxies are commonly active, yet it is the disk which suffers the most disruption, and is most likely, initially to accumulate fresh material from a neighbour. Condon (1983) finds strong radio emission, associated with a young stellar population, from the disks of late type spirals, and suggests that in the majority of cases this star formation has been caused by interaction with other galaxies or inter-galactic gas clouds. Comparison of small aperture nuclear photometry with large aperture IRAS photometry provides a way to investigate this question for a large sample of clearly interacting galaxies. Since the IRAS photometry had apertures of ~ several arcmin, it will include a large component due to interstellar dust heated by a combination of late-type stars and any newly born early-type stars across the entire disk of the galaxy or galaxies (cf. Jura 1982). For those galaxies in which the nuclear starburst component has been quantified by mid-IR mapping, the nuclear and disk contributions to the IRAS data can be separated out. The resultant disk emission can be used to provide quantitive estimates of non-nuclear starformation rates in these interacting galaxies

5.6 Future IR studies

As the preeceding discussion shows there are two types of IR observations which it is important to extend to as many interacting galaxies as possible. The first of these is mapping the extent of the 20μm emission around the nucleus. This will enable a clearer distinction between starburst and "monster" activity to be made and for this reason it is probably the single most important measurement to obtain for these galaxies. The second type of IR study, near infrared spectroscopy of galactic nuclei, is still in its infancy, but is potentially a very rich field. Observations of H recombination lines can be used to estimate numbers of early type stars for starburst models, while H_2 emission may provide information about molecular flows in star forming regions, or most excitingly, the detailed physics of the interaction. Because so little is known about the excitation of H_2 in galactic nuclei, to investigate the phenomenology of this as yet unexplored field, the observations of interacting galaxies need to be complemented by studies of the near-IR spectra of galaxies of all types, normal, starburst or monsters. With just these two types of observations of interacting galaxies, significant progress can be made towards solving all of the astrophysical questions raised above. Finally, with the advent of IRAS data, the time is right to begin the development of IR studies of galaxy disks, with particular reference to understanding of the effects of interactions.

REFERENCES

Aldrovandi, S.M.V. & Contini, M., 1983. Astr. Astrophys., **127**, 15

Allen, D.A., 1976. Astrophys. J., **207**, 367.

Arp, H., 1966. Atlas of Peculiar Galaxies, California Institute of Technology, Pasadena.

Baldwin, J.A., Phillips, M. & Terlevich, R., 1981. Pub. Astron. Soc. Pacific., **93**, 5.

Balick, B. & Heckman, T.M., 1982. Ann. Rev. Astr. Astrophys., **20**, 431.

Balzano, V.A., 1983. Astrophys. J., **268**, 602.

Becklin, E.E., 1984. Preprint

Becklin, E.E., 1985. Private Communication.

Beckwith, S., 1981. In Infrared Astronomy, IAU Symp. 96, p.167, eds. Wynn-Williams, C.G & Cruikshank, D.P., Reidel, Dordrecht, Holland.

van den Bergh, S., 1969. Astrophys. J. Lett., **4**, 117.

Bergvall, N., 1981. Uppsala Observatory Report No. 19.

Biermann, P. & Fricke, K., 1977. Astr. Astrophys., **54**, 461.

Black, J.H. & Dalgarno, A., 1976. Astrophys. J., **203**, 132.

Boisse, P., Gispert, R., Coron, N., Wijnbergen, J.J., Serra, G., Ryter, C. & Puget, J.L., 1981. Astr. Astrophys., **94**, 265.

Brosch, N., Greenberg, J.M., Rahe, J. & Shaviv, G., 1984. Astr. Astrophys., **65**, 37.

Brosch, N. & Shaviv, G., 1982. Astrophys. J., **253**, 526.

Burke, B.F. & Miley, G.K., 1973. Astr. Astrophys., **28**, 379.

Bushouse, H.A. & Gallagher, J.S., 1985. Preprint.

Carozzi-Meyssonnier, N., 1978. Astr. Astrophys., **63**, 415.

Cohen, M. & Kuhi, L., 1979. Astrophys. J. Suppl., **41**, 743.

Condon, J.J., 1980. Astrophys.J., **242**, 894.

Condon, J.J., 1983. Astrophys. J. Suppl., **53**, 459.

Condon, J.J., Condon, M.A., Gisler, G. & Puschell, J., 1982. Astrophys. J., **252**, 102.

Cutri, R.M. & McAlary, C.W., 1985. Astrophys. J., **296**, 90.

Dahari, O., 1985. Astrophys. J. Suppl., **57**, 643.

Davies, R.D., 1978. In Structure and properties of nearby galaxies, IAU Symp. 77, p.274, eds. Berkhuijsen, E.M. & Wielebinski, R., Reidel, Dordrecht, Holland.

Demoulin, M.H., 1968. Astrophys. J., **153**, 31.

Demoulin, M.H., 1969. Astrophys. J., **156**, 325.

Draine, B.T., 1981. Astrophys. J., **245**, 880.

Draine, B.T. & Salpeter, E.E., 1979. Astrophys. J., **231**, 438.

Elias, J.H., Ennis, D.J., Gezari, D.Y., Hauser, M.G., Houck, J.R., Lo, K.Y., Matthews, K., Nadeau, D., Neugebauer, G., Werner, M.W. & Westbrock, W.E., 1978. Astrophys. J., **220**, 25.

Elias, J.H., Frogel, J.A., Matthews, K. & Neugebauer, G., 1982. Astr. J., **87**, 1029.

Ellis, R.S., Gondhalekar, P.M. & Efstathiou, G., 1982. Mon. Not. R. astr. Soc., **201**, 223.

Fabbiano, G., Feigelson, E. & Zamorani, G., 1982. Astrophys. J., **256**, 397.

Feast, M.W. & Robertson, B.S.C., 1978. Mon. Not. R. astr. Soc., **185**, 31.

Feldman, F.R., Weedman, D.W., Balzano, V.A. & Ramsey, L.W., 1982. Astrophys. J., **256**, 427.

Ferland, G.J. & Netzer, H., 1983. Astrophys. J., **264**, 105.

Fisher, J., Simon, M., Benson, J. & Solomon, P.M., 1983. Astrophys. J. Lett., **273**, L27.

Fosbury, R.A.E. & Wall, J.V., 1979. Mon. Not. R. astr. Soc., **189**, 79.

Fried, J.W. & Schultz, H., 1980. Astr. Astrophys., **118**, 166.

Gallagher, J.S., Knapp, G.R. & Faber, S.M., 1981. Astr. J. **86**, 1781.

Gallouet, L. & Heidmann, N., 1971. Astr. Astrophys. Suppl., **3**, 325.

Gallouet, L. Heidmann, N., & Dampierre, F., 1973. Astr. Astrophys. Suppl., **12**, 89.

Gallouet, L. Heidmann, N., & Dampierre, F., 1975. Astr. Astrophys. Suppl., **19**, 1.

Gehrz, R.D., Hackwell, J.A. & Jones, T.W., 1974. Astrophys. J., **191**, 675.

Gehrz, R.D., Sramek, R.A. & Weedman, D.W., 1983. Astrophys. J., **267**, 551.

Giles, K., 1977. Mon. Not. R. astr. Soc., **180**, 57P.

Gioia, I.M., Gregorini, L. & Klein, U., 1982. Astr. Astrophys., **116**, 164.

Glass, I.S., 1973. Mon. Not. R. astr. Soc., **164**, 155.

Graham, J.R., Wright, G.S., Meikle, W.P.S., Joseph, R.D. & Bode, M.F., 1984. Nature, **310**, 213.

Griersmith, D., Hyland, A.R. & Jones, T.J., 1982. Astr. J., **87**, 1106.

Gunn, J.E., 1979. In Active Galactic Nuclei, p.213, eds. Hazard, C. & Milton, S., Cambridge University press, UK.

Habing, H.J. & Israel, F.P., 1979. A. Rev. Astr. Astrophys., **17**, 345.

Halpern, J.P. & Steiner, J.E., 1983. Astrophys. J. Lett., **269**, L37

Harwit, M. & Pacini, F., 1975. Astrophys. J. Lett., **200**, L127.

Heckman, T.M., 1980. Astr. Astrophys., **87**, 152.

Heckman, T.M., 1983. Astrophys. J., **268**, 628.

Heckman, T.M., Miley, G.K., van Breugal, W.J.M. & Butcher, H.R., 1981. Astrophys. J., **247**, 403.

Heckman, T.M., Balick, B., van Breugal, W.J.M. & Miley, G.K., 1983a. Astr. J., **88**, 583.

Heckmann, T.M., van Breugal, W.J.M., Miley, G.K. & Butcher, H.R., 1983b. Astr. J., **88**, 1077.

Hildebrand, R.H., Whitcomb, S.E., Winston, R., Stiening, R.F., Moseley, S.H., & Harper, D.A., 1977. Astrophys. J., 216, 698.

von Hoerner, S., 1975. In HII Regions and Related topics, p.53, eds. Wilson, T.L. & Downes, D., Springer-Verlag, Heidelberg.

Hollenbach, D. & McKee, C.F., 1979. Astrophys. J. Suppl., **41**, 555.

Hollenbach, D. & Shull, J.M., 1977. Astrophys. J., **216**, 419.

Houck, J.R., Schneider, D.P., Danielson, G.E., Biechman, C.A., Lonsdale, C.J., Neugebauer, G. & Soifer, B.T., 1985. Astrophys. J., **278**, L63.

Huchra, J.P., 1977. Astrophys. J., **217**, 928.

Huchra, J.P., Davies, M., Latham, D. & Tonry, J., 1983. Astrophys. J. Suppl., **52**, 89.

van der Hulst, J.M., 1978. In Structure and Properties of Nearby Galaxies, IAU Symp. 77, p.269, eds. Berkhuijsen, E.M. & Wielebinski, R., Reidel, Dordrecht, Holland.

Hummel, E., 1980. Astr. Astrophys. Suppl., **41**, 151.

Hummel, E., 1981. Astr. Astrophys., **96**, 111.

Hummel, E., van der Hulst, J.M., Dickey, J.M., 1984. Astr. Astrophys., **134**, 207.

Hutchings, J.B., Campbell, B. & Crampton, D., 1982. Astrophys. J. Lett., **261**, L23.

Iben, I. & Tutukov, A.V., 1984. Astrophys. J. Suppl., **54**, 335.

Isreal, F. & van de Hulst, J.M., 1983. Astron. J. **88**, 1736.

Jenkins, C.R., 1984. Astrophys. J., **277**, 501.

Johnson, H.L., 1966. Astrophys. J., **143**, 187.

Johnson, H.L., 1968. In Nebulae and Interstellar Matter, p167, eds. Middlehurst, B.M. & Aller, L.H., University of Chicago Press.

Jura, M., 1984. Astrophys. J., **191**, 375.

Jura, M., 1982. Astrophys. J., **254**, 70.

Kahn, F.D., 1974. Astr. Astrophys., **37**, 149.

Karachentsev, I.D., 1972. Cummun. Spec. Astrophys. Obş. USSR., **7**, 1.

Karachentseva, V.E., 1973. Cummun. Spec. Astrophys. Obs. USSR., **8**, 1.

Keel, W.C., 1983. Astrophys. J., **269**, 460.

Keel, W.C., Kennicutt, R.C., Hummel, E. & van der Hulst, J.M., 1985. Astr. J. **90**, 708.

Kellerman, K.I., Shaffer, D.B., Pauling-Toth, I.I., Preuss, E. & Witzel, A., 1976. Astrophys. J. Lett. **210**, L121.

Klein, U., Grave, R. & Wielebinski, R., 1983. Astr. Astrophys., **117**, 332.

Kleinmann, D.E. & Low, F.J., 1970. Astrophys. J. Lett., **159**, L165.

Kronberg, P.P. & Biermann, P., 1981. Astrophys. J., **243**, 89.

Kronberg, P.P., Biermann, P. & Schwab, F., 1985. Astrophys. J., **291**, 693.

Krumm, N. & Shane, W.W., 1982. Astr. Astrophys., **116**, 237.

Kwan, J., 1977. Astrophys. J., **216**, 713.

Kwan, J. & Scoville, N., 1976. Astrophys. J. Lett., **210**, L39.

Larson, R.B., 1977. In The Evolution of galaxies and stellar populations, p97, eds. Tinsley, B.M. & Larson, R.B., Yale University Press, New Haven.

Larson, R.B., 1978. In Infrared Astronomy, p137, eds. Setti,G., & Fazio, G.G., Reidel, Dordrecht, Holland.

Larson, R.B. & Tinsley, B.M., 1978. Astrophys. J., **219**, 46.

Lawrence, A., Ward, M., Elvis, M., Fabbiano, G., Willner, S.P., Carleton, N.P. & Longmore, A., 1985. Astrophys. J., **291**, 117.

Lebofsky, M.J. & Reike, G.H., 1979. Astrophys. J., **229**, 111.

Lequex, J., 1980. In Star Formation, p. 75, eds. Maeder, A. & Martinet, L., Geneva Observatory, Switzerland.

Lequex, J., Maucherat-Joubert, M., Deharveng, J.M. & Kunth, D., 1981. Astr. Astrophys., **103**, 305.

Lonsdale, C.J., Persson, S.E. & Matthews, K., 1984. Astrophys. J., **287**, 95

Loose, H.H., Krugel, E. & Tutukov, A., 1982. Astr. Astrophys., **105**, 342.

Low, F.J. & Johnson, H.L., 1965. Astrophys. J., **141**, 366.

Madore, B.F., 1980a. In The Structure and Evolution of Normal Galaxies, p. 239, eds. Fall, S.M. & Lynden-bell, D., Cambridge University Press.

Madore, B.F., 1980b. Astr. J., **85**, 507.

Maihara, T., Oda, N., Sugiyama, T. & Okuda, H., 1978. Publ. Astr. Soc. Japan, **30**, 1.

Matthews, T.A. & Sandage, A.R., 1963. Astrophys. J., **138**, 30.

Matthews, W.G. & Baker, J.C., 1971. Astrophys. J., **170**, 241.

Miller, G.E. & Scalo, J.M., 1979. Astrophys. J. Suppl., **41**, 513.

Mountain, C.M., 1983. Ph.D. Thesis, University of London.

D'Odorico, S., 1970. Astrophys. J., **160**, 3.

Pacholczyk, A.G. & Weymann, R.J., 1968. Astr. J., **73**, 850.

Panagia, N., 1973. Astr. J., **78**, 929.

Penston, M.V., 1973. Mon. Not. R. astr. Soc., **162**, 359.

Peterson, S.D. & Shostak, G.S., 1974. Astr. J., **79**, 767.

Raymond, J.C., 1979. Astrophys. J. Suppl., **39**, 1.

Rickard, L.J., Palmer, P., Morris, M., Turner, B.E. & Zukerman, B., 1977. Astrophys. J., **213**, 673.

Rieke, G.H., 1976. Astrophys. J., **206**, L15.

Rieke, G.H., 1978. Astrophys. J., **226**, 550.

Rieke, G.H., 1978. In Infrared Astronomy, p. 220, ed. Fazio, G.G., Dordrecht, Holland.

Rieke, G.H., 1981. In Infrared Astronomy, IAU Symp. 96, p 317, eds. Wynn-Williams, C.G., & Cruikshank, D.P., Riedel, Dordrecht, Holland.

Rieke, G.H., Harper, D.A., Low, F.J., & Armstrong, K.R., 1973. Astrophys. J., 183, L67.

Rieke, G.H., Cutri, R.M., Black, J.H., Kailey, W.F., McAlary, C.W., Lebofsky, M.J. & Elston, R., 1985. Astrophys. J., **290**, 116.

Rieke, G.H. & Lebofsky, M.J., 1978. Astrophys. J., **220**, L37.

Rieke, G.H., & Lebofsky, M.J., 1979. A. Rev. Astr. Astrophys., **17**, 477.

Rieke, G.H., Lebofsky, M.J., Thompson, R.I., Low, F.J. & Tokunaga, A.T., 1980. Astrophys. J., **238**, 24.

Rieke, G.H. & Low, F.J., 1972. Astrophys.J., **176**, L95.

Rieke, G.H. & Low, F.J., 1975. Astrophys. J., **197**, 17.

Rubin, V.C. & Ford, W.K., 1968. Astrophys. J., **154**, 431.

Rubin, V.C., Ford, W.K. & D'Odorico, S., 1970. Astrophys. J., **160**, 801.

Salpeter, E.E., 1955. Astrophys. J., **121**, 161.

Sandage, A.R., 1973. Astrophys. J., **183**, 711.

Sandage, A.R., Becklin, E.E. & Neugebauer, G., 1969. Astrophys. J., **157**, 55.

Schweizer, F., 1977. Astrophys. J., **211**, 324.

Schweizer, F., 1978. In Structure and Properties of Nearby Galaxies, IAU Symp. 77, p. 279, eds. Berkuijsen, E.M. & Wielebiniski, R., Reidel, Dordrecht, Holland.

Schweizer, F., 1982. Astrophys. J., **252**, 455.

Schweizer, F., 1983. In Internal Kinematics and Dynamics of Galaxies, IAU Symp. 100, p. 319, ed. Athanassoula, E., Reidel, Dordrecht, Holland.

Scoville, N.Z., Hall, D.N.B., Kleinmann, S.G., & Ridgway, S.T., 1982. Astrophys. J., **253**, 136.

Scoville, N.Z., Becklin, E.E., Young, J.S. & Capps, R.W., 1983. Astrophys. J., **271**, 512.

Searle, L., Sargent, W.L.W. & Bagnuolo, W.G., 1973. Astrophys. J., **179**, 427.

Sellgren, K., 1984. Astrophys. J., **277**, 623.

Serra, G., Pujet, J.L. & Ryter, C.E., 1980. Astr. Astrophys., **84**, 220.

Seyfert, C.K., 1943. Astrophys. J., **97**, 28.

Sharp, N. & Jones, B., 1980. Nature, **283**, 275.

Sheilds, G.A. & Tinsley, B.M., 1976. Astrophys. J., **203**, 66.

Silk, J., 1980. In Star Formation, p. 131, eds. Maeder, A. & Martinet, L., Geneva Observatory, Switzerland.

Silk, J., & Norman, C., 1981. Astrophys. J., **247**, 59.

Simkin, S.M., Su, H.J. & Schwarz, M.P., 1980. Astrophys. J., **237**, 404.

Smirnov, M.A., & Komberg, B.V., 1980. Astrofizika, **16**, 431.

Smith, M.G., 1985. In Active Galactic Nuclei ed. Dyson, J.E. preprint.

Smith, J., 1982. Astrophys. J., **261**, 463.

Soifer, B.T., Helou, G., Lonsdale, C.J., Neugebauer, G., Hacking, P., Houck, J.R., Low, F.J., Rice, W. & Rowan-Robinson, M., 1984. Astrophys. J. Lett., **278**, L71.

Stasinska, G., 1982. Astr. Astrophys. Suppl., **48**, 299.

Stocke, J.T., 1978. Astr. J., **83**, 348.

Stocke, J.T., Tifft, W.G. & Kaftan-Kassim, M.A., 1978. Astr. J., **83**, 322.

Stockton, A. & Bertola, F., 1980. Astrophys. J., **235**, 37.

Struck-Marcell, C. & Tinsley, B.M., 1978. Astrophys. J., **221**, 5.

Sulentic, J.W., 1976. Astrophys. J. Suppl., **32**, 171.

Sulentic, J.W., & Arp, H., 1983. Astr. J., **88**, 489.

Sulentic, J.W. & Kaftan-Kassim, M.A., 1973. Astrophys. J. Lett., **182**, L17.

Telesco, C.M., 1984. In Proceedings of the Edinburgh Star Formation Workshop, page 183, ed. Wolstencroft, R.D., Royal Observatory, Edinburgh, U.K.

Telesco, C.M., 1985. Preprint. To be published in Proceedings of the RAL Workshop on Extra-galactic IR Astronomy, ed. Gondhalekar, P.M., Rutherford-Appleton Laboratory, Chilton, U.K.

Telesco, C.M. & Harper, D.A., 1980. Astrophys. J., **235**, 392.

Telesco, C.M. & Gatley, I., 1984. Astrophys. J., **284**, 557.

Telesco, C.M., Decher, R. & Gatley, I., 1985. Preprint submitted to Astrophys. J.

Telesco, C.M., Becklin, E.E., Wynn-Williams, C.G. & Harper, D.A., 1984. Astrophys. J., **282**, 427.

Terlevich, R. & Melnick, J., 1985. Mon. Not. R. astr. Soc., **213**, 841.

Thompson, R.I., Lebofsky, M.J. & Reike, G.H., 1978. Astrophys. J. Lett., **222**, L49.

Toomre, A., 1977. In Evolution of Galaxies and Stellar Populations, p. 401, eds. Tinsley, B.M. & Larson, R.B., Yale University

Observatory, New Haven, Connecticut.

Toomre, A. & Toomre, J., 1973. Scientific American, **229**, 38.

Toomre, A. & Toomre, J., 1972. Astrophys. J., **178**, 623.

Turner, J.L. & Ho, P.T.P., 1983. Astrophys. J. Lett., **268**, L79.

Turner, J., Kirky-Dochen, K., & Dalgarno, A., 1977. Astrophys. J. Suppl. **35**, 381.

Ulrich, M.H., 1972. Astrophys. J., **178**, 113.

Ulvestad, J.S., 1982. Astrophys. J., **259**, 96.

de Vaucouleurs, G., de Vaucouleurs, A. & Corwin, H.G., 1976. Second Reference Catalogue of Bright Galaxies, University of Texas Press, Austin.

Vorontsov-Velyaminov, B.A., 1977. Astr. Astrophys. Suppl. **28**, 1.

Vorontsov-Velyaminov, B.A., 1969. In Problems of Exrta-galactic Research, IAU Symp. 15, p.194, ed. McVittie, G.C., Macmillan,

Wade, R., 1983. Proceedings S.P.I.E. **445**, 47.

White, S.D.M., & Valdes, F., 1980. Mon. Not. R. astr. Soc., **190**, 55.

Woodward, P.R., 1976. Astrophys. J., **207**, 466.

Wright, A.E., 1972. Mon. Not. R. astr. Soc., **157**, 309.

Wright, A.E., 1974. Mon. Not. R. astr. Soc., **167**, 251.

APPENDIX

PUBLICATIONS

The following research papers, to which I have cotributed, are enclosed.

1) Recent star formation in interacting galaxies -- I. Evidence from JHKL photometry
   R.D. Joseph, W.P.S. Meikle, N.A. Robertson & G.S. Wright, 1984.
   Mon. Not. R. astr. Soc., **209**, 111.

2) The ultraluminous interacting galaxy NGC6240
   G.S. Wright, R.D. Joseph & W.P.S. Meikle, 1984.
   Nature, **309**, 430.

3) NGC3256: an emerging elliptical galaxy
   J.R. Graham, G.S. Wright, W.P.S. Meikle & R.D. Joseph, 1984.
   Nature, **310**, 213.

4) Detection of molecular hydrogen in two merging galaxies
   R.D. Joseph, G.S. Wright & R. Wade, 1984.
   Nature, **311**, 132.

5) Recent star formation in interacting galaxies -- II. Super starbursts in merging galaxies
   R.D. Joseph & G.S. Wright, 1985.
   Mon. Not. R. astr. Soc., **214**, 87.

6) Near infrared spectroscopy of galaxies
   G.S. Wright, R.D. Joseph, R. Wade, J.R. Graham & I. Gatley, 1985.
   to be published in Proc. RAL Workshop on Extragalactic IR Astronomy.

Recent star formation in interacting galaxies – I. Evidence from *JHKL* photometry

R. D. Joseph, W. P. S. Meikle, N. A. Robertson* and G. S. Wright *The Blackett Laboratory, Imperial College, Prince Consort Road, London SW7 2BZ*

Received 1983 November 29; in original form 1983 June 7

Summary. We have carried out a survey using *JHKL* photometry to investigate recent star formation in interacting galaxies. The objective was to look for a $K-L$ excess produced by 'warm' dust heated by a putative burst of star formation. We find $K-L$ excesses suggesting that interactions induce starbursts with an efficiency approaching 100 per cent. The appearance of these inferred starbursts in interacting systems of different morphological types is qualitatively consistent with dynamical studies of galaxy interactions. However, the common occurrence of such starbursts shows that interactions have implications for the astrophysics of galaxies well beyond purely morphological effects.

1 Introduction

Toomre & Toomre (1972, TT), in a classic numerical study of the tidal effects of interactions between pairs of galaxies, showed that such interactions could result in the redistribution of substantial quantities of material into deeply-plunging orbits in the galaxies. They suggested that this injection of fresh material deep into the potential well of a galaxy could result in a rapid burst of star formation.

The quest for evidence of recent star formation in interacting galaxies has been pursued in studies ranging from radio to X-ray wavelengths with tantalizing, if somewhat ambiguous, results. Radio observations by Sulentic & Kaftan-Kassim (1973), Allen & Sullivan (1973) and Wright (1974) failed to reveal enhanced radio emission in the interacting galaxies they studied. Sulentic (1976) found excess radio emission in multiple systems, but it was not correlated with any optical morphological evidence for interactions. Stocke (1978) and Hummel (1981) found a higher detection rate for pairs than for isolated galaxies, and evidence that closer physical separation is correlated with a higher probability of detection.

Larson & Tinsley (1978) compared the *UBV* colours of a sample of interacting and peculiar galaxies with the colours of more normal galaxies. They found significantly more

* Now at Department of Natural Philosophy, University of Glasgow, Glasgow G12.

scatter in the colours of the interacting galaxies, and interpreted this scatter as an indication of recent star formation in the interacting systems.

Fabbiano, Feigelson & Zamorani (1982) detected 40 per cent of a sample of peculiar galaxies in the X-ray band using the *Einstein Observatory*. They conclude that the X-ray emission is most likely due to Population I X-ray binary systems, with young supernova remnants possibly adding a contribution.

If interactions do indeed induce bursts of star formation, evidence of this activity should be apparent in infrared observations. Many galactic nuclei are known to have very large infrared luminosities (*cf.* Rieke & Lebofsky 1979), and for all but the most energetic of these galaxies, this luminosity is generally attributed to massive young stars produced in a recent burst of star formation. The stellar radiation is thermalized by dust associated with the star formation regions, and re-radiated in the infrared (*cf.* Rieke *et al.* 1980). If such bursts of star formation are present in interacting galaxies, then it is likely that they will have infrared spectra and luminosities similar to those found in the bright infrared galaxies. In fact Rieke (1978a) has commented that interacting galaxies seem to be more luminous than normal galaxies in the infrared.

To follow up these ideas we have embarked on a programme to study star formation in interacting galaxies. Our initial objective was to carry out an infrared survey of a variety of morphological types of interacting systems to search for evidence of recent bursts of star formation. Strong evidence that a starburst of large scale has occurred is obtained by observing large infrared luminosities and correspondingly small mass–luminosity ratios (M/L). A good measurement of the bolometric luminosity requires middle- and far-infrared (10–100 μm) photometry, which is difficult to obtain for a large number of objects. However, if there is substantial far-infrared luminosity, then its presence will be reflected in $K-L$ colours which are significantly redder than normal galaxy colours, as may be seen from the 'blackbody' line in Fig. 1. This is illustrated by the two archetypal starburst galaxies, M82 and NGC253, in contrast with M31. The $K-L'$ colours of the former are 0.86 and 1.38 respectively (L' is 3.6 μm), and the corresponding M/L ratios in solar units are 0.04 and 0.002 (Rieke *et al.* 1980; Rieke & Low 1975; Telesco & Harper 1980; Rieke & Lebofsky 1978). By contrast, M31 has a nuclear $K-L$ colour of 0.34 (Sandage, Becklin & Neugebauer 1969) and a M/L ratio of 48 (Rieke & Lebofsky 1978) which is easily maintained by a normal population of stars. Since photometry at $JHKL$ can be done relatively quickly, we chose to carry out our survey of interacting galaxies at these wavelengths and to look for $K-L$ excesses as evidence for recent bursts of star formation.

2 Observations

The group of galaxies chosen for study was selected from the *Atlas of Peculiar Galaxies* (Arp 1966), covering a wide variety of morphological types. These included spiral galaxies with small compact companions ('M51' types), systems with both weak and well-developed tails, and systems in which one or both galaxies have a peculiar, highly distorted appearance. Within this range the selection criteria favoured the brighter examples. The 51 programme galaxies are listed in Table 1.

It is likely that all the galaxies listed in Table 1 are paired with a companion, even though this is not always apparent from the photographs in the *Atlas of Peculiar Galaxies*. Physical association is indicated by the clear bridges of matter joining the galaxies, their apparent proximity, and the lack of significant differences in their recessional velocities. As may be seen from Table 1, the maximum velocity difference is ~ 600 km s^{-1} and the mean is ~ 130 km s^{-1}. The two galaxies for which companionship is least secure are denoted by the comment 'probable companion' in Table 1.

The UK Infrared Telescope (UKIRT) was used during 1982 March and September to obtain $JHKL$ photometry for both members of 22 pairs of galaxies, and for only one member of six additional pairs. The galaxies were located using either the coordinates for optical nuclei published by Gallouet, Heidmann & Dampierre (1971, 1973, 1975), or coordinates measured from the Palomar Sky Survey plates.

The infrared signal was detected at K with 1 s integration time and the location where this signal peaked was found. In most cases this position coincided with the optical nucleus to within the aperture employed. Apertures of 12 arcsec were used in 1982 March, while 8 arcsec apertures were used in September. In three cases, noted in Table 1, the source was extended beyond 12 arcsec at K. Large chopper throws, 60–100 arcsec, were used to minimize contamination of the nuclear colours by disc material.

The faint standard stars HD1160, GL105.5, BD+2.2957, BS9524, 6353, 1552 and 4550 were used to provide calibration and correction for atmospheric extinction. De-reddening using the van de Hulst curve 15 (Johnson 1968) was based on the extinction-free polar cap model (Sandage 1973). The corrected photometric data is listed in Table 1, together with an estimate of the errors in the $K-L$ colour index. Typically the errors in $J-H$ and $H-K$ are ~ 0.03 mag and are due to uncertainties in calibration. The photometric precision at L is limited chiefly by the signal-to-noise ratio achieved, and this is the major source of uncertainty in the quoted $K-L$ colour index.

3 Results and discussion

3.1 Interpretation of $K-L$ excess

The nuclei of normal galaxies are generally considered to have the colours $H-K = 0.3 \pm 0.1$ and $K-L = 0.3 \pm 0.2$ (*cf.* Johnson 1966; Sandage *et al.* 1969; Glass 1973; Allen 1976). These are the colours expected for a galaxy whose light is dominated by that from late-type stars.

The data from Table 1 is plotted in an HKL colour–colour diagram in Fig. 1. The ellipse outlines the region occupied by normal galaxies. This figure shows that, whereas nearly all the galaxies have normal $H-K$ colours, about half exhibit a distinct $K-L$ excess, i.e. $K-L > 0.5$.

This $K-L$ excess cannot be due to reddening. Fig. 1 shows the reddening line in the HKL plane. Clearly, reddening sufficient to produce a $K-L$ colour excess would also produce an $H-K$ colour vastly larger than that of any of the $K-L$ excess galaxies. (For Arp 242, the JHK colours indicate at most 2 magnitudes of visual extinction, and this is insufficient to account for the observed $K-L$ excess.) There is, moreover, no correlation between galaxy inclination and $K-L$ colour, in contrast to what might be expected if the $K-L$ colour excess were due to internal reddening in the galaxies.

There are several reasons why optically-thin free–free emission is unlikely to be responsible for most of the $K-L$ excesses observed. First, the 'free–free' line in Fig. 1 shows that a significant contribution from free–free emission would result in $H-K$ colours significantly redder than those of the $K-L$ excess galaxies.

Secondly, limits to the free–free flux density at 3.5 μm can be obtained from radio data for the six $K-L$ excess galaxies listed in Table 2. These are the only galaxies in the $K-L$ excess group for which we have found radio measurements with angular resolution sufficient to distinguish between the galaxies. As the table shows, the nuclear radio sources have angular sizes comparable to the apertures used for the infrared measurements. Since the radio spectra are generally non-thermal, any free–free emission must be a small fraction of the radio flux densities listed in Table 2. If we extrapolate any presumed infrared free–free emission to the radio region using the Gaunt factor for an optically thin plasma, the flux

Table 1. *JHKL* observations of interacting galaxies.

Arp number	NGC/other identity	V_0^*	J	$J-H$	$H-K$	$K-L$	Aperture (arcsec)	Notes
318	0833		11.81	0.59	0.58	0.2 ± 0.2	8	
	0835		11.29	0.81	0.36	0.3 ± 0.1	8	
200	1134	3595	11.86	0.79	0.40	0.4 ± 0.1	8	Probable companion UGC 02362
143	2444	3994	11.86	0.79	0.22	0.3 ± 0.08	12	
	2445	4020	12.81	0.84	0.37	0.8 ± 0.2	12	IR source 3″E, 3″S of nucleus
82	2535	4016	12.84	0.71	0.25	0.3 ± 0.2	12	
	2536	4061	13.20	0.67	0.20	0.8 ± 0.2	12	
283	2798	1709	11.08	0.83	0.40	0.69 ± 0.04	12	†
	2799	1738	13.99	0.74	0.22	0.1 ± 0.4	12	
94	3226	1254	11.42	0.82	0.18	0.13 ± 0.06	12	
	3227	1050	10.74	0.86	0.43	0.81 ± 0.03	12	Seyfert galaxy
270	3395	1595	12.57	0.59	0.43	0.4 ± 0.1	12	
	3396	1650	12.61	0.63	0.24	0.7 ± 0.1	12	
214	3718	1095	10.83	0.93	0.30	0.33 ± 0.03	12	Companion NGC 3729
294	3786	2745	11.88	0.79	0.39	0.63 ± 0.06	12	
	3788	2323	11.72	0.77	0.28	0.14 ± 0.06	12	
83	3799	3479	13.42	0.66	0.21	0.4 ± 0.2	8	
	3800	3462	12.53	0.75	0.37	0.6 ± 0.1	8	
244	4038	1447	11.86	0.79	0.34	0.3 ± 0.05	12	
	4039	1430	11.88	0.78	0.25	0.34 ± 0.06	12	
18	4088	822	11.67	0.83	0.35	0.62 ± 0.06	12	† Companion NGC 4085
120	4435	793	10.19	0.85	0.29	0.23 ± 0.03	12	
	4438	182	10.28	0.97	0.33	0.32 ± 0.02	12	
242	4676A	6631	12.58	0.77	0.67	0.6 ± 0.1	12	
	4676B	6590	12.48	0.80	0.27	0.1 ± 0.2	12	
240	5257	6791	12.59	0.82	0.35	0.4 ± 0.1	12	
	5258	6615	12.27	0.79	0.38	0.6 ± 0.1	12	†
239	5278	7710	12.84	0.72	0.33	0.15 ± 0.2	8	
	5279	7744	13.25	0.66	0.33	0.26 ± 0.15	8	
84	5394	3496	12.05	0.88	0.34	0.5 ± 0.1	12	
	5395	3505	12.21	0.84	0.25	0.1 ± 0.1	12	
271	5426	2296	11.97	0.73	0.28	0.3 ± 0.09	12	
	5427	2483	12.04	0.74	0.28	0.6 ± 0.1	12	
199	5544	3292	12.70	0.71	0.25	0.7 ± 0.2	12	
	5545	3302	12.98	0.74	0.33	0.3 ± 0.2	12	
297	5753		12.26	0.84	0.16	0.05 ± 0.1	12	† 2 galaxies in field of 4
	5755		13.17	0.96	0.33	0.69 ± 0.07	12	
90	5929	2696	11.97	0.83	0.27	0.4 ± 0.1	12	
	5930	2875	11.52	0.83	0.34	0.63 ± 0.06	12	
91	5954	2210			0.26	0.3 ± 0.2	8	K = 10.29; Companion 5953
188	A1605+55		12.91	0.80	0.39	0.1 ± 0.2	8	Probable companion MCG 09-26-54
102	A1718+49B	7420	12.65	0.80	0.45	0.7 ± 0.2	8	Companion A1718+49A; Source 3″W of nucleus
93	7284		12.33	0.76	0.40	0.4 ± 0.3	8	
	7285		12.76	1.49	0.22	0.6 ± 0.2	8	
319	7318A	6976	12.16	0.73	0.31	0.2 ± 0.1	8	
	7318B	6011	12.64	0.65	0.35	0.1 ± 0.1	8	
	7319	6878	13.05	0.60	0.48	0.8 ± 0.1	8	
86	7752	5125	13.26	0.71	0.36	1.2 ± 0.4	8	
	7753	5328	12.64	0.85	0.38	0.4 ± 0.2	8	
112	7805	4948				0.3 ± 0.1	8	K = 10.8
	7806	4827			0.44	0.7 ± 0.1	8	K = 11.18

Notes

* Velocities from de Vaucouleurs, de Vaucouleurs & Corwin (1976) except for N2445 and N5395, which are from Bottinelli, Gouguenheim & Paturel (1982), and N1134, N7805 and N7806 from Huchra *et al.* (1983).

† Source was extended in north–south direction at K.

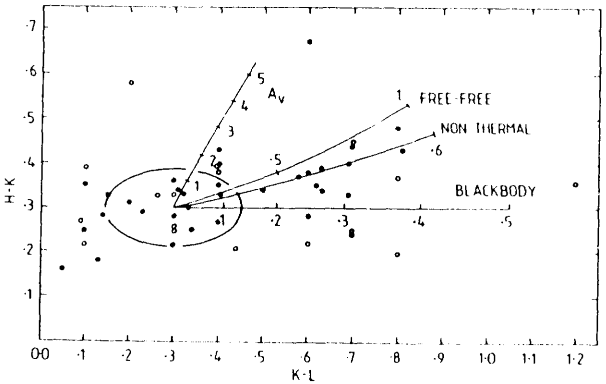

Figure 1. *HKL* colour–colour diagram for all the galaxies listed in Table 1. Normal galaxy colours lie within the ellipse. Tick marks on the reddening line indicate magnitudes of extinction at V. Tick marks on the free–free, non-thermal and blackbody lines correspond to the fraction of the total flux at *L* contributed by these components. The blackbody line corresponds to any temperature ≲ 300 K. An open circle is used to indicate data with errors in *K–L* ≳ 0.1

density at 2695 MHz should be about ten times that at 3.5 μm. Comparison of radio and infrared flux densities in Table 2 shows that infrared free–free emission must be negligible for these six *K–L* excess galaxies. This result, which includes two of the four galaxies lying closest to the free–free line in Fig. 1, *viz.* NGC 2798 and 3227, is likely to typify the entire *K–L* excess group. We therefore conclude that free–free emission does not make a significant contribution to the observed *K–L* excesses.

A *K–L* excess could also be due to non-thermal emission processes. Such emission might be expected if there were a massive object in the nucleus of a *K–L* excess galaxy, and the interaction were providing fuel to 'feed the monster' as suggested by Gunn (1979).

There are two arguments which suggest that non-thermal emission is unlikely to account for most of the *K–L* excesses we observe. First, limits to any contribution to the 3.5 μm flux density from the same source responsible for the non-thermal radio emission can be obtained by extrapolation of the available radio data into the infrared. We have taken radio flux densities and spectral indices from the literature for 10 unresolved pairs of *K–L* excess galaxies, in addition to the six pairs listed in Table 2, and extrapolated them to 3.5 μm. A spectral index of –0.7 was adopted where no index has been measured. This results in 3.5 μm flux densities too small by factors of 200–10000 to account for the *excess* over a 3500 K blackbody which we find for these galaxies. In fact, this upper limit is even stronger since the continuum spectra of non-thermal extra-galactic sources generally steepen between the radio and infrared regions.

Secondly, the *HKL* colours may be compared with the 'non-thermal' line in Fig. 1. This line has been calculated by adding a non-thermal component with spectrum $S_\nu \propto \nu^{-1.5}$ to the stellar continuum. Of course, choice of a steeper power law will bring the 'non-thermal' line in Fig. 1 down toward the 'blackbody' line. However, a spectral index of –1.5 should be representative of a putative non-thermal component in the nuclei of these galaxies. It typifies those Rieke (1978b) found for Seyfert 1 galaxies after subtracting the stellar con-

Table 2. Radio data for pairs with a *K–L* excess.

Arp number	NGC	*K–L*	Radio flux density (mJy)	Radio spectral index	Radio size (arcsec)	Infrared flux density (3.5 μm) (mJy)
143	2445	0.8	20*		<22	12
	2444	0.3	< 6			
283	2798	0.7	66†	0.6	2.5 × 2.5	54
	2799	0.1	< 20			
94	3227	0.8	54†	0.7	3 × 3	87
	3226	0.3	20			
242	4676A	0.6	~21*		<22	15
	4676B	0.1	~5			
84	5394	0.5	18†	0.6	5 × 6	20
	5395	0.1	< 20‡			
90	5930	0.6	40†	1.0	3 × 5	32
	5929	0.4	23			

Notes

* Radio data at 1415 MHz from Burke & Miley (1973).

† Radio data at 2695 MHz from Stocke, Tifft & Kaftan-Kassim (1978).

‡ Radio upper limit at 1415 MHz from Hummel (1981).

tinuum, and also characterizes the optical–infrared spectra of quasars (Neugebauer *et al.* 1979). Given that the *JHK* colours suggest the presence of about one magnitude of reddening, it is evident that the 'non-thermal' line in Fig. 1 does not fit the *HKL* colours of the *K–L* excess galaxies at all well.

The remaining possibility is that suggested in the Introduction. If the *K–L* excess galaxies have experienced bursts of star formation and the stellar radiation is thermalized and re-radiated by dust, then the spectra should be similar to those of well-known 'infrared' galaxies, such as M82 and NGC 253. The *K–L* excess is then due to the addition of a warm (50–100 K) but very luminous quasi-thermal spectrum to the ~ 3500 K stellar spectrum exhibited by normal galaxies in the *JHKL* wavebands. This is illustrated by the 'blackbody' line in Fig. 1. The addition of a warm blackbody is seen to give a normal galaxy a *K–L* excess, while hardly affecting the *H–K* colour. As Fig. 1 shows, the *K–L* excess galaxies have *H–K* colours which are not significantly different from those galaxies with normal *K–L* colours.

If this interpretation of the *K–L* excess is correct, and a *K–L* excess indicates that recent bursts of star formation have occurred in the nuclei of these galaxies, then there should be evidence of this activity at other wavelengths. The radio data in Table 2 provides one example supporting this interpretation. For all six pairs of interacting galaxies it is the *K–L* excess galaxy which is the brighter radio source in the pair. The radio luminosities of the bright components are comparable to those obtained in radio-bright spirals (Condon *et al.* 1982) and also exhibit non-thermal spectra. These features have been interpreted by Condon *et al.* as due to the injection of relativistic electrons resulting from a high rate of supernovae. Thus this correlation further confirms the interpretation of a *K–L* excess as evidence of a recent burst of star formation.

3.2 RELATIONS BETWEEN MORPHOLOGY AND RECENT STAR FORMATION

We have argued that the $K-L$ excess present in about half of the programme galaxies in Fig. 1 is evidence that they have experienced recent bursts of star formation. We now examine the occurrence of $K-L$ excesses in the various types of interacting systems observed, to explore possible relations between the morphology of the interaction and recent star formation. We shall then attempt to relate these features to the physical picture of interactions that emerges from the dynamical studies of TT and Wright (1972).

3.2.1 Star bursts in interacting pairs of all types

The data in Table 1 includes *JHKL* photometry on both members of 22 pairs of galaxies. The *HKL* colours are shown in Fig. 2. For 18 of the 22 pairs one galaxy has a $K-L$ excess and the other member of the pair has a normal $K-L$ colour index. This suggests a frequency of star bursts in interacting systems of ~80 per cent. In fact, it is likely to be even higher. Two of the four pairs with no $K-L$ excess have well-developed tidal tails. As we discuss in Section 3.2.2 below, this could indicate that the interaction is sufficiently old that evidence of the starburst would have faded away. Thus we find that interactions are extremely efficient in triggering bursts of star formation in the nuclei of galaxies.

An important, but at first sight rather puzzling aspect of our data is that in no case have *both* galaxies in an interacting pair shown a $K-L$ excess. This is even more curious for several systems in which both galaxies are remarkably similar in morphology and size (e.g. Arp 242, 271, 240). However, *this feature of our results can be understood on the basis of the* numerical studies of TT and Wright (1972). They find that maximum tidal disruption and transfer of material occur when the accreting galaxy orbits the 'victim' galaxy (to use the Toomres' terminology) in the same plane and sense of direction as the rotation of the 'victim'. Since in any arbitrary interaction between two galaxies conditions close to these are more likely to be met for one galaxy than for the other, it is not surprising that a burst of star formation preferentially appears in one member of the pair.

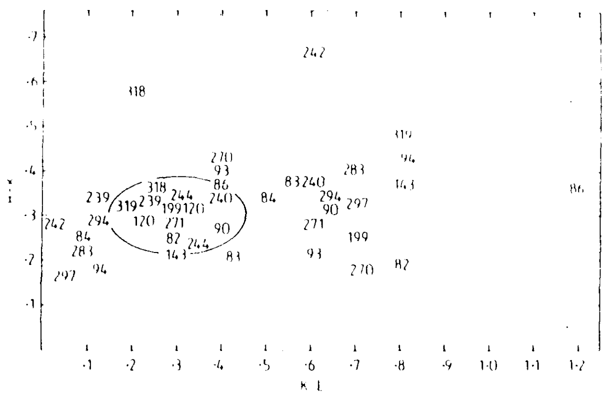

Figure 2. *HKL* colour–colour diagram for 22 pairs of galaxies. The members of each pair are identified by their number in the *Atlas of Peculiar Galaxies*.

3.2.2 Starbursts in pairs with well-developed 'tails'

Another subset of the programme galaxies comprises those with well-developed tails. The criterion for membership of this class is somewhat arbitrary, but we have selected those galaxies with tails whose length is at least twice the galaxy diameter and which seem to be unbound, in contrast with what appear to be loosely-wound spiral arms. The 13 galaxies fitting this criterion, including two marginal cases, are plotted in the *HKL* plane in Fig. 3. We have included in this figure galaxies which do not have tails themselves if they are paired with a companion which does have a well-developed tail. This figure shows that for four of the seven pairs of galaxies with tails, one member of the pair has a $K-L$ excess and has evidently experienced a recent burst of star formation.

The fact that a significant number of the galaxies in systems with tails exhibit a $K-L$ excess suggests immediately that either starburst activity can have a duration as long as the time required to develop a tail, or that starbursts may be delayed, or both. TT find that significant tail-building requires a period $\sim 10^8$ yr. Larson & Tinsley (1978) and Rieke *et al.* (1980) found the durations of starbursts which best fit their data were generally $< 10^8$ yr. This suggests that starburst activity has been delayed in some of the systems which we observed.

The results on two of the systems with well-developed tails are, at first sight, surprising. Arp 242 'The Mice', and Arp 244 'The Antennae', are among the most striking objects in the *Atlas of Peculiar Galaxies*. Both contain two galaxies of fairly equal size and similar morphology, with long tidal tails pointing away from the centre of mass of the system. We might have expected similar $K-L$ colours in these two systems from their superficially similar appearance, but in fact one of the galaxies in 'The Mice' has a $K-L$ excess whereas both galaxies in 'The Antennae' have normal *HKL* colours. However, the TT simulations of these systems show that 'The Antennae' must be viewed much later *after the interaction* (7×10^8 yr) than 'The Mice' (1.2×10^8 yr), in order to match the larger ratio of tail length to body diameter in the former. From these ages it is more likely that any starburst activity will have

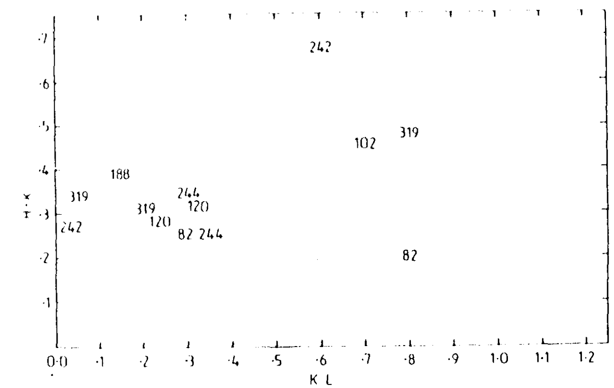

Figure 3. *HKL* colour–colour diagram for systems with well-developed tails, identified by their Arp numbers.

died out in 'The Antennae' than in 'The Mice'. Thus the $K-L$ excess and the inferred starburst that we find in 'The Mice' but not in 'The Antennae' is consistent with the relative ages of these systems in the TT models.

3.2.3 Starbursts in 'M51' types

The *HKL* colours for five 'M51-like' pairs of galaxies in our sample, those with a compact companion at the end of one arm of a large spiral galaxy, are presented in Fig. 4. The letters 'L' and 'S' denote the large and small members of each pair. In four of these systems, one galaxy has a $K-L$ excess and in three cases it is the compact companion which has the $K-L$ excess. This is unlikely to be an aperture effect, since one expects that the larger the aperture, relative to the galactic nucleus, the bluer the colour (*cf.* Griersmith, Hyland & Jones 1982; Aaronson 1981; Frogel *et al.* 1978). Thus we have found in our small statistical sample that a burst of star formation is preferentially triggered in the small companion.

M51 itself shows similar behaviour in fact. The smaller companion NGC 5195, has a $K-L$ colour of 0.5 (Penston 1973) whereas the colour of the nucleus of M51 itself is $K-L$ = 0.30 (Ellis, Gondhalekar & Efstathiou 1982). The M/L of M51 is 3 (Telesco & Harper 1980), which does not indicate the presence of a recent burst of star formation. The M/L of the companion is not available, but its infrared luminosity is only a factor of 2 less than that of M51 (Smith 1982). These points provide strong circumstantial evidence for a recent burst of star formation in the compact companion, but not in the nucleus of the larger galaxy of the pair.

That the starburst occurs preferentially in the compact companion can be qualitatively understood by how tightly material is bound in the two galaxies. Material in the outer regions of the larger galaxy will be relatively more loosely bound, and it is therefore more likely to be stripped and captured by the more compact companion. This effect has appeared in the TT simulation of an interaction between a disc of particles and a compact companion of smaller mass. Another point made by Wright (1972) is that the disruption caused by the

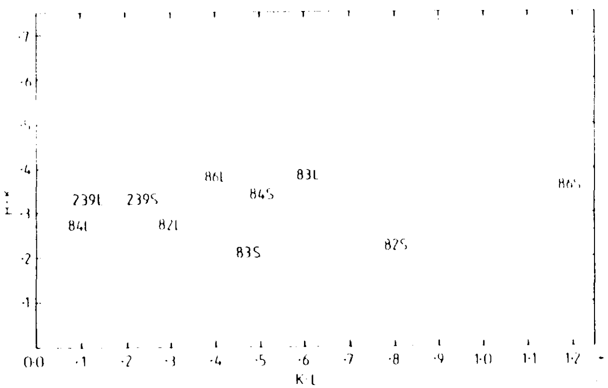

Figure 4. *HKL* colour–colour diagram for 'M51-like' pairs. Their Arp numbers are followed by 'L' and 'S' to denote the large and small member respectively.

larger galaxy on the smaller, is much less than vice versa. In terms of its own radius, the small galaxy is relatively further away from the large one and so is more likely to gain material than to lose it in the interaction.

4 Summary and conclusions

From our *JHKL* survey of 51 interacting galaxies of various types we find excesses in the $K-L$ colour index indicative of a large far-infrared luminosity for nearly half of the programme galaxies. There are three reasons why it is likely that these $K-L$ excesses and the accompanying far-infrared luminosities we infer are powered by, and are evidence for, recent bursts of star formation.

(1) The large far-infrared luminosities found in the nuclei of similar 'infrared' galaxies like M82 and NGC 253 are thought to be due to recent bursts of star formation.

(2) The occurrence of $K-L$ excesses in different morphological types of interacting systems is physically consistent with what would be expected on the basis of the dynamical models of Toomre & Toomre and others, if the $K-L$ excesses are indicative of recent star formation.

(3) Each $K-L$ excess galaxy in the six pairs for which radio maps are available is in every case the brighter radio source. The bright non-thermal radio emission is most likely due to a high supernova rate, thereby further supporting the correlation between a $K-L$ excess and recent star formation.

The major result of this survey is the strong evidence that interactions are extremely efficient in triggering bursts of star formation, with the efficiency apparently approaching 100 per cent. Starbursts never appear in both members of an interacting pair in our sample.

The data also suggest two other features which may characterize interaction-induced starbursts. (1) There is evidence of a delay of ~ 10^8 yr in the starburst activity after the time of closest approach in some systems. (2) In 'M51-like' systems, the compact companion is apparently more likely to acquire material from the larger galaxy and undergo a burst of star formation than vice versa.

It is clear that further infrared observations at longer wavelengths are required to confirm and make more quantitative the indications of recent star formation in interacting galaxies which we have inferred from our *JHKL* photometry. From the arguments we have adduced above it is apparent that interacting systems should be a seminal class of galaxies to study to obtain further insight into the detailed parameters of the rapid star formation process. Moreover, our observations of interaction-induced bursts of star formation are likely to be related to the mounting evidence that interactions are associated with the activity in Seyferts and radio galaxies (*cf.* Balick & Heckman 1982) and in low-redshift quasars (Stockton 1982).

Acknowledgments

It is a pleasure to thank the UKIRT staff, and especially Andy Longmore, for excellent advice and help in learning to use UKIRT with maximum efficiency. GSW holds an SERC studentship and NAR was an SERC post-doctoral research assistant.

References

Aaronson, M., 1981. *Infrared Astronomy, IAU Symp. 96*, p. 317, eds. Wynn-Williams, C. G. & Cruikshank, D. P., Reidel, Dordrecht, Holland.

Allen, D. A., 1976. *Astrophys. J.*, **207**, 367.
Allen, R. J. & Sullivan, W. T., 1973. *Astr. Astrophys.*, **25**, 187.
Arp, H., 1966. *Atlas of Peculiar Galaxies*, California Institute of Technology, Pasadena.
Balick, B. & Heckman, T. M., 1982. *A. Rev. Astr. Astrophys.*, **20**, 431.
Bottinelli, L., Gouguenheim, L. & Paturel, G., 1982. *Astr. Astrophys. Suppl.*, **47**, 171.
Burke, B. F. & Miley, G. K., 1973. *Astr. Astrophys.*, **28**, 379.
Condon, J. J., Condon, M. A., Gisler, G. & Puschell, J. J., 1982. *Astrophys. J.*, **252**, 102.
de Vaucouleurs, G., de Vaucouleurs, A. & Corwin, H. G., 1976. *Second Reference Catalogue of Bright Galaxies*, University of Texas Press, Austin.
Ellis, R. S., Gondhalekar, P. M., & Efstathiou, G., 1982. *Mon. Not. R. astr. Soc.*, **201**, 223.
Fabbiano, G., Feigelson, E. & Zamorani, G., 1982. *Astrophys. J.*, **256**, 397.
Frogel, J. A., Persson, J. E., Aaronson, M. & Matthews, K., 1978. *Astrophys. J.*, **220**, 75.
Gallouët, L. & Heidmann, N., 1971. *Astr. Astrophys. Suppl.*, **3**, 325.
Gallouët, L., Heidmann, N. & Dampierre, F., 1973. *Astr. Astrophys. Suppl.*, **12**, 89.
Gallouët, L., Heidmann, N. & Dampierre, F., 1975. *Astr. Astrophys. Suppl.*, **19**, 1.
Glass, I. S., 1973. *Mon. Not. R. astr. Soc.*, **164**, 155.
Griersmith, D., Hyland, A. R. & Jones, T. J., 1982. *Astr. J.*, **87**, 1106.
Gunn, J. E., 1979. *Active Galactic Nuclei*, p. 213, eds. Hazard, C. & Mitton, S., Cambridge University Press.
Huchra, J., Davis, M., Latham, D. & Tonry, J., 1983. *Astrophys. J. Suppl.*, **52**, 89.
Hummel, E., 1981. *Astr. Astrophys.*, **96**, 111.
Johnson, H. L., 1966. *Astrophys. J.*, **143**, 187.
Johnson, H. L., 1968. *Nebulae and Interstellar Matter*, p. 167, eds. Middlehurst, B. M. & Aller, L. H., University of Chicago Press.
Larson, R. B. & Tinsley, B. M., 1978. *Astrophys. J.*, **219**, 46.
Neugebauer, G., Oke, J. B., Becklin, E. E. & Matthews, K., 1979. *Astrophys. J.*, **230**, 79.
Penston, M. V., 1973. *Mon. Not. R. astr. Soc.*, **162**, 359.
Rieke, G. H., 1978a. *Infrared Astronomy*, p. 159, eds. Setti, G. & Fazio, G. G., Reidel, Dordrecht, Holland.
Rieke, G. H., 1978b. *Astrophys. J.*, **226**, 550.
Rieke, G. H. & Lebofsky, M. J., 1978. *Astrophys. J.*, **220**, 137.
Rieke, G. H. & Lebofsky, M. J., 1979. *A. Rev. Astr. Astrophys.*, **17**, 477.
Rieke, G. H., Lebofsky, M. J., Thompson, R. I., Low, F. J. & Tokunaga, A. T., 1980. *Astrophys. J.*, **238**, 24.
Rieke, G. H., & Low, F. J., 1975. *Astrophys. J.*, **197**, 17.
Sandage, A., 1973. *Astrophys. J.*, **183**, 711.
Sandage, A. R., Becklin, E. E. & Neugebauer, G., 1969. *Astrophys. J.*, **157**, 55.
Smith, J., 1982. *Astrophys. J.*, **261**, 463.
Stocke, J. T., 1978. *Astr. J.*, **83**, 348.
Stocke, J. T., Tifft, W. G. & Kaftan-Kassim, M. A., 1978. *Astr. J.*, **83**, 322.
Stockton, A., 1982. *Astrophys. J.*, **257**, 33.
Sulentic, J. W., 1976. *Astrophys. J. Suppl.*, **32**, 171.
Sulentic, J. W. & Kaftan-Kassim, M. A., 1973. *Astrophys. J.*, **182**, 117.
Telesco, C. M. & Harper, D. A., 1980. *Astrophys. J.*, **235**, 392.
Toomre, A. & Toomre, J., 1972. *Astrophys. J.*, **178**, 623.
Wright, A. E., 1972. *Mon. Not. R. astr. Soc.*, **157**, 309.
Wright, A. E., 1974. *Mon. Not. R. astr. Soc.*, **167**, 251.

The ultraluminous interacting galaxy NGC6240

G. S. Wright, R. D. Joseph & W. P. S. Meikle

Blackett Laboratory, Imperial College, London SW7 2BZ, UK

In the course of checking preliminary lists of IRAS (Infrared Astronomical Satellite) sources to see whether any of the interacting galaxies that we have been studying[1] were included, we discovered that the position of the IRAS source 1650+024PO4 (ref. 2) is within a few arc seconds of one of our programme interacting galaxies, NGC6240. Examination of the Palomar sky survey prints shows that NGC6240 is the only non-stellar object within the 1 arc min IRAS error box for this source. Photometry at 10 and 20 μm from the United Kingdom IR Telescope (UKIRT) confirms that this galaxy is among the most luminous IR galaxies yet discovered. An interaction-induced burst of star formation is the most likely source of the strong IR emission.

Photometry of NGC6240 using UKIRT was obtained on 29 February 1984. We first found the peak in the signal from NGC6240 at K (2.2 μm), and we used this position for the longer wavelength observations. This position coincides within our measurement errors of ~2 arc s, with the optical and radio positions discussed below. Our photometric results, obtained in a 4 arc s aperture, are shown in Fig. 1, together with the published preliminary IRAS data, and available optical and radio data. This reveals that the IRAS source is indeed NGC6240.

The nuclear 10-μm luminosity of NGC 6240, inferred from our UKIRT photometry in a 4 arc s aperture, is $1.2\times10^{10}\ L_{\odot}$, based on the measured redshift[3] (7,597 km s^{-1}) and a Hubble constant H_0 of 50 km s^{-1} Mpc^{-1}. Integration of the spectrum shown in Fig. 1 yields a bolometric luminosity (L_{bol}) of $2.4\times10^{12}\ L_{\odot}$. Most of this energy is emitted in the IR, with the optical and radio emission contributing only ~10% of the total. This interacting galaxy therefore has an IR luminosity 60 times larger than the archetypal starburst galaxies M82 and NGC253 (ref. 4), for which $L_{bol}\sim4\times10^{10}\ L_{\odot}$. Its IR luminosity is an order of magnitude larger than that of the Seyfert galaxy NGC1068 (ref. 5), and comparable with that of Mkn 231 (ref. 6), the most luminous IR galaxy known.

The IR luminosity is most easily understood as arising from a massive burst of star formation, in which the radiation from young, early-type stars is thermalized by dust, and re-radiated in the IR. The quasi-thermal IR spectrum, peaking at ~100 μm, is typical of that observed in known starburst galaxies. Comparing our 10- and 20-μm fluxes in a 4 arc s aperture with the IRAS photometry at 12.5 and 25 μm in a much larger aperture, suggests that about half of the IR emission comes from a region outside the central 4 arc s. The spatial extent of this emission rules out the possibility that the dust is heated by a single compact object in the nucleus, as has been suggested for some Seyfert galaxies.

However, NGC6240 is clearly not just another starburst galaxy. It is at least an order of magnitude more luminous than typical starburst galaxies, and the recent star formation appears to be extended over an enormous region in excess of 3 kpc, significantly larger than is generally found for starburst galaxies.

A comprehensive picture of the nature of NGC6240 can be obtained using available optical and radio studies. Photographs presented by Fosbury and Wall[7] reveal that it is an extremely chaotic interacting galaxy, with a prominent dust lane and three long plumes extending from the central region. Charge-coupled device (CCD) images obtained by Fried and Schulz[8] show two distinct nuclei separated by ~2 arc s. The spectra of Fosbury and Wall, and Fried and Schulz, show intense optical emission lines arising from a region extending over at least 10 arc s. These authors have used the optical emission line intensities to distinguish between different excitation mechanisms (see ref. 9), and they find that the optical emission is characteristic of shock excitation.

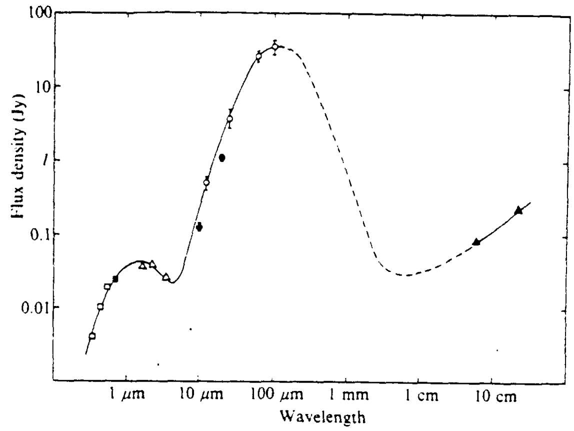

Fig. 1 Continuum spectrum of NGC6240. Data from: ●, this paper; ○, ref. 2; □, ref. 7; ■, ref. 8; △, ref. 15 and ▲, ref. 10. The dashed interpolation is a Rayleigh–Jeans Spectrum with emissivity proportional to λ^{-1} joined smoothly to the data at longer and shorter wavelengths.

NGC6240 is also a very bright radio source with a luminosity at 1,413 MHz (ref. 10) of 4.2×10^{22} W Hz^{-1} Sr^{-1}. The Very Large Array (VLA) maps of Condon *et al.*[10] show that the radio emission is coextensive with the region of intense optical line emission. The two nuclei are also clearly resolved at 4,885 MHz. Other bright radio galaxies in the Condon *et al.* sample have an IR (10 μm)-to-radio (1,445 MHz) flux density ratio of ~4. They suggest that this relation can be understood in terms of a starburst model, with the radio emission arising from supernova remnants associated with the starburst. Comparing our 10-μm flux density with the radio flux density for NGC6240 measured by Condon *et al.* for the central 5 arc s gives a ratio of 0.5. Evidently a simple starburst model is inadequate for NGC6240, and an additional energy source for the radio emission is required. Fosbury and Wall[7] suggest that the strong radio emission in NGC6240 is due to relativistic particles accelerated in the shock fronts. This interpretation appears to be more consistent with the small IR-to-radio flux density ratio we find for this galaxy.

The physical picture of NGC6240 which emerges from all of these studies is that of an interaction between two gas-rich galaxies. If the impact parameter is small enough, dynamical friction will be adequate to dissipate the orbital kinetic energy and a merger of the two galaxies will ensue, as discussed by Toomre[11] and others. Such interactions produce large non-circular gas motions and infall of material as the colliding galactic nuclei spiral towards each other. The resulting shocks in this material can trigger a massive burst of star formation. NGC6240 seems to be a clear example of this process. The two nuclei, and the strong evidence of shock excitation on large scales, support this model. Furthermore, the thermal character of the IR spectrum, the very large IR luminosity, the spatial extent of the IR emission, and the corresponding spatial extent of the ionized gas are strong circumstantial evidence of a massive burst of star formation, fuelled and triggered by the interaction.

These physical processes and events in NGC6240 are similar to those which we[1] and others (see, for example, ref. 12) are finding in studies of interacting galaxies. NGC6240 is remarkable because it is such a spectacular and energetic example.

There is mounting evidence that interactions are associated with other types of active galactic nuclei[13,14]. The properties of NGC6240 outlined above demonstrate that this association has physical plausibility. In particular, interaction-induced starbursts are capable of supplying luminosities at least as large as those characteristic of all but the most luminous active galaxies.

We thank Norna Robertson and James Graham for stimulating discussions on the physics of interacting galaxies and Dave King for assistance in measuring the source position. G.S.W. is an SERC-supported research student.

Received 15 March, accepted 30 April 1984.

1. Joseph, R. D., Meikle, W. P. S., Robertson, N. A. & Wright, G. S. *Mon. Not. R. astr. Soc.* **208** (in the press).
2. *Nature* **306**, 646 (1983).
3. de Vaucouleurs, G., de Vaucouleurs, A. & Corwin, H. G. *Second Reference Catalog of Bright Galaxies*, 217 (University of Texas Press, 1976).
4. Rieke, G. H., Lebofsky, M. J., Thompson, R. I., Low, F. J. & Tokunaga, A. T. *Astrophys. J.* **238**, 24–40 (1980).
5. Telesco, C. M., Becklin, E. E. & Wynn-Williams, C. G. *Astrophys. J.* (submitted).
6. Rieke, G. H. *Astrophys. J.* **226**, 550–558 (1978).
7. Fosbury, R. A. E. & Wall, J. V. *Mon. Not. R. astr. Soc.* **189**, 79–88 (1979).
8. Fried, J. W. & Schulz, H. *Astr. Astrophys.* **118**, 166–170 (1983).
9. Baldwin, J. A., Phillips, M. M. & Terlevich, R. *Publ. astr. Soc. Pacif.* **93**, 5–19 (1979).
10. Condon, J. J., Condon, M. A., Gisler, G. & Puschell, J. J. *Astrophys. J.* **252**, 102–124 (1982).
11. Toomre, A. in *Evolution of Galaxies and Stellar Populations*, (eds Tinsley, B. M. & Larson, R. B.) 401–426 (Yale University Observatory, 1977).
12. Gehrz, R. D., Sramek, R. A. & Weedman, D. W. *Astrophys. J.* **267**, 551–562 (1983).
13. Balick, B. & Heckman, T. M. *A. Rev. Astr. Astrophys.* **20**, 431–468 (1982).
14. Stockton, A. *Astrophys. J.* **257**, 33–39 (1982).
15. Allen, D. A. *Astrophys. J.* **207**, 367–375 (1976).

Printed in Great Britain by Macmillan Production Ltd., Basingstoke, Hampshire

NGC3256: an emerging elliptical galaxy

J. R. Graham, G. S. Wright, W. P. S. Meikle & R. D. Joseph

Astronomy Group, Physics Department, Imperial College of Science and Technology, Prince Consort Road, London SW7 2BZ, UK

M. F. Bode*

Los Alamos National Laboratory, Los Alamos, New Mexico 87545, USA

NGC3256 is a spectacular peculiar galaxy, with a highly chaotic nuclear region consisting of several bright knots. Two diffuse tidal tails are visible evidence of violent past history. The galaxy has been classified on the basis of this tidal damage as the remnant of two colliding galaxies in the final throes of merging[1]. The galaxy is highly luminous, with $M_B = -22.6$, as well as being a bright, narrow emission-line galaxy[2]. At radio wavelengths, NGC3256 is one of the brightest in Wright's survey[3] of interacting galaxies. We have discovered bright and exceptionally extended 10-μm emission that is evidence for an extremely luminous starburst extending over several kiloparsecs, which will leave the system severely gas-depleted. This depletion, in combination with the violent stellar relaxation which accompanies galaxy mergers, suggests that NGC3256 will become an elliptical galaxy.

NGC3256 was observed in February 1984 as part of our programme to investigate the IR properties of interacting galaxies[4]. Merging galaxies such as NGC3256 are an interesting subgroup of these, not only because the interactions are expected to be particularly violent, but also because of the suggestion[1] that a significant fraction of elliptical galaxies could be the endpoint of mergers. The 1.5-m telescope at the Cerro Tololo Inter-American Observatory was used to make measurements at *JHKL* (1.25, 1.65, 2.2, 3.5 μm) and 10 μm in a 15 arc s aperture centred on the optical nucleus. 3 × 3 maps using the same beam, with pixel centres displaced one half beamwidth, were also made at these wavelengths. In addition, *JHKL* measurements were made in a 30 arc s aperture on the nucleus. At 10 μm, the flux density measured on the nucleus was 1.7 ± 0.15 Jy. Emission was also detected in the pixels to the east and south-east at 1.2 ± 0.2 Jy and 1.3 ± 0.3 Jy respectively. The integrated flux of about 3 Jy makes this object one of the brightest extragalactic 10-μm sources. At the distance of 53 Mpc inferred from its redshift[5] ($H_0 = 50\ \mathrm{km\ s^{-1}\ Mpc^{-1}}$) the nuclear 10-μm luminosity of NGC3256 is $\approx 1.8 \times 10^{10}\ L_\odot$. This surpasses the 10-μm luminosity of all recognized 'starburst' galaxies by an order of magnitude, and rivals that of the powerful Seyfert galaxies. Extrapolating this spectrum into the far IR suggests a total IR luminosity of order $3 \times 10^{11}\ L_\odot$ (ref. 6). The mass contained within the central 15 arc s (4kpc) determined from the mean rotation curve[5] is $6 \times 10^9\ M_\odot$. Thus the mass/luminosity ratio in solar units is $\approx 0.02(H_0/50)$. Clearly this ratio cannot be sustained by normal star formation over the lifetime of the galaxy.

The 10-μm source must be extended on a scale of several arcseconds. This follows directly from consideration of the 10-μm fluxes observed at three positions together with the measured beam profile. In fact, the 10-μm emission is almost certainly more extended than these measurements suggest. A remarkably red $K - L$ colour ≈ 1.0, indicating a large excess at *L*, extends over most of the central 30 arc s (typical galaxy colours are ≈ 0.3). Furthermore, one third of the total luminosity at *L* measured in the 30 arc s beam falls beyond the central 15 arc s. The most plausible interpretation of these results is that a mammoth burst of star formation has been triggered by the violent gravitational tides and collisional shocks produced by the interaction. The steeply-rising IR spectrum looks very much like that typical of known starburst galaxies such as M82 (ref. 6). The very small mass/luminosity ratio, and the evidence for spatially extended 10-μm emission are features characteristic of starbursts. In a starburst, the luminosity at 10 μm and at *L* is due to massive early-type stars. The dust cocoon surrounding these stars at birth absorbs their light and reradiates it in the IR. The considerable variations we find in the *JHK* colours measured at different positions in our maps suggest that we have within the same aperture both the unreddened light from knots of less massive blue stars and emission from hot dust.

Apart from the intrinsic interest of an unusually luminous starburst, this discovery has one interesting further implication. There are both theoretical and observational arguments which support the suggestion that merging galaxies can evolve into ellipticals. Numerical simulations[1,7] show that the violent relaxation following a collision produces a stellar velocity distribution similar to that in ellipticals. Observations of galaxies like NGC7257 and NGC5128 show this effect in the stellar velocity distribution, as well as an $r^{1/4}$ luminosity profile[8]. However, as White[7] and others have pointed out, the ultimate fate of the gas which the two merging galaxies originally contain is an outstanding difficulty. If mergers generally result in powerful starbursts similar to that in NGC3256, this lacuna in the merger–elliptical evolution scenario is resolved. The massive early-type stars responsible for the high IR luminosity eventually become supernovae, and the mechanical energy in the supernovae ejecta is sufficient to drive a galactic wind which will leave the galaxy severely gas-depleted.

Galactic winds driven by supernovae have been discussed elsewhere[9] but we can argue that, on simple energetic grounds, the supernovae resulting from the starburst in NGC3256 will be able to sweep the galaxy free of gas. The IR luminosity L_{IR} is powered by early-type stars of average luminosity l_*, so the total mechanical energy supplied by the supernovae produced when these stars explode is $(L_{IR}/l_*)E_{SN}$, where $E_{SN} = 10^{51}$ erg is the energy liberated by each supernova. The condition that this ejected gas, and any remaining interstellar gas, escape from the galaxy is

$$\frac{GM^2}{r} < \frac{L_{IR}}{l_*} E_{SN} \qquad (1)$$

where we have made the conservative assumption that all the mass, *M*, inside a radius, *r*, is gas. In fact, a considerable fraction may be locked up in remant objects and low-mass main sequence stars. If the duration of the starburst, τ_b, exceeds the lifetime of a typical early-type star, τ_*, then additional generations of supernovae will contribute to the kinetic energy, increasing it by a factor τ_b/τ_*. We may therefore re-express the condition for gas ejection in terms of the mass/luminosity ratio:

$$\frac{M}{L_{IR}} < 1 \times \left(\frac{\tau_b}{2 \times 10^7\ \mathrm{yr}}\right)\left(\frac{m_*}{10\ M_\odot}\right)^{-1}\frac{M_\odot}{L_\odot} \qquad (2)$$

where m_* is the mass of a star characterizing the starburst. If we take a 10 $M_\odot$ star to typify the early-type stars in the burst[10], and we assume, conservatively, that there is only one generation of stars, (that which we are presently observing), then the condition for escape of all the gas is that $M/L_{IR} < 1$. As the observed M/L_{IR} for NGC3256 is 0.02, this condition is easily satisfied. Thus, there is more than enough mechanical energy to drive a galactic wind which will carry the gas out of the galaxy.

NGC3256 is, therefore, one of the most luminous examples of a starburst yet discovered. It also demonstrates that merger-induced star formation is sufficiently vigorous to produce a remnant as gas depleted as any elliptical galaxy. The discovery of the super-starburst in NGC3256 supports the idea that at least some of present-day elliptical galaxies could have been formed by mergers.

We thank the staff of the Cerro Tololo Inter-American Observatory, especially Jay Frogel, Brook Gregory and Oscar

* Present address: Department of Astronomy, The University, Manchester M13 9PL, UK.

Rivera, for support. We also thank Norna Robertson for helpful discussions. J.R.G. is a Department of Education for Northern Ireland supported research student. G.S.W. is an SERC supported research student. M.F.B. was supported by the Association of Universities for Research in Astronomy and by the US Department of Energy. J.R.G., W.P.S.M. and M.F.B. are visiting astronomers at Cerro Tololo Inter-American Observatory, which is operated by the Association of Universities for Research in Astronomy, Inc., under contract with the NSF.

Received 6 April; accepted 25 May 1984.

1. Toomre, A. in *Evolution of Galaxies and Stellar Populations* (eds Tinsley, B. M. & Larson, R. B.) 401–426 (Yale University Observatory, 1977).
2. de Vaucouleurs, G. & de Vaucouleurs, A. *Mem. R. astr. Soc.* **68**, 69–87 (1961).
3. Wright, A. E. *Mon. Not. R. astr. Soc.* **167**, 251–272 (1974).
4. Joseph, R. D. Meikle, W. P. S., Robertson, N. A. & Wright, G. S. *Mon. Not. R. astr. Soc.* (in the press).
5. Feast, M. W. & Robertson, B. S. C. *Mon. Not. R. astr. Soc.* **185**, 31–46 (1978).
6. Telesco, C. M. & Harper, D. A. *Astrophys. J.* **235**, 392–404 (1980).
7. White, S. D. M. *Mon. Not. R. astr. Soc.* **184**, 185–203 (1978).
8. Schweizer, F. in *Internal Kinematics and Dynamics of Galaxies, IAU Symp.* No. 100, 319–329 (1983).
9. Mathews, W. G. & Baker, J. C. *Astrophys. J.* **170**, 241–259 (1971).
10. Rieke, G. H., Lebofsky, M. J., Thompson, R. I., Low, F. J. & Tokunaga, A. T. *Astrophys. J.* **238**, 24–40 (1980).

Printed in Great Britain by Macmillan Production Ltd., Basingstoke, Hampshire

Detection of molecular hydrogen in two merging galaxies

R. D. Joseph & G. S. Wright

Blackett Laboratory, Imperial College, London SW7 2BZ, UK

Richard Wade

Royal Observatory, Blackford Hill, Edinburgh EH9 3HJ, UK

NGC6240 and Arp 220 (IC4553) are two of the most luminous IR galaxies known[1,2]. They are also both thought to be examples of galaxy–galaxy mergers. As part of our study of interacting and merging galaxies[1,3,4] we have obtained IR spectra in the 2-μm region of NGC6240 and Arp 220 and detected the $v = 1\text{–}0$ S(1) quadrupole rotation–vibration emission line of H_2 (rest wavelength 2.122 μm) in both galaxies. (This line in NGC6240 has also recently been detected by E. E. Becklin *et al.*, personal communication.) These detections, which double the number of previously published measurements of extragalactic H_2 (refs 5, 6) suggest that the merger of two galaxies results in the production of massive quantities of shocked molecular gas. This shocked gas must cool and collapse, leading to an enormous burst of star formation. These measurements of shocked H_2 thus strengthen our earlier interpretation[1] of the extremely large IR luminosity of NGC6240 in terms of a 'super-starburst'. Arp 220 may be undergoing similar activity. We suggest that merging galaxies are a unique new class of ultra-luminous IR galaxies.

The spectra were measured on the UK Infrared Telescope (UKIRT) on the nights of 10 and 11 April 1984 using a seven-channel cooled grating spectrometer (CGS-2) with a 5 arc s aperture[7]. Wavelength calibration and the instrumental resolution of 550 km s^{-1} were derived from observations of Brackett γ (λ 2.166 μm) in the planetary nebula NGC7027. Spectra of the star BS5447 provided flux calibration. The spectra were measured at positions defined by the peak of the IR emission for NGC6240, and by the peak of the optical emission for Arp 220. The spectral coverage of the seven-channel spectrometer, ~0.023 μm, was centred on the $v = 1\text{–}0$ S(1) line of H_2 (hereafter, the S(1) line) redshifted to the recessional velocities of the galaxies. The full spectra obtained are shown in Fig. 1. The S(1) line is clearly detected in both galaxies and probably also resolved in both. The corresponding fluxes and luminosities, for $H_0 = 50$ km s^{-1} Mpc^{-1}, are given in Table 1. The luminosity in the S(1) line for NGC6240 of $10^8\ L_\odot$ may be compared with luminosities of $3\times10^6\ L_\odot$ and $3\times10^7\ L_\odot$ in this line for NGC1068 (ref. 5) and NGC3690 (ref. 6) respectively.

Using the data in Table 1 we can develop the following physical picture of the H_2 excitation in these two merging galaxies. First, this gas is almost certainly excited by shock-heating, as is the case for virtually all known examples of H_2 quadrupole emission[8]. In NGC6240, the width of the S(1) line, ~800 km s^{-1}, is identical to the widths of optical emission lines seen in a similar aperture on the nucleus, and which are thought to be shock-excited[9]. Fluorescence following absorption of UV photons is considered to be the most plausible alternative mechanism for excitation of these rotation–vibration levels. In this case, the $v = 2\text{–}1$ S(1) line should have about half the intensity of the $v = 1\text{–}0$ S(1) line[10]. Our failure to detect the $v = 2\text{–}1$ S(1) line in NGC6240 at a sensitivity similar to that reached for the $v = 1\text{–}0$ S(1) line detection, suggests that UV pumping does not contribute significantly to the excitation, and shocks remain as the most likely excitation mechanism.

Second, the mass of hot gas may be estimated by assuming local thermodynamic equilibrium at a temperature of 2,000 K (ref. 8). The luminosities in Table 1 then imply masses of excited molecular gas of $\sim10^5\ M_\odot$ and $\sim10^4\ M_\odot$ for NGC6240 and Arp 220 respectively.

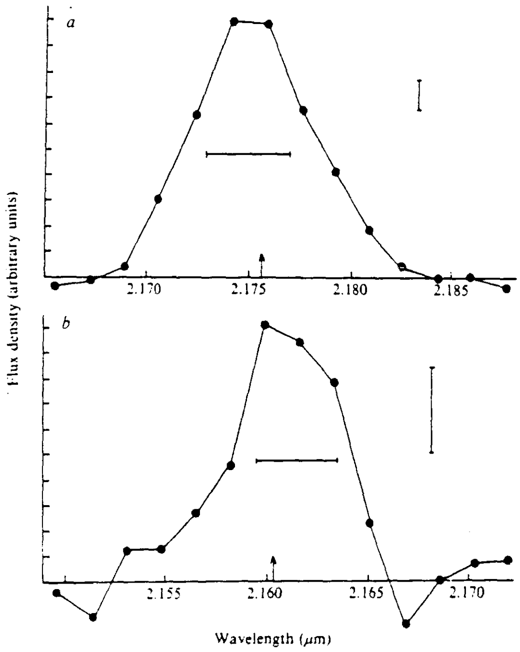

Fig. 1 Near IR spectrum of the nucleus of *a*, NGC6240; *b*, Arp 220 in a 5 arc s aperture. The arrow shows the wavelength of the 2.122 μm S(1) line redshifted to the radial velocity of the respective galaxies. The spectrum has been ratioed with the standard, smoothed using a triangular function, and the baseline has been subtracted off. The vertical bar represents the 1σ error per point, and the horizontal bar represents the instrumental resolution.

Third, we can use simple energetic arguments to investigate the underlying source driving the shocks. The gas cools to a temperature <1,000 K in about 3 yr (ref. 11), so in NGC6240 the shock excites about $3\times10^4\ M_\odot$ of gas per year. The force, $\dot{m}v$, required to drive such a shock at a speed of ~20 km s^{-1} is $\sim5\times10^{36}$ dynes. By comparison, the radiation pressure, L/c, of these ultra-luminous galaxies, with $L_{IR} \sim 10^{12}\ L_\odot$, is $\sim10^{35}$ dynes. Despite the high luminosities, radiation pressure is clearly insufficient to drive the shocks which we infer are present in these galaxies.

These objects are the results of galaxy–galaxy mergers, and are both likely to be examples of 'super-starbursts'[1,2]. Two obvious mechanisms for driving the shocks are either the relative kinetic energy of the collision, or mass outflow from the early-type stars in the starbursts. To investigate the relative contributions of these two processes we can use the ratios of the luminosities in the S(1) lines to the total IR luminosities. This ratio should have a characteristic value if the H_2 is excited by mass outflow from young stars, and the IR luminosity is provided by the luminosity of the early-type stars which is thermalized by dust and re-radiated in the IR. These ratios are presented in Table 2, along with that for Orion, a 'typical' star formation

Table 1 Fluxes and luminosities in the S(1) line

Galaxy	Flux (W m^{-2})	$L(L_\odot)$
NGC6240	$(15\pm1)\times10^{-17}$	1×10^8
Arp 220	$(2.5\pm0.5)\times10^{-17}$	9×10^6

Table 2 The ratio of luminosity in the S(1) line to total, IR luminosity

Object	Ratio ($L(S(1))/L_{IR}$)
NGC6240	20×10^{-5}
Arp 220*	1.2×10^{-5}
Orion	1.2×10^{-5}
NGC3690	3×10^{-5}
NGC1068	0.9×10^{-5}

* See comments in text.

region in the Galaxy[12]. For comparison, we have also included these ratios for the other two galaxies in which H_2 has been detected, NGC1068 and NGC3690 (refs 6 and 12). We have used our 10–20 μm UKIRT photometry[1] to obtain the appropriate IR luminosity for the nucleus of NGC6240 in a 5 arc s aperture, similar to that used for the S(1) observations. These measurements give an IR continuum spectrum of similar shape to the large aperture IRAS photometry[1] and imply a luminosity $L_{IR} \sim 5 \times 10^{11} L_{\odot}$, a factor of 4 less than that inferred from the IRAS results. We have, therefore, used a similar factor to scale the IRAS luminosity for Arp 220 (ref. 2) to that expected in a 5 arc s aperture.

Table 2 shows that all the galaxies, with the exception of NGC6240, could be excited by mass outflow from star formation regions similar to Orion. NGC6240 is clearly the exception, by a factor of more than 10, and it is likely that mechanical energy in the galaxy–galaxy collision has provided most of the energy required to heat the H_2 gas. If we assume a galaxy mass of $\sim 10^{12} M_{\odot}$, 10% of which is gas, and a relative velocity between the colliding galaxies of ~ 300 km s^{-1}, then this process supplies an energy of $\sim 10^{59}$ ergs. For an efficiency of 0.002 in coupling shock energy into the S(1) line[13], the mechanical energy in the collision can excite the gas at the observed rate for a time $\sim 2 \times 10^7$ yr. For Arp 220 the luminosity ratio in Table 2 is entirely consistent with excitation by mass outflow from star formation regions. However, it is very likely that we have not measured the maximum S(1) line intensity in Arp 220, since we observed only the optical nucleus. Given the physical similarity between NGC6240 and Arp 220, it would be surprising if a better measurement of the S(1) line flux did not result in a luminosity ratio closer to that for NGC6240.

There are several important conclusions to be drawn from these measurements. First, the existence of massive quantities of shocked molecular gas, in excess of that expected for star formation regions alone, is consistent with what might be expected when galaxies merge, and tends further to confirm other indications that NGC6240 is indeed the merger of two gas-rich galaxies. Second, both these galaxies are probably undergoing an episode of star formation of exceptional intensity, with shocked, and, therefore, dense H_2 produced at the rate of 3×10^3 to $3 \times 10^4 M_{\odot}$ yr^{-1}. This gas will cool rapidly, collapse and fragment, and result in a burst of star formation. The enormous mass of molecular gas that is shocked over any reasonable lifetime for this process, and its expected spatial extent on a scale of kpc if the shocks are merger-driven, as seems to be the case for NGC6240 at least, will produce an episode of rapid star formation of unusual spatial extent and intensity, that is, a 'super-starburst'. Finally, because dust is required to form the H_2 molecules[14], there must be dust present. It will thermalize the radiation from the newly-formed stars and re-radiate it in the IR. Thus these super-starbursts are likely to produce ultraluminous IR galaxies. We have suggested previously[1] that NGC6240 is a paradigmatic example of such a process, and the detection of shocked H_2 strongly supports this interpretation. As a consequence, merging galaxies may be a unique new class of galaxies exhibiting super-starbursts and ultra-large IR luminosities.

This picture of interaction-induced shocks, which then trigger a super-starburst in merging galaxies, is physically coherent and plausible. However, there remain some fundamental unanswered questions concerning the details of these processes. First, how common might such a phase of vigorous H_2 excitation be among merging galaxies generally? As these two galaxies were selected for study on the basis of their large IR luminosities, it is difficult to attempt generalizations about the time scale of the phase of luminous H_2 emission on the basis of these measurements alone. However, the fact that the S(1) line is so luminous in two merging galaxies suggests that the episode of this activity may be a significantly large fraction of the time over which the morphological disturbance would be recognized as a merger. The dynamical simulations of Toomre and Toomre[15] and Wright[16] suggest that the tidal 'tails' resulting from an interaction persist for periods of the order of 10^9 yr. This is longer than the 2×10^7 yr estimated above for the time merger-driven shocks can excite the gas in NGC6240 at the observed rate. Despite the rather large uncertainties in this estimate, the duration of luminous H_2 emission powered by the merger is unlikely to be more than 10^8 yr. Even if the H_2 were mostly excited by mass outflows from star formation regions, the time scale for such starbursts is probably $\leq 10^8$ yr (ref. 17). This is also rather short compared with the merger lifetime. So, if these time scales are approximately correct, we would expect that only $\sim 10\%$ of the galaxies recognizable as mergers from their morphologies are currently undergoing a phase of activity similar to that in NGC6240.

Perhaps even more intriguing is the fact that we failed to detect the Paschen α hydrogen recombination line in NGC6240 at a comparable sensitivity to that reached in the S(1) line measurements. (We measured Paschen α because Brackett α, at a rest wavelength of 4.051 μm, is at the edge of the atmospheric transmission window at the redshift of NGC6240.) For those objects in which the H_2 excitation is thought to be due to mass outflows in star formation regions—NGC1068, NGC3690, and Orion—the Brackett γ line flux is within a factor of 2 of the S(1) line flux. Although we have shown that in NGC6240 the S(1) line is ~ 20 times stronger than expected for excitation from star formation regions, the Paschen α line is also expected to be about 12 times stronger than Brackett γ from recombination theory[18,19]. Because it is difficult to avoid the conclusion that the high IR luminosity of NGC6240 is due to a massive burst of star formation[1], our failure to detect the Paschen α recombination line is indeed surprising. Whether this can be understood in terms of a complex geometry for dust extinction, self-shielding by the H_2, or perhaps a starburst initial mass function with fewer high mass stars, requires further detailed analysis. Such an analysis, supplemented by additional spectroscopic results for these and other interacting galaxies, is in preparation.

We thank Charles Telesco, James Graham and especially Ian Gatley for stimulating and informative discussions. G.S.W. is a research student supported by the UK SERC.

Note added in proof: Molecular hydrogen emission has been discovered in these two galaxies by several independent observers as listed in IAU Circ. No. 3968.

Received 20 June; accepted 8 August 1984.

1. Wright, G. S., Joseph, R. D. & Meikle, W. P. S. *Nature* **309**, 430–431 (1984).
2. Soifer, B. T. *et al. Astrophys. J.* (submitted).
3. Joseph, R. D., Meikle, W. P. S., Robertson, N. A. & Wright, G. S. *Mon. Not. R. astr. Soc.* **209**, 111–122 (1984).
4. Graham, J. R., Wright, G. S., Meikle, W. P. S., Joseph, R. D. & Bode, M. F. *Nature* **310**, 213–214 (1984).
5. Thompson, R. I., Lebofsky, M. J. & Rieke, G. H. *Astrophys. J. Lett.* **222**, L49–L53 (1978).
6. Fischer, J., Simon, M., Benson, J. & Solomon, P. M. *Astrophys. J. Lett.* **273**, L27–L30 (1983).
7. Wade, R. *Proc. S.P.I.E.* **445**, 47–50 (1983).
8. Shull, J. M. & Beckwith, S. *A. Rev. Astr. Astrophys.* **20**, 163–190 (1982).
9. Fosbury, R. A. E. & Wall, J. V. *Mon. Not. R. astr. Soc.* **189**, 79–88 (1979).
10. Black, J. H. & Dalgarno, A. *Astrophys. J.* **203**, 132–142 (1976).
11. Kwan, J. *Astrophys. J.* **216**, 713–723 (1977).
12. Beckwith, S. in *Infrared Astronomy* (eds Wynn-Williams, C. G. & Cruikshank, D. P.) 167–178 (Reidel, Dordrecht, 1981).
13. Kwan, J. & Scoville, N. *Astrophys. J. Lett.* **210**, L39–L43 (1976).
14. Hollenbach, D. & McKee, C. F. *Astrophys. J. Suppl.* **41**, 555–592 (1979).
15. Toomre, A. & Toomre, J. *Astrophys. J.* **178**, 623–666 (1972).
16. Wright, A. E. *Mon. Not. R. astr. Soc.* **157**, 309–333 (1972).
17. Rieke, G. H., Leboksky, M. J., Thompson, R. I., Low, F. J. & Tokunaga, A. *Astrophys. J.* **238**, 24–40 (1980).
18. Giles, K. *Mon. Not. R. astr. Soc.* **180**, 57P–59P (1977).
19. Osterbrock, D. E. *Astrophysics of Gaseous Nebulae*, 65–66 (Freeman, San Francisco, 1974).

Printed in Great Britain by Macmillan Production Ltd., Basingstoke, Hampshire

Mon. Not. R. astr. Soc. (1985) **214**, 87–95

Recent star formation in interacting galaxies – II. Super starbursts in merging galaxies

R. D. Joseph and G. S. Wright *The Blackett Laboratory, Imperial College, Prince Consort Road, London SW7 2BZ*

Accepted 1984 December 13. Received 1984 December 13; original form 1984 September 11

Summary. The subset of galaxy–galaxy interactions which have resulted in a merger are, as a class, ultraluminous IR galaxies. Their IR luminosities span a narrow range which overlaps with the most luminous Seyfert galaxies. However, in contrast with Seyfert galaxies, the available optical, IR, and radio properties of mergers show no evidence for a compact non-thermal central source, and are easily understood in terms of a burst of star formation of extraordinary intensity and spatial extent: they are 'super starbursts.' We argue that super starbursts occur in the evolution of most mergers, and discuss the implications of super starbursts for the suggestion that mergers evolve into elliptical galaxies. Finally, we note that merger-induced shocks are likely to leave the gas from both galaxies in dense molecular form which will rapidly cool, collapse, and fragment. Thus a merger might in fact be expected to result in a burst of star formation of exceptional intensity and spatial extent, i.e. a super starburst.

1 Introduction

Large and often dominant IR luminosities characterize the continuum spectra of many types of galactic nuclei. Surveys of bright spiral galaxies by Rieke & Lebofsky (1978) and by Scoville *et al.* (1983) have shown that many, perhaps most of these galaxies exhibit flux densities at 10 μm which are substantially in excess of that expected from stellar emission alone. These authors have interpreted this 'infrared excess' as the thermal re-radiation by interstellar dust of starlight from luminous early-type stars produced in a recent burst of star formation.

Surveys by Rieke (1978), Neugebauer *et al.* (1979), and others, show that active galactic nuclei, such as Seyfert galaxies and quasars, also display large infrared luminosities. Both thermal and non-thermal processes have been discussed for the IR emission from these galaxies.

Interacting galaxies are another class of galaxies which seem to exhibit large infrared excesses (Gehrz, Sramek & Weedman 1983; Joseph *et al.* 1984 (Paper I); Lonsdale, Persson & Matthews 1984). These authors have all suggested that starbursts are the underlying sources of the infrared luminosities of these galaxies. The tidal forces induced by the interaction result in substantial redistribution of material in and between the galaxies (*cf.* Toomre & Toomre 1972), and this evidently provides the fuel for a rapid burst of star formation in the nucleus of one member of the interacting pair of galaxies.

Merging galaxies are a subset of interacting galaxies which, as a class, have not previously been investigated in the infrared. However, if distant interactions can induce starbursts, galaxy–galaxy mergers might be expected to result in even more impressive bursts of star formation, since the mergers will provide significantly more fuel for star formation than will non-merging interactions. Indeed, Heckman (1983) has found that his sample of *merging* galaxies is more likely to be radio-loud than ordinary spiral galaxies and non-merging interacting spiral galaxies. As part of our study of interacting galaxies of various morphological types (Joseph *et al.* 1984 (Paper I); Joseph *et al.*, in preparation; Wright, Joseph & Meikle 1984; Graham *et al.* 1984), we have investigated the infrared features of merging galaxies.

2 The sample

There are several different, but overlapping, lists of candidates for galaxy–galaxy mergers in the literature (*cf.* Toomre 1977; Schweizer 1983; Heckman 1983). For this study we have imposed a more restrictive criterion for a merger than is generally adopted. We have limited attention to highly disturbed systems in which two disc galaxies have lost their individual identities and appear as a single, coalesced object. The primary morphological indication of such a merger is the presence of two tidal 'tails' (Toomre & Toomre 1972), since numerical simulations of galaxy interactions show that when two disc galaxies of approximately equal mass interact two tidal tails are produced. Probably the major consequence of these restrictions is to limit attention to systems within a more narrow range of merger ages than is the case for many of the galaxies in the lists of mergers cited above. This is illustrated by the pictures of our sample in Plate 1, which show that the tidal tails of these galaxies have diffused away more than, for example, those in NGC 4676A/B ('The Mice') and in NGC 4038/39 ('The Antennae').

In Plate 1 we show pictures of the nine mergers in our sample. We emphasize that they are the *only* merging galaxies of which we are aware which satisfy these morphological criteria and for which mid-infrared photometry is available. They are all generally considered to be examples of mergers (Toomre 1977; Schweizer 1983; Fried & Schultz 1980; Stockton & Bertola 1980; Balick & Heckman 1981). Evidence that these systems are indeed the products of a merger includes tidal tails (NGC 520, 3256, 2623) or the remnants thereof (NGC 6240, IC 4553, NGC 1614, 4194), double nuclei (NGC 6240, 2623), or the presence of two velocity systems (NGC 520). The 'shells' or 'ripples' seen in NGC 3310 are also thought to be the result of a collision between two galaxies (Schweizer 1983).

IR photometry for these nine galaxies is presented in Table 1. Photometry at 10 μm has been obtained by us and our colleagues for NGC 2623, 6240 (Wright *et al.* 1984), and NGC 3256 (Graham *et al.* 1984). Infrared photometry for the other five galaxies has been taken from the literature, as indicated in Table 1.

3 Infrared luminosities

As Table 1 shows, all these merging galaxies are relatively bright at 10 μm. However, it is the unusually large infrared luminosities which these flux densities imply which are of physical interest. In Table 1 we list the 10-μm luminosities for these galaxies, computed from the formula

$$L_{10}=4\pi D^2 \nu S_\nu \qquad (1)$$

where D is the distance and S_ν is the 10-μm flux density. With the exception of IC 4553 the

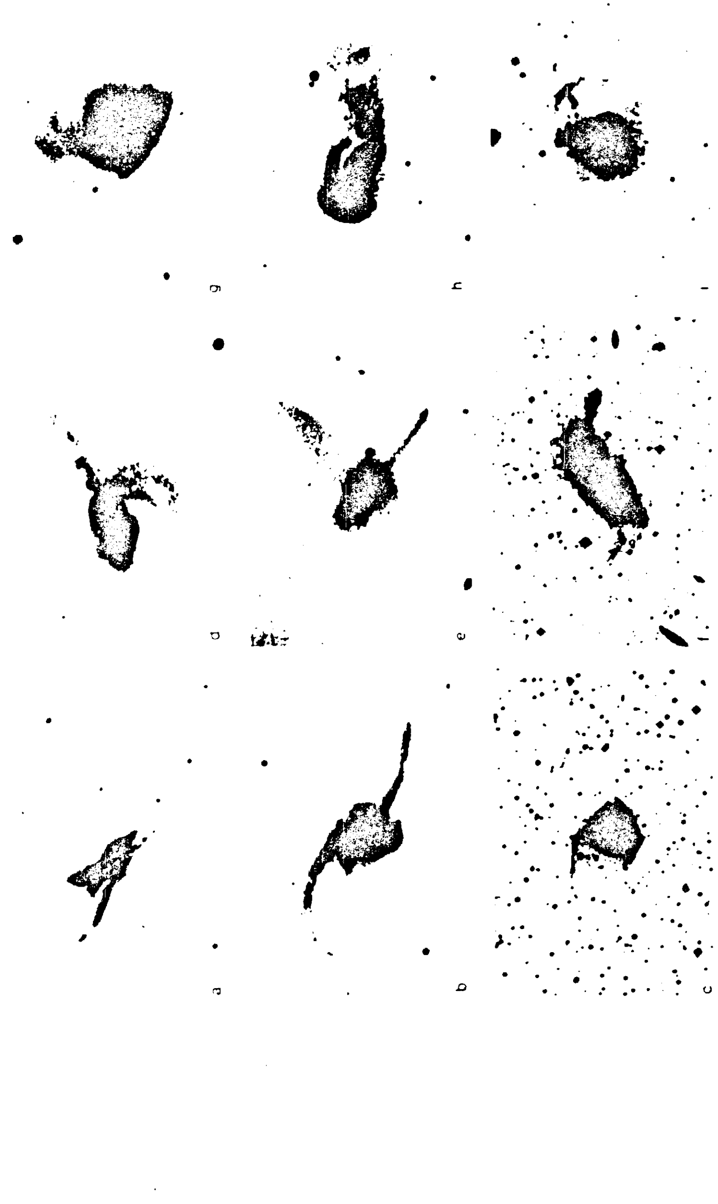

Plate 1. Pictures of the nine merging galaxies in our sample. The photographs have been reproduced from the Arp (1966) Atlas, except for NGC 3256, which is reproduced from the ESO/SERC Southern Sky Survey IIIaJ plate taken with the UK Schmidt Telescope, and for NGC 6240, which is reproduced from a plate published by Fosbury & Wall (1979). Ordered approximately according to relative merger age, the galaxies are (a) NGC 520, (b) NGC 2623, (c) NGC 3256, (d) NGC 1614, (e) IC 883, (f) NGC 6240, (g) IC 4553, (h) NGC 4194, (i) NGC 3310.

[*facing page* 88]

Table 1. Infrared photometry of merging galaxies.

NGC/IC	ARP/VV	Distance (Mpc)	S_{10}(mJy)	$L_{10}(L_{\odot})$	References
6240		150	120	2×10^{10}	Wright *et al.* (1984)
3256	VV65	50	2000	4×10^{10}	Graham *et al.* (1984)
2623	A243	110	80	8×10^{9}	
4553	A220	110(a)	480	5×10^{10}	Soifer *et al.* (1984)
1614	A186	90	630	4×10^{10}	Lebofsky & Rieke (1979)
520	A157	46	460	8×10^{9}	Condon *et al.* (1982)
4194	A160	53	320	7×10^{9}	Rieke & Low (1972)
3310	A217	20	100	1×10^{9}	Telesco & Gatley (1984)
883	A193	140	154	2.5×10^{10}	Lonsdale *et al.* (1984)

(a) Soifer *et al.* (1984)

distances in Table 1 have been determined using redshifts from RC2 (de Vaucouleurs, de Vaucouleurs & Corwin 1976), assuming $H_0=50\,\mathrm{km\,s^{-1}\,Mpc^{-1}}$.

The significance of these luminosities is best appreciated by comparison with the 10-μm luminosities of other classes of galaxies. Luminosities calculated using equation (1), and the same value for H_0, for several classes of galaxies are shown in Table 2. It is evident that the merging galaxies are two orders of magnitude more luminous at 10 μm than bright spiral galaxies in general, and about one order of magnitude more luminous than archetypal starburst galaxies such as NGC 253 and M82. Of perhaps greater interest and significance is comparison with Seyfert galaxies. The merging galaxies may be seen to overlap with the more luminous Seyferts, and only a few of the most luminous Seyferts outshine the merging galaxies at 10 μm. Our conclusion from the luminosities in Table 2 is that these merging galaxies are among the most luminous IR galaxies known.

Table 2. Comparison of 10 μm luminosities

Class of galaxies	Range of $L_{10}(L_{\odot})$	References
Merging galaxies	1×10^{9}–5×10^{10}	This work
Seyfert galaxies	1×10^{8}–10^{11}	Rieke (1978)
Starbursts: M82	10^{9}	Rieke *et al.* (1980)
NGC 253	6×10^{8}	Rieke & Lebofsky (1978)
Bright spirals	10^{8}–7×10^{8}	Rieke & Lebofsky (1978)

This conclusion is even stronger when we consider the total IR luminosities of two galaxies in this group, NGC 6240 and IC 4553, for which far-IR photometry from *IRAS* has been reported (Wright *et al.* 1984; Soifer *et al.* 1984). Both of these galaxies have total IR luminosities $\sim2\times10^{12}L_{\odot}$. This is within a factor of 2 of that of Mkn 231, until recently the most luminous IR galaxy discovered. Aaronson & Olszeweski (1984) have measured the redshift of the morphologically peculiar galaxy which they suggest is associated with the *IRAS* source 0422+009 and derive a similar luminosity for this object. The 10-μm luminosities in Table 2, together with the fact that two (or three?) of the four most luminous IR galaxies known are mergers, suggests that merging galaxies, as a class, are indeed ultraluminous IR galaxies.

4 Emission mechanisms and energy sources

In Fig. 1 we plot the continuum spectra for these merging galaxies. Despite the incompleteness of several of the spectra, it is clear that they are all very similar. The steep mid-IR spectrum rises to a peak near 100 μm and then falls two or three orders of magnitude to the radio. Such a spectrum is

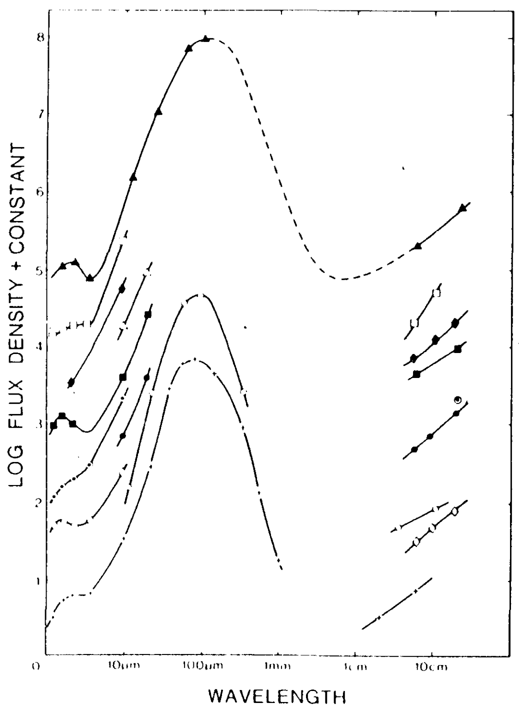

Figure 1. Continuum spectra of merging galaxies and the starburst galaxy NGC 253. The mid and far infrared data are taken from the references in Table 1. Near-infrared and radio measurements are from: NGC 6240 (▲), Allen (1976) and Condon *et al.* (1982); NGC 3256 (○), Graham *et al.* (1984) and Wright (1974); NGC 520 (◆), Glass (1973), Condon (1980) and Condon *et al.* (1982); NGC 1614 (△), NGC 3310 (■), Telesco & Gatley (1984), Hummel (1980) and Sramek (1975); NGC 2623 (●), Condon (1980); NGC 4194 (□), Balzano (1983), Sulentic (1976) and Hummel, van der Hulst & Dickey (1984); IC 4553 (○), Condon (1980), Stocke, Tifft & Kaftan Kassim (1978) and Emerson *et al.* (1984); IC 883 (×), Lonsdale *et al.* (1984) and Sulentic (1976). The dashed interpolation is a Rayleigh–Jeans spectrum with emissivity proportional to λ^{-1} joined smoothly to the data at longer and shorter wavelengths. For NGC 253 (+) the data have been taken from Glass (1973), Rieke *et al.* (1973), Rieke & Low (1975), Hildebrand *et al.* (1977), Elias *et al.* (1978), Rieke & Lebofsky (1978), Telesco & Harper (1980) and Turner & Ho (1983). To avoid crowding the figure the spectra have been shifted vertically by an arbitary amount.

commonly interpreted as thermal emission from dust grains with a colour temperature of ~50 K. Continuum spectra with these features for galactic nuclei are generally assumed to be indicative of a recent burst of star formation, with the ultraviolet radiation from massive, early-type stars thermalized by dust and re-radiated in the IR.

There are several observational tests of this interpretation which can be applied to this group of merging galaxies. First, are the optical spectra of these galaxies suggestive of recent star formation? There are optical spectra in the literature for six of these galaxies, NGC 6240 (Fosbury

& Wall 1979), NGC 1614 (Aitken, Roche & Phillips 1981), NGC 4194 (Balzano 1983), NGC 3310 (Heckman 1980), NGC 520 (Stockton & Bertola 1980), and NGC 3256 (Feast & Robertson 1978). For NGC 1614, 3310, and 4194 the relative intensities of [O III]/Hβ and/or [N II]/Hα are similar to those found in H II regions, whereas for NGC 6240 the line intensities suggest shock excitation (*cf.* Baldwin, Phillips & Terlevich 1981). For NGC 3256 and 520 only qualitative descriptions of the spectra have been given, but for both galaxies the spectra are characterized by narrow linewidths, $< 30\,\mathrm{km\,s^{-1}}$, indicative of starbursts (*cf.* Feldman *et al.* 1982). Thus none of the available optical spectra indicate Seyfert-type activity, and most are consistent with what is expected from H II regions.

Secondly, the IR emission from starburst galaxies is characterized by spatial extent on scales of 100's of parsec (Rieke 1976). For several of the merging galaxies there is evidence that the IR emission is extended on scales exceeding 1 kpc. Wright *et al.* (1984) argue from the difference between their small aperture 10 and 20 μm photometry and large aperture *IRAS* measurements that the IR emission in NGC 6240 must be extended on scales ≳3 kpc, and this is confirmed in recent measurements by Cutri *et al.* (1984). For NGC 3310 the maps of Telesco & Gatley (1984) show that star formation has been triggered across the entire galaxy, and intense 10-μm emission in this galaxy extends for more than 5 kpc. Maps at 10 μm and multiaperture photometry at 3.45 μm of NGC 3256 are used by Graham *et al.* (1984) to infer that the emission is extended over at least 4 kpc. Finally, Cutri *et al.* (1984) have recently mapped IC 4553 at 10 μm, and find the source to be larger than 2 kpc. Spatial extent at 10 μm on this scale cannot be produced by a single compact source heating the dust, as would be required if the underlying energy source were accretion onto a compact object. There must be sources distributed throughout the emitting region in these merging galaxies. Such a distribution of luminosity sources is a natural consequence of a starburst interpretation.

Further evidence in support of the starburst interpretation comes from radio observations. High angular resolution radio measurements, referenced in Fig. 1, are available for all of these galaxies except NGC 3256. In every case the nuclear radio source is resolved, with a characteristic extent of ~1.5 kpc, and has a non-thermal spectrum, typically of index ~ −0.7. These are not the characteristics of radio emission associated with Seyfert-type activity. Such radio properties are generally interpreted as due to supernova remnants associated with recent bursts of star formation (*cf.* Condon *et al.* 1982).

Taken together, the IR, optical, and radio measurements on this group of merging galaxies provides strong and consistent evidence that the large IR luminosities which apparently characterize merging galaxies are powered by recent bursts of star formation. However, the star formation activity present in these systems must be at least an order of magnitude more vigorous than in other classes of starburst galaxies to account for their extreme IR luminosities. Moreover, for at least four of these galaxies the starburst must be extended over scales of several kpc, again significantly larger than other known starburst galaxies. The starbursts in merging galaxies are, indeed, 'super starbursts.'

5 Discussion

Since all the merging galaxies for which IR photometry is available appear to be undergoing a super starburst phase can we expect that most merging galaxies will be found to be ultraluminous IR galaxies? The dynamical simulations of Toomre & Toomre (1972) and Wright (1972) suggest that the morphological evidence for an interaction (or a merger) in the form of tidal 'tails' will persist for times of order 10^9 yr. By selecting merger candidates whose tidal tails have begun to disappear, we estimate the remaining morphological distortions will have disappeared in about 5×10^8 yr (*cf.* Toomre 1977). Models of rapid star formation episodes in these galaxies (*cf.* Rieke

Table 3. Infrared luminosities and M/L ratios for merging galaxies in order of increasing 'age'

Galaxy	$L_{IR}(L_\odot)^{(a)}$	Mass ($M_\odot$)	M/L_{IR}
NGC 520	1×10^{11}	$1\times10^{9(b)}$	0.01
NGC 2623	1×10^{11}		
NGC 3256	6×10^{11}	$6\times10^{9(c)}$	0.01
NGC 1614	6×10^{11}	$>2\times10^{9(d)}$	>0.003
IC 883	4×10^{11}		
NGC 6240	5×10^{11}	$<5\times10^{10(e)}$	<0.08
IC 4553	7×10^{11}		
NGC 4194	1×10^{11}	$3\times10^{9(f)}$	0.03
NGC 3310	6×10^{10}		

Notes

(a) See text.

(b) Mass estimated by assuming the linewidths in Stockton & Bertola (1980) are due to doppler broadening due to rotation.

(c) Mass derived from the rotation curve in Feast & Robertson (1978).

(d) Mass taken from Ulrich (1972).

(e) Mass estimated by assuming that all of the optical line widths in Fosbury & Wall (1979) are due to doppler broadening due to rotation.

(f) Mass taken from Demoulin (1969).

et al. 1980; Cutri *et al.* 1984) result in starburst lifetimes of $\sim10^8$ yr. Given the uncertainties in these numbers, it is probably not surprising that a significant fraction of the galaxies recognizable as mergers from the morphological criteria outlined above should be found in the super-starburst phase in their evolution.

Despite the relatively narrow age range of our sample, it seems to be possible to account for some of the spread in luminosities within our sample in terms of the age of the merger process. In Table 3 and Plate 1 we have attempted to place these galaxies in a rough order of age. We have used the faintness of the tidal 'tails' and the degree of coalescence as indicators of relative merger age, as was done by Toomre (1977). Although such an ordering is somewhat subjective, it is rather clear that NGC 520 must be one of the youngest mergers in this group, since it is the only member of the sample in which two velocity systems are present in the spectra. NGC 3310 must also be the oldest, since it has no tails remaining at all, and its 'shells' or 'ripples' indicate a very late stage in a merger (*cf.* Schweizer 1983). Comparing the IR luminosities in Table 3 it is apparent that the two youngest and the two oldest mergers are less luminous than the four 'middle-aged' mergers. There seems to be a peak in the distribution of luminosities as a function of age of the merger process. This suggests that merging galaxies undergo a phase of starburst activity of characteristic luminosity $\sim10^{12}L_\odot$. The younger mergers in our sample may not quite have reached this stage, while in the older systems the starburst has begun to die away.

The appearance of a super starburst as the natural consequence of a merger may also be significant for theories of the origin of (some) elliptical galaxies. Toomre (1977) and others have argued from the expected stellar velocity distributions and luminosity profiles of merger remnants that merging galaxies evolve into objects resembling elliptical galaxies. However, if this suggestion is correct, there must be some way for the embryonic elliptical galaxy to divest itself of the gas belonging to the galaxies before they merged. The super starburst phase of merger evolution can provide the mechanism for this. Massive, early-type stars produced in the starburst will end their lives as supernovae. Galactic winds driven by these supernovae may then sweep the galaxy free of gas (Matthews & Baker 1971). As Graham *et al.* (1984) have shown in the case of NGC 3256, an *exceptionally extended* starburst with a bolometric mass-to-light ratio less than unity (solar units) can provide sufficient mechanical energy for ejection of all the gas its vicinity.

In Table 3 we present bolometric mass-to-light ratios for those galaxies for which rotation curves or line-widths exist. For NGC 6240 we have estimated the bolometric luminosity in a small aperture from the *IRAS* photometry, and for the others we have made a conservative extrapolation of the 10-μm luminosities to total IR luminosities by multiplying by a factor of 15 (*cf.* Scoville *et al.* 1983; Telesco & Gatley 1984). Masses have been estimated as described in the footnotes to Table 3. It is evident from Table 3 that the mass-to-light ratios in these merging galaxies are similar to NGC 3256, and substantially less than one. For NGC 6240, 3310, and IC 4553 the starburst is extended on scales similar to that in NGC 3256. If, as we expect, the M/L ratios and spatial extent are similar for the other merging galaxies in the sample, the remnant objects from all these mergers will be severely gas-depleted. Provided the other arguments relating mergers to ellipticals are valid, then it seems inevitable that these merging galaxies will indeed become indistinguishable from elliptical galaxies.

The IR luminosities typical of these merging galaxies require star formation rates larger than those in any other known classes of galaxies by at least an order of magnitude. The detection of molecular hydrogen (Joseph, Wright & Wade 1984; Becklin *et al.* 1984) in two of these galaxies, NGC 6240 and IC 4553, provides a clue to the detailed mechanism by which these super starbursts are engendered. We imagine two gas-rich galaxies which approach each other at a relative velocity of a few hundred km s^{-1}. As the galaxies begin to merge fast shocks of velocity $\lesssim100$ km s^{-1} are induced in the gas due to cloud–cloud collisions. Any H_2 present before the interaction will be dissociated by such shocks. However, Draine & Salpeter (1979) have shown that a significant fraction of refractory dust grains survive shocks up to ~300 km s^{-1}. Although Draine & Salpeter considered gas densities of ~40 cm^{-3}, Hollenbach & McKee (1979) argue that this conclusion remains valid for densities up to $\sim10^7$ cm^{-3}. These dust grains will provide sites for post-shock formation of H_2. Hollenbach & McKee go on to show that if the initial density is $>10^3$ cm^{-3} and the shock velocity is <300 km s^{-1}, the post-shock gas can be fully molecular. Our detections of H_2 imply that $3\times10^3 M_\odot$ yr^{-1} are shocked in NGC 6240. For any reasonable lifetime assumed for this process, it is evident that there must be an efficient mechanism for H_2 formation, such as that discussed by Hollenbach & McKee operating in these systems. (For IC 4553 strong OH maser emission also suggests that there are large quantities of molecular gas in the nuclear region of this galaxy (Baan & Haschick 1984).) The dense H_2 will rapidly cool, collapse, and fragment, producing a burst of star formation. Under such conditions we would expect gas to be converted into stars with exceptional efficiency, thus producing an episode of star formation of ultra-high luminosity. Since the gas clouds experiencing these shocks will be distributed across the central regions of the two merging galaxies, we would also expect the rapid star formation activity to have unusually large spatial extent. These are precisely the features we have identified in this sample of merging galaxies.

6 Conclusions

We suggested in the Introduction that, if an interaction between two galaxies results in a burst of star formation in the nucleus of one of the two galaxies, it would be surprising if such bursts of star formation did not occur with significantly more vigour in merging systems. The observational evidence we have adduced above confirms this conjecture. Beginning from a rather restrictive definition of a merging galaxy we have found that, for all the galaxies fitting this description for which mid-IR photometry is available, their IR luminosities are larger than most other classes of IR galaxies and they rival the most luminous Seyfert galaxies. From the shape of the continuum spectra, optical emission line intensities, and spatial extent of the IR and radio emission, we argued that the energy source powering these large IR luminosities is a 'super' starburst. There seems to be some suggestion of a rise and fall of star formation rate with merger evolution in our sample. The peak IR luminosities characterizing a merger-induced starburst are $\sim 10^{12} L_{\odot}$. One interesting consequence of these super starbursts is that the remnant of the merger is likely to be swept free of gas by winds driven by supernovae resulting from the starburst, thus lending further support to suggestions that mergers will evolve into objects greatly resembling elliptical galaxies.

Finally, we outlined a physical picture for the process by which a merger triggers such super starbursts. Shocks generated in the interaction result in rapid and efficient formation of H_2 on the surfaces of dust grains. This dense gas very quickly engenders a burst of star formation. The dust grains on which the H_2 formed thermalize the radiation from the luminous, hot stars and re-radiate it in the IR, providing the ultra-large IR luminosities which we have found to be a characteristic feature of merging galaxies.

Acknowledgments

It is a pleasure to thank James Graham, Norna Robertson, and Alar Toomre for helpful discussions and correspondence on various aspects of this subject. GSW is a research student supported by the SERC.

References

Aaronson, M. & Olszewski, E. W., 1984. *Nature*, **309**, 414.
Aitken, D. K., Roche, P. F. & Phillips, M. M., 1981. *Mon. Not. R. astr. Soc.*, **196**, 101P.
Allen, D. A., 1976. *Astrophys. J.*, **207**, 367.
Arp, H., 1966. *Atlas of Peculiar Galaxies*, California Institute of Technology, Pasadena.
Baan, W. A. & Haschick, A. D., 1984. *Astrophys. J.*, **279**, 541.
Balick, B. & Heckman, T. M., 1981. *Astr. Astrophys.*, **96**, 271.
Baldwin, J. A., Phillips, M. & Terlevich, R., 1981. *Publs astr. Soc. Pacif.*, **93**, 5.
Balzano, V. A., 1983. *Astrophys. J.*, **268**, 602.
Becklin, E., Black, J., Cutri, R., DePoy, D., Elston, R., Impey, C., Joseph, R., Kailey, W., Lebofsky, M., McAlary, C., Rieke, G., Seab, C., Wade, R., Werner, M., Wright, G. & Wynn-Williams, C., 1984. *IAU Circ. No. 3968*.
Condon, J. J., 1980. *Astrophys. J.*, **242**, 894.
Condon, J. J., Condon, M. A., Gisler, G. & Puschell, J., 1982. *Astrophys. J.*, **252**, 102.
Cutri, R. M., Rieke, G. H., Black, J. H., Kailey, W. F., McAlary, C. W., Lebofsky, M. J. & Elston, R., 1984. Preprint.
Demoulin, M. H., 1969. *Astrophys. J.*, **156**, 325.
Draine, B. T. & Salpeter, E. E., 1979. *Astrophys. J.*, **231**, 438.
de Vaucouleurs, G., de Vaucouleurs, A. & Corwin, H. G., 1976. *Second Reference Catalogue of Bright Galaxies*, University of Texas Press, Austin.
Elias, J. H., Ennis, D. J., Gezari, D. Y., Hauser, M. G., Houck, J. R., Lo, K. Y., Matthews, K., Nadeau, D., Neugebauer, G., Werner, M. W. & Westbrook, W. E., 1978. *Astrophys. J.*, **220**, 25.
Emerson, J. P., Clegg, P. E., Gee, G., Cunningham, C. T., Griffin, M. J., Brown, L. M. J., Robson, E. I. & Longmore, A. J., 1984. *Nature*, **311**, 237.
Feast, M. W. & Robertson, B. S. C., 1978. *Mon. Not. R. astr. Soc.*, **185**, 31.
Feldman, F. R., Weedman, D. W., Balzano, V. A. & Ramsey, L. W., 1982. *Astrophys. J.*, **256**, 427.
Fosbury, R. A. E. & Wall, J. V., 1979. *Mon. Not. R. astr. Soc.*, **189**, 79.
Fried, J. W. & Schultz, H., 1980. *Astr. Astrophys.*, **118**, 166.
Gehrz, R. D., Sramek, R. A. & Weedman, D. W., 1983. *Astrophys. J.*, **267**, 551.
Glass, I. S., 1973. *Mon. Not. R. astr. Soc.*, **164**, 155.
Graham, J. R., Wright, G. S., Meikle, W. P. S., Joseph, R. D. & Bode, M. F., 1984. *Nature*, **310**, 213.
Heckman, T. M., 1980. *Astr. Astrophys.*, **87**, 152.
Heckman, T. M., 1983. *Astrophys. J.*, **268**, 628.
Hildebrand, R. H., Whitcomb, S. E., Winston, R., Stiening, R. F., Harper, D. A. & Moseley, S. H., 1977. *Astrophys. J.*, **216**, 698.
Hollenbach, D. & McKee, C. F., 1979. *Astrophys. J. Suppl.*, **41**, 555.
Hummel, E., 1980. *Astr. Astrophys. Suppl.*, **41**, 151.

Hummel, E., van der Hulst, J. M. & Dickey, J. M., 1984. *Astr. Astrophys.*, **134**, 207.
Joseph, R. D., Meikle, W. P. S., Robertson, N. A. & Wright, G. S., 1984. *Mon. Not. R. astr. Soc.*, **209**, 111 (Paper I).
Joseph, R. D., Wright, G. S. & Wade, R., 1984. *Nature*, **311**, 132.
Lebofsky, M. J. & Rieke, G. H., 1979. *Astrophys. J.*, **229**, 111.
Lonsdale, C. J., Persson, S. E. & Matthews, K., 1984. Preprint.
Matthews, W. G. & Baker, J. C., 1971. *Astrophys. J.*, **170**, 241.
Neugebauer, G., Oke, J. B., Becklin, E. E. & Matthews, K., 1979. *Astrophys. J.*, **230**, 79.
Rieke, G. H., 1976. *Astrophys. J.*, **206**, L15.
Rieke, G. H., 1978. *Astrophys. J.*, **226**, 550.
Rieke, G. H. & Lebofsky, M. J., 1978. *Astrophys. J.*, **220**, L37.
Rieke, G. H., Lebofsky, M. J., Thompson, R. I., Low, F. J. & Tokunaga, A. T., 1980. *Astrophys. J.*, **238**, 24.
Rieke, G. H., Harper, D. A., Low, F. J. & Armstrong, K. R., 1973. *Astrophys. J.*, **183**, L67.
Rieke, G. H. & Low, F. J., 1972. *Astrophys. J.*, **176**, L95.
Rieke, G. H. & Low, F. J., 1975. *Astrophys. J.*, **197**, 17.
Schweizer, F., 1983. *Internal Kinematics and Dynamics of Galaxies*, p. 319, ed. Athanassoula, E., Reidel, Dordrecht, Holland.
Scoville, N. Z., Becklin, E. E., Young, J. S. & Capps, R. W., 1983. *Astrophys. J.*, **271**, 512.
Soifer, B. T., Helou, G., Lonsdale, C. J., Neugebauer, G., Hacking, P., Houck, J. R., Low, F. J., Rice, W. & Rowan-Robinson, M., 1984. *Astrophys. J.*, **283**, L1.
Sramek, R., 1975. *Astr. J.*, **80**, 71, 77.
Stocke, J. T., Tifft, W. G. & Kaftan Kassim, M. A., 1978. *Astr. J.*, **83**, 322.
Stockton, A. & Bertola, F., 1980. *Astrophys. J.*, **235**, 37.
Sulentic, J. W., 1976. *Astrophys. J. Suppl.*, **32**, 171.
Telesco, C. M. & Harper, D. A., 1980. *Astrophys. J.*, **235**, 392.
Telesco, C. M. & Gatley, I., 1984. *Astrophys. J.*, **284**, 557.
Toomre, A., 1977. *Evolution of Galaxies and Stellar Populations*, p. 401, eds Tinsley, B. M. & Larson, R. B., Yale University Observatory, New Haven, Connecticut.
Toomre, A. & Toomre, J., 1972. *Astrophys. J.*, **178**, 623.
Turner, J. L. & Ho, P. T. P., 1983. *Astrophys. J.*, **268**, L79.
Ulrich, M. H., 1972. *Astrophys. J.*, **178**, 113.
Wright, A. E., 1972. *Mon. Not. R. astr. Soc.*, **157**, 309.
Wright, A. E., 1974. *Mon. Not. R. astr. Soc.*, **167**, 251.
Wright, G. S., Joseph, R. D. & Meikle, W. P. S., 1984. *Nature*, **309**, 430.

NEAR INFRARED SPECTROSCOPY OF GALAXIES

G.S. Wright & R.D. Joseph
Blackett Laboratory, Imperial College, London SW7 2BZ.
R. Wade
Royal Observatory, Blackford Hill, Edinburgh EH9 3HJ.
J.R. Graham
Lawrence Berkeley Laboratory, Berkeley, CA94720.
I. Gatley
United Kingdom Infrared Telescope, Hilo, Hawaii 96720.

1. Introduction

It is only with the advent of sensitive spectrometers at UKIRT that the serious and systematic development of IR spectroscopy for extragalactic astronomy has become possible. Until last year there were only two published detections of the 2.122μm v=1-0 S(1) rotation-vibration line of H_2 in galactic nuclei. The first extragalactic measurement was in NGCC1068 (Thompson et al. 1978) and spectra of NGC3690 have also been presented (Fischer et al. 1983). Likewise, the 1.644μm forbidden line of FeII had been detected only in the nuclei of M82 and NGC4151 (Rieke et al. 1980, Rieke and Lebofsky 1981). Additionally, less than a dozen detections of the IR H recombination lines (Brα, Brγ) in galaxies have been reported.

We have obtained spectra in the H and K windows for about 12 galaxies, and, most importantly, have measured several lines for most of these galaxies. These results were obtained very recently and the data reduction and analysis are still at a very preliminary stage. In this paper, therefore, we will attempt only to give a broad overview of the results and their implications.

2. Rationale for this study

We had two principal objectives in begining the exploration of near-IR spectroscopy for extra-galactic astronomy. Firstly, H_2 emission is observed from star-forming regions in molecular clouds (e.g. Beckwith 1981), and strong [FeII] emission has been observed from young supernova remnants (Allen et al. 1985). Temperatures ≥ 8000K are required to excite [FeII], whereas H_2 can be excited by temperatures as low as 1000K. For these reasons measuring both these lines, as well as H recombination lines, provides physical and astrophysical diagnostic information for galactic nuclei, and in particular, the detailed properties of starbursts. Secondly, in interacting and merging galaxies large scale shocks are expected. Since both the H_2 and [FeII] can be collisionally excited, observation of these lines also holds the promise of providing a better understanding of the physics of the interaction between two galaxies.

3. Results

In this paper we will discuss only the K and H window spectra of 8 interacting galaxies and NGC253. These spectra were obtained using the UKT9 CVF spectrometer at UKIRT. The spectral resolution was ~ 130, and we employed apertures ranging from 5 to 19.6 arcsec. Sample spectra, shown in Figures 1-3, illustrate the dominant spectral features in all our data. These are the H_2 lines (especially v=1-0 S(1), and v=1-0 Q (blended 1-7)), Brackett γ, and the $a^4F_{7/2}$ - $a^4D_{9/2}$ 1.644μm forbidden line of FeII.

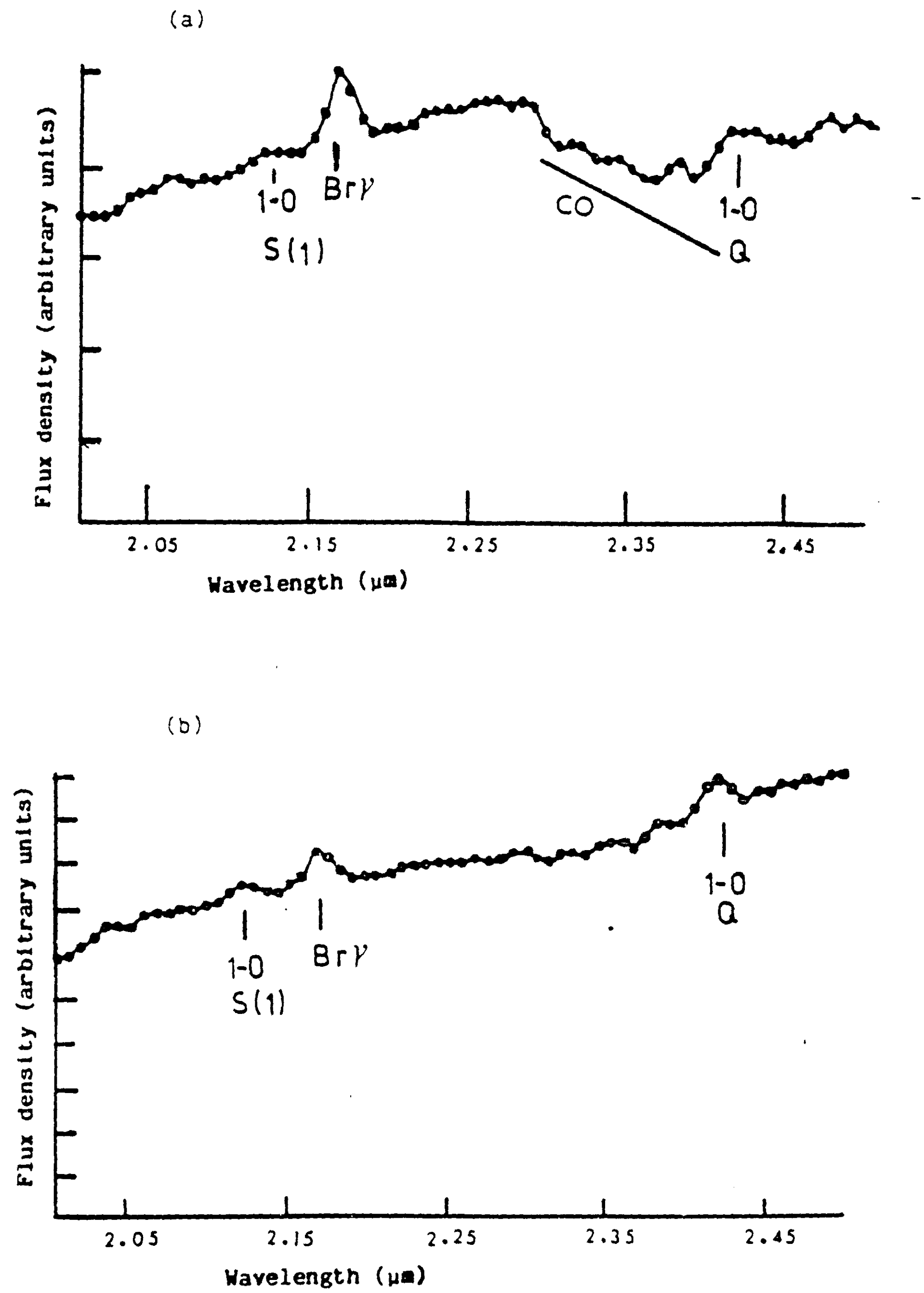

Figure 1

K-window spectra of NGC253. The vertical lines indicate the wavelengths of the H_2 and Brγ lines at the redshift of NGC253. The error per point is smaller than the size of the dots. In (a) the spectrum has been ratioed with an early type star to show the CO absorption (Brγ is therefore artificially enhanced). In (b) the CO absorption is removed by ratioing with a supergiant and the V= 1-0 Q lines of H_2 are clearer.

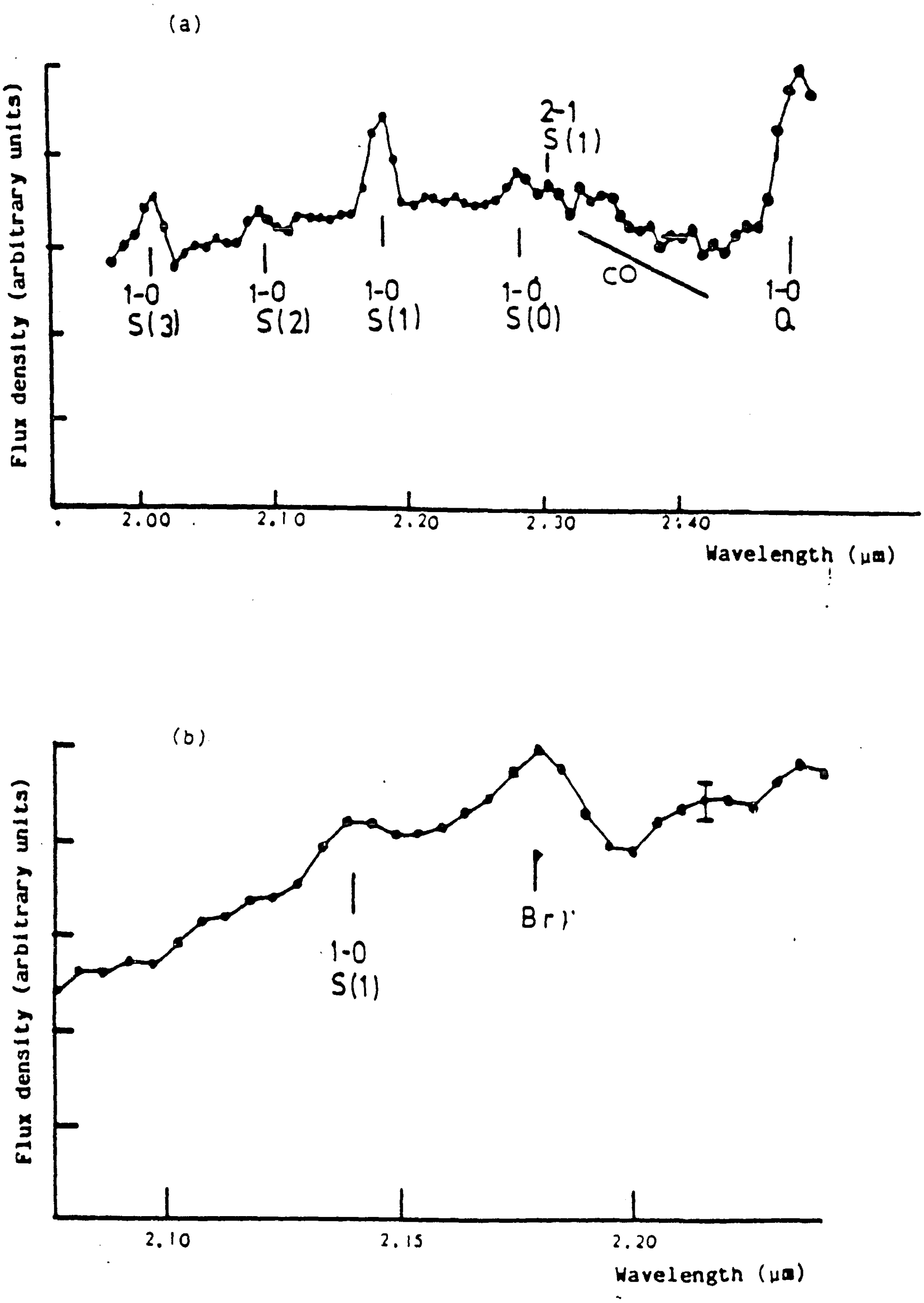

Figure 2

K-window spectra of (a) NGC6240 and (b) NGC2798. The H_2 and Brγ lines are indicated on the figures. The spectra have been ratioed with a standard and that of NGC2798 has been smoothed with a triangular function. For NGC6240 the error per point is smaller than the size of the dots and for NGC2798 a typical error bar is shown.

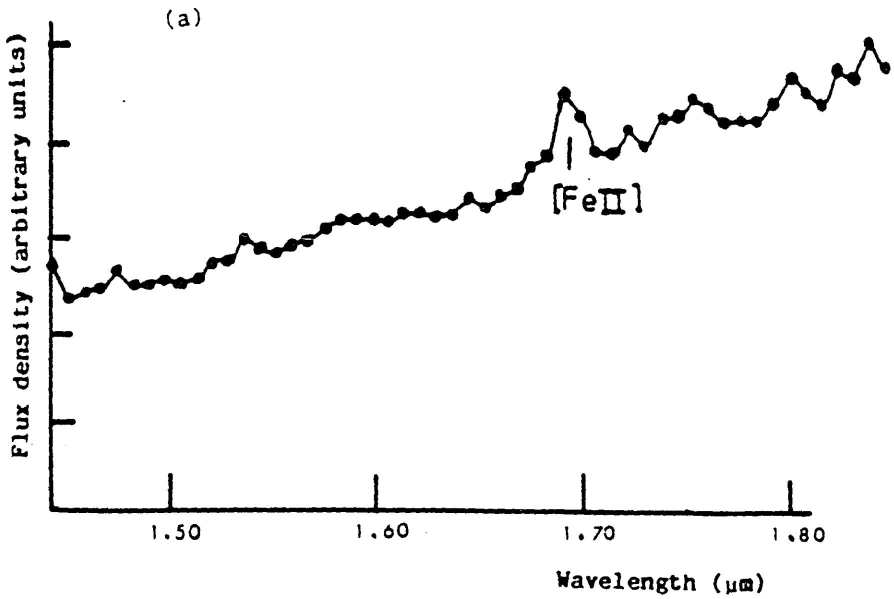

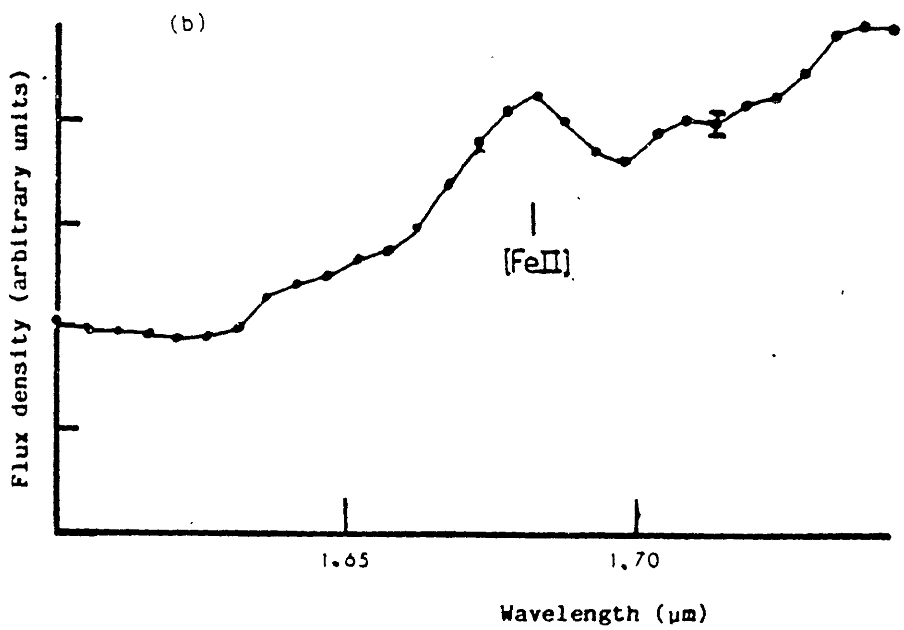

Figure 3

H-window spectra of (a) NGC6240 and (b) NGC1614. The wavelengths of the 1.644μm [FeII] line at the redshifts of the galaxies are shown by the vertical lines. For NGC1614 a typical error bar is drawn, while for NGC6240 the typical error per point is smaller than the size of the dots. Both spectra are ratioed with standard spectra and the spectrum of NGC1614 has been smoothed using a triangular function.

4. Excitation of the H_2 and [FeII]

Although we do not have measures of excitation-temperature-sensitive H_2 line ratios (e.g. v=2-1 S(1) / v=1-0 S(1)) for all of the galaxies, for those in which we have detected several lines (NGC6240, IC4553, NGC1614) the line ratios are more consistent with collisional excitation models (e.g. Shull and Hollenbach 1978) than with models for fluorescence following absorption of UV photons (e.g. Black and Dalgarno 1976). Additionally, in NGC6240 we have resolved the 1-0 S(1) H_2 line and its width, ~ 800 kms^{-1}, is similar to the widths of optical lines which are also thought to be shock excited (Fosbury and Wall 1979). For the [FeII] lines, in NGC1614 the ratios of other lines within the multiplet (at 1.600μm and 1.664+1.677μm) to the 1.644μm line are consistent with collisional population of the upper term in dense gas. Furthermore we did not detect other strong forbidden IR lines from higher excited states, which fell within our K-window scans (e.g. $a^4G_{7/2}$-$b^2G_{7/2}$). In summary, our results suggest that both the H_2 and the [FeII] are collisionally excited. In the following we investigate possible sources of this excitation.

5. Interpretation

Our H_2 detections imply luminosities in the 1-0 S(1) line ranging from ~ 10^5 - $3x10^8$ L⊙, and corresponding masses of excited gas of ~ $5x10^2$ - $2x10^5$ M⊙. Thus the excitation rate for H_2 is phenomenal, ~ 10^2 - $7x10^4$ M⊙ of H_2 per year.

We can use the ratio of the luminosity in the 1-0 S(1) line, L(S(1)), to the total IR luminosity, L(IR), to investigate whether this H_2 is excited predominantly by mass outflow from star-forming regions or by interaction driven shocks. This ratio should have a characteristic value if the H_2 is excited by mass outflow from young stars, and the IR luminosity is provided by the luminosity of the same stars, thermalised by dust. We have used IRAS data to estimate the total IR luminosities for all the galaxies. The ratio L(S(1))/L(IR) is within a factor of 2 of the value for Orion, 1 x 10^{-5} (Beckwith 1981), for all of the galaxies except NGC6240. NGC6240 is clearly an exception, with excess H_2 by a factor of more than 15, and it is likely that interaction - induced shocks have provided most of the energy to heat the H_2 gas (Joseph et al. 1984). For all of the other galaxies the H_2 could be excited by mass outflow from star-formation regions as in Orion.

Although L(S(1))/L(IR) lies in the range (0.5-1.4) x 10^{-5}, the ratio L(S(1))/L(Brγ) seems to show slightly more variation, 0.3-5, again excluding NGC6240. This is surprising since the ratio L(S(1))/L(Brγ) should be unaffected by extinction. If the IR emission is due to a burst of star formation, it is possible that this ratio may depend on the age of the starburst or variations in the IMF due to local conditions. This suggestion can be tested by plotting L(S(1))/L(Brγ) against L(Brγ)/L(IR). The ratio L(Brγ)/L(IR) should be a function of the effective temperature of the stars dominating the luminosity of the starburst. Figure 4 shows that there is a clear correlation between L(S(1))/L(Brγ) and L(Brγ)/L(IR). There is surprisingly little scatter in this correlation due to variations in extinction from galaxy to galaxy (the ratio L(Brγ)/L(IR) is extinction dependent). Most importantly, the fact that there is such a good correlation suggests that there must be some "age dependence" in the ratio L(S(1))/L(Brγ), i.e. in some galaxies the IR luminosity and H_2 excitation seems to be predominantly due to stars of later spectral type than in others.

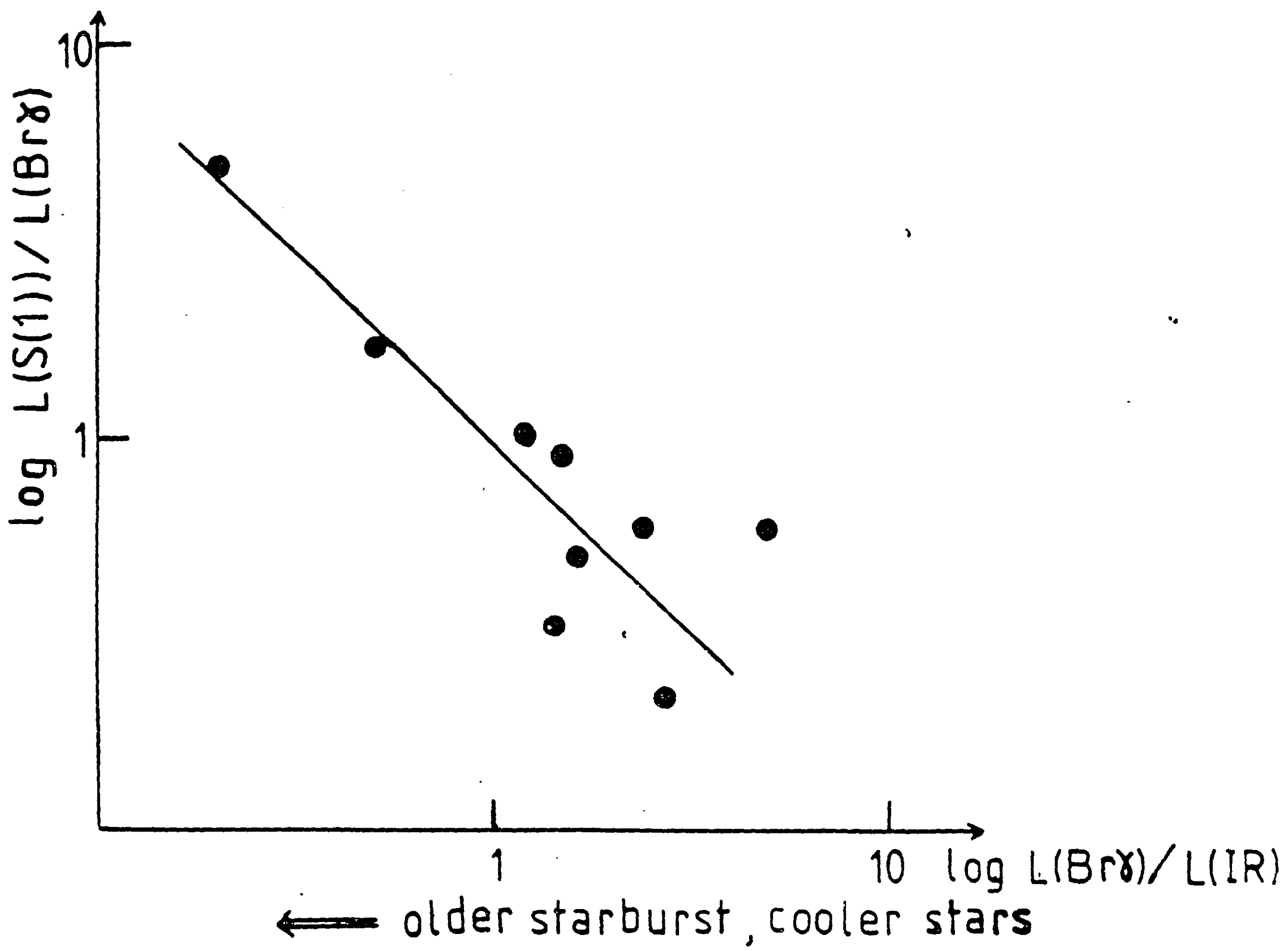

Figure 4

The correlation between L(S(1))/L(BrY) and L(BrY)/L(IR)

For the [FeII] emission no strong correlations with Brγ, the v=1-0 S(1) line, IR luminosity, or combinations thereof are apparent. This is unexpected because, if the [FeII] were due to, for example, supernova remnants as mentioned above, we might expect to find a correlation between, for example, L([FeII])/L(IR) (supernova rate per unit luminosity) and L(Brγ)/L(IR), since the supernova rate should be proportional to the age of the starburst and hence to the latter ratio. The apparent absence of such correlations may indicate that the [FeII] excitation is not related directly to the starburst and is instead excited by interaction induced shocks, as the H_2 is in NGC6240. However, the 1.644μm [FeII] line is more likely to be affected by extinction than the 1-0 S(1) line or Brγ and differential extinction between H and K may have the effect of introducing scatter to the correlations. This, coupled with the fact that we have fewer galaxies in which we have measured the [FeII] line, means that at present it is difficult to draw any firm conclusions about the source of the [FeII] excitation.

For several of the galaxies we have measured a very large spatial extent for the H_2 emission. In NGC253 we have detected H_2 over an angular extent of ~ 40 arcsec. This extent is considerably larger than the apparent extent of the starburst inferred from 10μm photometry (Rieke et al. 1980). It is possible that we are observing excitation induced by the bar (cf. Scoville et al. 1985), by outflow from the nucleus, or due to spiral density waves. For two of the interacting galaxies, NGC2798 and NGC3227, the ratio L(S(1))/L(Brγ) increases by about a factor of 2 between a small and a large aperture measurement. This suggests that in these galaxies also, the H_2 excitation is more extended than the starburst. Although much of the H_2 may be excited in star formation regions, the large spatial extent indicates that the situation is complex and there is also excitation of the H_2 by interaction induced shocks, as we observe in the extreme example of NGC6240.

6. Discussion and Conclusions.

In NGC6240, the existence of massive quantities of shocked molecular gas, greatly in excess of that expected from star-forming regions alone, provides a clue to the detailed mechanism by which the interaction of two galaxies could trigger a luminous starburst. Shocks generated in the interaction result in the rapid and efficient formation of H_2 on the surfaces of dust grains. This dense gas will cool rapidly, collapse and fragment, resulting in a burst of star formation (cf. Joseph and Wright 1985). Our measurements of extended H_2 in the barred spiral NGC253, and in interacting galaxies, suggest that a similar process operating at a less extreme level may be playing a critical role in the common occurence of starbursts in interacting and barred galaxies.

In conclusion, there is strong evidence for shock excitation of both H_2 and [FeII], and the latter implies that the shock velocities are $\gtrsim$ 30 kms^{-1}. The correlation between L(S(1))/L(Brγ) and L(Brγ)/L(IR) suggests that outflow from star formation regions is the dominant excitation mechanism for the H_2 emission. However, the spatial extent of the H_2 excitation in some of these galaxies implies that other excitation mechanisms are also present. For the [FeII], excitation related to the starburst e.g. in supernova remnants, is an attractive possibility but we are unable to find quantitative support for this suggestion. Despite the preliminary stage of the reduction and analysis, the data presented here illustrate some of the potential of near-infrared spectroscopy as a diagnostic tool for detailed investigation of physical processes in galaxies.

References

Allen, D.A., Jones, T.J. & Hyland, A.R., 1985. Mon. Not. R. astr. Soc., **219**, 280.

Beckwith, S. 1981 in "Infrared Astronomy" (eds. Wynn-Williams, C.G., & Cruikshank, D.P) .167-178 (Reidel, Dordrecht)

Black, J.H. & Dalgarno, A., 1976. Astrophys. J., **203**, 132.

Fischer, J., Simon, M., Benson, J. & Solomon, P.M., 1983. Astrophys. J. Lett., **273**, L27.

Fosbury, R.A.E. & Wall, J.V., 1979. Mon. Not. R. astr. Soc., **189**, 79.

Joseph, R.D., Wright, G.S. & Wade, R., 1984. Nature, **311**, 132.

Joseph, R.D. & Wright, G.S., 1985. Mon. Not. R. astr. Soc., **214**, 87.

Rieke, G.H., Lebofsky, M.J., Thompson, R.I., Low, F.J. & Tokunaga, A., 1980. Astrophys. J., **238**, 24.

Rieke, G.H. & Lebofsky, M.J., 1981. Astrophys. J., **250**, 87.

Scoville, N.Z., Soifer, B.T., Neugebauer, G., Young, J.S., Matthews, K. & Yerka, J., 1985. Astrophys. J., **289**, 129.

Shull, J.M. & Hollenbach, D.J., 1978. Astrophys. J., **220**, 525.

Thompson, R.I., Lebofsky, M.J. & Rieke, G.H., 1978 Astrophys. J. Lett. **222**, L49.